

ISSN 2518-1491 (Online),
ISSN 2224-5286 (Print)

ҚАЗАҚСТАН РЕСПУБЛИКАСЫ
ҰЛТТЫҚ ҒЫЛЫМ АКАДЕМИЯСЫНЫҢ

Д.В.СОКОЛЬСКИЙ АТЫНДАҒЫ «ЖАНАРМАЙ,
КАТАЛИЗ ЖӘНЕ ЭЛЕКТРОХИМИЯ ИНСТИТУТЫ» АҚ

Х А Б А Р Л А Р Ы

ИЗВЕСТИЯ

НАЦИОНАЛЬНОЙ АКАДЕМИИ НАУК
РЕСПУБЛИКИ КАЗАХСТАН

АО «ИНСТИТУТ ТОПЛИВА, КАТАЛИЗА И
ЭЛЕКТРОХИМИИ ИМ. Д.В. СОКОЛЬСКОГО»

NEWS

OF THE ACADEMY OF SCIENCES
OF THE REPUBLIC OF KAZAKHSTAN

JSC «D.V. SOKOLSKY INSTITUTE OF FUEL,
CATALYSIS AND ELECTROCHEMISTRY»

ХИМИЯ ЖӘНЕ ТЕХНОЛОГИЯ СЕРИЯСЫ



СЕРИЯ ХИМИИ И ТЕХНОЛОГИИ



SERIES CHEMISTRY AND TECHNOLOGY

6 (432)

**ҚАРАША – ЖЕЛТОҚСАН 2018 ж.
НОЯБРЬ – ДЕКАБРЬ 2018 г.
NOVEMBER – DECEMBER 2018**

1947 ЖЫЛДЫҢ ҚАҢТАР АЙЫНАН ШЫҒА БАСТАҒАН
ИЗДАЕТСЯ С ЯНВАРЯ 1947 ГОДА
PUBLISHED SINCE JANUARY 1947

ЖЫЛЫНА 6 РЕТ ШЫҒАДЫ
ВЫХОДИТ 6 РАЗ В ГОД
PUBLISHED 6 TIMES A YEAR

NAS RK is pleased to announce that News of NAS RK. Series of chemistry and technologies scientific journal has been accepted for indexing in the Emerging Sources Citation Index, a new edition of Web of Science. Content in this index is under consideration by Clarivate Analytics to be accepted in the Science Citation Index Expanded, the Social Sciences Citation Index, and the Arts & Humanities Citation Index. The quality and depth of content Web of Science offers to researchers, authors, publishers, and institutions sets it apart from other research databases. The inclusion of News of NAS RK. Series of chemistry and technologies in the Emerging Sources Citation Index demonstrates our dedication to providing the most relevant and influential content of chemical sciences to our community.

Қазақстан Республикасы Ұлттық ғылым академиясы "ҚР ҰҒА Хабарлары. Химия және технология сериясы" ғылыми журналының Web of Science-тің жаңаланған нұсқасы Emerging Sources Citation Index-те индекстелуге қабылданғанын хабарлайды. Бұл индекстелу барысында Clarivate Analytics компаниясы журналды одан әрі the Science Citation Index Expanded, the Social Sciences Citation Index және the Arts & Humanities Citation Index-ке қабылдау мәселесін қарастыруда. Web of Science зерттеушілер, авторлар, баспашылар мен мекемелерге контент тереңдігі мен сапасын ұсынады. ҚР ҰҒА Хабарлары. Химия және технология сериясы Emerging Sources Citation Index-ке енуі біздің қоғамдастық үшін ең өзекті және беделді химиялық ғылымдар бойынша контентке адалдығымызды білдіреді.

НАН РК сообщает, что научный журнал «Известия НАН РК. Серия химии и технологий» был принят для индексирования в Emerging Sources Citation Index, обновленной версии Web of Science. Содержание в этом индексировании находится в стадии рассмотрения компанией Clarivate Analytics для дальнейшего принятия журнала в the Science Citation Index Expanded, the Social Sciences Citation Index и the Arts & Humanities Citation Index. Web of Science предлагает качество и глубину контента для исследователей, авторов, издателей и учреждений. Включение Известия НАН РК в Emerging Sources Citation Index демонстрирует нашу приверженность к наиболее актуальному и влиятельному контенту по химическим наукам для нашего сообщества.

Б а с р е д а к т о р ы
х.ғ.д., проф., ҚР ҰҒА академигі **М.Ж. Жұрынов**

Р е д а к ц и я а л қ а с ы:

Ағабеков В.Е. проф., академик (Белорус)
Волков С.В. проф., академик (Украина)
Воротынцев М.А. проф., академик (Ресей)
Газалиев А.М. проф., академик (Қазақстан)
Ергожин Е.Е. проф., академик (Қазақстан)
Жармағамбетова А.К. проф. (Қазақстан), бас ред. орынбасары
Жоробекова Ш.Ж. проф., академик (Қырғыстан)
Иткулова Ш.С. проф. (Қазақстан)
Манташян А.А. проф., академик (Армения)
Пралиев К.Д. проф., академик (Қазақстан)
Баешов А.Б. проф., академик (Қазақстан)
Бүркітбаев М.М. проф., академик (Қазақстан)
Джусипбеков У.Ж. проф. корр.-мүшесі (Қазақстан)
Молдахметов М.З. проф., академик (Қазақстан)
Мансуров З.А. проф. (Қазақстан)
Наурызбаев М.К. проф. (Қазақстан)
Рудик В. проф., академик (Молдова)
Рахимов К.Д. проф. академик (Қазақстан)
Стрельцов Е. проф. (Белорус)
Тәшімов Л.Т. проф., академик (Қазақстан)
Тодераш И. проф., академик (Молдова)
Халиков Д.Х. проф., академик (Тәжікстан)
Фарзалиев В. проф., академик (Әзірбайжан)

«ҚР ҰҒА Хабарлары. Химия және технология сериясы».

ISSN 2518-1491 (Online),

ISSN 2224-5286 (Print)

Меншіктенуші: «Қазақстан Республикасының Ұлттық ғылым академиясы» Республикалық қоғамдық бірлестігі (Алматы қ.)

Қазақстан республикасының Мәдениет пен ақпарат министрлігінің Ақпарат және мұрағат комитетінде 30.04.2010 ж. берілген №1089-Ж мерзімдік басылым тіркеуіне қойылу туралы куәлік

Мерзімділігі: жылына 6 рет.

Тиражы: 300 дана.

Редакцияның мекенжайы: 050010, Алматы қ., Шевченко көш., 28, 219 бөл., 220, тел.: 272-13-19, 272-13-18,
www.nauka-nanrk.kz / chemistry-technology.kz

© Қазақстан Республикасының Ұлттық ғылым академиясы, 2018

Типографияның мекенжайы: «Аруна» ЖК, Алматы қ., Муратбаева көш., 75.

Главный редактор
д.х.н., проф., академик НАН РК **М. Ж. Журинов**

Редакционная коллегия:

Агабеков В.Е. проф., академик (Беларусь)
Волков С.В. проф., академик (Украина)
Воротынцев М.А. проф., академик (Россия)
Газалиев А.М. проф., академик (Казахстан)
Ергожин Е.Е. проф., академик (Казахстан)
Жармагамбетова А.К. проф. (Казахстан), зам. гл. ред.
Жоробекова Ш.Ж. проф., академик (Кыргызстан)
Иткулова Ш.С. проф. (Казахстан)
Манташян А.А. проф., академик (Армения)
Пралиев К.Д. проф., академик (Казахстан)
Баешов А.Б. проф., академик (Казахстан)
Буркитбаев М.М. проф., академик (Казахстан)
Джусипбеков У.Ж. проф. чл.-корр. (Казахстан)
Мулдахметов М.З. проф., академик (Казахстан)
Мансуров З.А. проф. (Казахстан)
Наурызбаев М.К. проф. (Казахстан)
Рудик В. проф., академик (Молдова)
Рахимов К.Д. проф. академик (Казахстан)
Стрельцов Е. проф. (Беларусь)
Ташимов Л.Т. проф., академик (Казахстан)
Тодераш И. проф., академик (Молдова)
Халиков Д.Х. проф., академик (Таджикистан)
Фарзалиев В. проф., академик (Азербайджан)

«Известия НАН РК. Серия химии и технологии».

ISSN 2518-1491 (Online),

ISSN 2224-5286 (Print)

Собственник: Республиканское общественное объединение «Национальная академия наук Республики Казахстан» (г. Алматы)

Свидетельство о постановке на учет периодического печатного издания в Комитете информации и архивов Министерства культуры и информации Республики Казахстан №10893-Ж, выданное 30.04.2010 г.

Периодичность: 6 раз в год

Тираж: 300 экземпляров

Адрес редакции: 050010, г. Алматы, ул. Шевченко, 28, ком. 219, 220, тел. 272-13-19, 272-13-18,
<http://nauka-nanrk.kz / chemistry-technology.kz>

© Национальная академия наук Республики Казахстан, 2018

Адрес редакции: 050100, г. Алматы, ул. Кунаева, 142,
Институт органического катализа и электрохимии им. Д. В. Сокольского,
каб. 310, тел. 291-62-80, факс 291-57-22, e-mail: orgcat@nursat.kz

Адрес типографии: ИП «Аруна», г. Алматы, ул. Муратбаева, 75

E d i t o r i n c h i e f

doctor of chemistry, professor, academician of NAS RK **M.Zh. Zhurinov**

E d i t o r i a l b o a r d :

Agabekov V.Ye. prof., academician (Belarus)
Volkov S.V. prof., academician (Ukraine)
Vorotyntsev M.A. prof., academician (Russia)
Gazaliyev A.M. prof., academician (Kazakhstan)
Yergozhin Ye.Ye. prof., academician (Kazakhstan)
Zharmagambetova A.K. prof. (Kazakhstan), deputy editor in chief
Zhorobekova Sh.Zh. prof., academician (Kyrgyzstan)
Itkulova Sh.S. prof. (Kazakhstan)
Mantashyan A.A. prof., academician (Armenia)
Praliyev K.D. prof., academician (Kazakhstan)
Bayeshov A.B. prof., academician (Kazakhstan)
Burkitbayev M.M. prof., academician (Kazakhstan)
Dzhusipbekov U.Zh. prof., corr. member (Kazakhstan)
Muldakhmetov M.Z. prof., academician (Kazakhstan)
Mansurov Z.A. prof. (Kazakhstan)
Nauryzbayev M.K. prof. (Kazakhstan)
Rudik V. prof., academician (Moldova)
Rakhimov K.D. prof., academician (Kazakhstan)
Streltsov Ye. prof. (Belarus)
Tashimov L.T. prof., academician (Kazakhstan)
Toderash I. prof., academician (Moldova)
Khalikov D.Kh. prof., academician (Tadjikistan)
Farzaliyev V. prof., academician (Azerbaijan)

News of the National Academy of Sciences of the Republic of Kazakhstan. Series of chemistry and technology.
ISSN 2518-1491 (Online),
ISSN 2224-5286 (Print)

Owner: RPA "National Academy of Sciences of the Republic of Kazakhstan" (Almaty)

The certificate of registration of a periodic printed publication in the Committee of Information and Archives of the Ministry of Culture and Information of the Republic of Kazakhstan N 10893-Ж, issued 30.04.2010

Periodicity: 6 times a year

Circulation: 300 copies

Editorial address: 28, Shevchenko str., of. 219, 220, Almaty, 050010, tel. 272-13-19, 272-13-18,
<http://nauka-nanrk.kz/chemistry-technology.kz>

© National Academy of Sciences of the Republic of Kazakhstan, 2018

Editorial address: Institute of Organic Catalysis and Electrochemistry named after D. V. Sokolsky
142, Kunayev str., of. 310, Almaty, 050100, tel. 291-62-80, fax 291-57-22,
e-mail: orgcat@nursat.kz

Address of printing house: ST "Aruna", 75, Muratbayev str, Almaty

NEWS

OF THE NATIONAL ACADEMY OF SCIENCES OF THE REPUBLIC OF KAZAKHSTAN

SERIES CHEMISTRY AND TECHNOLOGY

ISSN 2224-5286

<https://doi.org/10.32014/2018.2518-1491.20>

Volume 6, Number 432 (2018), 6 – 15

UDC 542.943; 547.211; 661.961; 661.993

**S.A. Tungatarova^{1,2}, G. Xanthopoulou³, G.N. Kaumenova^{1,2}, M. Zhumabek¹,
T.S. Baizhumanova¹, V.P. Grigorieva¹, L.V. Komashko¹, G.U. Begimova^{1,2}**

¹JSC “D.V. Sokolsky Institute of Fuel, Catalysis and Electrochemistry”, Almaty, Kazakhstan;

²Al-Farabi Kazakh National University, Almaty, Kazakhstan;

³Institute of Nanoscience and Nanotechnology, NCSR Demokritos, Athens, Greece

tungatarova58@mail.ru

DEVELOPMENT OF COMPOSITE MATERIALS BY COMBUSTION SYNTHESIS METHOD FOR CATALYTIC REFORMING OF METHANE TO SYNTHESIS GAS

Abstract. In the modern world, natural gas is the main source for obtaining synthesis-gas from methane. Production of synthesis-gas is constantly improved, as the demand for this raw material in the petrochemical industry is growing every year. Also, synthesis gas is used as an environmentally friendly source of heat and energy. Therefore, finding ways to activate CH₄ for synthesis of products is an important task of petrochemical industry. La – Mg – Mn – Ni - Al catalysts were prepared by the self-propagating high-temperature synthesis method, namely its modern modification - the solution combustion synthesis. The optimum content of metals in the catalyst was determined by varying the ratio of elements in samples. The conditions for conversion of methane to synthesis-gas were determined. It was found that the highest results on oxidative conversion to synthesis-gas can be obtained at 900°C and a space velocity of 2500 h⁻¹ over 5% La + 10% Mg + 5% Mn + 20% Ni + 10% Al + 50% glycine catalyst. The catalysts were examined by a complex of physical and chemical methods, as a result of which it was established that a number of changes occur in the catalyst structure during the testing in a flowing catalytic installation. It has been shown that simple and mixed oxides, metal aluminates and spinel-type structures, the presence of which promotes the active work of catalysts for the oxidative conversion of methane, are present in the catalyst. In addition, elastic carbon nanotubes wrapped in a spiral with diameters of 40 - 50 - 70 nm were detected on the surface.

Key words: methane, hydrogen, synthesis gas, self-propagating high-temperature synthesis, solution combustion.

Introduction

Continuous increase in fuel consumption in the energy sector, in various branches of the chemical, petrochemical industry and transport leads to an increase in the volume of harmful substances entering the atmosphere. This is becoming more urgent due to the toughening of the requirements to the quality of the produced base and raw intermediate products of the petrochemical industry [1-4]. Therefore, studies aimed at developing of various catalysts for the complex treatment of gas emissions of industry, as well as catalysts that work effectively in the field of synthesis-gas production under more favorable conditions, are strategically important [5-9].

It is known that the activity of multicomponent catalysts is a complex function of the chemical composition and parameters of the micro- and macrostructure. Nature of the active centers, dispersion of the active components, morphology of the surface, presence of microstrains and defects in the structure are determined by the conditions of synthesis and subsequent heat treatment of the samples. Therefore, an intensive search of new methods for the preparation of catalysts for production of synthesis-gas has been carried out recently [10-14].

Solution combustion synthesis (SCS), self-propagating high-temperature synthesis (SHS) and other methods of preparation, in which the energy of exothermic reactions is used to prepare the active

components of catalysts, relate to such promising methods [15-19]. The main advantages of these methods are: low energy costs, short synthesis times, no need for expensive equipment, the possibility of a one-stage conversion of inorganic materials to final products using chemical reaction energy, an increase in non-stoichiometric phases of products due to high thermal gradient and rapid cooling rate [20-22].

Experimental

Catalyst preparation

Nitric acid salts of various metals, in particular: lanthanum (III) nitrate, manganese (II) nitrate, magnesium nitrate, nickel nitrate, aluminum nitrate, and glycine were used to synthesize the desired catalysts. Preliminary calcination and treatment of salts were not performed. All used salts were weighed and thoroughly mixed in an agate mortar. Then the mixture of salts was placed in a quartz glass, into which 10 ml of distilled water, preheated to 80°C, was poured. The glass with the solution was transferred to the muffle furnace, preheated to 500°C, after complete dissolution of all salts. After 5-8 minutes, enough heat is generated to ensure the propagation of the combustion front, advancing with high speed and self-generation of heat. This leads to a sharp increase in temperature. The temperature inside the reaction front is so high that impurities with a low boiling point is evaporated, facilitating the production of more pure products. As a result, structures with a high concentration of defects of intermediate and non-stoichiometric compounds, which are one of the reasons for the high activity of SCS catalysts, are formed. After cooling, the catalysts were placed in a glass weighing bottles for storage.

Characterization techniques

Studies of the developed catalysts were carried out by various methods: elemental analysis, X-ray phase analysis (XRD), transmission electron microscopy on an EM-125K device. These analyzes were performed both before and after the tests of the synthesized catalysts in reactor of the flowing catalytic unit (FCU-1). Composition of the initial reaction mixture and reaction products was studied on the "Chromos GC-1000" chromatograph with "Chromos" computer software. XRD analysis was carried out on a DRON-4-0.7 diffractometer with CoK α radiation in the range of angles $2\theta = 6 - 100^\circ$. Conditions for conducting of the XRD analysis: initial angle = 6.00; end angle = 100.00; step = 0.020; exposure dose = 0.6; speed = 2 g/min; the maximum number of pulses is 821. Samples were studied by the method of shooting to lumen in the form of dry suspensions using microdiffraction on the EM-125K transmission electron microscope.

Catalytic reaction

A series of samples with various components in the La – Mg – Mn – Ni - Al catalyst was prepared by solution combustion synthesis method. The activity of the developed catalysts in the reaction of oxidative conversion of methane by oxygen was determined in a flowing catalytic unit FCU-1 at atmospheric pressure in a quartz reactor at the temperature range from 600 to 900°C. For the studies, a mixture of gases CH₄ : O₂ : Ar = 2 : 1 : 2.8, CH₄ : O₂ : Ar = 34 % : 17 % : 49 % was used.

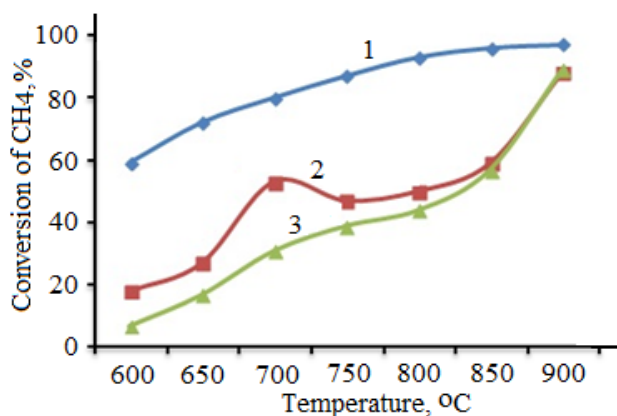
Results and discussion

The following optimal conditions: a space velocity (GHSV) 2500 h⁻¹ in the 600 - 900°C temperature range were selected to determine the activity of La – Mg – Mn – Ni - Al catalysts after careful study of the literature data. In the process of repeatability tests, it was established that the maximum yield of methane to synthesis-gas is reached at 900°C. Table 1 shows the results of CO and H₂ yields for each catalyst with a specific set of metals. It is seen from the Table 1 that 5 % La + 10 % Mg + 5 % Mn + 20 % Ni + 10 % Al + 50 % glycine catalyst is the most active with CO and H₂ yield up to 21 % and 65 %, respectively.

Table 1 - Catalysts prepared by SCS method for the oxidation of methane to synthesis gas

No	Chemical composition of catalysts, % wt.	Yield, %	
		CO	H ₂
1	5 % La + 20 % Mg + 10 % Mn + 5 % Ni + 10 % Al + 50 % glycine	3	7
2	5 % La + 10 % Mg + 20 % Mn + 5 % Ni + 10 % Al + 50 % glycine	11	44
3	5 % La + 10 % Mg + 5 % Mn + 20 % Ni + 10 % Al + 50 % glycine	21	65
4	5 % La + 10 % Mg + 10 % Mn + 5 % Ni + 20 % Al + 50 % glycine	10	42

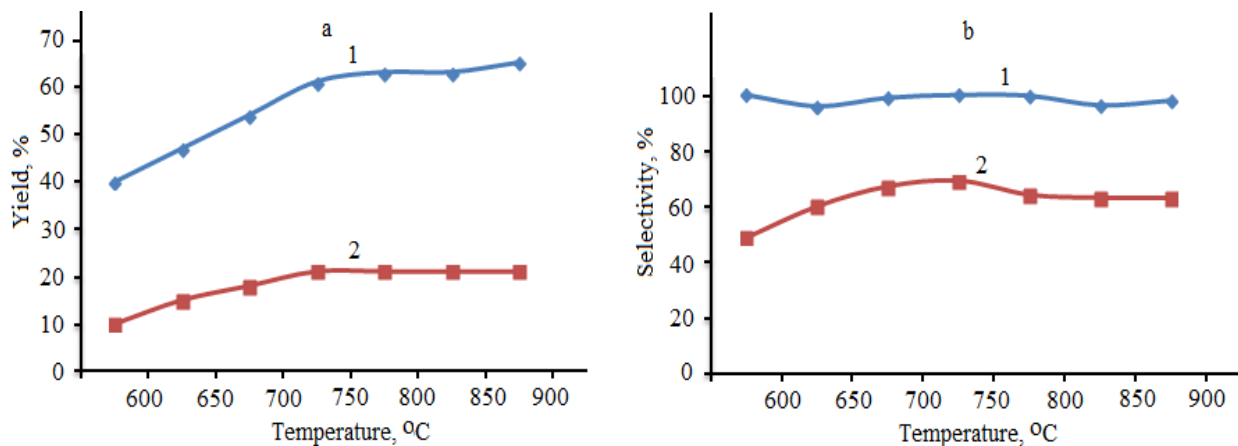
Effect of the variation of space velocity on the process indicators was investigated on the most active 5 % La + 10 % Mg + 5 % Mn + 20 % Ni + 10 % Al + 50 % glycine catalyst. The results of the experiments are shown in Figure 1. As can be seen from Figure 1, the increase in space velocity does not promote the growth of conversion of methane to synthesis gas. This may be due to the fact that the gas does not have time to come into contact with catalyst to convert organic molecule to the target products in the process of increasing the space velocity.



GHSV, h⁻¹: 1 – 2500, 2 – 4500, 3 – 6500.

Figure 1 - Conversion of methane over the 5 % La + 10 % Mg + 5 % Mn + 20 % Ni + 10 % Al + 50 % glycine catalyst at different space velocities

The following graphs in Figure 2 show that the highest yields of H₂ (65 %), CO (21 %) with selectivity for H₂ (98 %) and CO (63 %) are achieved at a space velocity of 2500 h⁻¹. Optimal yields and selectivities were recorded in the temperature range 800 - 900°C and pressure 0.39 MPa.



a – yield: 1 – H₂, 2 – CO; b – selectivity: 1 – H₂, 2 – CO.

Figure 2 - Effect of the reaction temperature on the yield and selectivity of process over 5 % La + 10 % Mg + 5 % Mn + 20 % Ni + 10 % Al + 50 % glycine catalyst

Figure 3 shows the XRD spectra of 5 % La + 10 % Mg + 5 % Mn + 20 % Ni + 10 % Al + 50 % glycine catalyst. As a result of the obtained data, it was shown that the following phases are present in the catalysts: Ni (reflexes, Å: 2,03₃₅; 1,89₅₂; 1,76₁₂; 1,26₉₄; 1,24₅₃ – ASTM, 4-850); MgO periclase (reflexes, Å: 2,51₅₄; 2,41₈₂; 1,48₅₂; 1,36₂₆; 1,33₀₄; 1,21₅₉ - ASTM, 4-829); La₂NiO₄ (reflexes, Å: 3,78₇₅; 3,12₄₀; 2,90₁₅; 2,72₆₆; 2,18₇₁; 2,09₆₇; 1,68₇₇; 1,65₂₀ – ASTM, 34-314); and Mn₃O₄ (low-intensity reflexes, Å: 5,04₁₁; 2,53₈₄; 3,33₀₃ – ASTM, 4-732).

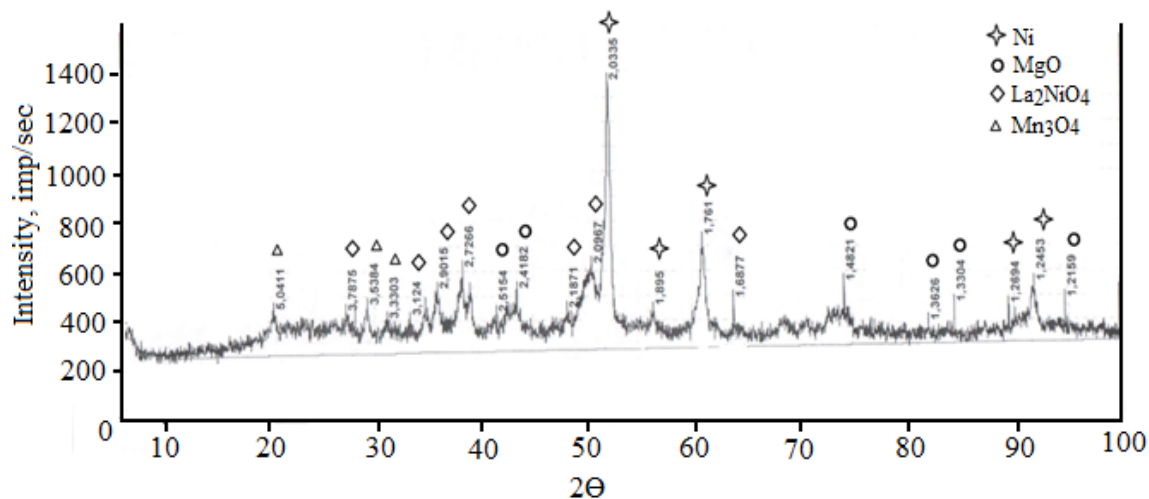


Figure 3 - XRD spectrum of the 5 % La + 10 % Mg + 5 % Mn + 20 % Ni + 10 % Al + 50 % glycine catalyst

In the course of the study, the transmission electron microscope showed the results for the 5 % La + 10 % Mg + 5 % Mn + 20 % Ni + 10 % Al + 50 % glycine catalyst before and after investigations on flow catalytic unit FCU-1. Figure 4a shows the accumulation of large particles isothermal shape with a size of 100 - 500 nm. The microdiffraction pattern is represented by a small set of reflexes, which can be attributed to MgNiO_2 (JSPDS, 24-712). Figure 4b shows an aggregate of large semitransparent particles with a size of 70 - 100 nm or more. However, small amorphous particles with a size of 10 - 15 nm are visible inside these particles on translucent edges. The microdiffraction pattern is represented by a small set of reflexes arranged in rings, which can be attributed equally to $\text{Al}_9\text{N}_7\text{O}_3$ (JSPDS, 35-830) or possibly to $\text{LaAl}_{11}\text{O}_{18}$ (JSPDS, 33-699).

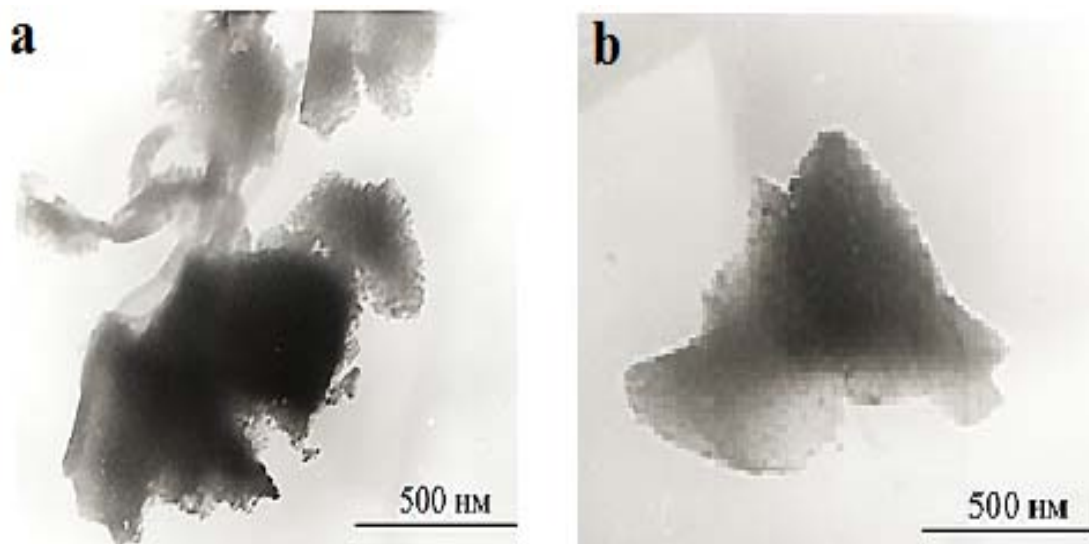


Figure 4 - TEM images of the 5 % La + 10 % Mg + 5 % Mn + 20 % Ni + 10 % Al + 50 % glycine catalyst before the tests

Properties of catalysts after testing on the FCU-1 installation were studied repeatedly. The presence of carbon nanotubes was detected during the transmission electron microscope analysis. Nanotubes are elastic, often wrapped in a spiral, whose diameters reach 40 - 50 - 70 nm, Figure 5.

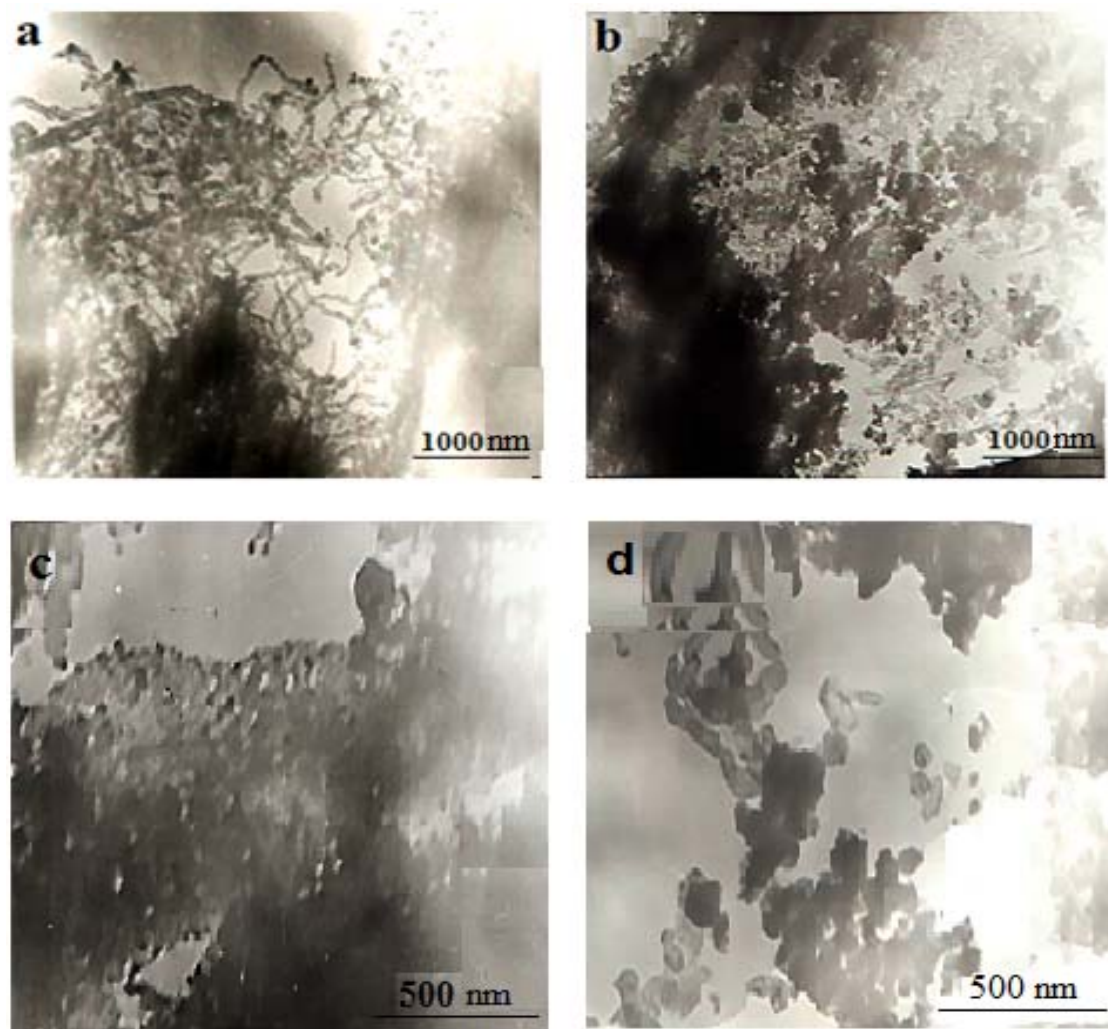


Figure 5 – TEM images of the 5 % La + 10 % Mg + 5 % Mn + 20 % Ni + 10 % Al + 50 % glycine catalyst after tests

Figures 5a and 5b, presented at low magnification, show the accumulation of carbon nanotubes and dense round-shaped particles with a size of 50 - 70 - 100 nm. The microdiffraction pattern is represented by a large set of rings and reflexes corresponding to δ - MgAl_2O_4 (JSPDS, 20-660), it is possible presence of the La_2O_3 (JSPDS, 24-554) and LaN (JSPDS, 15-892) in mixture. Figure 5b shows a small aggregate of dense particles 60 - 100 nm in size (there are nanotubes), which can be attributed to $\text{LaAl}_{11}\text{O}_{18}$ (JSPDS, 33-699).

Figures 5c and 5d show aggregates of various shapes and densities with particle sizes from 10 - 20 to 50 - 100 nm. The diffraction pattern is represented by a large set of rings and reflexes and can be attributed to phase mixtures of Mg_2NiH_4 (JSPDS, 36-916), NiLa_2O_4 (JSPDS, 11-557), HNi_2 (JSPDS, 33-606), Mg_2C_3 (JSPDS, 1-1138), Al_2O_3 (JSPDS, 33-699), $\text{La}_2\text{MnAl}_{11}\text{O}_{19}$ (JSPDS, 36-1317) and MgO (periclase) (4-829).

5 % La + 10 % Mg + 5 % Mn + 20 % Ni + 10 % Al + 50 % glycine catalyst was investigated on a scanning electron microscope; the elemental composition of sample was established during the analysis. Figure 6 illustrates the results of these analyzes.

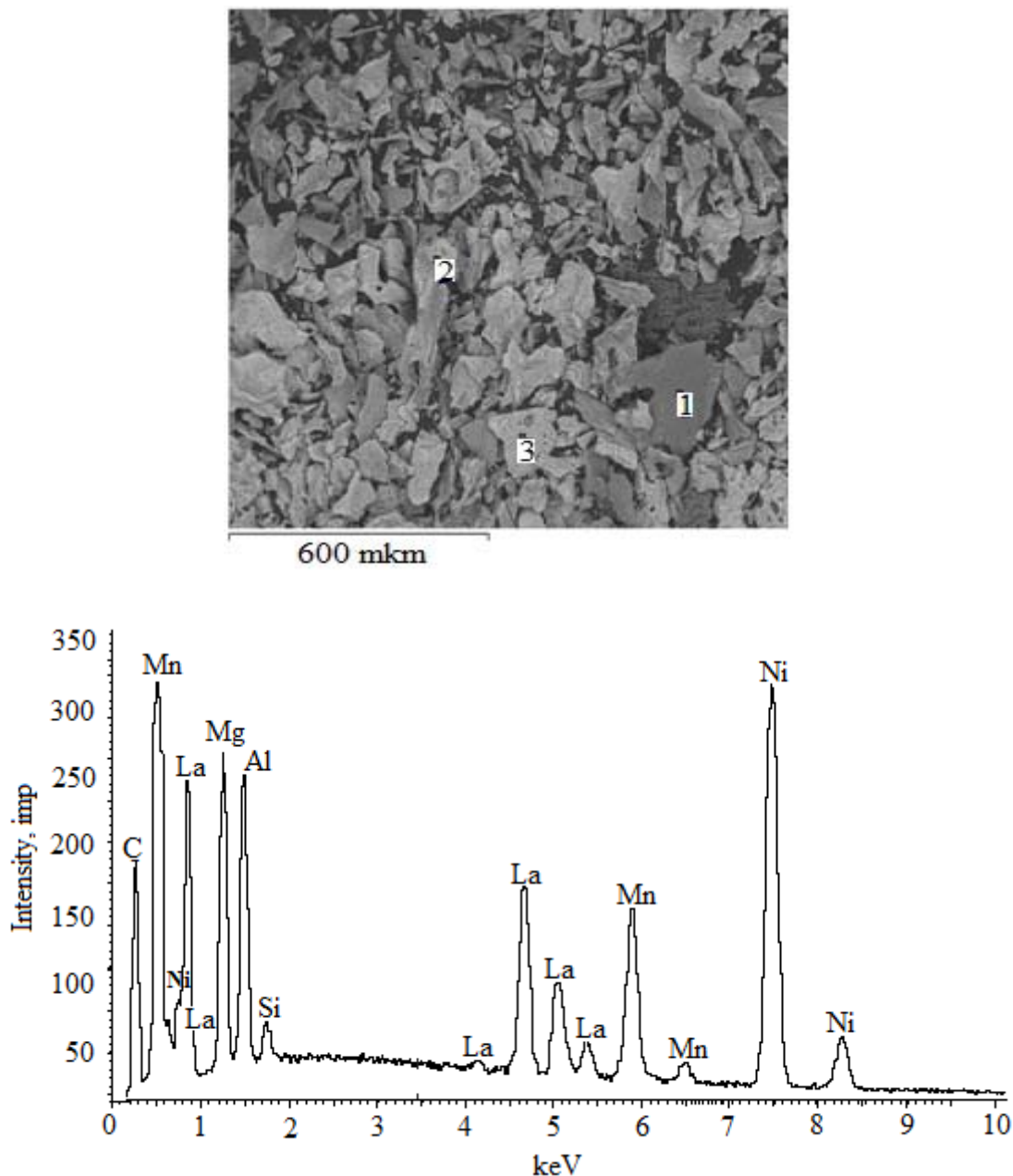


Figure 6 - SEM images of the 5 % La + 10 % Mg + 5 % Mn + 20 % Ni + 10 % Al + 50 % glycine catalyst before the tests

The results of elemental analysis for catalyst at the points indicated in the images correspond to the experimental data. It was shown that the surface of catalyst is not homogeneous.

Figure 7 shows the results of the sample analysis on a scanning electron microscope after the tests. According to elemental analysis, only a decrease in oxygen was detected, as well as a lack of nitrogen in the sample. This is connected, apparently, with the fact that their volatilization from the catalyst occurs at high temperatures. The percentage of nickel and lanthanum increased, which indicates the compaction of these components in the mass of catalyst.

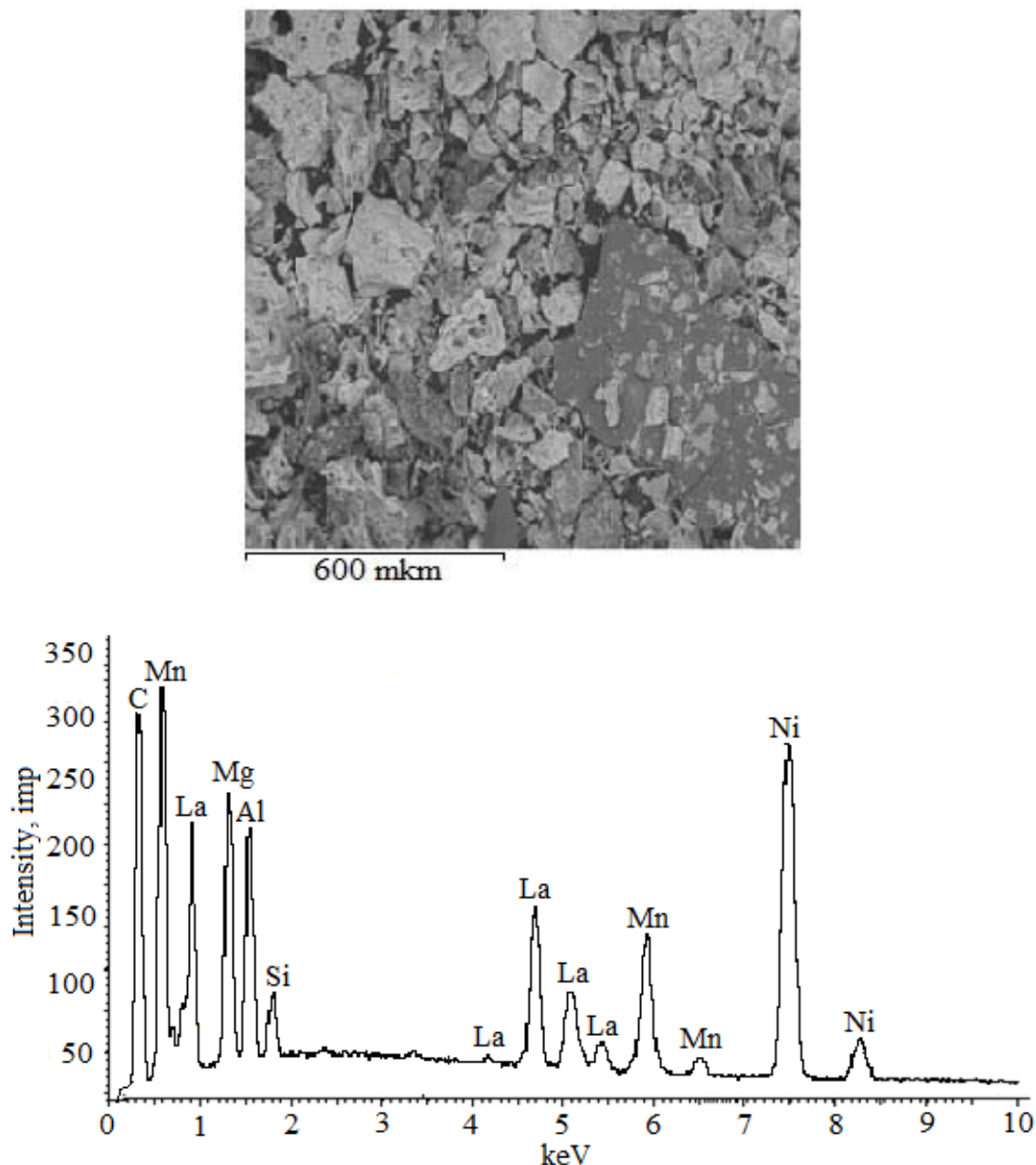


Figure 7 - SEM images of the 5 % La + 10 % Mg + 5 % Mn + 20 % Ni + 10 % Al + 50 % glycine catalyst after the tests

Conclusion

Based on the results of the tests, the following conclusions can be drawn:

- 5 % La + 10 % Mg + 5 % Mn + 20 % Ni + 10 % Al catalyst was the most active for conversion of methane to synthesis gas from numerous combinations of catalysts with the following set of La – Mg – Mn – Ni - Al components prepared by solution combustion synthesis;
- space velocity of 2500 h^{-1} at temperature of 900°C are optimal conditions for the active operation of this catalyst;
- the presence of simple and mixed oxides, metal aluminates and spinel-type structures in the catalyst, the presence of which promotes their active work in the process of oxidative conversion of methane, was established by TEM and SEM research. The presence of carbon nanotubes was also established. Nanotubes are elastic, often wrapped in a spiral with diameters of 40 - 50 - 70 nm.

Acknowledgments

The work was supported by the Ministry of Education and Science of the Republic of Kazakhstan (Grant No AP05132348).

REFERENCES

- [1] Hiblot H, Ziegler-Devin I, Fournet R, Glaude PA (2016) Steam reforming of methane in a synthesis gas from biomass gasification, *Int J Hydrogen Energ*, 41:18329-18338. <http://dx.doi.org/10.1016/j.ijhydene.2016.07.226> (in Eng).
- [2] Angeli SD, Turchetti L, Monteleone G, Lemonidou AA (2016) Catalyst development for steam reforming of methane and model biogas at low temperature, *Appl Catal B: Environ*, 181:34-46. <https://doi.org/10.1016/j.apcatb.2015.07.039> (in Eng).
- [3] Kho ET, Scott J, Amal R (2016) Ni/TiO₂ for low temperature steam reforming of methane, *Chem Eng Sci*, 140:161-170. <https://doi.org/10.1016/j.ces.2015.10.021> (in Eng).
- [4] Dedov AG, Loktev AS, Komissarenko DA, Parkhomenko KV, Roger A-C, Shlyakhtin OA, Mazo GN, Moiseev II (2016) High-selectivity partial oxidation of methane into synthesis gas: the role of the red-ox transformations of rare earth-alkali earth cobaltate-based catalyst components, *Fuel Process Technol*, 148:128-137. <https://doi.org/10.1016/j.fuproc.2016.02.018> (in Eng).
- [5] Palcheva R, Olsbye U, Palcut M, Rauwel P, Tyuliev G, Velinov N, Fjellvag HH (2015) Rh promoted La_{0.75}Sr_{0.25}(Fe_{0.8}Co_{0.2})_{1-x}Ga_xO₃-perovskite catalysts: Characterization and catalytic performance for methane partial oxidation to synthesis gas, *Appl Surf Sci*, 357:45-54. <http://dx.doi.org/10.1016/j.apsusc.2015.08.237> (in Eng).
- [6] Rogatis LD, Mortini T, Cognigni A, Olivi L, Fornasiero P (2009) Methane partial oxidation on NiCu-based catalysts, *Catal Today*, 145:176-185. <https://doi.org/10.1016/j.cattod.2008.04.019> (in Eng).
- [7] Makarshin LL, Sadykov VA, Andreev DV, Gribovskii AG, Privezentsev VV, Parmon VN (2015) Syngas production by partial oxidation of methane in a microchannel reactor over a Ni-Pt/La_{0.2}Zr_{0.4}Ce_{0.4}O_x catalyst, *Fuel Process Technol*, 131:21-28. <https://doi.org/10.1016/j.fuproc.2014.10.031> (in Eng).
- [8] Dedov AG, Loktev AS, Komissarenko DA, Mazo GN, Shlyakhtin OA, Parkhomenko KV, Kiennemann AA, Roger AC, Ishmurzin AV, Moiseev II (2015) Partial oxidation of methane to produce syngas over a neodymium-calcium cobaltate-based catalyst, *Appl Catal A*, 489:140-146. <https://doi.org/10.1016/j.apcata.2014.10.027> (in Eng).
- [9] Peymani M, Alavi SM, Rezaei M (2016) Preparation of highly active and stable nanostructured Ni/CeO₂ catalysts for syngas production by partial oxidation of methane, *Int J Hydrogen Energ*, 41:6316-6325. <https://doi.org/10.1016/j.ijhydene.2016.03.033> (in Eng).
- [10] Vella LD, Specchia S (2011) Alumina-supported nickel catalysts for catalytic partial oxidation of methane in short-contact time reactors, *Catal Today*, 176:340-346. doi:10.1016/j.cattod.2010.11.068 (in Eng).
- [11] Kim HW, Kang KM, Kwak H-Y (2009) Preparation of supported Ni catalysts with a core/shell structure and their catalytic tests of partial oxidation of methane, *Int J Hydrogen Energ*, 34:3351-3359. doi:10.1016/j.ijhydene.2009.02.036 (in Eng).
- [12] Zhang J, Jin L, Li Y, Hu H (2013) Ni doped carbons for hydrogen production by catalytic methane decomposition. *Int. J. Hydrogen Energy*. 38:3937-3947. <https://doi.org/10.1016/j.ijhydene.2013.01.105> (in Eng).
- [13] González-Cortés SL, Imbert FE (2013) Fundamentals, properties and applications of solid catalysts prepared by solution combustion synthesis (SCS), *Appl Catal A*, 452:117-131. <http://dx.doi.org/10.1016/j.apcata.2012.11.024> (in Eng).
- [14] Kirillov VA, Fedorova ZA, Danilova MM, Zaikovskii VI, Kuzin NA, Kuzmin VA, Krieger TA, Mescheryakov VD (2011) Porous nickel based catalysts for partial oxidation of methane to synthesis gas, *Appl Catal A*, 401:170-175. <https://doi.org/10.1016/j.apcata.2011.05.018> (in Eng).
- [15] Kaddeche D, Djaidja A, Barama A (2017) Partial oxidation of methane on co-precipitated Ni-Mg/Al catalysts modified with copper or iron, *Int J Hydrogen Energ*, 42:15002-15009. <https://doi.org/10.1016/j.ijhydene.2017.04.281> (in Eng).
- [16] Khan NA, Kennedy EM, Dlugogorski BZ, Adesina AA, Stockenhuber M (2014) Partial oxidation of methane with nitrous oxide forms synthesis gas over cobalt exchanged ZSM-5, *Catal Commun*, 53:42-46. <https://doi.org/10.1016/j.catcom.2014.04.012> (in Eng).
- [17] Larimi AS, Alavi SM (2012) Ceria-Zirconia supported Ni catalysts for partial oxidation of methane to synthesis gas, *Fuel*, 102:366-371. <https://doi.org/10.1016/j.fuel.2012.06.050> (in Eng).
- [18] Tungatarova SA, Dossunov K, Baizhumanova TS, Popova NM (2010) Nanostructured supported Pt-, Ru- and Pt-Ru catalysts for oxidation of methane into synthesis-gas, *J Alloys Compd*, 504: 349-352. doi:10.1016/j.jallcom.2010.04.223 (in Eng).
- [19] Lim M-W, Yong S-T, Chai S-P (2014) Combustion-synthesized Nickel-based catalysts for the production of hydrogen from steam reforming of methane, *Energy Procedia*, 61:910-913. <https://doi.org/10.1016/j.egypro.2014.11.993> (in Eng).
- [20] Kostenko SS, Ivanova AN, Karnaukh AA, Polianczyk EV (2017) Conversion of methane to synthesis gas in a non-premixed reversed-flow porous bed reactor: A kinetic modeling, *Chem Eng Process*, 122:473-486. <https://doi.org/10.1016/j.cep.2017.05.014> (in Eng).
- [21] Pruksawan S, Kitiyanan B, Ziff RM (2016) Partial oxidation of methane on a nickel catalyst: Kinetic Monte-Carlo simulation study, *Chem Eng Sci*, 147:128-136. <https://doi.org/10.1016/j.ces.2016.03.012> (in Eng).
- [22] Velasco JA, Fernandez C, Lopez L, Cabrera S, Boutonnet M, Jaras S (2015) Catalytic partial oxidation of methane over nickel and ruthenium based catalysts under low O₂/CH₄ ratios and with addition of steam, *Fuel*, 153:192-201. <https://doi.org/10.1016/j.fuel.2015.03.009> (in Eng).

ӨОК 542.943; 547.211; 661.961; 661.993

С.А. Тунгатарова^{1,2}, Г. Ксандопуло³, Г.Н. Кауменова^{1,2},
М. Жумабек¹, Т.С. Байжуманова¹, В.П. Григорьева¹, Л.В. Комашко¹ Г.У. Бегимова^{1,2}

¹Д.В. Сокольский атындағы «Жанармай, катализ және электрохимия институты» АҚ, Алматы, Қазақстан;

²Әл-Фараби атындағы Қазақ ұлттық университеті, Алматы, Қазақстан;

³Нанотехнология және наноғылым институты, «Демокрит» ҰҒЗО, Афины, Греция

МЕТАНДЫ СИНТЕЗ ГАЗҒА КАТАЛИТИКАЛЫҚ РИФОРМИНГЛЕУДЕ ЖАНУ ӘДІСІМЕН КОМПОЗИТТИ МАТЕРИАЛДАРДЫ ЖАСАУ

Аннотация. Қазіргі заманда метаннан синтез-газ алудың негізгі көзі табиғи газ болып табылады. Мұнай-химия өнеркәсібінде синтез-газды өндіру үнемі осы шикізатқа деген қажеттіліктің жыл сайын артуына әкелуде. Сонымен қатар, синтез-газ экологиялық таза жылу және энергия көзі ретінде пайдаланылады. Сондықтан мұнай-химия өнеркәсібінде органикалық синтездің жартылай өнімдерін алу мақсатына бағытталған және метанды белсендіру жолдарын табу маңызды міндет болып табылады. Осыған байланысты жоғарытемпературада өздігінен жану синтезі әдісі, әсіресе оның заманауи түрлендірілген ерітіндіде жану үрдісі бойынша La – Mg – Mn – Ni – Al катализаторлары дайындалды. Зерттеу метанның конверсиясының синтез-газға айналуының оңтайлы жағдайлары және элементтердің қатынасын түрлендіру нәтижесінде катализатордың құрамындағы металдардың мөлшері анықталды. Метанның синтез-газға тотыға айналу барысында 5% La + 10% Mg + 5% Mn + 20% Ni + 10% Al + 50% глицин катализаторында температура 900°C болғанда және 2500 сағ⁻¹ көлемдік жылдамдықта анағұрлым жоғары нәтижелерді алуға болатыны анықталды. Катализаторларды ағымды каталитикалық кондырғада зерттегеннен соң, физика-химиялық әдістерімен зерттеу барысында катализаторлардың құрылымы өзгеріске ұшырайтыны кешенді анықталды. Зерттеу барысында катализаторлардың құрамында металл алюминаттары мен құрылымы шпинель түріндегі жәй және аралас оксидтерінің бар болуы анықталынып, олардың метанның тотыға айналуына белсенді әсер ететіндігі көрсетілген. Сонымен қатар, беткі қабатында диаметрі 40 - 50 - 70 нм-болатын спиральға жиі оралған иілімді көміртекті нанотүтікшелердің түзілгені анықталды.

Түйін сөздер: метан, сутек, синтез-газ, жоғарытемпературада өздігінен жану синтезі, ерітіндіде жану.

УДК 542.943; 547.211; 661.961; 661.993

С.А. Тунгатарова^{1,2}, Г. Ксандопуло³, Г.Н. Кауменова^{1,2}, М. Жумабек¹,
Т.С. Байжуманова¹, В.П. Григорьева¹, Л.В. Комашко¹ Г.У. Бегимова^{1,2}

¹АО «Институт топлива, катализа и электрохимии им. Д.В. Сокольского», Алматы, Казахстан;

²Казахский национальный университет им. аль-Фараби, Алматы, Казахстан;

³Институт нанонауки и нанотехнологий, ИЦНИ Демокрит, Афины, Греция

РАЗРАБОТКА КОМПОЗИТНЫХ МАТЕРИАЛОВ МЕТОДОМ ГОРЕНИЯ ДЛЯ КАТАЛИТИЧЕСКОГО РИФОРМИНГА МЕТАНА В СИНТЕЗ-ГАЗ

Аннотация. В современном мире природный газ является основным источником получения синтез-газа из метана. Производство синтез-газа постоянно совершенствуется, так как спрос на это сырье в нефтехимической промышленности растет с каждым годом. Кроме того, синтез-газ используется в качестве экологически чистого источника тепла и энергии. Поэтому поиск путей активации CH₄ для синтеза продуктов является важной задачей нефтехимической промышленности. Методом самораспространяющегося высокотемпературного синтеза, а именно современной его модификацией - процессом горения в растворе были приготовлены La – Mg – Mn – Ni - Al катализаторы. В результате варьирования соотношения элементов в образцах было установлено оптимальное содержание металлов в катализаторе и определены условия конверсии метана в синтез-газ. Найдено, что при 900°C и объемной скорости 2500 ч⁻¹ на катализаторе 5% La + 10% Mg + 5% Mn + 20% Ni + 10% Al + 50% глицин возможно получение наиболее высоких результатов по окислительному превращению в синтез-газ. Катализаторы были исследованы комплексом физико-химических методов, в результате чего установлено, что в процессе проведения

испытаний на проточной каталитической установке в структуре катализатора происходит ряд изменений. Показано, что в катализаторе присутствуют простые и смешанные оксиды, алюминаты металлов и структуры шпинельного типа, присутствие которых способствует активной работе катализаторов окислительного превращения метана. Кроме того, на поверхности обнаружены эластичные, часто завернутые в спирали с диаметрами 40 - 50 - 70 нм углеродные нанотрубки.

Ключевые слова: метан, водород, синтез-газ, самораспространяющийся высокотемпературный синтез, горение в растворе.

Information about authors:

S.A. Tungatarova – Chief Researcher, Doctor of Chemical Sciences, Laboratory of Organic Catalysis, JSC “D.V. Sokolsky Institute of Fuel, Catalysis and Electrochemistry”, Al-Farabi Kazakh National University, Almaty, Kazakhstan. Tel: +77272916632. tungatarova58@mail.ru. **ORCID** 0000-0001-6005-747X

G. Xanthopoulou - Professor, PhD, DSc, Laboratory of Modern Ceramics, Institute of Nanoscience and Nanotechnology, NCSR “Demokritos”, Athens, Greece. g.xanthopoulou@inn.demokritos.gr. **ORCID** 0000-0002-1788-141X

G.N. Kaumenova - PhD Doctoral Student, Al-Farabi Kazakh National University, Laboratory of Organic Catalysis, JSC “D.V. Sokolsky Institute of Fuel, Catalysis and Electrochemistry”, Almaty, Kazakhstan. Tel: +77272916632. kaumenova.gulnar@mail.ru. **ORCID** 0000-0002-6448-6607

M. Zhumabek - Junior Researcher, Laboratory of Organic Catalysis, JSC “D.V. Sokolsky Institute of Fuel, Catalysis and Electrochemistry”, Almaty, Kazakhstan. Tel: +77272916632, manapkhan_86@mail.ru. **ORCID** 0000-0002-2026-0577

T.S. Baizhumanova - Leading Researcher, Candidate of Chemical Sciences, Laboratory of Organic Catalysis, JSC “D.V. Sokolsky Institute of Fuel, Catalysis and Electrochemistry”, Almaty, Kazakhstan. Tel: +77272916632. baizhuma@mail.ru. **ORCID** 0000-0001-9851-2642

V.P. Grigorieva - Scientific Researcher, Laboratory of Physical Methods of Research, JSC “D.V. Sokolsky Institute of Fuel, Catalysis and Electrochemistry”, Almaty, Kazakhstan. Tel: +77272916632. ifce@ifce.kz. **ORCID** 0000-0002-8188-536X

L.V. Komashko - Scientific Researcher, Laboratory of Physical Methods of Research, JSC “D.V. Sokolsky Institute of Fuel, Catalysis and Electrochemistry”, Almaty, Kazakhstan. Tel: +77272916632. ifce@ifce.kz. **ORCID** 0000-0002-1976-1104

G.U. Begimova – PhD, Scientific Researcher, Laboratory of Organic Catalysis, JSC “D.V. Sokolsky Institute of Fuel, Catalysis and Electrochemistry”, Senior Lecturer of Al-Farabi Kazakh National University, Almaty, Kazakhstan. Tel: +77272916632, zeynep80@mail.ru. **ORCID** 0000-0002-8188-536X

NEWS

OF THE NATIONAL ACADEMY OF SCIENCES OF THE REPUBLIC OF KAZAKHSTAN

SERIES CHEMISTRY AND TECHNOLOGY

ISSN 2224-5286

<https://doi.org/10.32014/2018.2518-1491.21>

Volume 6, Number 432 (2018), 16 – 22

UDC 574.635

**Johann Dueck¹, Roza Tatayeva², Aliya Baymanova³,
Zhumbike Bakeshova², Baurzhan Kapsalyamov²**

¹Friedrich-Alexander-University Erlangen-Nuremberg, Germany;

²Gumilev Eurasian National University, Astana, Kazakhstan;

³Karaganda State Medical University, Karaganda, Kazakhstan

johanndueck@yandex.com, rktastana@bk.ru, Baymanova@kgmu.kz,
zhumka.73@mail.ru, 19575859@mail.ru

BIOLOGICAL TREATMENT OF WASTE WATER: THEORETICAL BACKGROUND AND EXPERIMENTAL RESEARCH

Abstract. Recent years have seen a rising interest in biofilters. This is due to the application of new materials for particles in the charge and small energy expenditures. Biological purification before other methods has a number of significant advantages. Microorganisms complete the decomposition of domestic sewage to neutral products (gas and water), while ensuring the circulation of substances in nature. Thus, biological purification, unlike other methods, does not extract and does not transfer contamination to other forms, which ensures practically no-waste production. At the same time, biological methods are less expensive, since, with the exception of capital investments, they almost do not require operating costs. All methods of biological purification are mainly divided into aerobic and anaerobic. In aerobic method, microorganisms use dissolved oxygen in waste water, while in anaerobic process, microorganisms do not have access to oxygen.

The further development of the bio-purification technology will be promoted by the elaboration of effective methods for simulating the processes in purifying plants.

In the present paper, a model for calculating the bio-purification in a continuous reactor supported by experiments on a laboratory facility is developed. Below, instead of empirical assumptions about the exponential dependence of the decrease in the substrate concentration on the distance from the inlet to a reactor with parameters having no clear physical meaning and determined from experiments, this law is calculated directly with the use of the kinetics and mass transfer.

Key words: biofilm, water purification, modeling, biofilter.

Introduction

Environmental biotechnology uses microorganisms to improve environmental quality. This improvement includes preventing the discharge of pollutants into environment and cleaning up the contaminated mediums.

Nowadays there are sorbents, both natural, and artificial, which allow to clear waters from variety of pollutants simultaneously, for example from ions of heavy metals and petroleum. Below we explore a modified sorbent based on the use of one of a sol – gel process [1].

One of them is the biological treatment. Microorganisms capable of water remediation occur in nature as suspended flocs and attached biofilms. Flocs are formed without a solid substratum, while biofilms adhere to a solid substratum, i.e. on the surface of minerals.

Biofilms, which are naturally immobilized cells, occur ubiquitously in nature and are increasingly important in processes used in pollution control, such as trickling filters, rotating biological contactors and anaerobic filters. On the surface of the granules, microorganisms form a film into which the water-dissolved contaminants diffuse to serve as substrates for microbial proliferation.

A mathematical modelling by a biofilm under steady state conditions is discussed. The nonlinear differential Equations in biofilm reaction is solved using the Adomian decomposition method [2].

Biofilters are used successfully in cleaning water from various pollutants [3-5].

In works [6-8] some modern methods of sewage treatment are presented. However, in these works, water purification is not related to the activity of living microorganisms, which is characteristic of biological water treatment technologies.

The analysis of traditional (nitrification-denitrification) and the latest biotechnology wastewater from inorganic nitrogen has been done. Current status of the present key technologies of nitrogen removal from wastewater has been formulated. The main advantages and disadvantages of these biotechnologies are described in [9].

Biofilm formation and adherence properties of bacterial strains commonly found in wastewater treatment systems were studied in pure and mixed cultures using a crystal microtiter plate assay. These results on attachment and biofilm formation can serve as a tool for the design of tailored systems for the cleaning of municipal and industrial wastewater [10].

The stable effective operation of the biofilter is determined by a number of factors both promoting reproduction of microorganisms (conditions of the biochemical reaction, transport intensity of impurities and metabolic products) and inhibiting this process (film erosion by water flow, filling of charge pores, inhibition of bio-reactions by products of their own vital activity).

The further development of the bio-purification technology will be promoted by the elaboration of effective methods for simulating the processes in purifying plants.

In the paper, a model for calculating the bio-purification in a continuous reactor supported by experiments on a laboratory facility is developed. This approach was proposed in describing the processes proceeding in the biofilm [11].

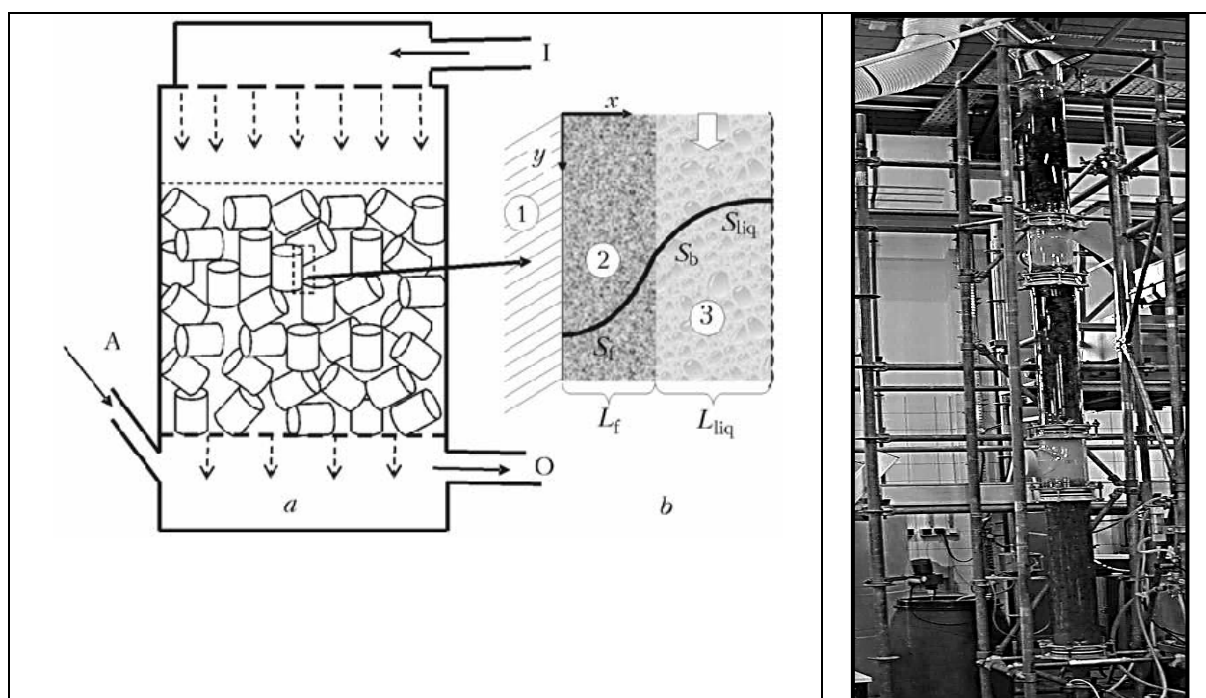


Figure 1 -Schematic representation of the water purification process:

a) biofilter: I, inflowing water; O, outflowing water; A, air inflow;

b) part near the ring surface: 1) ring; 2) biofilm of thickness L_f ; 3) water film of thickness L_{liq} . c) Laboratory-scale plant

Experimental facility

Below we describe measurements of the efficiency of purification of an artificially prepared water representing a low-concentration meat broth (the total inlet content of carbon in the aqueous solution was varied from 5 to 58 mg/l). Experiments were performed on a drop biofilter representing a vertical pipe

(Fig.1) with a working section length equal to 268 cm. The diameter of the pipe was 15 cm. The charge grains represented Raschig rings of height 1.67 mm, inner diameter 1.23 cm, and outer diameter 1.47 cm. Water was supplied to the reactor through a sprinkler in the form of a downflow of drops equidistributed over the reactor cross-section, and the trickling filtrate was removed upon reaching the bottom hole. Microorganisms on the particle surface represented mixed cultures.

Samples of water were taken at both the reactor inlet and outlet and also at two other points at a distance of 78 and 173 cm from the inlet.

The following indices were measured:

1. Total organic carbon. Hard balls of the biofilm carried out by the flow were filtered off from the samples, and the water was investigated for the total organic carbon with the use of a TOC-analyzer of the Groeger&Obst company (Germany).

2. Specific mass of the biofilm. At the same sampling points as for the analysis of water, ten rings were taken out. The weight difference of rings covered with the biofilm and without it gives the mass of the biofilm. Knowing the surface of the rings and measuring the biofilm density, we determined its total volume. On the assumption of a uniform distribution of the biofilm over the surface of the rings its average thickness was calculated.

MODEL OF WATER PURIFICATION IN THE BIOFILTER

Water running down in the biofilter flows over the biofilm surface on particles (Fig. 1a). The flow rate of water is selected so that it flows around the porous charge grains in the form of film and there is enough air between grains to provide aerobic microorganisms with oxygen.

1. Through the biofilm-water layer interface transport of the substrate into the biofilm occurs, so that in the direction of the flow (y) the substrate concentration in the water decreases:

$$Q_2 \frac{dS_1(y)}{dy} = -\beta_w (S_1(y) - S_b(y)), \quad (1)$$

where the value of the substrate concentration on the biofilm surface S_b is not known in advance.

2. The distribution of the substrate concentration in the biofilm is described by the equation

$$D_f \frac{\partial^2 S_f}{\partial x^2} = q \frac{S_f}{K + S_f} X_f \quad (2)$$

with the boundary conditions:

$$\frac{\partial S_f}{\partial x} = 0 \text{ at } x = 0, \text{ and } \beta_w (S_1 - S_f(L_f)) = D_f \frac{\partial S_f}{\partial x} \text{ at } x = L_f, S_1(L_f(y)) = S_b(y). \quad (3)$$

The biomass production rate is equal to the death rate of microorganisms taken, as in proportional to the squared concentration of the active biomass:

$$Yq \frac{S_f}{K + S_f} X_f = bX_f^2 \quad (4)$$

Equations (2) and (4) lead jointly to the relation

$$D_f \frac{d^2 S_f}{dx^2} = \frac{q^2 Y}{b} \left(\frac{S_f}{K + S_f} \right)^2 \quad (5)$$

3. The biofilm thickness is determined by the equality of the production rate of biomass across the whole width and the rate of its ablation:

$$\frac{Yq}{\rho} \int_0^{L_f} \frac{S_f}{K + S_f} X_f dx = rL_f \quad (6)$$

In view of (4)–(6) the biofilm thickness is defined as

$$L_f = \frac{Y}{r_p} \beta_w (S_1 - S_b), \quad (7)$$

A major quantity found from the calculation is the quantity of substrate taken up from the water by the film.

Finding the diffusion flow of the substrate into the film $J = D_f \left. \frac{dS_f}{dx} \right|_{z=L_f}$ from Eq. (5) at the boundary

conditions (3) and equating it to the substrate flow from the water into the film $J = \beta_w (S_1(y) - S_b)$, we obtain equations for finding S_b .

Analysis of problem (3), (5) shows [12], that two reaction regimes can be distinguished: 1) in a relatively thick film, substrate consumption occurs not across its whole width, but only in the water-contacting layer (diffusion regime, unsaturated biofilm); 2) a relatively thin film is saturated with substrate due to the diffusion and its consumption occurs across its whole width at an approximately equal rate (kinetic regime, saturated biofilm).

For calculations, the following diffusion kinetic parameters were taken: $D_{liq} = 0.8$ cm²/day, $D_f = 0.64$ cm²/day, $K = 0.01$ mg/day, $q = 8$ days⁻¹, $Y = 0.5$, $b = 0.5$ cm³/(day/mg), $R_{col} = 7.5$ cm, $R = 0.6775$ cm, $H = 1.67$ cm, $\varepsilon = 0.704$.

COMPARISON OF CALCULATIONS AND MEASUREMENTS

Calculations were performed with varying rate of substrate flow through the reactor Q and substrate concentration $S_{liq}(0)$ in water at the reactor inlet (column at $y = 0$). Measurements were made at the Q values given in the Table 1.

Table 1 - Various variants of the flow velocity measurements

Variant number	1	2	3	4	5	6	7	8	9
Q , cm/min	3.28	4.47	5.26	5.32	5.82	5.89	6.56	10.63	11.32

The change in $S_{liq}(y)$ along the working channel of the biofilter was measured.

Figure 2 presents the results of the calculations (curves) and the experimental values (dots) for all variants of the values of substrate flow rates given in table 1. In all cases, there is a fairly good agreement between the experimental and calculated data.

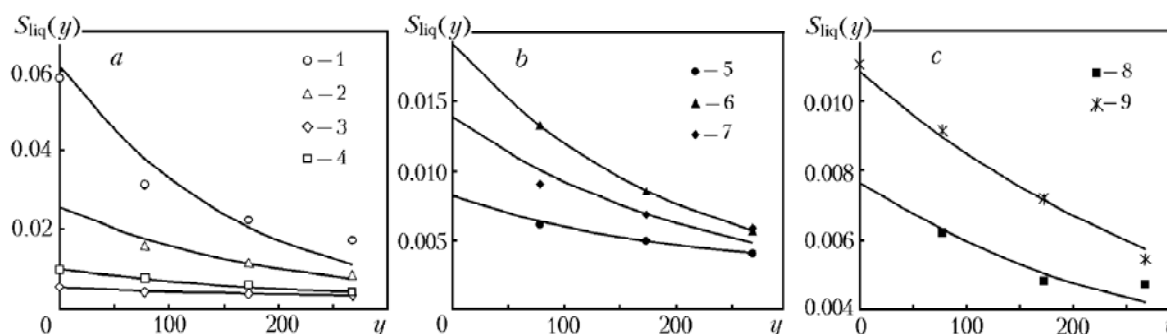


Figure 2 - Substrate concentration in the liquid $S_{liq}(y)$ versus the distance y down the bioreactor column (curves show calculations, dots — experiments): a) relatively low flow rates of the substrate solution; b) moderate flow rate of the substrate; c) relatively high flow rates of the substrate solution.

The curve number corresponds to the variant number in the table.

Both the experiment and the numerical calculation show that for high flow rates Q the efficiency of water purification, i.e., the ratio between the carbon concentrations at the reactor outlet and inlet,

decreases. This is likely to be due to the reduction of the residence time of the substrate solution in the reactor in spite of some increase in the mass transfer intensity.

The calculations provide an additional possibility of judging the behavior of other, not measured, variables defining the process of water purification such as the substrate flow into the biofilm and the biofilm thickness in each section of the biofilter.

However, comparison between measured and calculated thicknesses of the biofilm (Fig. 3) does not always give a satisfactory result for several reasons, including the following ones:

1. Modeling of the biofilm as a smooth layer characterized by the thickness alone is obviously insufficient. Models describing two-dimensional films are rather complicated and are under development [13].

2. Measurements were taken after about a week upon variation of the feed rate of the substrate solution or its concentration. During this time, probably, the microflora concentration and, accordingly, the substrate flow in the film manage to adjust themselves to the new conditions, and the corresponding change in the biofilm thickness strongly depends on the erosion intensity and requires much more time.

3. Measurements of the thickness of the biofilm through measurements of the mass or its volume may not be accurate enough, since they do not take into account the non-uniformity of the film distribution over the surface of grains.

It is important to know the film thickness, because this characteristic correlates with the substrate flow into the film. Figure 3 shows the curves reflecting the change in the biofilm thickness along the working channel of the biofilter. It is seen that the biofilm thickness decreases with decreasing concentration of the substrate in the liquid flow.

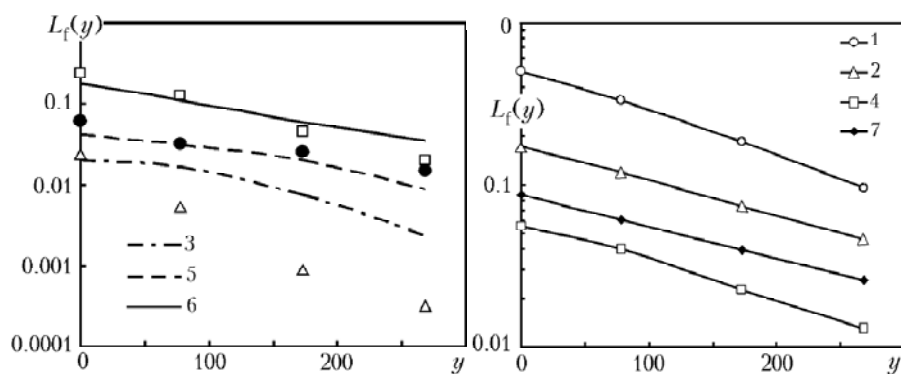


Figure 3 - Comparison of some of the calculated and measured thicknesses of the biofilm L_f in various sections along the reactor y and under various flow conditions: 1, 2, 3, 4, 5, 6, 7) variant number. y , L_f , cm

The decrease in L_f with y happens due to the decrease in the substrate concentration in water. On the other hand, a decrease in L_f leads to a decrease in the working volume of the biofilm, which in turn decreases the intensity of water purification.

Conclusions

The developed theoretical model of water bio-purification in the biofilter agrees well with the experimental data obtained on a laboratory bio-column. The agreement between calculations and measurements of the decrease in the substrate concentration down the column is much better than the corresponding comparison for the film thickness.

REFERENCES

- [1] Privalova N.M., Dvadenko M.V., Nekrasova A.A., Privalov D.M. (2017) Perfection of cleaning of waters from petroleum technology. Polytematic network electronic scientific magazine of kuban state agrarian university №127. P. 380-389. <https://cyberleninka.ru/article/v/sovershenstvovanie-tehnologii-ochistki-vod-ot-nefteproduktov-1>
- [2] Subramanian Muthukaruppan, Alagu Eswari, Lakshmanan Rajendran (2013) *Mathematical modelling of a biofilm: The Adomian decomposition method*. Natural Science, Vol.5 No.4, April 19. <https://www.ncbi.nlm.nih.gov/pubmed/17070991>

- [3] C.Cortes-Lorenzo, M.L.Molina-Munoz, B.Comez-Villalbat, R.Vilhez, A. Ramost, B.Rodelas, E.Hontoria, J.Gonzales-Lopez. (2006). Analysis of community composition of biofilms in a submerged filter system for the removal of ammonia and phenol from industrial wastewater, *Biochem. Soc. Trans.*, 34, 165. www.ncbi.nlm.nih.gov/pubmed/16417512
- [4] J.Chung, B.E. Rittmann. (2007). Bio-reductive dechlorination of 1,1,1-trichloroethane and chloroform using a hydrogen-based membrane biofilm reactor, *Biotechnol./Bioeng.*, 97, 52. onlinelibrary.wiley.com/doi/10.1002/bit.21212/abstract
- [5] Qi Lang, Shumei Ren, Peiling Yang, Zejun Tang, Lu Lu, Yunkai Li, Huiping Zhou, Nuan Sun, Wen Qi. (2016) Effect of Aquatic Plants Combined with Compound Microorganism Preparations Control on Eutrophication in Reclaimed Water. *Oxidation communications*. 3 (1) .2447 scibulcom.net/ocr.php?gd=2016&bk=3
- [6] Harlamova T.A., Kolesnikov A.V., Sarbaeva M.T., Bayeshov A.B., Sarbaeva G.T.(2013) Advanced electrochemical methods of waste water treatment. The bulletin of the national academy of sciences of the Republic of Kazakhstan.№5. P. 33-44. <http://www.bulletin-science.kz/index.php/en/arhive>. <https://doi.org/10.32014/2018.2518-1467>
- [7] Turebekova G. Z., Dosbayeva A.M., Sihynbaeva Zh.S., Sataeva L.M., Orazymbetova A.O. (2014) Application of new surfactants to improve sewage chemical production. The bulletin of the national academy of sciences of the Republic of Kazakhstan.№4.P. 28-31. <http://www.bulletin-science.kz/index.php/en/arhive>. <https://doi.org/10.32014/2018.2518-1467>
- [8] Zhumamurat M.S., Ahmetova A.B.(2017) Selection of natural sorbents for wastewater treatment. NEWS of the academy of sciences of the Republic of Kazakhstan. Series chemistry and technology №1 (421). P.59-66. <http://chemistry-technology.kz/index.php/en/arhiv>. <https://doi.org/10.32014/2018.2518-1491>
- [9] O.M. Shved, R.O. Petrunina, O. J. Karpenko, V.P. Novikov (2014): Modern technologies nitrogen extraction from sewage water // *Biotechnologia ACTA*, V. 7, №5.http://biotechnology.kiev.ua/index.php?option=com_content&view=category&id=129&Itemid=150&lang=ru
- [10] Sofia Andersson: Characterization of Bacterial Biofilms for Wastewater Treatment. School of Biotechnology, Royal Institute of Technology (KTH), Sweden. <http://www.diva-portal.org/smash/get/>
- [11] J. Dueck, S. Pylnik. (2008). Rate of the biochemical Reaction in a Biofilm in Contact with a Flowing Liquid. *Theoretical Foundations of Chemical Engineering*, Vol. 5, 536 <https://www.sparrho.com/rate-of-the-biochemical-reaction>
- [12] J.Dueck, S.V. Pylnik, A.V.Gorin. (2009) On the mass transfer in a sprinkled biofilter. *Journal of Engineering Physics and Thermophysics*, 6(82), 86. <https://www.deepdyve.com/on-the-mass-transfer-in-a-sprinkled-biofilter>
- [13] M.C.Van Loosdrecht, J.J.Heinen, H.Eberl, J.Kref, C.Picioreanu. (2002). Mathematical modeling of biofilm structures, 81, 245 https://www.researchgate.net/11020038_Mathematical_modeling_of_biofilm_structures

UDC 574.635

Johann Dueck¹, Роза Татаева, Алия Байманова, Жұмабике Бакешова, Бауыржан Капсаламов¹Фридрих-Александр-Университеті, Эрланген-Нюрнберг, Германия;²Л.Н.Гумилев атындағы Еуразия ұлттық университеті, Астана, Kazakhstan;³Қарағанды мемлекеттік медицина университеті, Қарағанды, Қазақстан**АҚАБА СУЛАРДЫ БИОЛОГИЯЛЫҚ ӨНДЕУ:
ТЕОРИЯЛЫҚ НЕГІЗДЕРІ ЖӘНЕ ЭКСПЕРИМЕНТТІК ЗЕРТТЕУЛЕР.**

Аннотация. Бұл жұмыста ағынды реакторда биологиялық тазартуды есептеу үшін теориялық модель ұсынылған. Модель су ағынындағы контаминанттардың көмірсутектері субстрат ретінде қызмет атқаратын, биопленканың түзілуін есепке алуға негізделген. Есептеулер тазарту процесі кезінде биопленканың өсуін қамтамасыз ететін, Рашиг сақиналарымен толтырылған зертханалық түтіккі реакторда жүргізілген эксперименттермен жасалды.

Ағынмен шығарылған, биопленканың қатты бөлшектері үлгілерден сүзілді, және су сынама алуға арналған төрт нүктеден алынып, Groeger & Obst (Германия) фирмасының ТОС-анализаторын қолданып, жалпы органикалық көміртегінің құрамына зерттелді.

Биопленканың меншікті салмағы анықталды. Дәл сол су сынамасы алынатын нүктелерден он сақина қайтып алынды. Биопленкамен жабылған сақиналардың салмағының айырмашылығы, биопленканың салмағын береді. Сақинаның бетін біліп және биопленканың тығыздығын өлшей отырып, біз оның жалпы көлемін анықтадық. Сақиналардың бетінде биопленканың біркелкі екендігін ескеріп, оның орташа қалыңдығы есептелді.

Биофильтраттағы суды биологиялық тазартудың теориялық моделі зертханалық биоколоннада алынған эксперименттік деректермен жақсы үйлеседі. Пленка қалыңдығымен салыстырғанда, колонна бойындағы субстрат концентрациясының азаюының өлшемдері мен есептеулері арасындағы сәйкестік әлдеқайда көп.

Түйін сөздер: биопленка, суды тазарту, модель, биофильтр.

UDC 574.635

Johann Duesck¹, Роза Татаева, Алия Байманова, Жумабике Бакешова, Бауыржан Капсаламов

¹Фридрих-Александр-Университет, Эрланген-Нюрнберг, Германия;

²Евразийский национальный университет им.Л.Н.Гумилева, Астана, Kazakhstan;

³Карагандинский государственный медицинский университет, Караганда, Казахстан

БИОЛОГИЧЕСКАЯ ОБРАБОТКА СТОЧНЫХ ВОД: ТЕОРЕТИЧЕСКАЯ ОСНОВА И ЭКСПЕРИМЕНТАЛЬНЫЕ ИССЛЕДОВАНИЯ

Аннотация. В данной работе предложена теоретическая модель для расчета биоочистки в проточном реакторе. Модель основывается на расчёте образования биопленки, субстратом для которой служат углеводороды контаминантов в потоке воды. Расчёты сопровождались экспериментами на лабораторном трубчатом реакторе, заполненном кольцами Рашига, на которых в процессе очистки нарастала биоплёнка.

Твердые частички биопленки, вынесенные потоком, отфильтровывались из образцов, и вода в четырёх точках отбора проб исследовалась на содержание общего органического углерода с использованием ТОС-анализатора фирмы Groeger & Obst (Германия).

Определялась удельная масса биопленки. В тех же точках отбора проб, что и для анализа воды, изымалось по десять колец. Разница в весе колец, покрытых биопленкой и без нее дает массу биопленки. Зная поверхность колец и измеряя плотность биопленки, мы определили ее общий объем. В предположении равномерного распределения биопленки на поверхности колец была рассчитана её средняя толщина.

Разработанная теоретическая модель биоочистки воды в биофильтре хорошо согласуется с экспериментальными данными, полученными на лабораторной биоколонне. Согласие между расчетами и измерениями падения концентрации субстрата вдоль колонны намного лучше, чем при соответствующем сравнении толщины пленки.

Ключевые слова: биопленка, очистка воды, модель, биофильтр.

NEWS

OF THE NATIONAL ACADEMY OF SCIENCES OF THE REPUBLIC OF KAZAKHSTAN

SERIES CHEMISTRY AND TECHNOLOGY

ISSN 2224-5286

<https://doi.org/10.32014/2018.2518-1491.22>

Volume 6, Number 432 (2018), 23 – 28

UDC 613.32

IRSTI 76.33.35

**G.E. Orymbetova¹, D. Conficoni², M.K. Kassymova³,
Z.I. Kobzhasarova⁴, E.M. Orymbetov⁵, G.D. Shambulova⁶**

^{1,3,4}M.Auezov South-Kazakhstan State University, Shymkent, Kazakhstan;

²Padova University, Italy;

⁵South Kazakhstan Medical Academy, Shymkent, Kazakhstan;

⁶Almaty Technological University, Almaty, Kazakhstan

e-mail: orim_77@mail.ru

RISK ASSESSMENT OF LEAD IN MILK AND DAIRY PRODUCTS

Abstract. In the present study, a quantitative dietary exposure assessment of lead was conducted using the contamination data of milk and dairy products. Milk and dairy products (n = 120) were analyzed for the presence of toxic elements, such as lead. Milk and dairy products were collected in markets and supermarkets of Shymkent, in accordance to structured sampling plan and analyzed, during the period from January 2016 till October 2017. The usual intake of these food groups was estimated from the results of a social survey of consumption of dairy products. According to a probabilistic exposure analysis, the mean (and P95) lead for milk and dairy products was 0.00138 (0.00318, P95) mg kg⁻¹ body weight day⁻¹. These values were below the tolerable daily intake (TDI) levels for lead (0.007 mg kg⁻¹ body weight day⁻¹). The absolute level exceeding the TDI for milk and dairy products was calculated, and recorded 0.1% of population.

Key words: risk, lead, hazard, milk, dairy products, heavy metals.

Introduction

Exposure to toxic elements (“heavy metals”) causes health problems such as toxicity of the liver, kidneys, hematopoietic system, and nervous system. Metals differ from other pollutants in that they are neither created nor destroyed and occur naturally in the environment. Anthropogenic activity largely contributes to human exposure because metals are bioconcentrated from the environment, people are exposed to toxic elements through a variety of routes, such as second hand exposure to pollution in the workplace, everyday household products [1-3].

Lead is one of the most common and hazardous toxicants. Lead is used in production of batteries, ammunition, metal products (solder and pipes), alloys, pigments and compounds, cable sheathing, and devices to shield X-rays. The risk of lead for a person is determined by its significant toxicity and ability to accumulate in the body. Most of the lead comes from food products (from 40 to 70% in different countries and in different age groups), and also with drinking water, atmospheric air, smoking, with accidental ingestion of lead-containing paint or lead-contaminated soil into the esophagus. With atmospheric air, small amount of lead is supplied 1-2%, but most of this lead is absorbed in the human body. The highest levels of lead are observed in canned foods in tin cans, fresh and frozen fish, wheat bran, gelatin, mollusks and crustaceans. A high content of lead is observed in root crops and other plant products grown on lands near industrial areas and along roads [4-6].

For all food products, the maximum permissible levels of heavy metals are established. The relevant authorities monitor compliance with standards. The presence of each metal in food is controlled by methods of chemical analysis, and in the human body by norms of maximum permissible concentrations [7].

The maximum permissible concentration of lead in tap water is 0.03 mg kg^{-1} . The total content of lead in the human body is 120 mg. TDI - 0.007 mg kg^{-1} body weight [4,5].

In an adult human body, an average of 10% of lead is absorbed, in children 30-40%, 90% of lead is excreted with physiological fluids, the biological half-life is 20 days in blood, and 20 years in bone [3-8].

The mechanism of lead toxic effect is determined in two main directions: 1) blockade of functional sulfhydryl groups of proteins, that leads to inhibition of many vital enzymes; 2) penetration of lead into nerve and muscle cells, formation of lead lactate by interaction with lactic acid, then the formation of lead phosphate, which creates a barrier to the penetration of nerve and muscle cells of calcium ions, and -as result - development of paralysis. Thus, main targets under the influence of lead are hematopoietic, nervous, food systems and kidneys. It noted its effect on sexual function of the body [4, 9-13].

The individual susceptibility to lead poisoning varies widely, and same doses of lead may have greater or lesser effect for different people. Characteristic symptoms of poisoning are pallor of face, loss of attention, poor sleep, tendency to frequent mood changes, increased irritability, aggressiveness, fatigue, and metallic taste in the mouth.

Measures to prevent lead food contamination include departmental and state control of emissions, control over the use of tinned, glazed, ceramic food utensils.

The most consumed group of food products (on average per capita) in Kazakhstan households is milk and dairy products (Statistics Committee of the Ministry of National Economy of the Republic of Kazakhstan).

People of Kazakhstan on average consume 290 kg of dairy products per year per person [14].

The aim of the work is to determine the content of lead in milk and dairy products and the potential risk to the health of population of the South Kazakhstan Region (SKR).

Objects and methods of research

As objects of research, dairy products, sold in markets and supermarkets of Shymkent (SKR), were chosen. In the city, a large part of population satisfies the needs for food products at expense of local and own products.

Sampling and sample preparation were carried out in accordance with the regulatory documentation for each type of product. The lead content in dairy products was evaluated on an inductively coupled plasma mass spectrometer (ICP-MS) device in accordance with ST RK ISO 17294-06 [15].

A total of 120 milk and dairy products samples were selected and analyzed.

The research was carried out in the laboratories of the "Food Engineering" department and in testing regional laboratory of engineering profile "Structural and Biochemical Materials" at M. Auezov SKSU.

A social survey (interview) of the population of Shymkent on consumption of milk and dairy products was conducted. The age of population that participated in survey was 12 years and older.

The usual food intake was expressed as $\text{mg kg}^{-1} \text{ bw day}^{-1}$ using self-reported body weight (bw) data collected during survey.

Three different scenarios were included for the lead dietary exposure assessment in relation to the data treatment of the non-detects (< LOD): lower, medium and upper bound.

Non-detects were considered as zero, 1/2 LOD and LOD for lower, medium and upper bound, respectively.

Calculations of probabilistic exposure assessment were executed using the software *@Risk* for Microsoft Excel version 7 (Palisade Corporation, USA). Best fit was based on chi-square statistics. The probability/probability plots (P/P) and the quantile/quantile plots (Q/Q), resulting from the cumulative distributions, were a parameter if the cumulative distributions corresponded to the theoretical cumulative distributions. First order Monte Carlo simulations were performed considering 10000 iterations. The estimated intake of lead (mean, maximum and percentiles) was determined. Output of exposure was compared to lead TDI [16,17].

Results and discussion

The results of lead content in dairy products produced in SKR are presented in table 1.

The calculation of food contaminants daily load on population was carried out on basis of data from the social survey on volume of consumption of foodstuffs with rations.

The results of the research establish that not all dairy products contain lead.

Based on data of the social survey of Shymkent population (280 people), lead intake with food products was established. Contribution of milk origin products to the total value of the population exposure is determined.

Table 1 - Calculations of concentration of Pb in products (mg kg^{-1}) and consumption product ($\text{kg day}^{-1} \text{bw}^{-1}$)

Concentration Pb in products, mg kg^{-1}	Consumption milk and dairy products, g day^{-1} (bw, kg)	Consumption milk and dairy products, $\text{kg day}^{-1} \text{bw}$
0.03	450 (52)	0.0086
0.02	300 (49)	0.0061
0.01	200 (67)	0.0029
0.02	350 (55)	0.0060
0.3	250 (50)	0.005
0.01	220 (55)	0.004
0.03	200 (58)	0.0034
0.02	180 (65)	0.0027
...
0.01	100 (55)	0.0018

Recently, studies have reported the concentrations of heavy metals, including Pb, in various milk samples, the results of which showed that the content of heavy metals did not exceed the maximum allowable concentrations specified in the technical regulations [18]. The presence of Pb through plants in milk can arise from environmental sources (region, climate, and soil composition) and anthropogenic sources (by fertilizers and chemical protection of plants) toxic metals come from soil, water. [19]. Since pollutants are able to disperse via air, surface water, and groundwater, heavy metal contamination can be a serious problem in crop production [20].

The overall results of Pb exposure are shown in Tables 2 and 3 (probabilistic).

Since the mean, the 95 percentiles as the maximum exposure are above the TDI value, there is a small risk for the population.

In probabilistic analysis every possible value that each variable can have. The mean of each possible scenario is taken into consideration, therefore allowing a more accurate lead intake estimation. Best fit distributions were formed for lead concentrations in milk and dairy products and all consumption data.

The best fit distributions determined for the upper bound scenario of lead concentrations in products, further applied for the probabilistic calculations are listed in Table 2.

Table 2 - Cumulative distribution of the risk analysis of exposure to Pb

Probabilistic	
Distribution consumption	0.003649 Risk Invgauss (0.003401;0.00688;Risk Shift(0.0001998))
Fraction of consumption	0.058
R and between	1
Distribution Total population	0.002715

Table 3 represent the probabilistic estimates of lead intake (mean, standard deviation, maximum, percentiles) ($\text{mg kg}^{-1} \text{bw day}^{-1}$) by population for the upper bound (worst case scenario) of dairy products.

Table 3 showed for lead that 0.1% of population SKR exceeds the TDI of $0.007 \text{ mg kg}^{-1} \text{bw day}^{-1}$, potentially indicating that the concentrations found in the analyzed foods cause on daily scale exposure on the health population.

Table 3 - Predictive analysis of Pb estimate for consumption of milk products (mean, percentiles, $\text{mg kg}^{-1} \text{bw d}^{-1}$) by the population of Shymkent.

	All Intake (for consumer)
Min	0.000197
SD	0.00092
Mean	0.00138
Max	0.00993
Med (P50)	0.00112
P90	0.00253
P95	0.00318
P99	0.00475
P(X<TDI)	99.9%
Fraction population exceeding	0.1%

The interpretations of risk analysis results are shown in figures 1. The 0.1 % of the population is exposed to concentration of Pb that is above the MPL value of 0.1 mg kg^{-1} : there is possible hazard for the population.

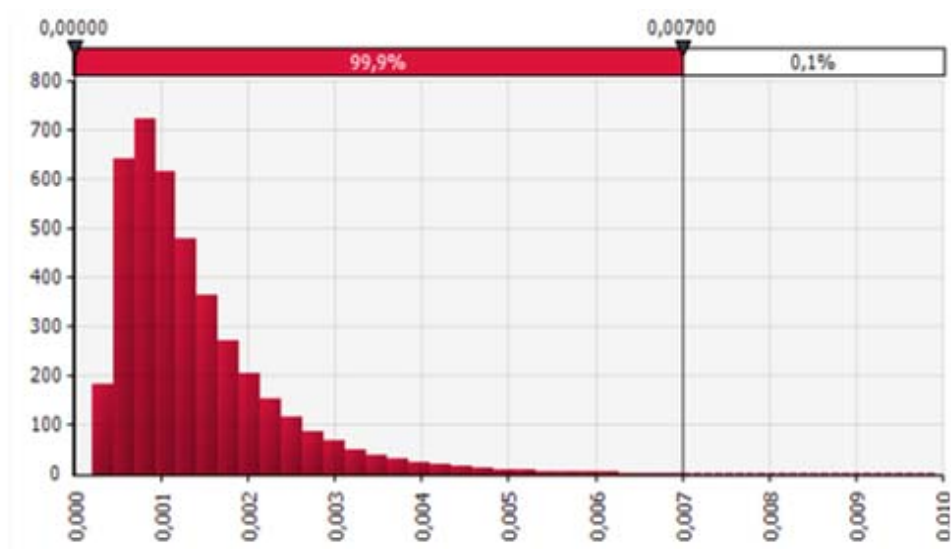


Figure 1 - Predictive risk of consumption of milk and dairy products contaminated by lead ($\text{mg kg}^{-1} \text{bw day}^{-1}$)

The obtained results show that 0.1% of the population is exposed to possible risk at consumption of milk and dairy products contaminated by Pb.

Conclusion

Thus, levels of lead in milk and dairy products are established, risks of adverse effects of controlled lead coming from finished products produced in SKR are calculated, need to conduct constant monitoring of food safety is confirmed. According to probabilistic impact analysis, the mean (and P95) lead intake for dairy products was 0.00138 (0.00318 , P95) $\text{mg kg}^{-1} \text{body weight day}^{-1}$. These values were below permissible level of daily intake (TDI) for lead ($0.007 \text{ mg kg}^{-1} \text{body weight day}^{-1}$). To reduce the risk of population's morbidity by toxic elements like lead, it is necessary to carefully control emissions of industrial enterprises into the atmosphere, soil, water and avoid pastures for animals near industrial centers and major highways.

REFERENCES

- [1] Lauwerys RR, Hoet P. (2001) Industrial Chemical Exposure: Guidelines for Biological Monitoring. 3rd ed. Boca Raton, FL: Lewis Publishers. 638 p.
- [2] Gorospe E.C, Gerstenberger S.L. (2008) A typical sources of childhood lead poisoning in the United States: A systematic review from 1966-2006. Clin Toxicol (Phila). P.728-737.
- [3] Deborah E. Keil, Jennifer Berger-Ritchie, Gwendolyn A. McMillin (2011). Testing for Toxic Elements: A Focus on Arsenic, Cadmium, Lead, and Mercury. LABMEDICINE. Volume 42, Number 12. P.735-742.
- [4] Roeva N.N. (2005) Ecological examination of biological products [Ekologicheskaya ekspertiza biologicheskikh tovarov]. M.: MSUTU. 76 p. (In Russian)
- [5] Gabelko S.V. (2012) Safety of food raw materials and food products [Bezopasnost prodovolstvennogo syrya and produktov pitaniya]. Novosibirsk: NSTU. 183 p. (In Russian)
- [6] Klassen C. Casarett & Doull's (2013) Toxicology: the basic science of poisons, eighth edition. New York: McGraw-Hill Education. 1331 p.
- [7] Sverlova L.I., Voronina N.V. (2001) Pollution of the natural environment and ecological pathology of person [Zagryaznenie prirodnoy sredy and ekologicheskaya patologiya cheloveka]. Khabarovsk. 216 p. (In Russian)
- [8] Baars, A.J., Theelen, R.M.C., Janssen, P.J.C.M. et al. (2001) Re-evaluation of human toxicological maximum permissible risk levels. RIVM report 711701 025.
- [9] Poznyakovskiy V.M. (1999) Hygienic basis of nutrition, safety and examination of food products [Gigienicheskie osnovy pitaniya, bezopasnost i ekspertiza prodovolstvennykh tovarov]. – Novosibirsk. 448 p. (In Russian)
- [10] Daneshparvar M., Seyed-Ali Mostafavi, Zare Jeddi M., et al. (2016) The Role of Lead Exposure on Attention-Deficit/Hyperactivity Disorder in Children: A Systematic Review. Iranian Journal Psychiatry. V.11(1). P.1-14
- [11] Shilu Tong, Yasmin E. von Schirnding, Tippawan Prapamontol (2000). Environmental lead exposure: a public health problem of global dimensions. Bulletin of the World Health Organization, 78(9). P.1068-1077.
- [12] Kim H., Jang T., et al. (2015) Evaluation and management of lead exposure. Annals of Occupational and Environmental Medicine. P.1-9
- [13] Flora G, Gupta D, Tiwari A. (2012) Toxicity of lead: a review with recent updates. Interdiscip Toxicol. P.47–58.
- [14] <http://kazakh-zerno.kz>. (2015)
- [15] ST RK ISO 17294-2:2003 "Kachestvo vody. Primenenie mass-spektrometrii s induktivno-svyazannoy plazmoy (ICP-MS). 2. Chasst Opredelenie 62 elementov ". ("Water quality. Application of inductively coupled plasma mass spectrometry (ICP-MS) - Part 2: Determination of 62 elements, IDT"). Komichet po tehniyeshkomu regulirovaniyu i metrologii. Astana, 2006. 50 p. (In Russian)
- [16] Christian R., George C. (2004) Monte Carlo Statistical Methods. Springer. ISBN 978-1-4757-4145-2. P.204
- [17] Voise D. (1996) Quantitative Risk Analysis: A Guide to Monte Carlo Simulation Modelling. Ed. John Wiley & Sons. ISBN-10: 0471958034. 340 p.
- [18] Myrkalykov B.N. (2017) Development of a technique for technological audit of the production of dry powder from sheep's milk [Razrabotka metodiki tehnologicheskogo audita proizvodstva suhogo poroshka iz ovechego moloka]. Dissert.PhD, Almaty. 206 p. (In Russian)
- [19] Dubrovina T.N., Dubrovin P.V. (2011) Development of a new sour-milk product with cereal filler [Razrabotka novogo kislomolochnogo produkta s krupyanyim napolnitelem]. J.Bulletin of the Innovative Eurasian University. Vestnik inovatsionnogo evraziskogo universiteta]. N2. P.120-125 (In Russian)
- [20] Ivanova T.N., Eremin O.Yu. (2001) Migration properties of toxic elements of grain products [Migratsionnye svoystva toksichnykh elementov zernoproductov]. J.Storage and processing of agricultural raw materials [Hranenie i pererabotka selhozsyraya]. N 7. P. 10-12. (In Russian)

**Г.Э. Орымбетова, D. Conficoni, М.К. Касымова,
З.И. Кобжасарова, Э.М. Орымбетов, Г.Д. Шамбулова**

^{1,3,4}М.Әуезов атындағы Оңтүстік-Қазақстан Мемлекеттік Университеті, Шымкент, Қазақстан;

²Падова Университеті, Италия;

⁵Оңтүстік Қазақстан медицина академиясы, Шымкент, Қазақстан;

⁶Алматы Технологиялық Университеті, Алматы, Қазақстан

СҮТ ЖӘНЕ СҮТ ӨНІМДЕРІНДЕ ҚОРҒАСЫН ТӘУЕКЕЛІН БАҒАЛАУ

Аннотация. Зерттеу барысында сүт және сүт өнімдерінің ластануы туралы мәліметтерді пайдалана отырып, азық-түлік өнімдерінде сандық бағалау жүргізілді. Сүт және сүт өнімдері (n = 120) қорғасын тәрізді

улы элементтердің болуы үшін талданды. Шымкенттің нарықтарында және нарықтарында құрылымдық іріктеу жоспарына және талдауына сәйкес 2016 жылдың қаңтарынан 2017 жылдың қазанына дейін сүт және сүт өнімдері жиналды. Осы азық-түлік топтарының әдеттегі тұтынуы сүт өнімдерін тұтынуды әлеуметтік сауалнама нәтижелері бойынша бағаланды. Ыдырау ықтималды талдауына сәйкес сүт өнімдеріне арналған орта (және P95) қорғасын тұтыну тәулігіне 0,00138 (0,00318, P95) мг / кг дене салмағының 1 болған. Бұл мәндер қорғасын үшін тәуліктік қабылдаудың (рұқсат етілген күнделікті тұтыну-РКТ) рұқсат етілген деңгейінен төмен (0,007 мг/кг⁻¹ дене салмағының күніне⁻¹). Сүт және сүт өнімдері үшін РКТ-дан жоғары болатын абсолютті деңгей есептелді және халықтың 0,1% құрады.

Түйін сөздер: тәуекел, қорғасын, қауіп, сүт, сүт өнімдері, ауыр металдар.

**Г.Э. Орымбетова¹, D. Conficoni², М.К. Касымова³,
З.И. Кобжасарова⁴, Э.М. Орымбетов⁵, Г.Д. Шамбулова⁶**

^{1,3-5}Южно-Казахстанский Государственный Университет им. М.Ауэзова, Шымкент, Казахстан;

²Университет Падова, Италия;

⁵Южно-Казахстанская медицинская академия, Шымкент, Казахстан;

⁶Алматинский технологический университет, Алматы, Казахстан

ОЦЕНКА РИСКА СВИНЦА В МОЛОКЕ И МОЛОЧНОЙ ПРОДУКЦИИ

Аннотация. В настоящем исследовании была проведена количественная оценка содержания свинца в пищевых продуктах с использованием данных о контаминации молока и молочных продуктов. Были проанализированы молоко и молочные продукты (n = 120) на наличие токсичных элементов, как свинец. На рынках и маркетах г.Шымкента в соответствии со структурированным планом выборки и анализом в период с января 2016 года по октябрь 2017 года были собраны молоко и молочные продукты. Обычное потребление этих пищевых групп оценивалось по результатам социального опроса потребления молочных продуктов. В соответствии с вероятностным анализом воздействия, среднее (и P95) потребление свинца для молочных продуктов составляло 0,00138 (0,00318, P95) мг кг⁻¹ массы тела в день⁻¹. Эти значения были ниже допустимого уровня суточного потребления (ДСД) для свинца (0,007 мг кг⁻¹ массы тела в день⁻¹). Был рассчитан абсолютный уровень, превышающий ДСД для молока и молочных продуктов, и составил 0,1% населения.

Ключевые слова: риск, свинец, опасность, молоко, молочные продукты, тяжелые металлы.

NEWS

OF THE NATIONAL ACADEMY OF SCIENCES OF THE REPUBLIC OF KAZAKHSTAN

SERIES CHEMISTRY AND TECHNOLOGY

ISSN 2224-5286

<https://doi.org/10.32014/2018.2518-1491.23>

Volume 6, Number 432 (2018), 29 – 37

UDC 541.128.13:542.975:973:541.64

E.T. Talgatov, A.S. Auyezkhanova, N.Z. Tumabayev,
S.N. Akhmetova, K.S. Seitkaliyeva, Y.A. Begmat, A.K. Zharmagambetova

D.V. Sokolsky Institute of Fuel, Catalysis and Electrochemistry, Almaty, Kazakhstan
eldar-talgatov@mail.ru

POLYMER-PALLADIUM CATALYSTS ON MAGNETIC SUPPORT FOR HYDROGENATION OF PHENYLACETHYLENE

Abstract. Pd-polymer catalysts on magnetic support (MS) have been successfully prepared by adsorption method. The magnetic support was synthesized by co-precipitation of iron chlorides ($\text{Fe}^{3+}:\text{Fe}^{2+} = 2:1$) with sodium hydroxide. A series of colloidal palladium solutions was prepared by reduction of K_2PdCl_4 with sodium borohydride in the presence of polyacrylamide (PAM) and polyacrylic acid (PAA) with a different mole ratios of palladium to polymer (Pd:PAA = 1:5; Pd:PAM = 1:5; Pd:PAM = 1:10 and Pd:PAM = 1:15).

The initial components and catalysts were characterized by physicochemical methods. XRD measurement was used to identify the crystalline structure of the magnetic material. The results based on the crystal planes showed that the synthesized sample corresponds to maghemite with a spinal structure and an average particle size of 8.5 nm. The disappearance of the absorption band of PdCl_4^{2-} ions at 425 nm indicated a complete reduction of palladium. According to elemental analysis, the content of palladium in the catalysts was 1wt.% of the sum of all components which was close to the calculated data. This result indicated the quantitative fixation of polymer-protected palladium particles to a magnetic support.

The developed catalysts showed rather high activity and selectivity in the hydrogenation of phenylacetylene to styrene ($W_{\text{C=C}} = 0.73\text{-}1.36 \times 10^{-6}$ mol/s, $S_{\text{st}} = 80.9\text{-}89.2\%$). The PAM-stabilized catalysts were characterized by higher rate and yield of styrene to compare to the Pd-PAA/MS catalyst. The increase of the polymer content in the catalysts affects insignificantly the catalytic properties of the Pd-PAM/MS.

Keywords. Palladium, polymer, magnetic catalyst, hydrogenation, phenylacetylene.

Introduction

Recently, the interest of researchers of various fields of science and technology is focused on magnetic nanoparticles due to their unique properties as superparamagnetism, high coercivity, biocompatibility [1-3]. One of the promising areas of application of magnetic nanoparticles is design of catalysts. The uses of such nanoparticles as a support provides high effectiveness of disperse catalytic systems and the easiness of their separation from the reaction medium by magnetic field [4-5]. Platinum [6-8], palladium [9-11] and ruthenium [12, 13] are the most often used active phase of such type of catalysts.

Palladium magnetic catalysts exhibit high activity in cross-coupling reactions [14, 15] and hydrogenation of various classes of organic compounds [16-18]. However, despite a large number of methods for preparation of catalysts with magnetic properties [19-21], there are only few publications on optimization of their synthesis. The purpose of this work therefore is to develop palladium catalysts with magnetic properties, as well as to study the effects of the polymer-stabilizer nature and the ratio of Pd to polymer on catalytic properties of synthesized Pd-polymer/MS composites in the hydrogenation of phenylacetylene as model unsaturated hydrocarbon.

Experimental part

Reagents and materials

Phenylacetylene (98%, Aldrich) was purified by distillation, a purity was checked chromatographically. Ethanol (pure grade), PdCl₂ (59-60% Pd, Aldrich), KCl (pure grade), FeCl₂·4H₂O (pure grade), FeCl₃·6H₂O (pure grade), NaBH₄ (96%, Aldrich), NaOH (pure grade), polyacrylamide (PAM, $M_w = 1000000$) and polyacrylic acid (PAA, $M_v = 1250000$, Aldrich) were used without additional purification.

Synthesis of magnetic support (MS)

The iron salts (FeCl₃·6H₂O - 21.6 g and FeCl₂·4H₂O - 8.0 g) were dissolved in 200 mL of pre-boiled distilled water at room temperature, and placed to a thermostated round-bottom flask with three outlets and heated to 40°C. Then 100 mL of 3.2 M sodium hydroxide solution was added to the flask, stirred by bubbling nitrogen during 1 hour and then cooled to room temperature. The resulting black precipitate was separated from the supernatant by magnetic separation and washed several times with D.I. water and stored in ethanol.

The crystallinity of the prepared magnetite sample was studied by X-ray diffractometer DRON 3 with cobalt K α radiation ($\lambda = 0.179$ nm).

Synthesis of polymer-protected Pd nanoparticles

Freshly prepared aqueous solution of NaBH₄ (10 mL of 0.05 mmol, 1.9 mg) was rapidly added to 90 mL of an aqueous mixture of K₂PdCl₄ (0.1 mmol, 10.6 mgPd) and a polymer (0.5-1.5 mmol, 36.0-108.5 mg) under vigorous magnetic stirring. The amount of polymer was taken based on the calculation for preparing polymer-protected palladium nanoparticles with a molar ratios of Pd:polymer = 1: 5; 1:10 and 1:15.

The degree of palladium reduction was evaluated spectrophotometrically (SF-2000, Russia) by disappearance of the absorption band of palladium ions at 425 nm

Catalysts preparation

Pd colloidal solutions and a magnetic support amounts were taken from the calculation for obtaining 1% Pd catalysts. Palladium fixation to the magnetic support was assessed visually by brightening the mother liquor. The content of palladium in the catalysts was determined on a X-ArtM COMITA X-ray fluorescence spectrometer.

The prepared colloidal palladium solution (100 mL of 1×10^{-3} mol/L) was poured into 35 mL of ethanol suspension of the magnetic material (29 mg/mL). The mixture was stirred with a shaker for 30 minutes. The resulting catalyst was separated from the mother liquor by magnetic separation, washed with D.I. water and dried in the air.

Hydrogenation process

Hydrogenation of phenylacetylene (0.25 mL) was carried out in a thermostated glass reactor at 40 ° C and atmospheric hydrogen pressure in ethanol (25 mL) [22]. The catalyst amount was 0.02 g. The reaction rate was calculated based on the change in volume of uptaken hydrogen per second.

The reaction products were analyzed by gas chromatography on a Chromos GC-1000 chromatograph (Chromos, Russia) with the a flame ionization detector in the isothermal regime using a BP21 (FFAP) capillary column with a polar phase (PEG modified with nitroterephthalate) 50 m in length and 0.32 mm in inside diameter. The column temperature was 90°C, and the injector temperature was 200°C; helium served as the carrier gas; the injected sample volume was 0.2 μ L. The selectivity of the catalyst was evaluated as the ratio of the targeting product to the sum of all reaction products at a fixed conversion.

Results and discussion

Analysis of initial components and catalysts

Figure 1 shown XRD patterns of the synthesized magnetic sample. Seven characteristic peaks at 2 θ 21.564°, 35.297°, 41.629°, 50.600°, 63.595°, 67.540° and 74.556° were corresponding to the (111), (220), (311), (400), (422), (511) and (440) crystal planes of a maghemite with a spinal structure [23]. The average crystallite size calculated using the Debye-Scherrer equation was about 8.5 nm.

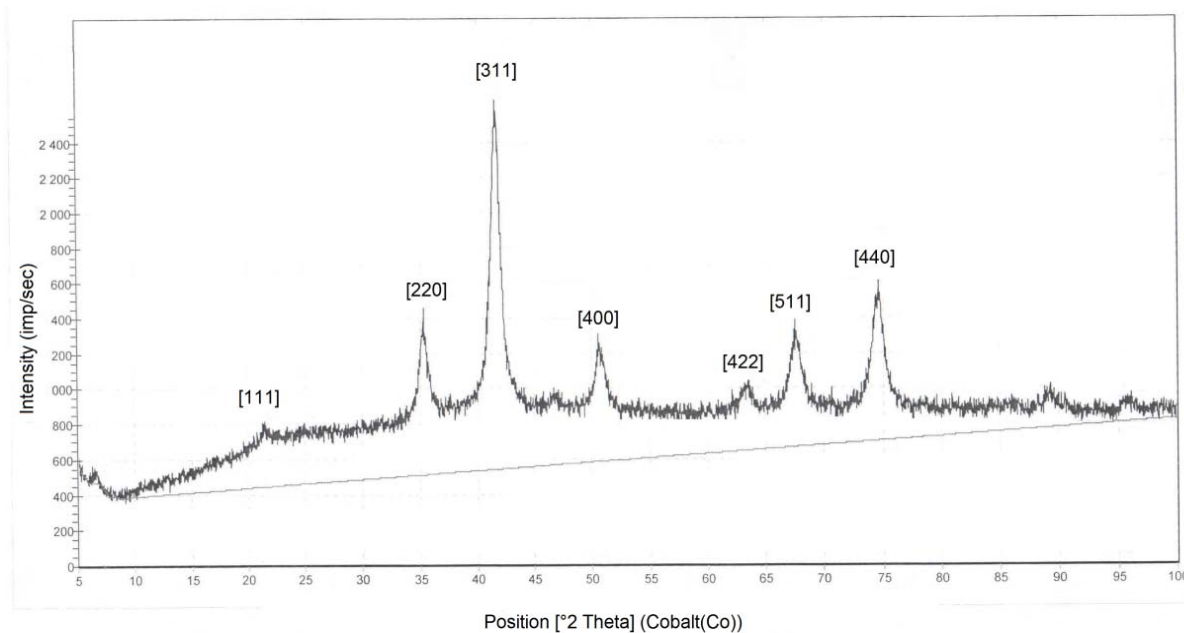


Figure 1 - X-ray diffraction pattern of the synthesized magnetic sample

According to spectrophotometric data, the addition of a reducing agent to a solution of palladium salt and a polymer leads to completely reduction of the metal ions at a ratio of $\text{Pd}:\text{NaBH}_4 = 2:1$. The disappearance of the absorption band of PdCl_4^{2-} ions at 425 nm in the spectrum of the reduced sample has confirmed the transition of Pd^{2+} to the zerovalent state (Figure 2).

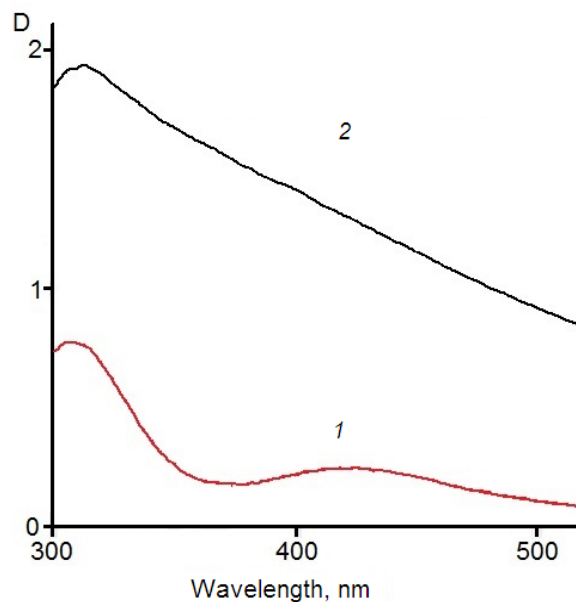


Figure 2 - The absorption spectrum of the palladium salt solution before (curve 1) and after (curve 2) metal reduction

The catalysts were prepared by adsorption of polymer-protected palladium particles onto the synthesized magnetic material. Clarity of the mother liquor after magnetic separation indicated the quantitative fixation of the metal-macromolecule active phase to the support (Figure 3). The active phase was probably fixed to support due to reducing the surface energy of the magnetic nanoparticles.

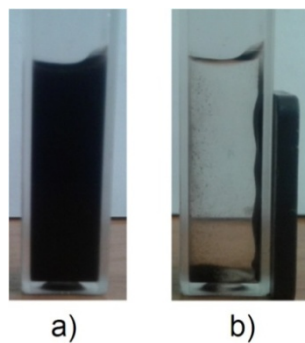


Figure 3 – Photos of the Pd-PAM(1:15) and MS mixture before (a) and after (b) magnetic separation

The complete Pd adsorption of on the magnetic sample was also confirmed by the results of the elemental analysis of the Pd-PAM(1:15)/MS catalyst (Table 1) in which the metal content was close to the calculated data and was 1wt.% of the sum of all components.

Table 1 – Elemental analysis data of the Pd-PAM(1:15)/MS catalyst

Element concentration, wt. %			
O	Cl	Fe	Pd
29.00	0.77	68.50	1.00

Catalytic properties of Pd-polymer/MS in phenylacetylene hydrogenation

Hydrogenation of phenylacetylene on 1% Pd-PAA(1:5)/MS in the first 70 minutes proceeds at a constant rate (0.7×10^{-6} mol/s) which in ~70 minutes insignificantly increased. The sharp slowing of the reaction begins at the 90th minute (Figure 4, curve 1). The activity of 1% Pd-PAM(1:5)/MS catalyst is 1.3-1.7 times higher than that of the catalyst stabilized with polyacrylic acid, however, the kinetic curve form was similar (Figure 4, curve 2).

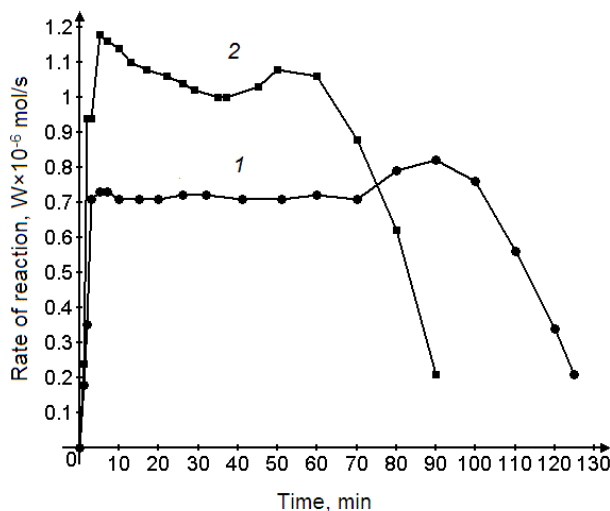


Figure 4 - Changes in the rate of phenylacetylene hydrogenation in the presence of (1) Pd-PAA(1:5)/MS and (2) Pd-PAM(1:5)/MS. Conditions: catalyst sample weight, 0.02 g; temperature, 40°C; H₂ pressure, 0.1 MPa; solvent, ethanol (25 mL); and initial phenylacetylene amount, 0.25 mL.

According to chromatographic analysis, a rapid increase in the styrene content occurred on Pd-PAA(1:5)/MS in the initial period of time. Then its amount decreased due to its reduction to ethylbenzene (Figure 5a). Similar changing the composition of the reaction products was observed during hydrogenation

of phenylacetylene on Pd-PAM(1:5)/MS (Figure 5b). The maximum styrene content reached at 70th minute (78.1%) and at 45th minute (81.0%) on PAA- and PAM-stabilized catalysts, correspondingly. These time values coincide with the time of increase in the reaction rates on these catalysts (Figure 4, curves 1 and 2)

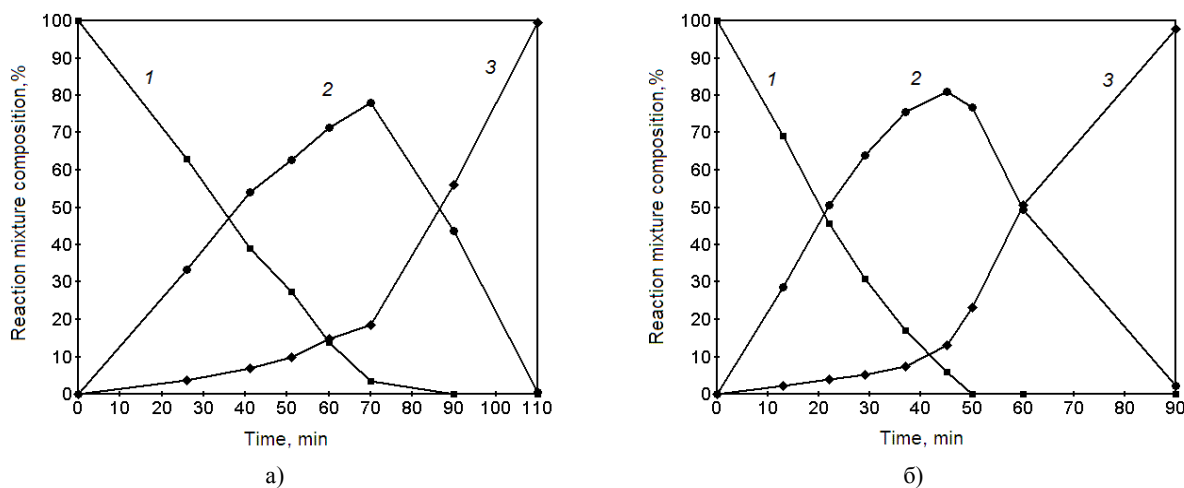


Figure 5 - Changes in the composition of reaction mixtures during of phenylacetylene hydrogenation on (a) Pd-PAA(1:5)/MS and (b) Pd-PAM(1:5)/MS: (1) phenylacetylene, (2) styrene, and (3) ethylbenzene. Conditions: catalyst sample weight, 0.02 g; temperature, 40°C; H₂ pressure, 0.1 MPa; solvent, ethanol (25 mL); and initial phenylacetylene amount, 0.25 mL.

The lower activity and selectivity of Pd-PAA(1:5)/MS (80.9%) compared with Pd-PAM(1:5)/MS catalyst (88.0%) (Table 2) was probably due to the stronger interaction of PAA with catalyst components [24], and, as a consequence, more difficult access of the substrate to palladium active centers.

Table 2 - Results of the hydrogenation of phenylacetylene (0.25 mL) on Pd-polymer/MS catalysts (0.02 g) in ethanol (25 mL) at 40°C and 0.1 MPa

Catalyst	W×10 ⁻⁶ , mol/s		Selectivity for styrene, %	Conversion, %
	C≡C	C=C		
Pd-PAA(1:5)/MS	0.73	0.82	80.9	96.5
Pd-PAM(1:5)/MS	1.18	1.08	88.0	92.0

The catalyst was easily separated from the reaction medium by magnetic field (Figure 6) at the end of the process indicating the prospect for development of such type of new nanosized magnetic materials for catalysis.

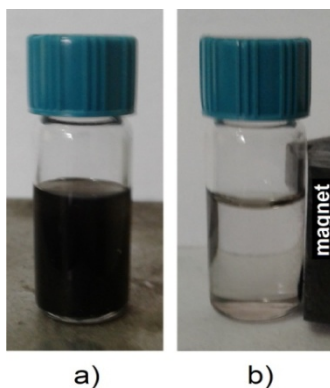


Figure 6 – Images of reaction mixture before (a) and after (b) magnetic separation of Pd-PAM/MS catalyst

The next step of study demonstrated the effect of the ratio of active phase components (Pd:PAM = 1:5, 1:10 and 1:15) on the catalytic properties of Pd-PAM/MS. It was found that the reaction rate increased with increasing polymer content in the catalysts. The highest rate (1.36×10^{-6} mol/s) of phenylacetylene hydrogenation showed the catalyst with the ratio of Pd:PAM=1:15 (Figure 7).

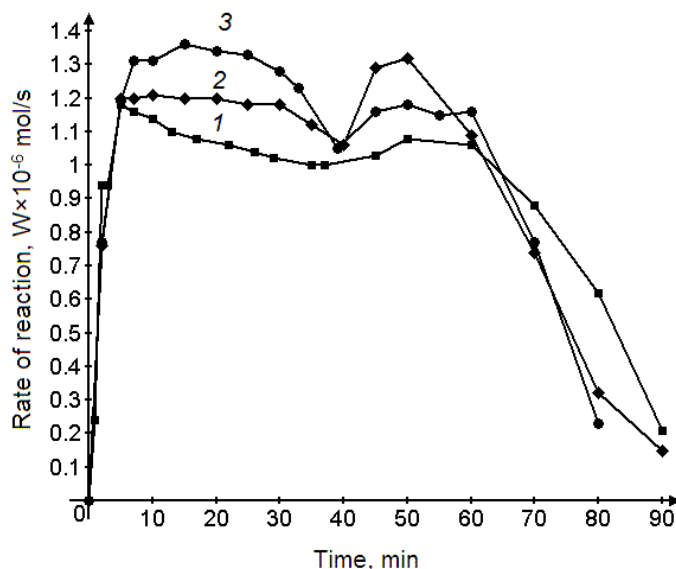


Figure 7 - Changes in the rate of phenylacetylene hydrogenation in the presence of Pd-PAM/MS catalysts: (1) Pd:PAM = 1:5; (2) Pd:PAM = 1:10 and (3) Pd:PAM = 1:15. Conditions: catalyst sample weight, 0.02 g; temperature, 40°C; H₂ pressure, 0.1 MPa; solvent, ethanol (25 mL); and initial phenylacetylene amount, 0.25 mL.

The selectivity for styrene on all studied Pd-PAM/MS catalysts was close to 88-89% at the substrate conversion of 92%. Thus, it has been shown that the activity of the catalysts increases with increasing polyacrylamide polymer content, while the selectivity of the process remains practically unchanged (Table 3). These results can indicate formation of uniform active centers on magnetic support.

Table 3 - Results of the hydrogenation of phenylacetylene (0.25 mL) on Pd-PAM/MS catalysts (0.02 g) in ethanol (25 mL) at 40°C and 0.1 MPa

Catalyst	W×10 ⁻⁶ , mol/s		Selectivity for styrene, %	Conversion, %
	C≡C	C=C		
Pd-PAM(1:5)/MS	1.18	1.08	88.0	92.0
Pd-PAM(1:10)/MS	1.21	1.32	88.1	95.1
Pd-PAM(1:15)/MS	1.36	1.18	89.2	93.0

Conclusion

A simple method for the synthesis of supported palladium hydrogenation catalysts with magnetic properties has been developed. The procedure consisted of mixing a colloidal solution of polymer-stabilized palladium with a suspension of a highly disperse magnetic support (γ -Fe₂O₃). The active phase was fixed due to reducing the surface energy of the magnetic nanoparticles as a result of the adsorption of the polymer-metal complex.

The results of testing the obtained catalysts in the hydrogenation of phenylacetylene have demonstrated their high activity (reaction rates are 0.73 - 1.36×10^{-6} mol/s) and selectivity for styrene (80.9-89.2%). The optimum catalytic properties showed the supported palladium composite stabilized with polyacrylamide with Pd:PAA ratio of 1:15. The advantage of the use of magnetic nanosized materials as supports is formation of dispersed catalysts close to colloidal systems and simplicity of their separation from reaction products by magnetic field.

Acknowledgments

The work was carried out with the financial support of the State Committee of Science of the Ministry of Education and Science of the Republic of Kazakhstan (grant AP05130377).

REFERENCES

- [1] Lu A-H, Salabas E L, Schuth F (2007) Magnetic nanoparticles: synthesis, protection, functionalization, and application, *Angew. Chem. Int. Ed.*, 46:1222-1244. DOI:10.1002/anie.200602866 (in Eng)
- [2] Mohammed L, Gomaa H G, Ragab D, Zhu J (2017) Magnetic nanoparticles for environmental and biomedical applications: a review, *Particuology*, 30:1-14. DOI:10.1016/j.partic.2016.06.001 (in Eng)
- [3] Wei Y, Han B, Hu X, Lin Y, Wang X, Deng X (2012) Synthesis of Fe₃O₄ nanoparticles and their magnetic properties, *Procedia Engineering*, 27:632-637. DOI:10.1016/j.proeng.2011.12.498 (in Eng)
- [4] Khojasteh H, Mirkhani V, Moghadam M, Tangestaninejad S, Mohammadpoor-Baltork I (2015) Palladium loaded on magnetic nanoparticles as efficient and recyclable catalyst for the Suzuki-Miyaura reaction, *J. Nano Struct.*, 5:271-280. DOI: 10.7508/jns.2015.03.009 (in Eng)
- [5] Liu W, Tian F, Yu J, Bi Y (2016) Magnetic mesoporous palladium catalyzed selective hydrogenation of sunflower oil, *J. Oleo Sci.*, 65:451-458. DOI:10.5650/jos.ess15169 (in Eng)
- [6] Abu-Reziq R, Wang D, Post M, Alper H (2007) Platinum nanoparticles supported on ionic liquid-modified magnetic nanoparticles: selective hydrogenation catalysts, *Adv. Synth. Catal.*, 349:2145-2150. DOI: 10.1002/adsc.200700129 (in Eng)
- [7] Guan H, Chao C, Kong W, Hu Z, Zhao Y, Yuan S, Zhang B (2017) Magnetic porous PtNi/SiO₂ nanofibers for catalytic hydrogenation of p-nitrophenol, *J. Nanopart. Res.*, 19:187-197. DOI: 10.1007/s11051-017-3884-9 (in Eng)
- [8] Zhang J, Wang Y, Ji H, Wei Y, Wu N, Zuo B, Wang Q (2005) Magnetic nanocomposite catalysts with high activity and selectivity for selective hydrogenation of ortho-chloronitrobenzene, *Journal of Catalysis*, 229:114-118. DOI:10.1016/j.jcat.2004.09.029 (in Eng)
- [9] Chen H, Zhang P, Tan W, Jiang F, Tang R (2014) Palladium supported on amino functionalized magnetic MCM-41 for catalytic hydrogenation of aqueous bromate, *RSC Adv.*, 4:38743-38749. DOI: 10.1039/C4RA05593D (in Eng)
- [10] Laska U, Frost C G, Price G J, Plucinski P K (2009) Easy-separable magnetic nanoparticle-supported Pd catalysts: kinetics, stability and catalyst re-use, *Journal of Catalysis*, 268:318-328. DOI:10.1016/j.jcat.2009.10.001 (in Eng)
- [11] Zhou P, Li D, Jin S, Chen S, Zhang Z (2016) Catalytic transfer hydrogenation of nitrocompounds into amines over magnetic graphene oxide supported Pd nanoparticles, *International Journal of Hydrogen Energy*, 41:15218-15224. DOI: 10.1016/j.ijhydene.2016.06.257 (in Eng)
- [12] Gyergyek S, Kocjan A, Bjelić A, Grilc M, Likozar B, Makovec D (2018) Magnetically separable Ru-based nano-catalyst for the hydrogenation/hydro-deoxygenation of lignin-derived platform chemicals, *Mater. Res. Lett.*, 6:426-431. DOI: 10.1080/21663831.2018.1477847 (in Eng)
- [13] Hu A, Yee G T, Lin W (2005) Magnetically recoverable chiral catalysts immobilized on magnetite nanoparticles for asymmetric hydrogenation of aromatic ketones, *J. Am. Chem. Soc.*, 127:12486-12487. DOI: 10.1021/ja053881o (in Eng)
- [14] Sydnes M O (2017) The use of palladium on magnetic support as catalyst for Suzuki-Miyaura cross-coupling reactions, *Catalysts*, 7:1-14. DOI:10.3390/catal7010035 (in Eng)
- [15] Biglione C, Cappelletti A L, Strumia M C, Martín S E, Uberman P M (2018) Magnetic Pd nanocatalyst Fe₃O₄@Pd for C-C bond formation and hydrogenation reactions, *J. Nanopart. Res.*, 20:127-142. DOI: 10.1007/s11051-018-4233-3 (in Eng)
- [16] Nasir Baig R B, Varma R S (2014) Magnetic carbon-supported palladium nanoparticles: an efficient and sustainable catalyst for hydrogenation reactions, *ACS Sustainable Chemistry & Engineering*, 2:2155-2158. DOI: 10.1021/sc500341h (in Eng)
- [17] Zhou J, Dong Z, Yang H, Shi Z, Zhou X, Li R (2013) Pd immobilized on magnetic chitosan as a heterogeneous catalyst for acetalization and hydrogenation reactions, *Applied Surface Science*, 279:360-366. DOI: 10.1016/j.apsusc.2013.04.113 (in Eng)
- [18] Shin J Y, Jung Y, Kim S J, Lee S (2011) Supported Pd nanocatalysts onto ionic silica-coated magnetic particles for catalysis in ionic liquids, *Bull. Korean Chem. Soc.*, 32:3105-3108. DOI: 10.5012/bkcs.2011.32.8.3105 (in Eng)
- [19] Gawande M B, Rathi A K, Branco P S, Varma R S (2013) Sustainable utility of magnetically recyclable nano-catalysts in water: applications in organic synthesis, *Appl. Sci.*, 3:656-674. DOI:10.3390/app3040656 (in Eng)
- [20] Mulahmetovic E, Hargaden G C (2017) Recent advances in the development of magnetic catalysts for the Suzuki reaction, *Review Journal of Chemistry*, 7:373-398. DOI: 10.1134/S2079978017030037 (in Eng)
- [21] Abu-Dief A M, Abdel-Fatah S M (2018) Development and functionalization of magnetic nanoparticles as powerful and green catalysts for organic synthesis, *Beni-Suef University Journal of Basic and Applied Sciences*, 7:55-67. DOI: 10.1016/j.bjbas.2017.05.008 (in Eng)
- [22] Zharmagambetova A K, Seitkalieva K S, Talgatov E T, Auezkhanova A S, Dzhardimalieva G I, Pomogailo A D (2016) Polymer-modified supported palladium catalysts for the hydrogenation of acetylene compounds, *Kinet. Catal.*, 57:360-367. DOI: 10.1134/S0023158416030174 (in Eng)

[23] Iconaru S L, Prodan A M, Motelica-Heino M, Sizaret S, Predoi D (2012) Synthesis and characterization of polysaccharide-maghemite composite nanoparticles and their antibacterial properties, *Nanoscale Research Letters*, 7:576. DOI: 10.1186/1556-276X-7-576

[24] Ospanova A K, Ashymhan N S, Berdybek G, Tastanov N (2014) Physico-chemical characteristics of complexation processes of transition metal ions with polyelectrolytes [Fiziko-khimicheskiye kharakteristiki protsessov kompleksobrazovaniya ionov perekhodnykh metallov s polielektrolitami], *News of the NAS RK. Series of chemistry and technology [Izvestiya NAN RK. Seriya khimii i tekhnologii]*, 4:59-65. <https://doi.org/10.32014/2018.%202518-1491> (In Russian) ЭОК 541.128.13:542.975'973:541.64

**Э.Т. Талғатов, А.С. Әуезханова, Н.Ж. Тумабаев, С.Н. Ахметова,
Қ.С. Сейтқалиева, Е.Ә. Бегмат, Ә.Қ. Жармағамбетова**

«Д.В. Сокольский атындағы жаңармай, катализ және электрохимия институты» АҚ, Алматы, Қазақстан

ФЕНИЛАЦЕТИЛЕНДІ ГИДРЛЕУГЕ АРНАЛҒАН МАГНИТТІ ТАСЫМАЛДАҒЫШҚА ОТЫРҒЫЗЫЛҒАН ПОЛИМЕР-ПАЛЛАДИЙ КАТАЛИЗАТОРЛАРЫ

Аннотация. Магнитті тасымалдағышқа отырғызылған Pd-полимер катализаторлары адсорбциялық әдіспен дайындалды. Магнитті тасымалдағыш темір хлоридтерін натрий гидроксидімен бірге $Fe^{3+}:Fe^{2+} = 2:1$ қатынаста біріктіріп отырғызу әдісімен синтезделінді. Палладидің коллоидты ертінділер сериясы полиакриламид (ПАА) және полиакрил қышқылдарының (ПАК) қатысуымен әртүрлі палладидің полимерге мольдік қатынасында ($Pd:ПАК = 1:5$; $Pd:ПАА = 1:5$; $Pd:ПАА = 1:10$ и $Pd:ПАА = 1:15$) натрий борогидридмен K_2PdCl_4 тотықсыздандыру арқылы алынды.

Бастапқы компоненттер және катализаторлар физико химиялық әдістермен зерттелінді. РФА нәтижелері синтезделген магнит үлгісі кристалдық беті бойынша шпинальды құрылысы бар маггемитқа сәйкес екендігі көрсетті және бөлшектердің орташа өлшемі 8,5 нм тең. 425 нм кезінде $PdCl_4^{2-}$ иондарының жұтылу сызықтарының жоғалуы палладидің толық қалпына келгенін дәлелдейді. Элементті анализ бойынша катализатордағы палладий мөлшері есептеп алынған нәтижеге жақын және барлық компоненттер суммасының $I_{мас. \%}$ құрайды, яғни магнитті тасымалдағышқа полимермен протектірленген палладий бөлшектерінің отырғанын растайды.

Фенилацетиленді гидрлеуде барлық катализаторлар жоғары белсенділік және стирол бойынша жоғары селективтілік ($W_{C=C} = 0,73-1,36 \times 10^{-6}$ моль c^{-1} , $S_{ст} = 80,9-89,2\%$) көрсетті. ПАА-тұрақтандырылған палладий катализаторы Pd-ПАК/МТ катализаторымен салыстырғанда стиролдың шығымы және реакцияның жылдамдығы жоғары болатындығын көрсетті. Полмердің мөлшерін арттыру Pd-ПАА/МТ катализаторының каталитикалық қасиетіне аздап әсер етеді.

Түйін сөздер. Палладий, полимер, магнитті катализатор, гидрлеу, фенилацетилен.

УДК 541.128.13:542.975'973:541.64

**Э.Т. Талғатов, А.С. Ауезханова, Н.Ж. Тумабаев, С.Н. Ахметова,
Қ.С. Сейтқалиева, Е.А. Бегмат, А.К. Жармағамбетова**

АО «Институт топлива, катализа и электрохимии им. Д.В. Сокольского», Алматы, Казахстан

ПОЛИМЕР-ПАЛЛАДИЕВЫЕ КАТАЛИЗАТОРЫ НА МАГНИТНОМ НОСИТЕЛЕ ДЛЯ ГИДРИРОВАНИЯ ФЕНИЛАЦЕТИЛЕНА

Аннотация. Pd-полимер катализаторы, нанесенные на магнитный носитель (МН), были успешно приготовлены адсорбционным методом. Магнитный носитель синтезировали методом соосаждения хлоридов железа гидроксидом натрия в соотношении $Fe^{3+}:Fe^{2+} = 2:1$. Серию коллоидных растворов палладия получали путем восстановления K_2PdCl_4 борогидридом натрия в присутствии полиакриламида (ПАА) и полиакриловой кислоты (ПАК) с различным мольным отношением палладия к полимеру ($Pd:ПАК = 1:5$; $Pd:ПАА = 1:5$; $Pd:ПАА = 1:10$ и $Pd:ПАА = 1:15$).

Исходные компоненты и катализаторы были охарактеризованы физико-химическими методами. Результаты РФА показали, что синтезированный магнитный образец по кристаллическим плоскостям соответствует маггемиту со шпинальной структурой и имеет средний размер частиц 8,5 нм. Исчезновение полосы поглощения ионов PdCl_4^{2-} при 425 нм свидетельствовало о полном восстановлении палладия. Согласно элементному анализу содержание палладия в катализаторах близко к расчетным данным и составляет 1мас.% от суммы всех компонентов, что свидетельствует о количественном закреплении полимер-протектированных частиц палладия на магнитном носителе.

Результаты гидрирования фенилацетилена показали, что все катализаторы проявляют достаточно высокую активность и селективность по стиролу ($W_{\text{с=с}} = 0,73-1,36 \times 10^{-6}$ моль с^{-1} , $S_{\text{ст}} = 80,9-89,2\%$). ПАА-стабилизированный палладиевый катализатор показал более высокую скорость и выход стирола по сравнению с Pd-ПАК/МН катализатором. Увеличение содержания полимера не значительно влияет на каталитические свойства Pd-ПАА/МН катализатора.

Ключевые слова. Палладий, полимер, магнитный катализатор, гидрирование, фенилацетилен.

Information about authors:

Talgatov E.T. - Senior Researcher, Doctor PhD, Laboratory of Organic Catalysis, JSC "D.V. Sokolsky Institute of Fuel, Catalysis and Electrochemistry", Almaty, Kazakhstan. Tel: +77272916972, e-mail: eldar-talgatov@mail.ru, ORCID iD 0000-0001-8153-4765;

Auyezkhanova A.S. - Leading Researcher, Candidate of Chemical Sciences, Laboratory of Organic Catalysis, JSC "D.V. Sokolsky Institute of Fuel, Catalysis and Electrochemistry", Almaty, Kazakhstan. Tel: +77272916972, e-mail: a.assemgul@mail.ru, ORCID 0000-0002-8999-2864;

Tumabayev N.Z. - Leading Researcher, Candidate of Chemical Sciences, Laboratory of Organic Catalysis, JSC "D.V. Sokolsky Institute of Fuel, Catalysis and Electrochemistry", Almaty, Kazakhstan. Tel: +77272916972, e-mail: muhamed_76@mail.ru, ORCID 0000-0002-4871-0541;

Akhmetova S.N. - Junior Researcher, Laboratory of Organic Catalysis, JSC "D.V. Sokolsky Institute of Fuel, Catalysis and Electrochemistry", Almaty, Kazakhstan. Tel: +77272916972, e-mail: sn.akhmetova@mail.ru, ORCID 0000-0003-1048-2640;

Seitkalieva K.S. - Junior Researcher, Laboratory of Organic Catalysis, JSC "D.V. Sokolsky Institute of Fuel, Catalysis and Electrochemistry", Almaty, Kazakhstan. Tel: +77272916972, e-mail: kuralai_seitkalieva@mail.ru, ORCID 0000-0002-1502-8845;

Begmat Y.A. - Senior laboratory assistant, Laboratory of Organic Catalysis, JSC "D.V. Sokolsky Institute of Fuel, Catalysis and Electrochemistry", Almaty, Kazakhstan. Tel: +77272916972, e-mail: begmat1995@mail.ru, ORCID 0000-0002-7308-3471;

Zharmagambetova A.K. - Head of the laboratory of Organic Catalysis, Doctor of Chemical Sciences, Professor, JSC "D.V. Sokolsky Institute of Fuel, Catalysis and Electrochemistry", Almaty, Kazakhstan. Tel: +77272916972, e-mail: zhalima@mail.ru, ORCID ID 0000-0002-7494-6005

NEWS

OF THE NATIONAL ACADEMY OF SCIENCES OF THE REPUBLIC OF KAZAKHSTAN

SERIES CHEMISTRY AND TECHNOLOGY

ISSN 2224-5286

<https://doi.org/10.32014/2018.2518-1491.24>

Volume 6, Number 432 (2018), 38 – 45

УДК 537.9

МРПТИ 29.19.23

**B.T. Ermagambet¹, G.E. Remnev², S.M. Martemyanov²,
A.A. Bukharkin², Zh.M. Kasenova¹, N.U. Nurgaliyev¹**

¹LLP "Institute of Coal Chemistry and Technology", Astana, Kazakhstan

²Tomsk polytechnic university, Tomsk, Russia

E-mail: coaltech@bk.ru, remnev@tpu.ru, martemyanov@tpu.ru, ater@tpu.ru,
zhanar_k_68@mail.ru, nurgaliyev_nao@mail.ru

DIELECTRIC PROPERTIES OF THE COALS OF MAYKUBEN AND EKIBASTUZ BASINS

Abstract. The paper describes the measurement of the frequency dependences of electrical conductivity, permittivity and loss factor in the frequency range from 25 Hz to 1 MHz for coals of Maykuben and Ekibastuz basins. Measurements were made on plates 2-4 mm thick in a two-electrode measuring system. The technique of preparation of samples and results of measurements are described. From the point of view of electrophysical characteristics fossil fuels refer to weakly conducting materials with heterogeneous structure. The frequency dependences of their dielectric properties are mainly investigated for the development of high-frequency heating technologies. Thus, the heat release under the action of the applied field depends on the electrical conductivity (resistive losses) and the loss tangent (dielectric losses). In addition, the process of electric discharge phenomena in such materials also depends on the dielectric properties.

Key words: coal, dielectric properties, permittivity, conductivity, loss factor.

Introduction

Fossil fuels are the most valuable raw material for energy production and chemical synthesis. Effective technologies for their processing can allow receiving products with high added value without damage to the environment. A number of such technologies can be based on pyrolytic processing. These include aboveground and underground pyrolytic conversion and gasification. Aboveground gasification of coal has a long history with periods of rapid development and recessions [1, 2]. To date, apart from traditional and industrially developed technologies, more promising ones have been developed, such as plasma, catalytic, layer gasification with reversed blowing [3, 4].

Underground conversion is realized by heating of the coal bed in situ and taking of pyrolysis products through the wells. This way of the coal deposits development looks the most promising and environmentally safe [5]. Access to the formation in this case organizes via wells. Heating can be realized by incomplete oxidation of the coal [6], heat-conducting heating [7, 8], electric heating [9, 10, 11], etc. In our opinion, one of the effective methods for coal heating is electrophysical heating, based on the action of an electromagnetic field of high voltage [12, 13].

From the point of view of electrophysical characteristics fossil fuels refer to weakly conducting materials with heterogeneous structure. The frequency dependences of their dielectric properties are mainly investigated for the development of high-frequency heating technologies [14-17]. Thus, the heat release under the action of the applied field depends on the electrical conductivity (resistive losses) and the loss tangent (dielectric losses). In addition, the process of electric discharge phenomena in such materials also depends on the dielectric properties. For example, the maximum electric field strength on the gas pores is determined by the relative permittivity [18]. Therefore, the dielectric properties will affect the

heat release, the electrical discharge phenomena (partial discharges, triaging) and, as a consequence, the technical characteristics of the equipment necessary for heating.

The paper describes the technique and results of measuring of frequency dependences of the specific electric conductivity, relative permittivity and loss tangent, measured in the coals taken from the Maykuben, Bogatyr and Saryadyr strip mines (Kazakhstan).

Research methodology

Measurement of dielectric properties requires the samples in the form of plates with a thickness of no more than 5 mm [19, 20]. Samples were cut from solid fragments of coal by a stone cutting machine with an abrasive-cut diamond-coated disc.

It is impossible to cut the plates directly from the coal fragment because of the cracks and low mechanical strength. To avoid the destruction, the samples were prepared as follows. A bar with dimensions $55 \times 55 \times 100$ mm was cut out from the initial fragment of coals (Figure 1,a). Then the bar was wrapped in a polyethylene film and poured into a solid ificated polyester resin (Figure 1,b).

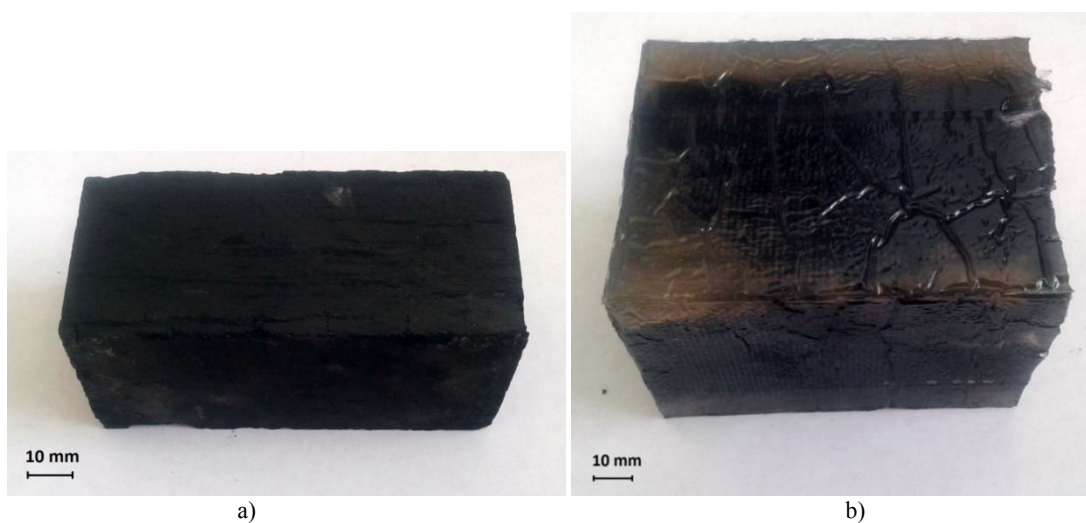


Figure 1 – Preparation of samples for dielectric properties measurement:
a) coal bar; b) bar, filled in polyester resin

Polyester resin gives the workpiece a mechanical strength and retains the coal during cutting. In this case, the layer of polyethylene film does not allow the resin to penetrate into the sample and further affect to the measurement results.

Then the resulting workpiece was cut into plates using an abrasive-cut diamond-coated disc (Fig. 2).

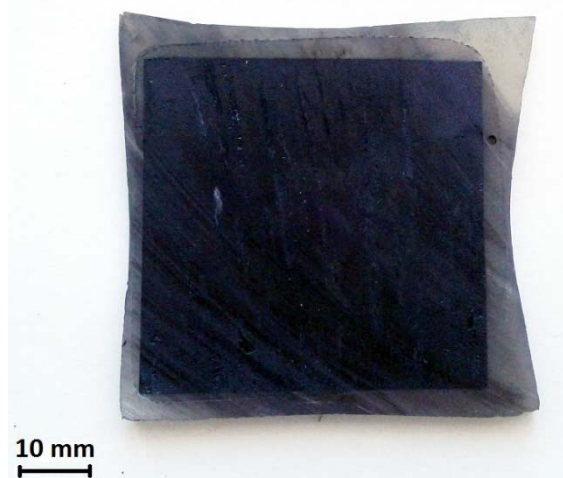


Figure 2 – Sample in the form of a plate for dielectric properties measurement

Since sedimentary rocks, including coal, have a layered structure, anisotropy of their dielectric properties is possible. If the applied electric field is oriented in the same direction as the layers in the coal, the value of the measured quantity can differ from the measurement, in which the applied field is oriented perpendicularly to the layers. Since in the developed technology of in-situ gasification the voltage applied to the electrodes will be oriented predominantly along the bedding layers of coals, the samples for measurement were made in such a way that the field of the measuring device was oriented along the layers of the sample.

Measurement of dielectric properties was carried out by the immittance meter E7-20 (MNIPI, Minsk, Belarus). The device generates a sinusoidal voltage of a specified frequency, applied to the measuring electrodes, and measures the electromagnetic response of the object. The meter has a PC-compatible interface RS-232C and can work under the control of a computer. Since measurements for the entire frequency range required the registration of a large number of measured values, software for controlling the instrument was designed to simplify the procedure.

In accordance with standard [19], measurements were made by the use of disk electrodes. Tool sets shown in Figure 3.

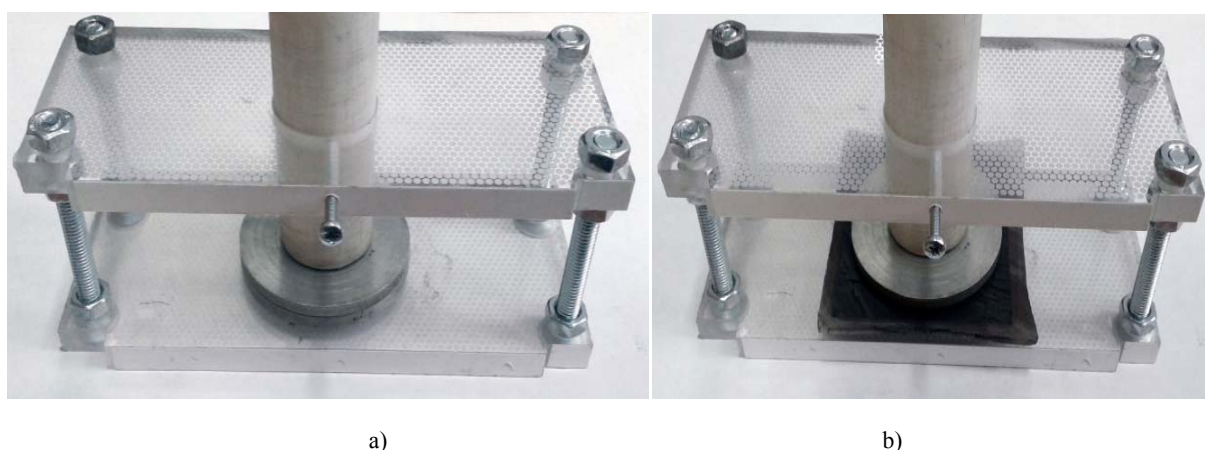


Figure 3 – Tool set for the measurement of dielectric properties:
a) without a sample, b) with an installed sample

The sample in the clamp is clamped between two disk aluminum electrodes with a diameter of 50 mm and a thickness of 3 mm. The thickness of the sample to ensure the necessary measurement accuracy should not exceed 5 mm.

The electrodes are connected to the immittance meter, and the measured values are recorded. The directly measured values are the loss tangent, the sample capacitance and the sample resistance. The specific permittivity ε is then calculated as the ratio of the measured capacitance of sample C and the capacitance of a similar air capacitor C_0 :

$$\varepsilon = \frac{C}{C_0}$$

The capacitance C_0 was measured in the absence of a sample and with inter electrode distance equal to the thickness of the sample. Specific electrical conductivity σ of the coal is defined as the ratio of the sample thickness h to the electrode area S and the measured resistance of the sample R :

$$\sigma = \frac{h}{S \cdot R}$$

For each of the investigated deposits, measurements were taken on 5 samples, after which the results of the measurements were averaged.

Results and discussion

Electric conductivity

The electrical conductivity σ characterizes the ability of a material to conduct an electric current. From the point of view of pyrolytic conversion technologies, the electrical conductivity along with the field strength E determines the heat energy P that will be released in the material from the flowing current:

$$P = \sigma \cdot E^2$$

Heating of materials having a low electrical conductivity value requires so high intensity of the applied field that industrial equipment for such heating is technologically unfeasible.

The measured frequency dependence of the electrical conductivity of investigated coals is shown in Figure 4.

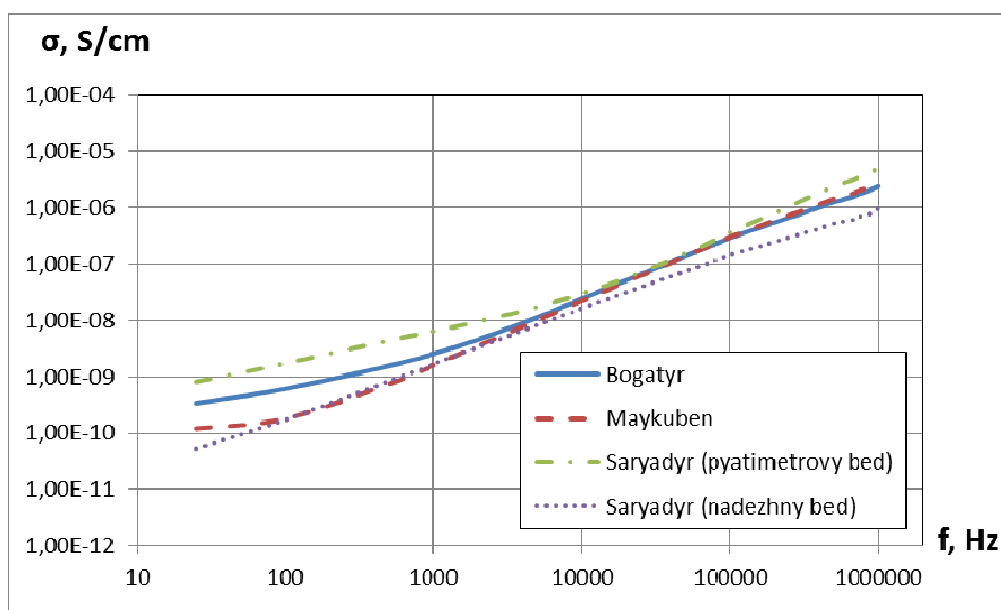


Figure 4 – Electric conductivity

In terms of the electrical conductivity, the coals are located on the boundary between semiconductors and dielectrics and belong to weakly conducting materials. Unlike materials with a homogeneous composition, coals tend to have a significant increase in electrical conductivity (by 3-4 orders of magnitude) with a frequency increasing from 25 Hz to 1 MHz. Presumably, this is connected with their mixed structure and the inclusion of a large number of crystallites and molecular clusters. At the boundaries of these macroscopic elements the energy structure of the electron shells of atoms and molecules is distorted, which is why free charge carriers with limited mobility and lifetime can arise in these places. The higher the frequency, the more such charge carriers can participate in conducting an electric current.

Since the electrical conductivity is very low at a low frequency, direct resistive heating of the investigated coals is possible only at high field strengths. Thus, by an electrical conductivity of 10^{-9} S/cm, field strength of 10^6 V/cm should be created to release the 1 kW of thermal energy.

Permittivity

The permittivity ε is an indicator of the polarization ability of the material. The higher its value, the greater the capacitive current can circulate through the material under the action of an alternating voltage. The results of measurements of the relative permittivity of the investigated coals are shown in Figure 5.

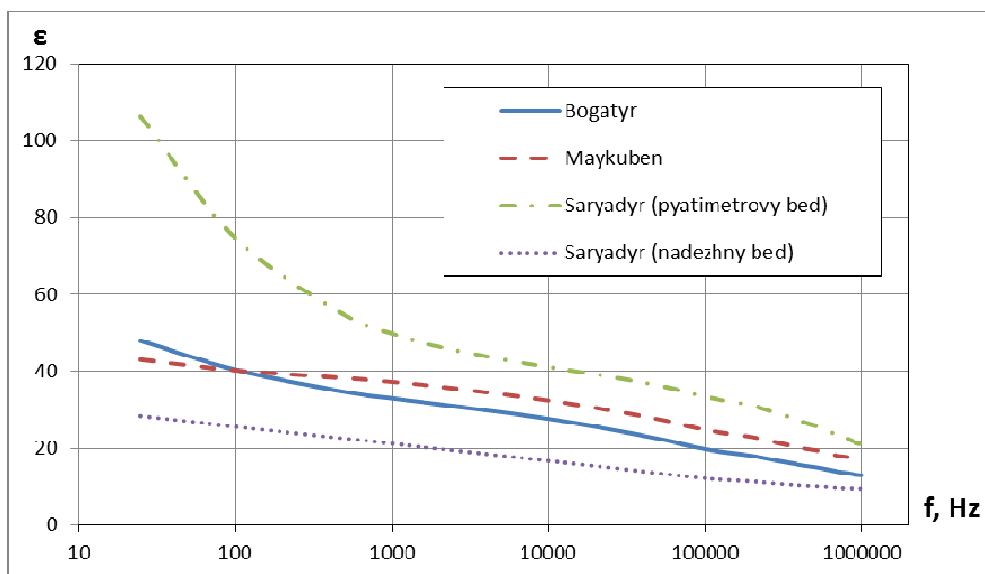


Figure 5 – Relative permittivity

As for most heterogeneous materials, the permittivity of coals decreases with an increasing of frequency from 25 Hz to 1 MHz in 3-5 times. For most mineral rocks in this frequency range ϵ is 3-10. For the coals in considered frequency range, the ϵ amounts to several tens, which indicates a very high polarization ability of the constituent components. Such components with high polarizability are water (sorbed, ion-bonded), OH groups, carboxyl groups, pyrite and other sulfur compounds.

In addition to the large value of the capacitive current, a high value of ϵ leads to an uneven distribution of the applied external voltage. As a result, significant field strength caused by the Maxwell-Wagner effect is concentrated in the pores and gaseous inclusions. In accordance with this phenomenon, a charge accumulates at the boundaries between the solid and gaseous phases, the value of which is proportional to the ratio of the permittivities. Thus, because of the high ϵ value of the coals, when the external electromagnetic field is applied to the coal, the significant part of the field will fall on the pores, causing partial discharges by a relatively low value of the voltage.

Loss tangent

The loss tangent $\tan(\delta)$ shows the ratio of active power to reactive power when applying an alternating voltage to a fragment of a dielectric material. Active power, which is the power of dielectric losses, arises as a result of the displacement of polar atomic groups under the action of an external field. For the most of dielectric materials the value of $\tan(\delta)$ decreases with increasing of frequency having a resonance maximum at some frequency. At this frequency the rate of change of the external field and the velocity of the free mobility of the dipoles of matter coincide. For materials with the mixed structure the frequency dependence of the loss tangent will be the envelope of the resonant peaks of the various components (Figure 6).

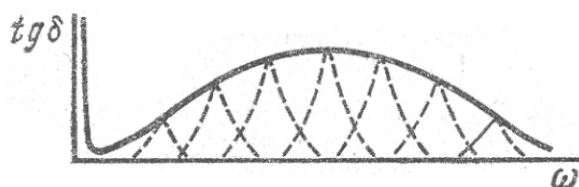


Figure 6 – Typical form of the curve $\tan(\delta) = f(\omega)$ for dielectric materials with the mixed structure [21]

This property is used in methods of high-frequency material heating, as, for example, by heating a subterranean oil reservoir, described in [22,23]. The measured frequency dependencies of $\tan(\delta)$ are shown in Figure 7.

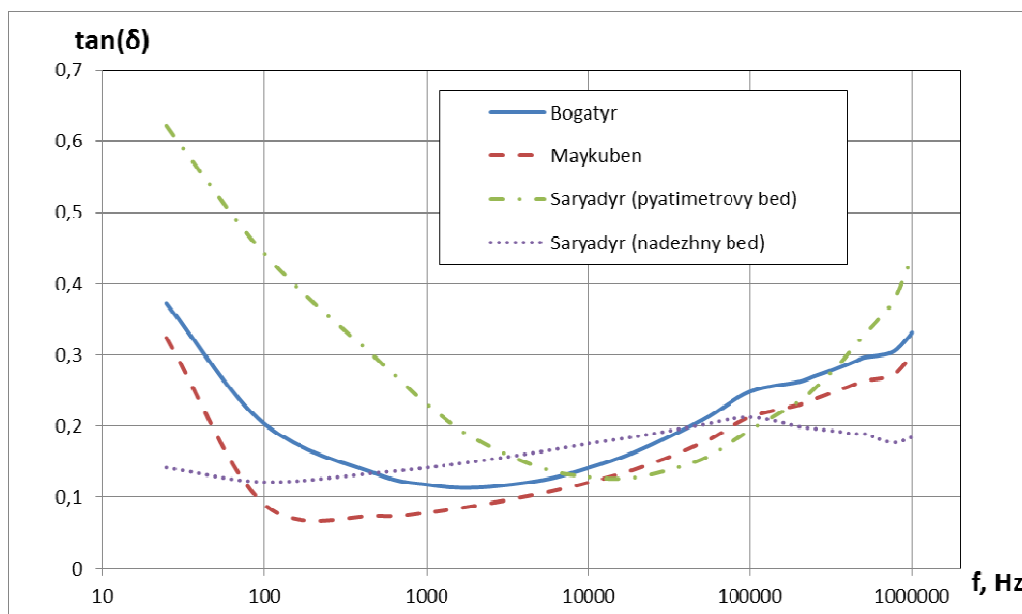


Figure 7 – Dielectric loss tangent

The measured dependencies shows that the peak values of $\tan(\delta)$ for the coals are outside the range of the considered frequencies. Therefore, the heating of these coals only due to dielectric losses needs to use the electromagnetic field of the frequency range > 1 MHz. The cost of powerful equipment operating at such frequencies is quite high. Thus, it can be assumed that the heating of the coals due to the dielectric losses of the high-frequency electromagnetic field is unlikely to be advisable. If we try to produce dielectric heating in the frequency range of < 1 MHz, a very large area of the electrodes will be required to provide heat release sufficient for heating.

Conclusions

The reaction of a substance to an electromagnetic field depends on the dielectric properties. For coals of different deposits, the dielectric properties can vary considerably. The described measurement results can be useful in the development of coals processing technologies which uses electromagnetic action, such as heating, enrichment, or electric discharge destruction. The described technic of samples making can be useful in carrying out similar measurements on solid fuels of other deposits.

Acknowledgement

The reported study was funded by the Ministry of Education and Science of Kazakhstan according to the research project IRN AP05131004 "Development of technology for underground gasification of coals of Ekibastuz and Maikuben basins and the creation of experimental industrial equipment".

REFERENCES

- [1] Delyagin G.N., Lebedev V.I., Permyakov B.A. (1987) Heat generating plants: Textbook for universities. *Stroyizdat, Moscow*.
- [2] Dyakova M.K., Lozovoy A.V. (1980) Hydrogenation of fuel. *ASUSSR, Moscow*.
- [3] Karpenko E.I. et al. (2000) Ecological and economic efficiency of plasma technologies for solid fuels processing. *Science, Novosibirsk*.
- [4] Karpenko E.I., Messerle V.E., Peregudov V.S. (2003) Method of plasma ignition of pulverized coal fuel [Sposob plazmennogo vosplamneniya pyleugol'nogo topliva]. Patent of the Russian Federation 2210700 [Patent Rossijskoj Federacii 2210700]. (In Russian).
- [5] Brandt A.R. (2009) Converting oil shale to liquid fuels: energy inputs and greenhouse gas emissions of the shell in-situ conversion process, *Environ. Sci. Technol.* 42(19):7489–7495. DOI:10.1021/es800531f (in Eng).
- [6] Kreinin E.V. (2016) Unconventional hydrocarbons sources, *Prospekt, Moscow*. ISBN: 978-5-392-19665-4.
- [7] Van Meurs P., DeRouffiguan E.P., Vinegar H.J., Lucid M.F. (1989) Conductively heating a subterranean oil shale to create permeability and subsequently produce oil. United States Patent 4886118.
- [8] Nicolas Kalmar (1984) In situ recovery oil from oil shale. United States Patent 4444258.

- [9] Passey Q.R., Thomas M.M., Bohacs K.M. (2001). Method for production of hydrocarbons from organic-rich rock. United States Patent 6918444.
- [10] Vinegar H.J., Sandberg C.L., C.K. Harris et al. (2013) High voltage temperature limited heaters. United States Patent 2013043029.
- [11] Vinegar H.J., Sandberg C.L., C.K. Harris et al. (2007) Systems, methods and processes for use in treating subsurface formations. Patent of Canada 2871784.
- [12] Lopatin V.V., Martemyanov S.M., Bukharkin A.A., Koryashov I.A. (2013) Underground pyrolytic conversion of oil shale. Proceedings of the 8th international forum on strategic technology, Ulaanbaatar. P.547-549.
- [13] Knyazeva A.G., Maslov A.L., Martemyanov S.M. (2018) A two-phase model of shale pyrolysis, *Fuel*, 228: 132–139. DOI:10.1016/j.fuel.2018.04.135 (in Eng).
- [14] Marland S., Merchant A., Rowson N. (2001) Dielectric properties of coal, *Fuel*, 80 (13):1839-1849. DOI:10.1016/S0016-2361(01)00050-3 (in Eng).
- [15] Salema A.A., Yeow Y.K., Ishaque K., Ani F.N., Afzal M.T., Hassan A. (2013) Dielectric properties and microwave heating of oil palm biomass and biochar, *Industrial Crops and Products*, 50: 366-374 (in Eng).
- [16] Nelson S.O., Beck-Montgomery S.R., Fanslow G.E., Bluhm D.D. (1981) Frequency dependence of the dielectric properties of coal, *Journal of Microwave Power*, 16(3): 319-326. DOI: 10.1080/16070658.1981.11689255 (in Eng).
- [17] Chatterjee I., Misra M. (1990) Dielectric properties of various ranks of coal, *Journal of microwave power and electromagnetic energy*, 25(4): 224-229. DOI:10.1080/08327823.1990.11688130 (in Eng).
- [18] Bukharkin A.A., Lopatin V.V., Martemyanov S.M., Koryashov I.A. (2014) Electrical discharge phenomena application for solid fossil fuels in-situ conversion, *Journal of Physics: Conference Series*, 552: 1-4. DOI:10.1088/1742-6596/552/1/012012 (in Eng).
- [19] State standard 25495-82. Rocks. Method for determining the permittivity and tangent of the dielectric loss angle [ГОСТ. Породы горные. Метод определения диэлектрической проницаемости и тангенса угла диэлектрических потерь]. Moscow, Russia, 1984. (In Russian).
- [20] Kazarnovskiy D.M., Tareev B.M. (1980) Control of insulating materials. *Energiya, Leningrad*.
- [21] Oreshkin P. T. (1977) Physics of Semiconductors and Dielectrics. *High school, Moscow*.
- [22] Dwight Eric Kinzer (2007). Processing hydrocarbons and Debye frequencies. United States Patent 7,312,428B2.
- [23] Zeilik B.S., Tyugay O.M. (2015) New Technology of Prognosis of Mineral Deposits (based on the concept of impact-explosive tectonics and Earth remote sensing data), *News of the National Academy of Sciences of the Republic of Kazakhstan*, Series of Geology and Technical Sciences, 3(411): 12-34. <https://doi.org/10.32014/2018.2518-170X> ISSN 2518-170X (Online), ISSN 2224-5278 (Print)

**Б.Т. Ермағамбет¹, Г.Е. Ремнев², С.М. Мартемьянов², А.А. Бухаркин²,
Ж.М. Касенова¹, Н.У. Нурғалиев¹**

¹«Көмір химиясы және технология институты» ЖШС, Астана қ, Қазақстан

²Томск политехникалық университеті, Томск, Ресей

МАЙҚҰБЫ ЖӘНЕ ЭКІБАСТҰЗ КӨМІР БАССЕЙНДЕРІНІҢ ДИЭЛЕКТРИКАЛЫҚ ҚАСИЕТТЕРІ

Аннотация. Мақалада Майкүбен және Екібастұз бассейндерінің көмірлері үшін 25 Гц-ден 1 МГц жиілік диапазонында электр өткізгіштігінің, диэлектрлік өтімділігінің және тангенс жоғалу бұрышының жиілік тәуелділігін өлшеу сипатталады. Екі электродты өлшеу жүйесінде қалыңдығы 2-4 мм пластинкаларда өлшеу жүргізілді. Үлгілерді дайындау әдістемесі және жүргізілген өлшемдердің нәтижелері сипатталған.

Қазба отыны электрофизикалық сипаттамалар тұрғысынан гетерофазды құрылымды әлсіз өткізгіш материалдарға жатады. Диэлектрлік қасиеттерінің жиіліктік тәуелділігі, негізінен, жоғары жиілікті жылу технологияларын әзірлеу мақсатында зерттеледі. Осылайша, берілген өрістің әсерінен жылу бөлу электр өткізгіштігіне (резистивті шығындар) және диэлектрлік шығынның тангенс бұрышына (диэлектрлік шығындар) байланысты. Мұндай материалдардағы электр пиролизінің ағымы жылуды өндіру үрдістеріне әсер ететін диэлектрлік қасиеттерге, электр разрядты құбылыстардың ағынына (ішінара разрядтар, қисық сызық) аса тәуелді.

Түйін сөздер: көмір, диэлектрикалық шығындар, диэлектрикалық өтімділігі, электр өткізгіштік, шығын коэффициенті

Б.Т. Ермагамбет¹, Г.Е. Ремнев², С.М. Мартемьянов², А.А. Бухаркин²,
Ж.М. Касенова¹, Н.У. Нурғалиев¹

¹ТОО «Институт химии угля и технологии», г.Астана, Казахстан

²Томский политехнический университет, Томск, Россия

ДИЭЛЕКТРИЧЕСКИЕ СВОЙСТВА УГЛЕЙ МАЙКУБЕНСКОГО И ЭКИБАСТУЗСКОГО БАССЕЙНОВ

Аннотация. В статье описано измерение частотных зависимостей электропроводности, диэлектрической проницаемости и тангенса угла потерь в частотном диапазоне от 25 Гц до 1 МГц для углей Майкубенского и Экибастузского бассейнов. Измерения проведены на пластинках толщиной

2-4 мм в двухэлектродной измерительной системе. Описана методика подготовки образцов и результаты проведенных измерений. Ископаемые угли с точки зрения электрофизических характеристик относятся к слабопроводящим материалам гетерофазного строения. Частотные зависимости их диэлектрических свойств исследуются, в основном, с целью разработки технологий высокочастотного нагрева. Так, выделение тепла под действием приложенного поля зависит от электропроводности (резистивные потери) и тангенса угла диэлектрических потерь (диэлектрические потери). Протекание электропиролиза в таких материалах сильно зависит от диэлектрических свойств, которые влияют на процессы выделение тепла, протекание электроразрядных явлений (частичные разряды, триинг).

Ключевые слова: уголь, диэлектрические потери, диэлектрическая проницаемость, электропроводность, коэффициент потерь

Information about the authors:

Yermagambet Bolat Toleukhanuly – Doctor of Chemical Science, Professor, Director of LLP "Institute of Coal Chemistry and Technology", Astana, Kazakhstan, e-mail: bake_yer@mail.ru;

Remnev Gennadiy Efimovich – Doctor of Technical Science, Professor, Tomsk polytechnic university, Tomsk, Russia, e-mail: remnev@tpu.ru;

Martemyanov Sergey Mikhaylovich – Candidate of Technical Science, Associate professor, Tomsk polytechnic university, Tomsk, Russia, martemyanov@tpu.ru;

Bukharkin Andrey Andreevich – Master of Technic and Technology, engineer, Tomsk polytechnic university, Tomsk, Russia, ater@tpu.ru;

Kassenova Zhanar Muratbekovna – Master of Chemical Sciences and Technology, Deputy Director of LLP "Institute of Coal Chemistry and Technology", Astana, Kazakhstan, e-mail: zhanar_k_68@mail.ru;

Nurgaliyev Nurken Uteuovich – Candidate of Chemical Science, Leading Researcher of LLP "Institute of Coal Chemistry and Technology", Astana, Kazakhstan, e-mail: nurgaliyev_nao@mail.ru

NEWS

OF THE NATIONAL ACADEMY OF SCIENCES OF THE REPUBLIC OF KAZAKHSTAN

SERIES CHEMISTRY AND TECHNOLOGY

ISSN 2224-5286

<https://doi.org/10.32014/2018.2518-1491.25>

Volume 6, Number 432 (2018), 46 – 52

A.R. Beisenbayev¹, A.N. Zhabayeva¹,
L.P. Suntsova², A.V. Dushkin², S.M. Adekenov¹

¹JSC International Research and Production Holding «Phytochemistry»,
4 M. Gazaliyev St., Karaganda, Kazakhstan;

²Institute of Solid Materials and Mechanochemistry of the RAS SB, 18 Kutateladze St.,
Novosibirsk, Russian Federation
e-mail: root@solid.nsc.ru; e-mail: phyto_pio@mail.ru

SYNTHESIS AND STUDY OF PINOSTROBIN OXIME SUPRAMOLECULAR COMPLEXES

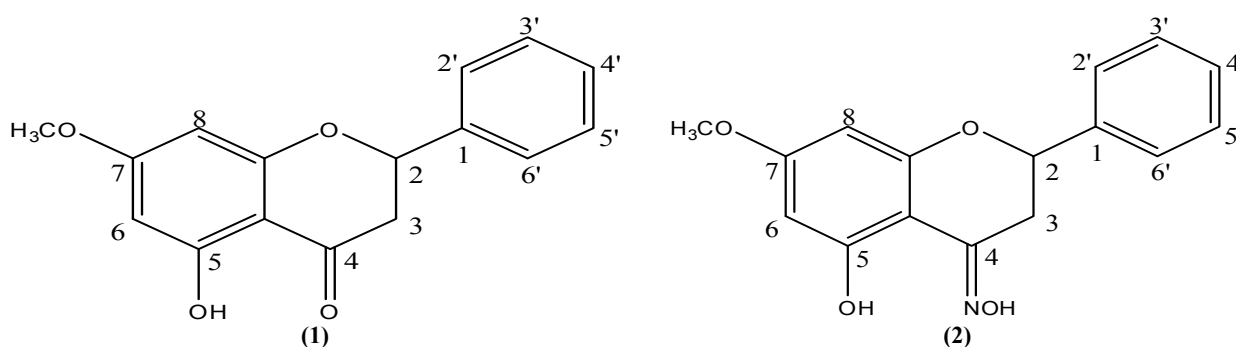
Abstract. The results of pinostrobin oxime derivatives studying, and its complexing ability with arabinogalactan, disodium salt of glycyrrhizic acid and magnesium carbonate, in particular, were discussed in this article. A supramolecular complex based on pinostrobin oxime with a higher water solubility was synthesized by mechanochemical treatment. Herewith, the complex of pinostrobin oxime with disodium salt of glycyrrhizic acid was shown to be the most effective. As the result, water solubility of this complex increased by 300 times.

Keywords: Pinostrobin oxime, arabinogalactan, disodium salt of glycyrrhizic acid, mechanochemical treatment, water solubility, supramolecular complexes.

1. Introduction

One of the priorities in the development of native pharmaceutical industry is a phytochemical manufacture development, based on original herbal drugs elaboration. In this case, herbal polyphenolic compounds perform a practical interest, as a new drug substance sources [1].

Flavonoids, including flavones, flavonols, flavanones and isoflavone, make large and important group of plant polyphenolic compounds. Pinostrobin (1), isolated from the *Populus balsamifera L.* buds, belongs to available flavanones.



It is known, that flavonoids isolated from *Populus balsamifera L.* buds have a hepatoprotective activity, a normalizing effect on synthesis of proteins in liver and prevent the cholestasis [2]. Antiproliferative, antimicrobial, neuroprotective and anti-inflammatory properties have been also found out in pinostrobin [3]. The development of pinostrobin chemical modification methods opens up new possibilities for obtaining original agents with specific biological activity.

A new high-potential compound pinostrobin oxime (PO) with hepatoprotective and antioxidant properties has been obtained by the reaction of pinostrobin with hydroxylamine hydrochloride [4].

On the basis of quantum chemical calculations [5], it can be said that the pinostrobin is a nucleophilic reagent with basic reaction centers at C3, C6, and C8 atoms, and the nucleophilic centers of pinostrobinoxime are O and N atoms, with the oxygen atom of the hydroxyl group at C5 possessing a relatively high electron density in comparison with the nitrogen atom of oxime.

The major disadvantage of PO, as well as other flavonoids, is its poor water solubility, which affects the bioavailability and inhibits pharmacological and preclinical studies, which makes it necessary to modify the molecules of active substances by transferring them to water-soluble salts. In this case, the emergence of drug side effects is possible, such as increased toxicity, which leads to the inexpediency of using original phytopreparations. The chemical behavior of flavonoids and their derivatives is unpredictable and unexpected in many cases, due to their polyfunctional nature. Various methods [6-13] of biologically active substances (BAS) water solubility enhancement are known, including a mechanochemical treatment. Mechanochemical treatment (MT) is a solid-phase reaction, it's a one-stage process with high efficiency and relative simplicity and it allows to avoid using solvents. The authors of [13-16] obtained supramolecular BAS complexes by mechanochemical treatment to increase bioavailability and noted the effectiveness of this method.

As a result of BAS mechanochemical treatment with an auxiliary component, which has an oligomeric, polymeric, or other macromolecular structure, a spontaneous association of an undetermined number of components occurs as spontaneous association of an indefinite number of components with the formation of supramolecular ensembles. Supramolecular ensembles have quite definite structural, conformational, thermodynamic, kinetic and dynamic properties; different types of interactions can be distinguished in them, differing in their strength, direction, dependence on distances and angles: coordination interactions with metal ions, electrostatic forces, hydrogen bonds, van der-Waals interactions, donor-acceptor interactions, etc. The strength of the interaction can vary over a wide range, depending on the type of bonds. In general, intermolecular bonds are weaker than covalent bonds, therefore they are less stable thermodynamically, but more flexible dynamically [17].

High-intensive MT can lead to rupture of strong covalent bonds, whereas low-intensive MT allows BAS molecules to "penetrate" into space inside the macromolecule or self-associative auxiliary substances, forming a supramolecular complex due to hydrogen bonds and van der Waals forces. Considering the absence of a covalent interaction between the molecules of BAS and the auxiliary substance, we can say that the structure of BAS remains unchanged.

Based on this, the actual task is the synthesis of a water-soluble complex with a biocompatible agent by MT, which allows to enhance water solubility of the substance and to preserve the molecule original structure.

2. Experimental part

2.1 PO complexes obtaining

The obtaining of solid dispersions was carried out in a BM-1 ball mill with a cylindrical vessel that has a fluoroplastic lining. Treatment mode: grinding media acceleration - 1g, total loading of processed mixture components – 18-22 g, vessel volume – 300 mL, grinding media – steel balls (steel grade III-X-15, diameter 22 mm, loading 675 g). Treatment duration was from 1 to 16 hours. Regardless of the barrel volume, the filling value of grinding media should be approximately 40%, and the filling value with processing material is 10-40%.

As complexing agents, we used:

- Arabinogalactan (3) (a good water soluble polysaccharide arabinogalactan (AG) isolated from *Larix dahurica*) produced by CJSC Ametis (Blagoveshchensk, Russia), Technical Specifications 9325-008-70692152-08. General formula $[(C_5H_8O_4)(C_6H_{10}O_5)_6]_n$. It is a solid amorphous substance, light brown in color, odorless, has a sweetish taste. Melting point is 240-250 °C. Easily soluble in water.

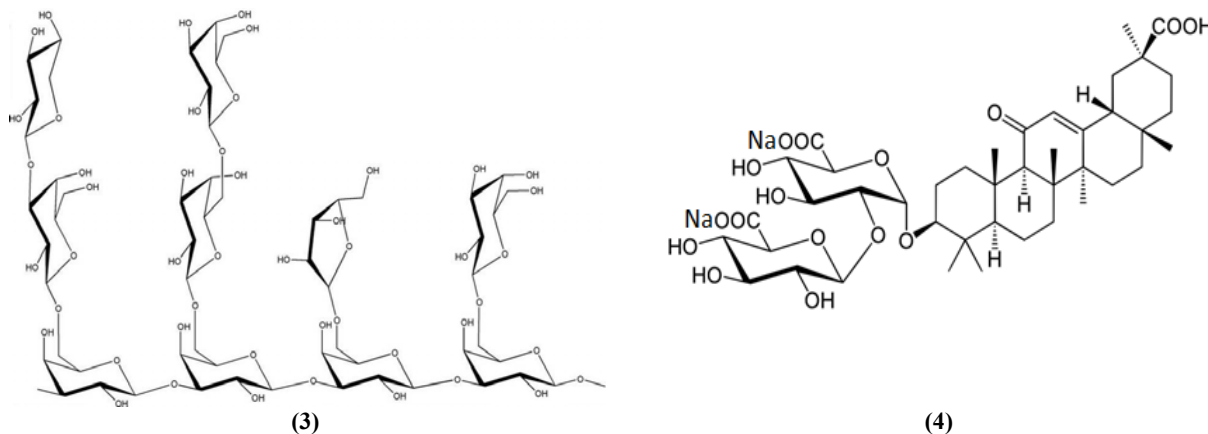
- Disodium salt of glycyrrhizic acid (4) (Na₂GA) – a natural saponin derivative, (CFS, 98%) produced by Shaanxi Sciphar Biotechnology Co., Ltd (Xi'an, China). The gross formula is C₄₂H₆₀O₁₆Na₂. It is a gray powder with a mustard tint. Does not melt. Tempered at a temperature of ~ 400 °C. Easily soluble in water.

- Polyvinylpyrrolidone (5) (PVP) is a synthetic polymer of Huangshan Bonsun Pharmaceuticals Co., Ltd. production (Huangshan, China). Common formula is C₆H₉NO)_n. It is a white, yellowish white powder

with no smell. It has sweetish taste. Fusion temperature is 150 °C. It is soluble in water, ethanol, and methanol.

- Magnesium carbonate substance ($MgCO_3$) of pharmacopeic purity (FSP42-3989-08)

Optimal mass ratio of components: PO/AG – 1:10, PO/ Na_2GA – 1:10, PO/ $MgCO_3$ – 5:1



2.2 High performance liquid chromatography (HPLC)

Agilent 1200 HPLC system with a reverse phase column (Zorbax Eclipse XDB-C18, 4.6×50 mm) was used to determine the concentration of PO. Column temperature is +30 °C. HPLC system equipped with diode-array detector and two pumps. The mobile phase is consisted of acetonitrile:acetate buffer (acetic acid/sodium acetate) pH=3,4, ratio is 60:40, flow rate is 1 mL/min and detector operated at 279 nm. PO concentration was determined in relation to a specially prepared alcohol solutions.

The dissolution kinetics of the initial PO was measured as a function of time to determine PO solubility, according to these data the optimal solution time was chosen. Then the sample weights of physical mixtures and mechanically treated PO mixtures\ auxiliary substance with pledged excess of PO were taken for obtaining of saturated solution. Sample weights were mixed in 10 ml of distilled water in incubator-shaker (37°C, 200 rpm) during the chosen period of time of solution (90 min). The the solution was centrifuged for 10 min (12000 rpm), supernatant liquid was filtered through the paper filter.

PO concentration in solution was determined by HPLC. PO concentration was determined in relation with prepared on purpose alcohol solutions.

2.3 Gel permeation chromatography (GPC)

The molecular weight distribution of the AG in complexes was analyzed by gel permeation chromatography on Agilent 1260. The solvent was a 0,1 M aqueous solution of $LiNO_3$, flow rate was 1 ml/min, sample concentration was 1 mg/mL. The calibration was based on standard dextrans with molecular weights of 25,12,5 kDa and D-galactose.

2.4 Scanning electron microscopy

Electronic images were acquired using a Hitachi TM-1000 microscope (Tokyo, Japan). Coating of samples with gold was performed by JEOL JFC-1600 auto fine coater. The coating parameters were as follows: amperage - 30mA, sputtering time - 30 s and film thickness was 15 nm.

3. Results and discussion

3.1 Obtained PO complexes

During the MT, the crystal particles of PO and the spherical particles of AG and Na_2GA are destroyed and a polydisperse powder is formed, consisting of 5-20 μm particles and their aggregates.

Arabinogalactan is a highly branched polysaccharide. This feature of the structure promotes the formation of strong supramolecular complexes with an active substance, the molecules of which can be bound by intermolecular bonds in the space formed by side chains.

There are hydrophilic and hydrophobic fragments in the molecule Na_2GA , so the possible mechanism of interaction of Na_2GA with PO in solution is the inclusion of molecules of these substances into micelles. Most probably, the Na_2GA molecules in a micelle are oriented by hydrophobic fragments inwards, and hydrophilic parts are oriented to the outer surface of the self-associates. In this case, the PO

molecules can be found in the internal hydrophobic part of the micelle and they also complex with external hydrophilic fragments.

PO refers to flavonoids, which are polyphenolic compounds with acidic properties. In alkaline pH ranges, their molecules are capable of ionization, and the ionized form, as a rule, has a higher water solubility. Thus, by shifting the equilibrium towards ionized molecules, we increased the total concentration of PO in the solution. As an alkaline agent, which allowed to "shift" the pH value to the required pH range of 10.2, we used a "pharmacopeia" substance of magnesium carbonate.

3.2 HPLC analyses result

The results shown in Fig. 1 display that after 16 hours of MT the water solubility of PO in complex with Na₂GA increased by 300 times, and in combination with AG - by 30 times, in complex with PVP by 42 times. After a 4-hour treatment, the water solubility of PO in a mixture with MgCO₃ increased 70-fold. After 1 and 2 hours of MT, the PO/MgCO₃ mixture proved to be more effective than other complexing agents, and the PO concentration during the long mechanical action changes insignificantly, and after four hours of treatment begins to decrease. The highest concentration of PO in solutions of the PO/AG complex is observed at 16 hours of MT, however, it does not differ much from the same value at 8 hours, which indicates that there is no need to increase the duration of the process. In the case of PO/Na₂GA, a significant increase in the water solubility of PO is observed with an increase in the processing time. Probably, the 24-hour MT of this complex will be even more effective.

Table 1 – HPLC analysis of supramolecular complexes of oximepinostrobin.

Substance	Mixing time, min	Mech. treatment time, h	The sample volume, μ l.	Peak time, h	Peak area	PO concentration, mg/l
PO	30	-	20	4,96	3,5	0,08
PO	60	-		4,96	12,92	0,33
PO	90	-		4,97	13,26	0,34
PO	137	-		4,96	22,00	0,57
PO	150	-		4,97	11,58	0,29
PO	180	-		4,97	11,32	0,29
PO	240	-		4,97	16,10	0,41
PO	300	-		4,97	16,66	0,43
PO+AG1/10	90	1		20	4,57	194,18
PO+AG1/10		2	4,96		229,08	6,08
PO+AG1/10		4	4,96		529,47	14,07
PO+AG1/10		8	4,96		669,89	17,81
PO+AG1/10		16	4,88		686,97	18,26
PO+AG1/10		120	16		4,89	781,03
PO+AG1/10	150	16	4,89	288,28	7,65	
PO+Na ₂ GA 1/10	90	1	5	4,95	140,39	14,92
PO+Na ₂ GA 1/10		2		4,92	187,08	19,89
PO+Na ₂ GA 1/10		4		4,93	397,24	42,26
PO+Na ₂ GA 1/10		8		4,94	662,89	70,53
PO+Na ₂ GA 1/10		16		4,87	1693,47	180,20
PO+Na ₂ GA 1/10		120		16	4,87	1403,08
PO+Na ₂ GA 1/10	150	16	4,87	1295,06	137,80	
PO+MgCO ₃ 5/1	90	1	20	4,93	1029,95	27,39
PO+MgCO ₃ 5/1		2	5	4,92	248,43	26,42
PO+MgCO ₃ 5/1		4	5	4,92	268,46	28,55
PO+MgCO ₃ 5/1		8	20	4,94	1017,84	27,06
PO+MgCO ₃ 5/1		16	20	4,95	550,76	14,64
PO+PVP1/10		90	1	20	4,77	489,75
PO+PVP1/10	2		4,6		914,97	24,33
PO+PVP1/10	4		4,62		605,35	16,09
PO+PVP1/10	8		4,86		606,83	16,13
PO+PVP1/10	16		4,92		963,33	25,61

The obtained results show that an increase in the water solubility of a substance based on pinostrobin oxime (PO) was achieved by the formation of supramolecular PO complexes by the method of mechanochemical treatment. Water-soluble polysaccharide arabinogalactan (AG) from Dahurian larch and

a vegetable saponin derivative disodium salt of glycyrrhizic acid (Na₂GA) were used as complexing agents. Structural features of complexing agents make it possible to form supramolecular complexes with the processed substance, molecules of what form hydrogen bonds in the intermolecular space formed by macromolecules of complexing substances. MgCO₃ was also used as an agent for shifting the pH of solid PO dispersions to a slightly alkaline range, what increases water solubility as well. The concentration of PO in the aqueous solutions of the obtained samples was determined by HPLC.

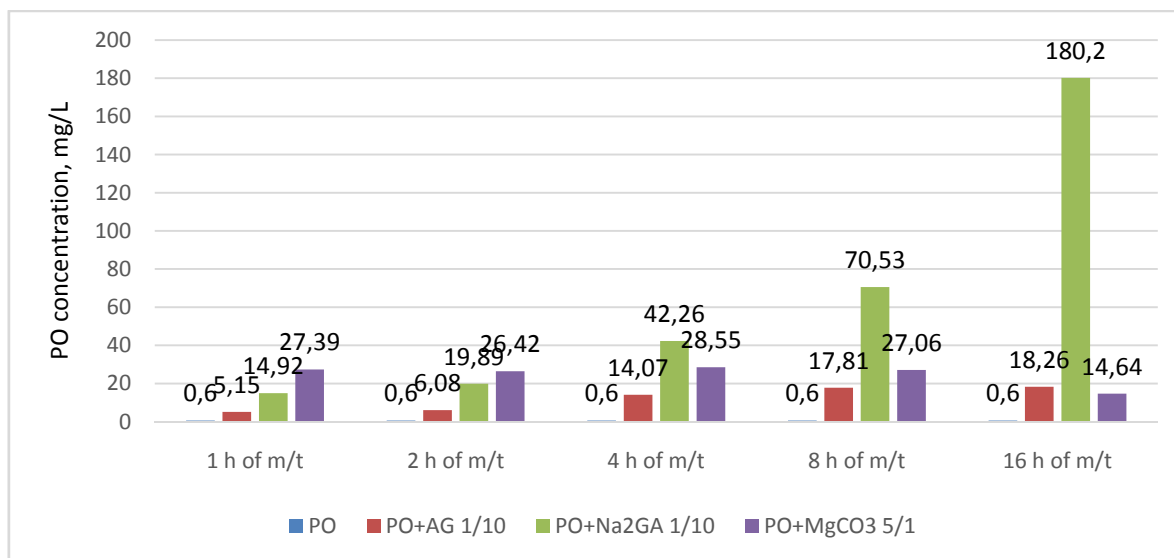


Figure 1 - Results of HPLC analysis of intermolecular complexes of oximepinostrobin. Dependence of the pinostrobinoxime concentration in solutions of intermolecular complexes on the time of MT.

3.3 GPC analyses of PO/AG

According to the data presented in Table 1, after MT of PO with AG, the average molecular weight of AG and the degree of polydispersity (M_w / M_n) change slightly. Also, MT of PO with AG leads to a slight decrease in the proportion of arabinose fragments in the molecule of the polysaccharide arabinogalactan, which does not depend on the time of mechanical action.

Table 1 - Molecular weight distribution of machined mixture of oxime pinostrobin with arabinogalactan

Sample	The conditions of MT, the ratio of OPB / AG	MM	M_w/M_n	Area of peaks with different MM
AG init.. reprecipitated	-	18060 445	1,44	99,9 0,1
PO/AG	1:5, $\tau=4$ h	18245 585	1,21 1,35	94,4 5,6
PO/AG	1:10, $\tau=4$ h	18105 550	1,37 1,13	98,4 1,6
PO/AG	1:15, $\tau=4$ h	18105 775	1,40 1,09	99,1 0,9
PO/AG	1:5, $\tau=8$ h	18290 570	1,38 1,2	94,9 5,1
PO/AG	1:10, $\tau=8$ h	18220 660	1,42 1,23	93,7 6,3
PO/AG	1:15, $\tau=8$ h	18200 570	1,42 1,1	99,0 1,0
PO/AG	1:5, $\tau=16$ h	17995 600	1,45 1,21	93,9 6,1
PO/AG	1:10, $\tau=16$ h	18155 570	1,44 1,12	98,6 1,4
PO/AG	1:15, $\tau=16$ h	18015 570	1,46 1,11	98,8 1,2

3.4 Electronic micrographs of samples

These micrographs shown in Fig.2 describe the morphology of the sample surface. The pure PO consists of crystalline particles and their agglomerates. AG is in the form of spherical particles with a porous surface. Na₂GA consists of spherical hollow particles with a smooth surface. After MT, the original shape of the particles of the original components has changed and it is impossible to separate the individual components, except the formed agglomerates. As it can be seen in Fig. 2, the obtained substances are polydisperse powders with particles with size of 5-20 μm and their aggregates.

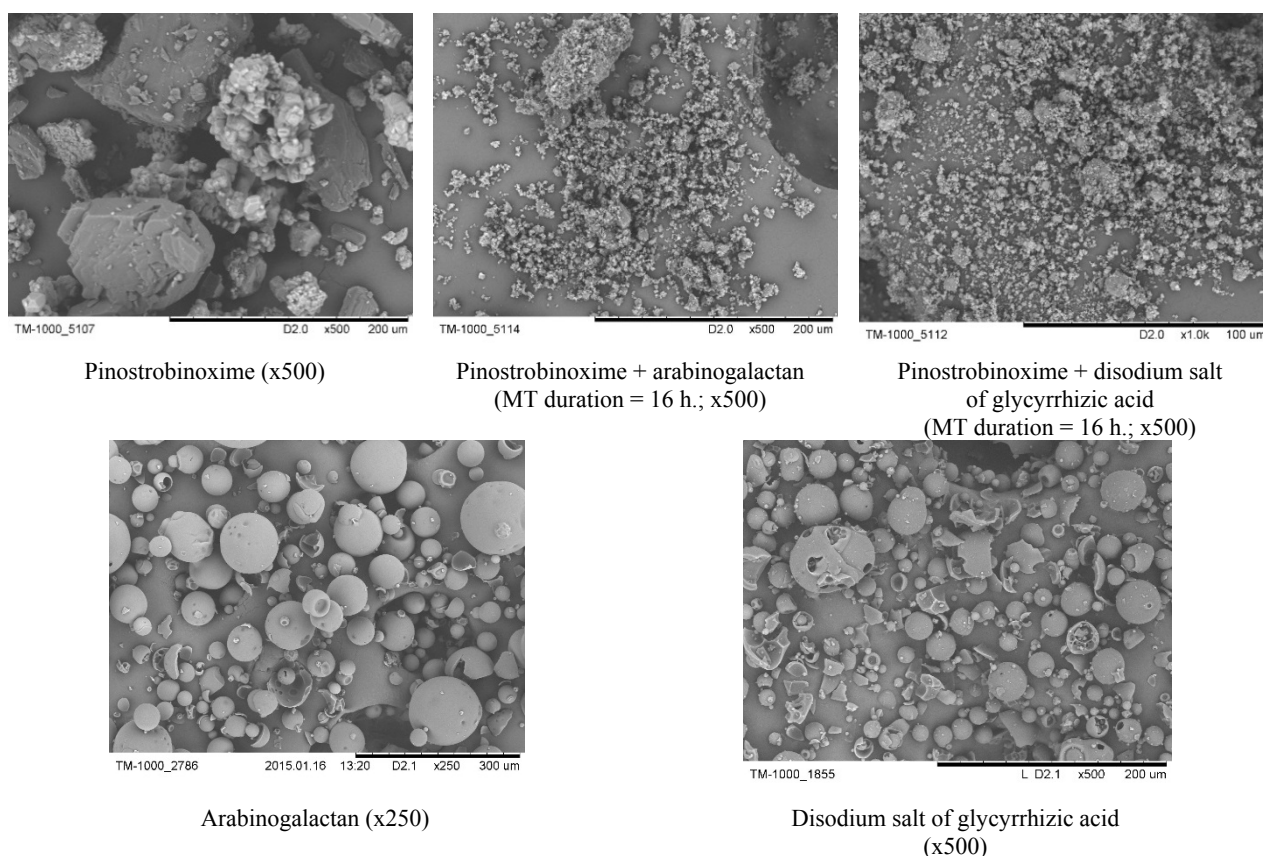


Figure 2- Electron micrographs of pinostrobinoxime and obtained complexes

4. Conclusion

Synthesis of supramolecular complex of pinostrobin oxime with arabinogalactan, disodium salt of glycyrrhizic acid and basic magnesium carbonate, selection of complexing agents, optimal compositions of water-soluble pinostrobin oxime complex have been carried out. The regime of obtaining a supramolecular complex is determined by the method of mechanochemistry. The obtained complexes have increased water solubility in comparison with pinostrobin oxime. The high water solubility of the pinostrobin oxime showed a complex with the disodium salt of glycyrrhizic acid. After mechanochemical treatment of the pinostrobin oxime with arabinogalactan, the average molecular weight of arabinogalactan changes insignificantly.

Acknowledgement

This work was supported by the Science Committee of the Ministry of Education and Science of the Republic of Kazakhstan on the project AP05130476 "Technology of water-soluble substances and ready-made dosage forms based on natural flavonoids and terpenoids."

REFERENCES

- [1] Andersen O.M., Markham K.R. (2006) Flavonoids: Chemistry, Biochemistry, and Applications. CRC Press Taylor & Francis Group, Boca Raton. ISBN: 0-8493-2021-6.
- [2] Simard F., Legault J., Lavoie S., Pichette A. (2014) Balsacones D-I, dihydrocinnamoylflavans from *Populus balsamifera* buds. *Phytochemistry*. 100: 141-149. DOI: [10.1016/j.phytochem.2013.12.018](https://doi.org/10.1016/j.phytochem.2013.12.018).
- [3] Mukusheva G.K., Lipseyeva A.V., Zhanymkhanova P.Z., Schultz E.E., Gatilov Y.V., Shakirov M.M., Adekenov S.M.1688. Flavanone pinostrobin in synthesis of coumarin chalkone hybrids with triazole linker(2015). *Heterocyclic compounds chemistry*. 52:146-152. (In Russian).
- [4] Adekenov S.M. Method of obtaining of hepatoprotective agent on basis of pinostrobin from buds of *Populus balsamifera* L. Eurasian patent No. 022691 dated 29.02.2016. (In Russian).
- [5] Donbayeva E.K., Turdybekov K.M., Sorokin R.N., Tuleuov B.I.). Квантово-химический расчет реакционной способности и компьютерный биоскрининг молекул некоторых метоксилированных флавоноидов (2008) PSU bulletin (chemical biological series). 4:82-89. (In Russian).
- [6] Sakuma S., Kikuawa K., Miyasaka R., Kabusiki K.. Method of increasing of water solubility of slightly soluble substances. RF patent No. 2517111 dated 27.05.2014. (In Russian).
- [7] Bekarev A.A. Method of increasing of bioavailability of drugs. RF patent No. 2328309 dated 10.07.2008. (In Russian).
- [8] Baranov V.D., Sotnikov P.S. Method of obtaining of water-soluble forms of biologically active substances. RF patent No. 2388491 dated 10.05.2010. (In Russian).
- [9] Sali N., Csepregi R., Kószegi T., Kunsági-Máté S., Sente L., Poór M. (2018). Complex formation of flavonoids fisetin and geraldol with β -cyclodextrins. *Journal of Luminescence*. 194:82-90. DOI: [10.1016/j.jlumin.2017.10.017](https://doi.org/10.1016/j.jlumin.2017.10.017).
- [10] Zhang K., Zhang M., Liu Z., Zhang Y., Gu L., Hu G., Chen X., Jia J. (2016). Development of quercetin-phospholipid complex to improve the bioavailability and protection effects against carbon tetrachloride-induced hepatotoxicity in SD rats. *Fitoterapia*. 113:102 – 109. DOI: [10.1016/j.fitote.2016.07.008](https://doi.org/10.1016/j.fitote.2016.07.008).
- [11] Lee J-S., Hong D. Y., Kim E. S., Lee H. G. (2017). Improving the water solubility and antimicrobial activity of silymarin by nanoencapsulation. *Colloids and Surfaces B: Biointerfaces*. 154:171-177. DOI: [10.1016/j.colsurfb.2017.03.004](https://doi.org/10.1016/j.colsurfb.2017.03.004).
- [12] Gonçalves V.S.S., Rodríguez-Rojo S., De Paz E., Mato C., Martín A., Cocero M.J. (2015). Production of water soluble quercetin formulations by pressurized ethyl acetate-in-water emulsion technique using natural origin surfactants. *Food Hydrocolloids*. 51:295 – 304. DOI: [10.1016/j.foodhyd.2015.05.006](https://doi.org/10.1016/j.foodhyd.2015.05.006).
- [13] Dushkin A.V., Tolstikov G.A., Meteleva E.S., Tolstikova T.G. Water soluble drug composition and its preparation. RF patent 2337710 dated 20.06.2009.
- [14] Kong R., Zhu X., Meteleva E. S., Chistyachenko Yu. S., Suntsova L.P., Polyakov N.E., Khvostov M.V., Baev D.S., Tolstikova T.G., Yu J., Dushkin A.V., Su W. (2017). Enhanced solubility and bioavailability of simvastatin by mechanochemically obtained complexes. *International Journal of Pharmaceutics*. 534:108-118. DOI: [10.1016/j.ijpharm.2017.10.011](https://doi.org/10.1016/j.ijpharm.2017.10.011).
- [15] Apanasenko I. E., Selyutina O.Yu., Polyakov N.E., Suntsova L.P., Meteleva E.S., Dushkin A.V., Vachali P., Bernstein P.S. (2015). Solubilization and stabilization of macular carotenoids by water soluble oligosaccharides and polysaccharides. *Archives of Biochemistry and Biophysics*. 572:58-65. DOI: [10.1016/j.abb.2014.12.010](https://doi.org/10.1016/j.abb.2014.12.010).
- [16] Neverova N.A., Medvedeva E.N., Babkin V.A., Larina L.I., Sapozhnikov A.N., Levchuk A.A., Kuzmin S.G. (2018). Synthesis and study of physical chemical properties of mechano-composites of arabinogalactan with cyclophosphamide. *Plant raw materials chemistry*. 1:37-44.
- [17] Zorkiy P.M., Lubina I.E. (1999). *Moscow Univ. Mess. Ser.2. Chemistry*. 5:300-307.

УДК 547.973:54.386

А.Р. Бейсенбаев¹, А.Н. Жабаяева¹, Л.П. Сунцова², А.В. Душкин², С.М. Адекенов¹

АО «Международный научно-производственный холдинг «Фитохимия»,
ул.М.Газалиева 4, г.Караганда, 100009, Республика Казахстан;
Институт Химии Твердого Тела и Механохимии СО РАН, ул. Кутателадзе 18, г.Новосибирск, Российская Федерация
e-mail: phyto_pio@mail.ru; e-mail: root@solid.nsc.ru

СИНТЕЗ И ИЗУЧЕНИЕ СУПРАМОЛЕКУЛЯРНОГО КОМПЛЕКСА ОКСИМА ПИНОСТРОБИНА

Аннотация. В статье обсуждаются результаты изучения оксимпроизводного пиностробина, в частности, способность комплексообразования их с арабиногалактаном, динатриевой солью глицирризиновой кислоты и основным карбонатом магния. Методом механохимической обработки на основе оксима пиностробина получен супрамолекулярный комплекс, обладающий повышенной водорастворимостью. При этом наибольшую эффективность показал комплекс оксима пиностробина с динатриевой солью глицирризиновой кислоты, в котором растворимость полученного комплекса повысилась в 300 раз.

Ключевые слова: Оксима пиностробина, арабиногалактан, динатриевая соль глицирризиновой кислоты, механохимическая обработка, водорастворимость, супрамолекулярный комплекс.

NEWS

OF THE NATIONAL ACADEMY OF SCIENCES OF THE REPUBLIC OF KAZAKHSTAN

SERIES CHEMISTRY AND TECHNOLOGY

ISSN 2224-5286

<https://doi.org/10.32014/2018.2518-1491.26>

Volume 6, Number 432 (2018), 53 – 56

A. S. Jadhav^a, G. T. Mohanraj^b, S. Mayadevi^c, A. N. Gokarn^d^{a,b} Birla Institute of Technology, Mesra, Ranchi, India;^{c,d} National Chemical Laboratory, Pune, IndiaEmail corresponding author: asj.paper@gmail.com

RAPID METHOD FOR DETERMINATION OF NANO SURFACE AREA OF ARECANUT SHELL DERIVED ACTIVATED CARBON BY IODINE ADSORPTION NUMBER

Abstract. Activated carbon is the most versatile and commonly used adsorbent. Activated carbon is prepared for 5e+10ng, 1e+11ng, and 3e+11ng batch size. Impregnation ratio maintained is 1:1,2:1,3:1,4:1. Nano activated carbon from arecanut shell is derived. Particles size diameter maintained to 53000 nm. In this study the specific surface area determination of activated carbon by means of the low-temperature argon adsorption (the BET method) is compared with the measurement of the surface area based on the adsorption of I₂ from the aqueous KI solution. The iodine adsorption number for the BET surface area is calculated. It is predicted iodine adsorption number S_{IN} method can be used for a quick estimation of the structure development of porous carbonaceous materials.

Keywords: Activated carbons, Iodine adsorption number (S_{IN}), Specific surface area (S_{BET}).

1. Introduction

First of all, raw material of the activated carbon is acquired by collecting arecanut shell store from Bangalore and Kerala. Highly porous carbon can be produced from a variety of natural and synthetic precursors [1,2] In its original state, the surface of a carbon is energetically heterogeneous [3], but as discovered by Beebe et al. [4] the heterogeneity is considerably reduced by heat treatment in an inert atmosphere. Precursor used for the production of activated carbon in this study is arecanut shell Activated carbon produced from residues would reduce the pressure on forests since wood is also commonly used for this purpose [5]. Many agricultural by-products such as coconut shell [6,7], grain sorghum [8], coffee bean husks [9], rubber wood sawdust [10], chestnut wood [11], have been discovered to be suitable precursors for activated carbon due to their high carbon and low ash contents

2. Experimental

2.1 Preparation of activated carbon

The carbonization Arecanut shell biomass is performed under a nitrogen flow of 100 cm³ min⁻¹ STP for 2hr. After activation, the activated carbon product removed and subsequently cleaned by removing the fibers and washing several times with distilled water to remove impurities The arecanut shell is chopped to pieces of ¼ inches, then dried at 110 °C until constant weight of the sample is reached. Then, dried and size-reduced arecanut shell is kept in a muffle furnace as raw material for activated carbon production.

Chemical activation method using phosphoric acid is used to activate the raw material. 5e+10ng, 1e+11ng, and 3e+11ng of raw material is impregnated by certain amount of 85 wt.% concentration phosphoric acid with occasional stirring. The amount of phosphoric acid solution used is adjusted to give a certain impregnation ratio (weight of activating agent/weight of raw material) of 1:1, 2:1, 3:1, and 4:1. The resulting slurry is then kept in a desiccator Overnight.

After 24 h, the mixture of raw material and phosphoric acid is then ready to have two-stage activation process with semi-carbonization as first stage [8]. In the first stage, the slurry is put in a horizontal tubular reactor and kept in a muffle furnace to experience semi-carbonization at a temperature 200 °C for 30 min. After semi-carbonization, the black and sticky dry powder is heated until certain activation and cooled in a desiccator. The activated carbon product is then repeatedly washed with warm distilled water (70 °C) until constant pH of the solution is reached. Finally, the activated carbon is dried in a vacuum oven at 110 °C for 24 h. The activated carbon is then stored in a desiccator for later experiment use. Finally the particle size maintained at 53000 nm.

Experimental is as shown in fig .1

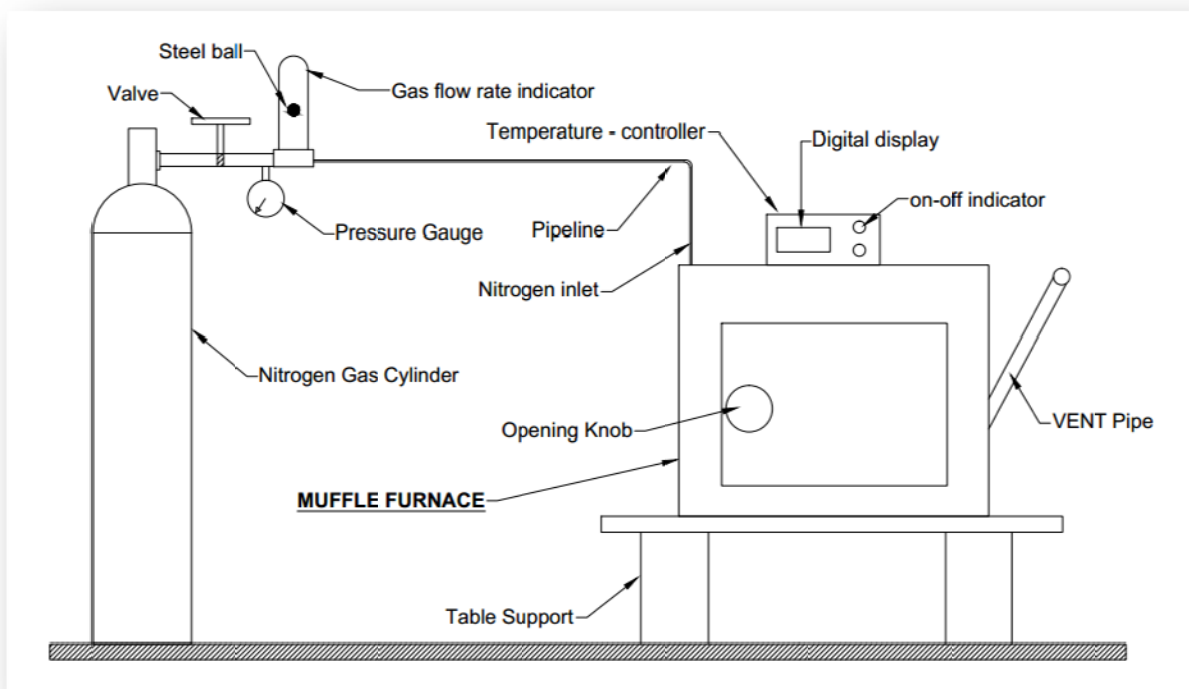


Fig: 1 Experimental Set Up

4.Result and Discussion

4.1Yield of activated carbon

In activated carbon preparation, yield is usually defined as final weight of activated carbon produced after activation, ishing, and drying, divided by initial weight of raw material; both on a dry basis [6]. Table.1 shows the yield of activated carbon.It is observed , yield of AC is increased with increase of impregnation upto 3:1 ratio and decreases from 3:1-4:1 impregnation ratio for each batch i.e 5e+10ng, 1e+11ng,and 3e+11ng

Table 1 - Yield of activated carbon prepared from biomass at 400⁰C from Arecanut Shell

Sample	Yield% (5e+10ng)	Yield% (1e+11ng)	Yield% (3e+11ng)
AS-PA-01 (1:1)	60.6	65.3	50.3
AS-PA-02 (1:2)	77.2	77	73.33
AS-PA-03 (1:3)	84	88	83.33
AS-PA-04 (1:4)	70	80	75.23

This is due to binding of O and H atoms decreases from 3:1 impregnation ratio. This led to decrease yield. The carbonization yield depends on the amount of carbon removed by binding with O and H atoms (Caturla et al., 1991).

4.2 Determination of Iodine Number

This is the most fundamental parameter used to characterize activated carbon performance. It is a measure of activity level (Higher degree indicates higher activation), often reported in mg/g (with typical range of $5 \times 10^8 - 1.2 \times 10^9$ ng/g). It is a measure of the microspore content of the activated carbon (values > 0 to 20 AO, or up to 2nm) by adsorption of iodine from solution. It is equivalent to surface area of activated carbon between $9000 \text{ nm}^2/\text{g}$ and $11000 \text{ nm}^2/\text{g}$ and. (Elliot et al., 1989). It tells of carbon that preferentially adsorb small molecules. High value indicate high degree of activation (Aziza et al., 2008; Elliot et al., 1989).

Table no: 2 Iodine number value of Arecanut shell

Sample	Iodine Number (5×10^8 ng)	Iodine Number (1×10^9 ng)	Iodine Number (3×10^9 ng)
AS-PA-01 (1:1)	692.81	829.63	812
AS-PA- 02 (1:2)	706.67	937.93	848
AS-PA- 03 (1:3)	822.57	976.6	906
AS-PA- 03 (1:4)	800.10	900	880

4.3 Determination of Iodine number surface Area

The aim of the current work is to calculate the surface area per iodine atom (ω_I), and then to determine the correlation between the specific surface area measured by the method of the low temperature argon adsorption (S_{BET}) and the surface area (S_{IN}) measured by the iodine adsorption number (IN) for activated carbons.

The analysis of the experimental adsorption isotherms (BET) in the relative pressure range of $p/p_0 = 0.05-0.4$ allows determining sorption capacities (a_m) which can then be used to calculate the specific surface area according Eq. (1)

$$S_{BET} = a_m \cdot N \cdot \omega_{Ar} \quad (1)$$

In this work, we assume the ω_{Ar} value equalled to equivalent surface measured according to the nitrogen standard. a_m : monolayer capacity, mole/g, N: Avogadro constant, $N = 6.023 \times 10^{23}$ 1/mole ω_{Ar} : surface area occupied by one of adsorbate (argon) atom

The determination of the iodine number is one of the methods often adopted in the industry utilizing activated carbons If we take into account the definition of the iodine adsorption number by the analogy to Eq. (1), Thus:

$$S_{BET} = \frac{IN \cdot 10^{-3}}{M_I} \cdot N \cdot \omega_I + \Delta S \quad (2)$$

Table no: 3 Iodine adsorption number of Arecanut shell

Sample	S_{IN} (5×10^8 ng)	S_{IN} (1×10^9 ng)	S_{IN} (3×10^9 ng)
AS-PA-01(1:1)	496.06	653.45	639.56
AS-PA- 02(2:1)	556.57	738.71	667.88
AS-PA- 03(3:1)	647.85	769.46	713.56
AS-PA- 04(4:1)	630.15	708.84	693.08

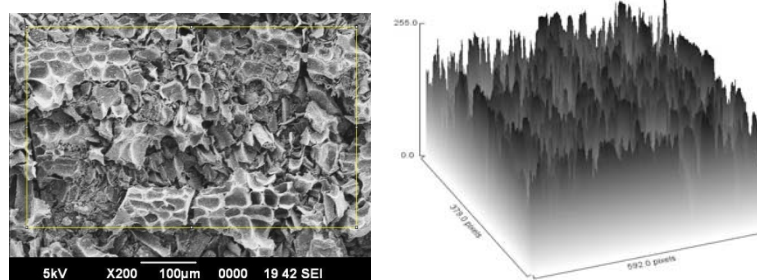


Fig: 2 - SEM of Arecanut shell carbon Fig: 3 Particle distribution image of ASAC

From table 3 iodine adsorption number shows same effect as shown by iodine number Value of iodine adsorption number increases uptill 3:1 and decreases from 3:1-4:1 impregnation ratio .Standard determination of the iodine adsorption number comprises the measurement of iodine amount in the adsorption layer of an activated carbon sample (in mg iodine/g adsorbent). The change of the bulk concentration results in the changes in the composition of the interfacial layers, which induces mutual displacements of the solution components from the adsorbed layer (Jankowska et al., 1991).

During excess adsorption from the solution there are no unoccupied sites on the surface, which implies that the same iodine amount occupies the same surface in the different carbon samples. It is worth noting that the specific surface area has been used most often for the characterization of the different porous solid bodies.

5. Conclusion

Arecanut shell derived activated carbon prepared in the form of the fine-grained (<0.080 mm) carbon samples, the iodine adsorption number in a range of $IN = 496060000-769460000$ ng/g can be recalculated into the specific surface area according to Eq. (2). If we analyze the procedure for the determination of the iodine adsorption number according to (PN-83/C-97555.04), this number equals the specific surface area S_{BET} . The determined iodine surface area, which amounts to $\omega_I = 0.2096$ nm², is a rough evaluation and has been calculated in proviso that iodine is covered hexagonally on the adsorbent surface .Iodine adsorption number to the specific surface area can be a rapid and efficient method for the evaluation of the surface area with a systematic error of a few nm²/g in relation to the S_{BET} value.

REFERENCE

- [1] F. Rouquerol, J. Rouquerol, K. Sing, Academic Press, San Diego 1999,
- [2] Rodriguez-Reinoso, F. (2002). [F. Schuth, K.S.W. Sing and]. Weitkamp, eds. Wiley/VCH, pp. 1766-827.
- [3] Sing, K.S.W. (1994). *Carbon*, 32,1311-7.
- [4] Beebe, R.A., Biscoe, J., Smith, W.R., and Wendell, C.B. (1947). Heats of adsorption on carbon black.]. *Am. Chern. Soc.*, 69, 95-101.
- [5] H.M. Mozammel, O. Masahiro, S.C. Bhattacharya, *Biomass Bioenergy* 22 (2002) 397-400.
- [6] M. Sekar, V. Sakthi, S. Rengaraj, *J. Colloid Interface Sci.* 279 (2004) 307-313.
- [7] Y. Diao, W.P. Walawender, L.T. Fan, *Bioresour. Technol.* 81 (2002) 45-52.
- [8] M.C. Baquero, L. Giraldo, J.C. Moreno, F. Su´arez-Garc´ia, A. Mart´inez-Alonso, J.M.D. Tasc´on, *J. Anal. Appl. Pyrolysis* 70 (2003) 779-784.
- [9] C. Srinivasakannan, M.Z.A. Bakar, *Biomass Bioenergy* 27 (2004) 89-96.
- [10] V. G´omez-Serrano, E.M. Cuerda-Correa, M.C. Fern´andez-Gonz´ales, M.F. Alexandre-Franco, A. Mac´ias-Garc´ia, *Mater. Lett.* 59 (2005) 846- 853.
- [11] A.M. Puziy, O.I. Poddubnaya, A. Mart´inez-Alonso, F. Su´arez-Garc´ia, J.M.D. Tasc´on, *Carbon* 43 (2005) 2857-2868.

NEWS

OF THE NATIONAL ACADEMY OF SCIENCES OF THE REPUBLIC OF KAZAKHSTAN

SERIES CHEMISTRY AND TECHNOLOGY

ISSN 2224-5286

<https://doi.org/10.32014/2018.2518-1491.27>

Volume 6, Number 432 (2018), 57 – 66

UDC 547.94 +547.458.68+543.429.2

O.A. Nurkenov¹, S.D.Fazylov¹, A.Zh.Issayeva¹,
T.M. Seilkhanov², T.S. Zhivotova¹, Z.T. Shulgau³, Zh.M. Kozhina⁴

¹ Institute of Organic Synthesis and Coal Chemistry the Republic of Kazakhstan, Karaganda, Kazakhstan,

² Sh. Ualikhanov Kokshetau state university, Kazakhstan,

³ RSE on the REM "National Center for Biotechnology" CS of the MES of the RK, Astana, Kazakhstan,

⁴ L.N. Gumilyov Eurasian national university, Kazakhstan.

e-mail: nurkenov_oral@mail.ru, iosu8990@mail.ru, ayauly_jan@mail.ru, tseilkhanov@mail.ru,
kozhina.janagul@yandex.ru

COMPLEXES OF INCLUSION OF FUNCTIONALLY-SUBSTITUTED HYDRASONS OF ISONICOTHIC ACID WITH CYCLODEXTRINES AND THEIR ANTIRADICAL ACTIVITY

Abstract. In the present work, supramolecular complexes based on N- (diethylamino) benzylidenisonicotinohydrazide and N- (2-bromo-3-phenyl) allylidenisonicotinohydrazide and cyclodextrins (β -CD, 2-GP- β -CD) were first obtained and studied. Comparison of the integral intensities of the ¹H NMR signals of substrate (hydrazone) and β - and 2-GP- β -CD- β receptors in supramolecular complexes showed that in all cases complexes of 1 guest molecule composition are formed for 2 host molecules. It was found that during the interaction they form an inclusion complex with the entry of the substrate molecule into the inner cavity of the receptor by the methylamine end. The resulting products form a mixture capable of dissolving in water or forming stable aqueous dispersions. The antiradical effect of synthesized supramolecular complexes on the DPPH radical was estimated. A concentration capable of 50% lowering the optical density of a 100 μ M solution of DPPH radical was determined. For a supramolecular complex based on N-(diethylamino)-benzylidenisonocinate-hydrazide and 2-GP- β -cyclodextrin, IC₅₀ (DPPH) was found to be 46.4 μ M.

Key words: β -cyclodextrin, 2-hydroxypropyl-cyclodextrin, supramolecular inclusion complexes, antiradical activity.

Hydrazones obtained on the basis of known isonicotinic acid hydrazide are used as antibacterial and antitubercular drugs, analytical reagents and dyes [1]. However, some of them have low solubility in water. At present, various ways of increasing the solubility of medicinal substances in water are developed and used: the use of special auxiliaries, including the inclusion of drugs in the complex of cyclodextrin [2].

Cyclodextrins (CD) are cyclic oligosaccharides that have a hydrophobic internal cavity and a hydrophilic outer shell [3]. Cyclodextrins (CD) are cyclic oligosaccharides that have a hydrophobic internal cavity and a hydrophilic outer shell [4]. By forming the inclusion complex, it is possible to increase the stability of low molecular substances sensitive to the action of light and air oxygen, increase their solubility in water, bioavailability, and reduce toxicity. Due to this, CSDs are widely used in the food, cosmetic, pharmaceutical industry, in the production of dyes, in analytical chemistry, in the elimination of environmental pollution by ecotoxicants, etc. [5-7].

The stability of the complexes is caused by the formation of a variety of non-covalent forces of interaction between the molecules of cyclodextrin and the "guest": Van der Waals, hydrophobic and etc. Cyclodextrin in the complex protects the guest molecule from damage by various reactive molecules and thereby reduces the rate of oxidation, steric rearrangement, hydrolysis, racemization and enzymatic degradation [8, 9].

It is promising to use the obtained hydrazones as a constituent supramolecular system (substrate) with a cyclic oligosaccharide - β -cyclodextrin (receptor) having a truncated cone molecule with internal protons H_3 and H_5 and external H_2 and H_4 protons (Fig. 1). The possibility of including the active substance in the capsule of β -cyclodextrin is due to hydrophobic interactions between the BAS and the complexing agent.

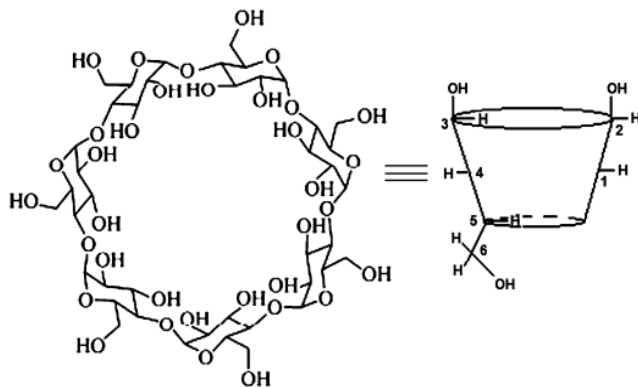
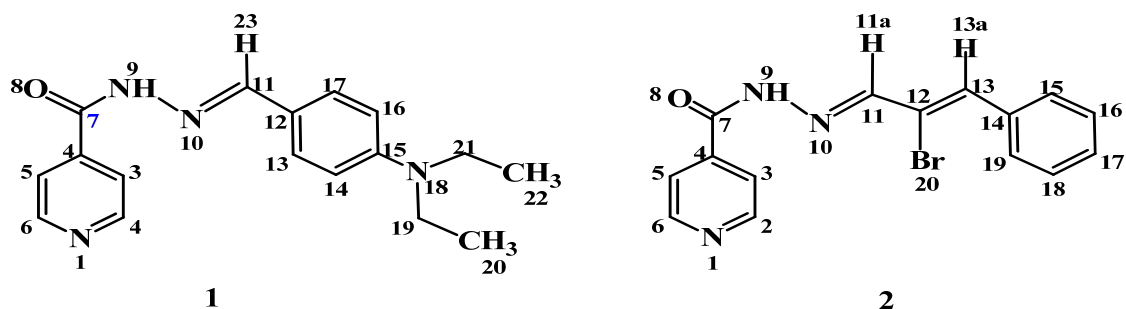


Figure 1 - Schematic representation of the structure of β -cyclodextrin molecules

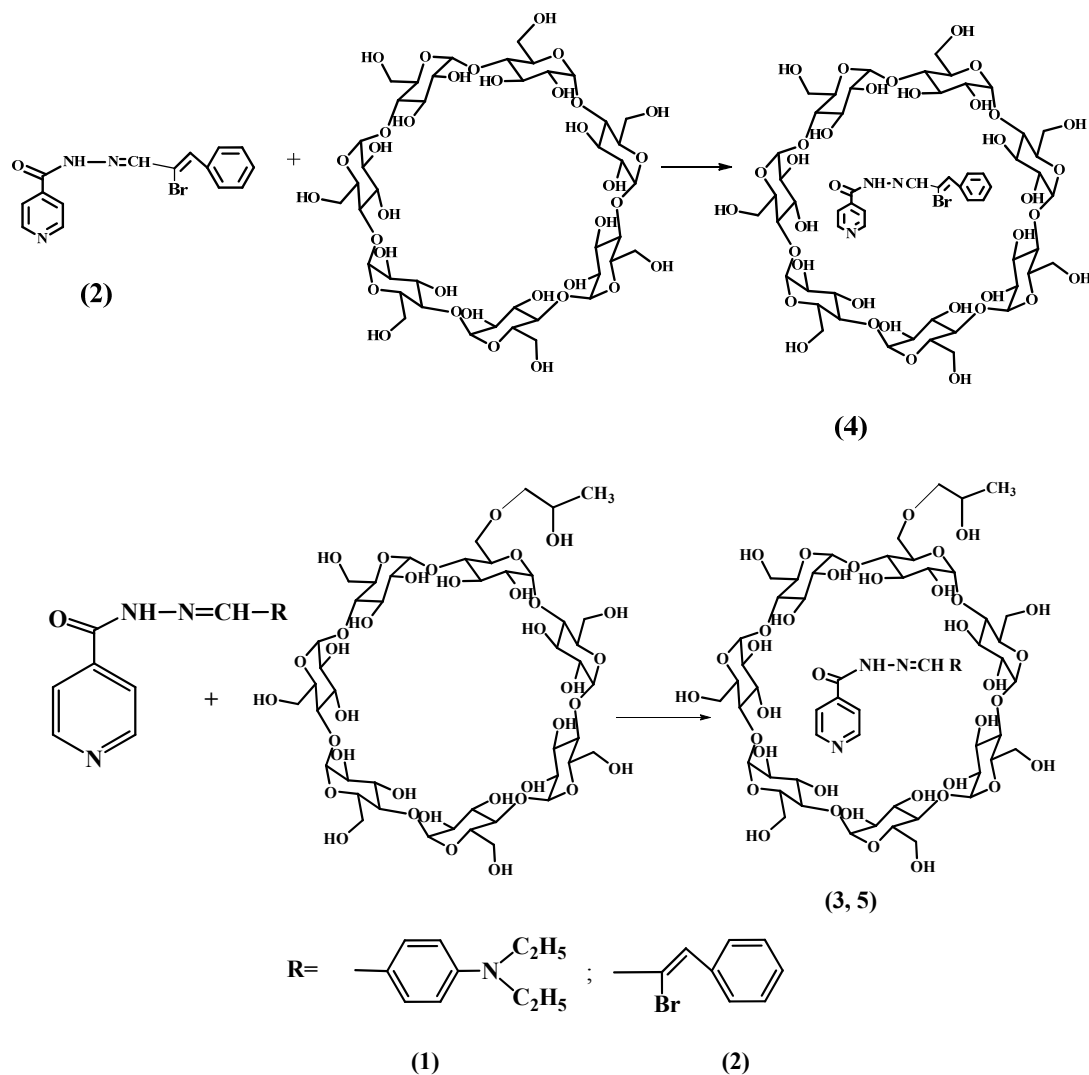
As hydrazones, N-(diethylamino)benzylidenisonicotinohydrazide (**1**) and N-(2-bromo-3-phenyl)allylideneisonicotinohydrazide (**7**) were selected as substrata for supramolecular self-assembly, which, according to the bioprospecting data, have high antituberculous, antimycobacterial activity and inhibitors of glutamine-phenylurea transaminase and threonine aldolase (see below), as well as poor solubility of the latter in water.



Supramolecular chemistry is dominated by the size and shape or geometric complementarity of the interacting components, therefore β -CD and its 2-hydroxy derivative-2-GP- β -CD were used to obtain inclusion complexes with substrates **1** and **2**.

Investigation by NMR spectroscopy of supramolecular complexes is based on the determination of the difference in the values of chemical shifts of ^1H and ^{13}C substrates (**1**, **2**) and receptors (β -CD, 2-GP- β -CD) in the free state and in the complexes as a result of intermolecular interaction. By the magnitude of chemical shifts of internal or external proton protons, it is possible to detect the formation of internal (inclusion) or external (without inclusion) complexes, respectively. The change in chemical shifts of ^1H and ^{13}C in the spectra of substrates makes it possible to determine the direction of occurrence of the latter in the CD cavity [10, 11].

The structure of substrates of supramolecular self-assembly **1** and **2** was established based on the results of ^1H and ^{13}C NMR spectroscopy obtained in DMSO-d_6 (Tables 1, 2 (**1**) and 1, 3, 4 (**2**)). The correctness of assigning one-dimensional NMR spectra of ^1H and ^{13}C **1** and **2** was confirmed by two-dimensional correlations of the NMR spectra of ^1H - ^1H COSY, ^1H - ^{13}C HMQC (Table 1).

Table 1 -NMR data of ^1H , ^{13}C , ^1H - ^1H COSY, ^1H - ^{13}C HMQC substrates 1 and 2

Substrate	δ , ppm, J, Hz			
	^1H	^{13}C	^1H - ^1H COSY	^1H - ^{13}C HMQC
1	1.06 t (6H, H-20,22, ^3J 6.9), 3.31-3.35 m (4H, H-19,21), 6.66 d (2H, H-14,16, ^3J 8.7), 7.48 d (2H, H-13,17, ^3J 8.7), 7.77 d (2H, H-3,5, ^3J 4.6), 8.25 s (1H, H-23), 8.72 d (2H, H-2,6, ^3J 4.6), 11.72 s (1H, H-9).	12.96 (C-20,23), 44.26 (C-19,21), 111.56 (C-14,16), 120.76 (C-12), 122.00 (C-3,5), 129.56 (C-13,17), 141.37 (C-4,11), 149.57 (C-2,6), 150.41 (C-15), 161.48 (C-7).	$\text{H}^{19,21}$ - $\text{H}^{20,22}$ (1.03, 3.33; 3.32, 1.05); $\text{H}^{13,17}$ - $\text{H}^{14,16}$ (6.65, 7.48; 7.48, 6.66); $\text{H}^{3,5}$ - $\text{H}^{2,6}$ (7.76, 8.72; 8.71, 7.77).	$\text{H}^{20,22}$ - $\text{C}^{20,22}$ (1.03, 12.93); $\text{H}^{14,16}$ - $\text{C}^{14,16}$ (6.63, 111.53); $\text{H}^{13,17}$ - $\text{C}^{13,17}$ (7.45, 129.54); $\text{H}^{3,5}$ - $\text{C}^{3,5}$ (7.76, 121.92); $\text{H}^{2,6}$ - $\text{C}^{2,6}$ (8.70, 150.73).
2	7.38-7.43 m (3H, H-15,19,17), 7.67 s (1H, H-13), 7.77 d (2H, H-3,5, ^3J 1.8), 7.84 d (2H, H-16,18, ^3J 6.4), 8.34 s (1H, H-11), 8.75 d (2H, H-2,6), 12.19 s (1H, H-9).	119.50 (C-12), 122.07 (C-3,5), 128.99 (C-15,19), 130.01 (C-17), 130.34 (C-16,18), 135.04 (C-14), 139.37 (C-13), 140.85 (C-4), 149.53 (C-11), 150.90 (C-2,6), 162.27 (C-7).	$\text{H}^{16,18}$ - $\text{H}^{15,17,19}$ (7.40, 7.84; 7.83, 7.43); $\text{H}^{2,6}$ - $\text{H}^{3,5}$ (7.76, 8.75; 8.74, 7.77).	$\text{H}^{15,19}$ - $\text{C}^{15,19}$ (7.40, 129.31); H^{13} - C^{13} (7.67, 139.39); $\text{H}^{3,5}$ - $\text{C}^{3,5}$ (7.76, 122.07); $\text{H}^{16,18}$ - $\text{C}^{16,18}$ (7.85, 130.14); H^{11} - C^{11} (8.32, 119.49); $\text{H}^{2,6}$ - $\text{C}^{2,6}$ (8.74, 150.97).

The ratio of the integrated intensities of the protons in the compounds in question corresponded to the structures 1 and 2 presented. NMR spectra of ^1H and ^{13}C β - and 2-GP- β -CD-nanov in the free state and supramolecular complexes 3-5 on their basis with substrates 1 and 2 are presented in Tables 2-4.

Table 2 – Chemical shifts of the ^1H and ^{13}C nuclei of substrate **1** and 2-GP- β -cyclodextrin in the free state (δ_0) and in the complex **3** (δ)

Atom number	Group	δ_0 , ppm.		δ , ppm.		$\Delta\delta = \delta - \delta_0$	
		^1H	^{13}C	^1H	^{13}C	^1H	^{13}C
Substrate 1							
2	CH	8.72	149.57	8.71	150.75	-0.01	1.18
3	CH	7.77	122.00	7.76	121.99	-0.01	-0.01
4	C		141.37		141.69		0.32
5	CH	7.77	122.00	7.76	121.99	-0.01	-0.01
6	CH	8.72	149.57	8.71	150.75	-0.01	1.18
7	C		161.48		163.82		2.34
9	NH	11.72		11.63		-0.11	
11	CH		141.37		141.69		0.32
12	C		120.76		120.94		0.18
13	CH	7.48	129.56	7.48	129.55	0	-0.01
14	CH	6.66	111.56	6.68	111.60	0.02	0.04
15	C		150.41		151.53		1.12
16	CH	6.66	111.56	6.68	111.60	0.02	0.04
17	CH	7.48	129.56	7.48	129.55	0	-0.01
19	CH_2	3.35	44.26	3.36	44.27	0.01	0.01
20	CH_3	1.06	12.96	1.00	12.84	-0.06	-0.12
21	CH_2	3.35	44.26	3.36	44.27	0.01	0.01
22	CH_3	1.06	12.96	1.00	12.84	-0.06	-0.12
23	CH	8.25		8.26		0.01	
2-HP-β-CD							
1	CH	4.79	102.33	4.80	102.29	0.01	-0.04
2	CH	3.26	72.56	3.28	72.94	0.02	0.38
3	CH	3.70	73.56	3.73	73.55	0.03	-0.01
4	CH	3.18	82.11	3.21	82.20	0.03	0.09
5	CH	3.56	72.56	3.60	72.30	0.04	-0.26
6	CH_2	3.56	60.40	3.60	60.43	0.04	0.03

Table 3 – Chemical shifts of the ^1H and ^{13}C nuclei of substrate **2** and β -cyclodextrin in the free state (δ_0) and in the complex **4** (δ)

Atom number	Group	δ_0 , ppm.		δ , ppm.		$\Delta\delta = \delta - \delta_0$	
		^1H	^{13}C	^1H	^{13}C	^1H	^{13}C
Substrate 2							
2	CH	8.75	150.90	8.38	150.98	-0.37	0.08
3	CH	7.77	122.07	7.95	124.49	0.18	2.42
4	C		140.85				
5	CH	7.77	122.07	7.95	124.49	0.18	2.42
6	CH	8.75	150.98	8.38	150.98	-0.37	0.08
7	C		162.27				
9	NH	12.19		12.19		0	
11	CH_a	8.34	149.53	8.38		0.04	
12	C		119.50				
13	CH_a	7.67	139.37	7.95		0.28	
14	C		135.04		133.50		-1.54
15	CH	7.43	128.99	7.53	129.42	0.10	0.43
16	CH	7.84	130.34	7.95	131.17	0.11	0.83
17	CH	7.43	130.01	7.53	132.11	0.10	2.10
18	CH	7.84	130.34	7.95	131.17	0.11	0.83
19	CH	7.43	128.99	7.53	129.42	0.10	0.43
β-CD							
1	CH	4.77	102.40	4.79	102.46	0.02	0.06
2	CH	3.26	72.83	3.27	72.93	0.01	0.10
3	CH	3.58	73.54	3.60	73.57	0.02	0.03
4	CH	3.28	81.98	3.31	82.07	0.03	0.09
5	CH	3.50	72.50	3.51	72.56	0.01	0.06
6	CH_2	3.58	60.42	3.60	60.45	0.02	0.03

Table 4 – Chemical shifts of the ^1H and ^{13}C nuclei of substrate **2** and 2-GP- β -cyclodextrin in the free state (δ_0) and in the complex of **5** (δ)

Atom number	Group	δ_0 , ppm.		δ , ppm.		$\Delta\delta = \delta - \delta_0$	
		^1H	^{13}C	^1H	^{13}C	^1H	^{13}C
Substrate 2							
2	CH	8.75	150.90	8.78	149.72	0.03	-1.82
3	CH	7.77	122.07	7.87	124.04	0.10	1.97
4	C		140.85		140.25		-0.60
5	CH	7.77	122.07	7.87	124.04	0.10	1.97
6	CH	8.75	150.98	8.78	149.72	0.03	-1.82
7	C		162.27		163.61		1.34
9	NH	12.19		12.19		0	
11	CH_a	8.34	149.53	8.38	149.72	0.04	0.19
12	C		119.50				
13	CH_a	7.67	139.37	7.87	139.64	0.20	0.27
14	C		135.04		131.18		-3.86
15	CH	7.43	128.99	7.52	129.00	0.09	0.01
16	CH	7.84	130.34	7.87	129.42	0.03	-0.62
17	CH	7.43	130.01	7.52	129.42	0.09	-0.59
18	CH	7.84	130.34	7.87	129.42	0.03	-0.62
19	CH	7.43	128.99	7.52	129.00	0.09	0.01
2-HP-β-CD							
1	CH	4.79	102.33	4.80	102.36	0.01	0.03
2	CH	3.26	72.56	3.28	72.91	0.02	0.35
3	CH	3.70	73.56	3.73	73.53	0.03	-0.03
4	CH	3.18	82.11	3.21	82.01	0.03	-0.10
5	CH	3.56	72.56	3.60	72.91	0.04	0.35
6	CH_2	3.56	60.40	3.60	60.66	0.04	0.20

Comparison of the integrated intensities of the signals of ^1H NMR of the molecules of substrates **1** and **2** and the receptors of β - and 2-GP- β -CD in supramolecular complexes **3-5** showed that in all cases complexes of the composition of the guest molecule are formed for **2** host molecules.

In the formation of the supramolecular complex **3**, as a result of the supramolecular self-assembly **1** with 2-GP- β -CD, changes in the proton chemical shifts in the cyclodextrin $\Delta\delta$ molecule occurred to a greater extent in the internal hydrophobic protons H-3, H-5, H-6 than in the external hydrophilic surface of protons H-1, H-2 and H-4. In molecule **1**, the largest changes in proton spectra are observed in diethylamine protons H-20, H-22, H-19, H-21 and located closer to the above protons in the phenylidene protons H-14 and H-16. The proton also undergoes screening in the process of complexation, the aromatic pyridine hydrophobic protons H-2,6 and H-3,5. It can be assumed that the greatest supramolecular interaction of host and host molecules is realized by means of the above protons during the formation of complex **3** (Fig. 2).

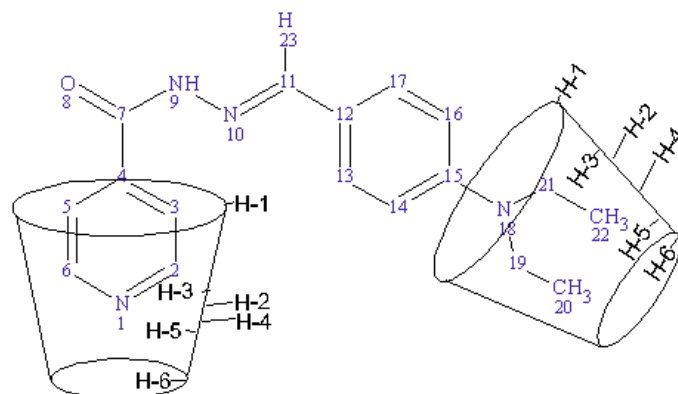


Figure 2 - Supposed supramolecular inclusion complexes **3**

Screening of external cyclodextrin protons is probably due to the intermolecular interaction of hydrophilic protons with external hydroxyl groups of 2-GP- β -CD-N, as well as the possible slight formation of external complexes [12-15]. The water-soluble aggregates formed in this way are capable of solubilizing the molecules of substrates through non-inclusive complexation [16-18]. A significant change in the chemical shifts of the imine proton H-9 is probably due to the hydrophilic interaction of its hydroxy-group receptor.

Supramolecular self-assembly of substrate **2** with β - and 2-GP- β -CDs with the formation of supracomplexes **4** and **5** was also accompanied by a change in internal hydrophobic protons of CD and insignificant screening of external proton receptors. In molecule **1**, the largest changes in proton chemical shifts occurred in the phenyl and pyridine fragments. When β -CD- β was used as the receptor, the greatest changes in proton chemical shifts were observed in the protons of the pyridine fragment of complex **4**, whereas the use of 2-GP- β -CD in supramolecular self-assembly with substrate **2** leads to the greatest change in the chemical shifts of the protons of the phenyl radical in the supracomplex **5**.

The proposed models of supracomplexes **4** and **5** are similar in structure and are shown in Figure 3. In order to study the biological activity of the obtained supramolecular inclusion complexes 3-5, their antiradical effect on the DPPH radical was evaluated. The antiradical action of the presented samples was investigated with respect to the radical 2,2-diphenyl-1-picryl hydrazyl (DPPH •) [19].

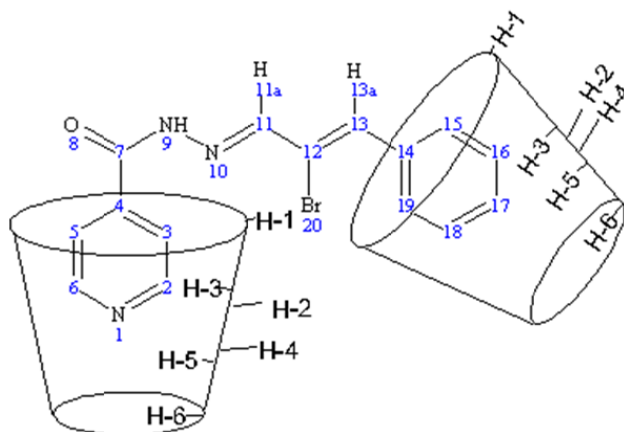


Figure 3 - Supposed supramolecular inclusion complexes **4** and **5**

A methanol solution of DPPH (100 μ M) was used for the initial evaluation of the antiradical activity of the samples under study in the DPPH-radical test. For the selection of substances with a pronounced antiradical activity, 2 ml of a 100 μ M methanolic solution of DPPH was mixed with 20 μ l of the test object dissolved in DMSO at a concentration of 5 mM. Thus, the final concentration of the test substance in the reaction mixture was 50 μ M. 10 minutes after the solution of the test compound was added to the DPPH radical solution, the optical density reduction at 515 nm was measured. For substances capable of reducing the optical density by more than 30%, an interaction test with DPPH radical was carried out at the final concentrations of the test substances 100, 75, 50, 25, 20, 10 and 5 μ M. Then, the concentration of the test substance was determined, which was able to reduce the optical density by 50% - IC₅₀ (DPPH) (Table 5). In control, a 100 μ M solution of DPPH was added with 20 μ l of a solvent - DMSO.

Table 5 - Optical density of the solution of a 100 μ M DPPH radical after a 10-minute incubation with the test substance at a final concentration of 50 μ M

№	Connection cipher	Optical density	The decrease in the optical density of the initial solution of DPPH-radical, in% of the control
1.	(3)	0,535	52,3
2.	(4)	1,094	2,5
3.	(5)	1,058	5,7
4.	Control (DPPH solution without test sample)	1,122	-

From Table 5 we see that Compound **3** in the final concentration of 50 μM reduces the optical density of the initial solution of DPPH radical by 52.3%, which means it is promising for further studies. The remaining compounds showed no pronounced antiradical activity under the conditions of this test system.

In the second series of experiments, we studied the ability of compound **3** at various concentrations (from 5.0 to 100 μM) to interact with the DPPH radical (Table 6).

Table 6 - Optical density of the solution of a 100 μM DPPG radical after a 10-minute incubation with **3** at the final concentrations in the reaction mixture of 100, 75, 50, 25, 20, 10 and 5 μM

№	The final concentration of 3 in the reaction mixture, μM	Optical density
1.	100	0,079
2.	75	0,275
3.	50	0,491
4.	25	0,723
5.	20	0,798
6.	10	0,907
7.	5	0,963
	Control (DPPH solution without test sample)	1,042

Using the constructed calibration curve (Fig. 4), the concentration of Compound **3** was determined, capable of 50% decrease in the optical density of a 100 μM solution of DPPH radical. For compound **3**, IC_{50} (DPPH) was found to be 46.4 μM .

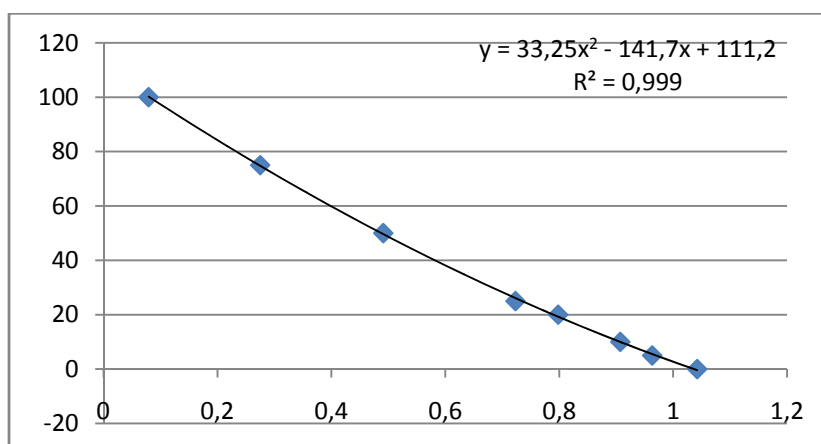


Figure 4 - Dependence of the optical density of the DPPH radical solution on the concentration of **3**

Using the constructed calibration curve (Table 7, Fig. 5), the concentration of ascorbic acid, capable of 50% lowering the optical density of 100 μM DPPH radical solution, was determined. For ascorbic acid, IC_{50} (DPPH) was found to be 21.14 μM .

Thus, supramolecular complexes based on the functionally substituted N-benzylidene- and allylidene-isonicotinohydrate with cyclodextrins ($\beta\text{-CD}$, hydroxypropyl- $\beta\text{-CD}$) were obtained and their structures studied by NMR spectroscopy. It is shown that the products obtained from a mixture that is capable of dissolving in water or forming stable aqueous dispersions.

Table 7 - Optical density of the solution of a 100 μM DPPG radical after a 10-minute incubation with ascorbic acid at the final concentrations in the reaction mixture of 25, 20, 10 and 5 μM

№	The final concentration of ascorbic acid in the reaction mixture, μM	Optical density
1.	25	0,429
2.	20	0,545
3.	10	0,792
4.	5	0,914
	Control (DPPH solution without test sample)	1,042

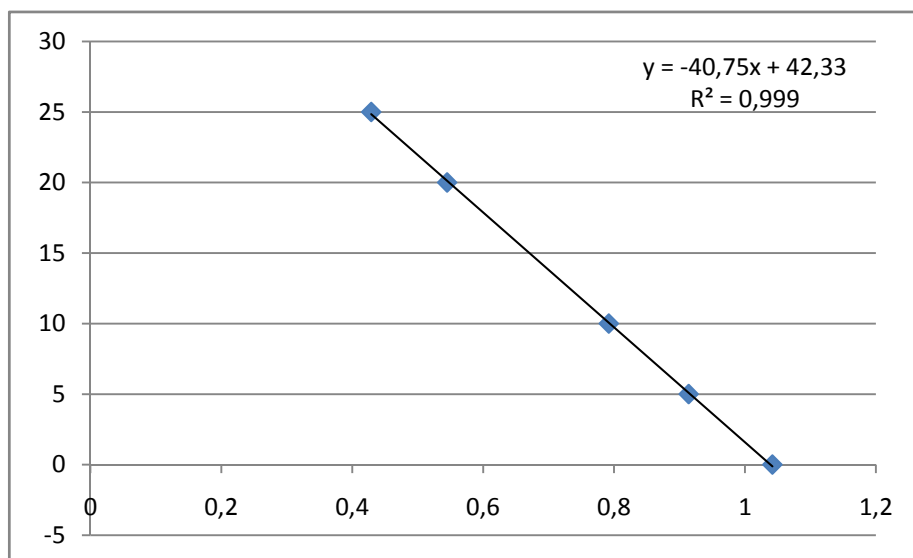


Figure 5 - Dependence of the optical density of the DPPH radical solution on the concentration of ascorbic acid

The antiradical effect of synthesized supramolecular inclusion complexes against DPPH radical was estimated. Antiradical activity under the conditions of this test system was shown in Sample 3, for which a concentration was determined capable of 50% decrease in the optical density of a 100 μM solution of DPPH radical. For compound 3, IC₅₀ (DPPH) was found to be 46.4 μM .

According to our data, the IC₅₀ (DPPH) (μM) for the reference sample, in this case for ascorbic acid, was 21.1 μM . The activity of the sample of Compound 3, for which IC₅₀ (DPPH) was 46.4 μM is inferior to the reference sample of ascorbic acid.

According to the literature data [20] IC₅₀ (DPPH) (μM) for ascorbic acid is 27, for glutathione - 49, for hydroquinone - 27, for trolox - 28, for α -tocopherol - 28. Thus, the activity of compound 3 is comparable with activity known antioxidant - glutathione.

Experimental part

β - and 2-GP- β -CDDs were used by Fluka companies with a purity of 99%. The ^1H and ^{13}C NMR spectra were recorded on a Jeol JNM-ECA 400 spectrometer (399.78 and 100.53 MHz on ^1H and ^{13}C nuclei, respectively) in a DMSO- d_6 solution at room temperature. Chemical shifts are measured relative to the residual signals of protons or carbon atoms DMSO- d_6 .

Preparation of inclusion complexes (3-5) of functionally substituted N-benzylidene- and allylideneisonicotinhydrazide (1, 2) with β - and hydroxypropyl- β -cyclodextrin. We chose the method of coprecipitation, since this method makes it possible to obtain a very pure preparation of the inclusion complex in a crystalline form. In a 1: 1 ratio, a saturated solution of cyclodextrin in water was added dropwise to a concentrated solution of the functionally substituted N-benzylidene- and allylideneisonicotinhydrazide in an organic solvent (ethanol, dioxane, DMF, etc.). After that, they interfered with a magnetic stirrer at a temperature of 85-90°C. The individuality of the proposed complexes was checked by thin-layer chromatography on Silufol UV-254 plates in isopropyl alcohol-25% ammonia-water 7:2:1 solution. The final product was dried at a temperature of 600°C in vacuum drying at atmospheric pressure of 0.4 kgf/cm². The inclusion complexes of hydrazones with cyclodextrins were obtained in the form of a powder.

The work was carried out with the financial support of the Committee of Science and the Ministry of Education of the Republic of Kazakhstan on "Grant Financing", No. Registration 0115PK01782, AP05131054 "Development of scientific bases and effective methods of creation of new polyfunctional pyridine compounds with the purpose of search on their basis of potential biological active substances for medicine".

REFERENCES

- [1] [Wiseman B](#), [Carpene X](#), [Feliz M](#), [Donald LJ](#), [Pons M](#), [Fita I](#), [Loewen PC](#). Isonicotinic acid hydrazide conversion to Isonicotinyl-NAD by catalase-peroxidases // [J Biol Chem](#), 2010, 285(34):26662-26673. DOI: 10.1074/jbc.M110.139428. (In Eng).
- [2] [Judge V](#), [Narasimhan B](#), [Ahuja M](#), [Balzarini J](#) and etc. Isonicotinic acid hydrazide derivatives: Synthesis, antimicrobial activity, and QSAR studies // *Med Chem Res*, 2012, 21:1451–1470. DOI 10.1007/s00044-011-9662-9. (In Eng).
- [3] Okumura H, Kawaguchi Y, and Harada A. Preparation and Characterization of Inclusion Complexes of Poly(dimethylsiloxane)s with Cyclodextrins // *Macromolecules*, 2001, 34 (18), pp 6338–6343. DOI: 10.1021/ma010516i. (In Eng)
- [4] Wenz G, Han B, and Muller A. Cyclodextrin Rotaxanes and Polyrotaxanes // *Chem. Rev.*, 2006, 106 (3), pp 782–817. DOI: 10.1021/cr970027+. (In Eng).
- [5] Liguori A, D'auria M, Emanuele L, Scrano L, Lelario F, Bufo S. Reactivity of rimsulfuron in newly formed inclusion combinations by using cyclodextrin and zeolite // *Int. Journ. Of Environmental Analit. Chem.*. 2007. V.87. P.1043-1052. DOI: [10.1080/03067310701440874](#). (In Eng).
- [6] Zimmer S, Grebe A, Bakke S, Bode N and etc. Cyclodextrin promotes atherosclerosis regression via macrophage reprogramming // *Science Translational Medicine*, 2016, V. 8, Issue 333, pp. 333ra50. DOI: 10.1126/scitranslmed.aad6100. (In Eng).
- [7] Loftsson T, Brewster M.E. Pharmaceutical applications of cyclodextrins: basic science and product development // *Journal of Pharmacy and Pharmacology*. 2010. V. 62. P. 1607-1621. DOI: 10.1111/j.2042-7158.2010.01030.x. (In Eng).
- [8] Kurkov S.V, Loftsson T. Cyclodextrins // *International Journal of Pharmaceutics*. – 2013, V. 453, pp 167-180. DOI:10.1016/j.ijpharm.2012.06.055. (In Eng).
- [9] Nowakowski M, Ejchart A. Complex formation of fenchone with α -cyclodextrin: NMR titrations // *J. Incl. Phenom. Macrocycl. Chem.*. 2014, V. 79. P. 337-342. DOI: 10.1007/s10847-013-0356-4. (In Eng).
- [10] Maheshwari A, Sharma M, Sharma D. Complexation of sodium picosulphate with beta cyclodextrin: NMR spectroscopic study in solution // *J. Incl. Phenom. Macrocycl. Chem.*, 2013, V. 77, pp 337-342. DOI: 10.1007/s10847-012-0251-4. (In Eng).
- [11] Huang Y.D. Comments on "Novel molecularly imprinted polymer based on β -cyclodextrin@graphene oxide: Synthesis and application for selective diphenylamine determination" // [J Colloid Interface Sci](#). 2018., P. 31042-31047. doi: 10.1016/j.jcis. 2018.09.001. (In Eng).
- [12] Maheshwari A., Sharma M., Sharma D. Complexation of sodium picosulphate with beta cyclodextrin: NMR spectroscopic study in solution // *J. Incl. Phenom. Macrocycl. Chem.*, 2013. V. 77, pp 337-342. DOI: 10.1007/s10847-012-0251-4. (In Eng).
- [13] Demarco P.V, Thakkar A.I. Cyclohepta-amilose Inclusion Complexes. A Proton Magnetic Resonance Study // *J. Chem. Soc., Chem. Commun*, 1970. P.2-4. DOI: [10.1039/c29700000002](#). (In Eng).
- [14] Hazra S, Hossain M, Kumar G.S. Studies on α -, β -, and γ -cyclodextrin inclusion complexes of isoquinoline alkaloids berberine, palmatine and coralyne // *J. Incl. Phenom. Macrocycl. Chem.*, 2014, V. 78, pp 311-323. DOI: 10.1007/s10847-013-0301-6. (In Eng)
- [15] Loftsson T, Masson M, Brewster M.E. Self-association of cyclodextrins and cyclodextrin complexes // *J. Pharm. Sci*. 2004. V. 93. P. 1091-1099. DOI: [10.1002/jps.20047](#). (In Eng).
- [16] Zhao D.G., Liao K.I., Ma X.Y., Yan X.H. Study of the supramolecular inclusion of β -cyclodextrin with andrographolide // *J. Inclusion Phenom. Macrocycl. Chem*. 2002. V. 43. № 3-4, pp 259-264. DOI: 10.1023/A:1021223407297. (In Eng).
- [17] Nacsá Á, Ambrus R, Berkesi O.J., Szabó-Révész P, Aigner Z. Water-soluble loratadine inclusion complex: analytical control of the preparation by microwave irradiation // *Pharm. Biomed. Anal.*. 2008. V. 48. № 3. P. 1020-1023. DOI: 10.1016/j.jpba.2008.07.001. (In Eng).
- [18] Cirri M, Maestrelli F, Mennini N, Mura P. Physicalchemical characterization of binary and ternary systems of ketoprofen with cyclodextrins and phospholipids // *J. Pharm. Biomed. Anal.*, 2009, V. 50, pp 683-689. DOI: [10.1016/j.jpba.2008.11.003](#). (In Eng).
- [19] Brand-Williams W., Cuvelier M.E., Berset C. Use of a free radical method to evaluate antioxidant activity // *Lebensm Wiss Technol*, 1995. V. 28. P. 25–30. DOI: [10.1016/S0023-6438\(95\)80008-5](#). (In Eng).
- [20] Plattner S. et al. Studying the reducing potencies of antioxidants with the electrochemistry inherently present in electrospray ionization-mass spectrometry // *Anal Bioanal Chem.*, 2014, pp 213–224. DOI: 10.1007/s00216-013-7445-5. (In Eng).

О.А. Нуркенов¹, С.Д. Фазылов¹, А.Ж. Исаева¹,
Т.М. Сейлханов², Т.С. Животова¹, З.Т. Шұлғау³, Ж.М. Қожина⁴

¹ҚР Органикалық синтез және көмір химиясы институты, Қарағанды қ., Қазақстан Республикасы;

²Ш. Уәлиханов атындағы Көкшетау мемлекеттік университеті, Қазақстан Республикасы;

³ҚР БҒМ ҒК «Ұлттық биотехнология орталығы» ШЖҚ-дағы РМК, Астана қ., Қазақстан Республикасы;

⁴Л.Н.Гумилев атындағы Еуразия ұлттық университеті, Астана қ., Қазақстан Республикасы,

ФУНКЦИОНАЛДЫҚ-ОРЫНБАСЫЛҒАН ИЗОНИКОТИН ҚЫШҚЫЛЫНЫҢ ГИДРАЗОНДАРЫ МЕН ЦИКЛОДЕКСТРИНДЕРДІҢ КОМПЛЕКСТІК КЕШЕНДЕРІ ЖӘНЕ ОЛАРДЫҢ АНТИРАДИКАЛДЫҚ БЕЛСЕНДІЛІКТЕРІ

Аннотация. Берілген жұмыста алғаш рет циклодекстриндердегі (β -ЦД, 2-ГП- β -ЦД) N-(диэтиламино) бензилиденизоникотиногидразид және N-(2-бромо-3-фенил)аллилиденизоникотиногидразидінің негізіндегі супрамолекулярлық кешендердің реакциялары қарастырылып, зерттелді. β - және 2-ГП- β -ЦД рецепторлары мен субстраттар (гидразондар) молекулаларының ¹H ЯМР интегралдық қарқындылық дабылдарын сәйкестендіру кезінде барлық жағдайда 1 қонақ молекуласының 2 рецептордың молекуласы құрамында болатын кешендер түзілетіні байқалды. Олардың субстрат молекуласының метиламиндік тобы жағынан рецептордың ішкі жағына кіруі арқылы қосылу кешені түзілетіні анықталды. Алынған өнімдер суда ери алатын қоспа түзеді немесе суда тұрақты дисперсиялар түзеді. Сонымен қатар, ДФПГ-радикалы қатысында циклодекстриндердегі гидразондардың супрамолекулярлық кешенінің антирадикалдық әсері бағаланды. ДФПГ-радикалының ерітіндісінің 100 μ M оптикалық тығыздықты 50%-ға дейін төмендете алатын концентрациясы анықталды. N-(диэтиламино)-бензилиденизоникотиногидразиді мен 2-ГП- β -циклодекстриннің супрамолекулярлық кешені үшін $IC_{50}(DPPH)$ 46,4 μ M тең.

Түйін сөз: β -циклодекстрин, 2-гидроксипропил- β -циклодекстрин, супрамолекулярлық қосылу кешендері, антирадикалдық белсенділік.

О.А. Нуркенов¹, С.Д. Фазылов¹, А.Ж. Исаева¹,
Т.М. Сейлханов², Т.С. Животова¹, З.Т. Шұлғау, ³ Ж.М. Қожина⁴

¹Институт органического синтеза и углекислотной химии РК, г. Караганда, Республика Казахстан;

²Кокшетауский государственный университет им. Ш. Уалиханова, Республика Казахстан;

³РГП на ПХВ «Национальный центр биотехнологии» КН МОН РК, г. Астана, Республика Казахстан;

⁴Евразийский национальный университет им. Л.Н. Гумилева, г. Астана, Республика Казахстан,

КОМПЛЕКСЫ ВКЛЮЧЕНИЯ ФУНКЦИОНАЛЬНО-ЗАМЕЩЕННЫХ ГИДРАЗОНОВ ИЗОНИКОТИНОВОЙ КИСЛОТЫ С ЦИКЛОДЕКСТРИНАМИ И ИХ АНТИРАДИКАЛЬНАЯ АКТИВНОСТЬ

Аннотация. В настоящей работе впервые были получены и изучены супрамолекулярные комплексы на основе N-(диэтиламино)бензилиденизони-котиногидразида и N-(2-бромо-3-фенил)аллилиденизоникотиногидразида и циклодекстринами (β -ЦД, 2-ГП- β -ЦД). Сопоставление интегральных интенсивностей сигналов ¹H ЯМР молекул субстратов (гидразонов) и рецепторов β - и 2-ГП- β -ЦД-на в супрамолекулярных комплексах показало, что во всех случаях образуются комплексы состава 1 молекула гостя на 2 молекулы хозяина. Установлено, что при взаимодействии они образуют комплекс включения с вхождением молекулы субстрата во внутреннюю полость рецептора метиламинным концом. Полученные продукты образуют смесь, способную растворяться в воде или образовывать устойчивые водные дисперсии. Оценено антирадикальное действие синтезированных супрамолекулярных комплексов в отношении ДФПГ-радикала. Определена концентрация, способная на 50% снизить оптическую плотность 100 μ M раствора ДФПГ-радикала. Для супрамолекулярного комплекса на основе N-(диэтиламино)-бензилиденизоникотиногидразида и 2-ГП- β -циклодекстрина, $IC_{50}(DPPH)$ оказалась равной 46,4 μ M.

Ключевые слова: β -циклодекстрин, 2-гидроксипропил- β -циклодекстрин, супрамолекулярные комплексы включения, антирадикальная активность.

NEWS

OF THE NATIONAL ACADEMY OF SCIENCES OF THE REPUBLIC OF KAZAKHSTAN

SERIES CHEMISTRY AND TECHNOLOGY

ISSN 2224-5286

<https://doi.org/10.32014/2018.2518-1491.28>

Volume 6, Number 432 (2018), 67 – 78

УДК 662.7

МРПТИ 61.53.91

**B.T. Yermagambet¹, N.U. Nurgaliyev¹, L.D. Abylgazina¹,
N.A. Maslov¹, Zh.M. Kasenova¹, B.K. Kasenov²**

¹LLP "Institute of Coal Chemistry and Technology", Astana, Kazakhstan;

²Chemical and Metallurgical Institute named after J. Abisheva, Karaganda

coaltech@bk.ru, nurgaliyev_nao@mail.ru, lilya_1501@mail.ru, nike.6484@mail.ru, zhanar_k_68@mail.ru,
kasenov1946@mail.ru

METHODS FOR EXTRACTION OF VALUABLE COMPONENTS FROM ASH-AND-SLAG COAL WASTES

Abstract. In the article the problems of ash and slag wastes processing, which are formed from coal combustion in CHP, are considered. General information is given on the chemical composition of ash and slag wastes and the content of valuable components of the most developed and used deposits in Kazakhstan and attractive from the point of view of extracting valuable materials from them. Among such deposits are the Karaganda basin, the Ekibastuz basin, the Maikuben basin, the Borly field, and the Kara-Zhyra field.

The literature review of the methods of leaching the elements from ash and slag waste from coals showed that the conditions of the process and the selection of the necessary reagents depend on the composition and the degree of preparation of the initial coal ash, and the concentration of the extracted component is an important component.

The most common and effective methods of extracting valuable components from ash are leaching with acids and alkalis. However, the use of such expensive reagents already in the production of these products requires the careful development of an appropriate technology (across the entire process chain), where it is also possible to recover the reagents. In addition, despite the relatively high degree of extraction of microelements, acid leaching has disadvantages associated with the use of expensive acid-fast processing equipment and the difficulty of separating siliceous sludge from acid solutions of salts and the difficulty of purifying aluminum salts from iron.

Promising technologies for extracting valuable components from ash are biochemical heap leaching with the use of thiobacteria *Th. Ferrooxidans*, fluoride technology (using fluorine and hydrogen fluoride, or fluoride and ammonium bifluoride).

Keywords: coal, ash, leaching, acid, alkali, metals, recovery, macroelements, microelements.

Introduction. Recently, more attention has been paid to environmental issues related to the development of technology and technology in Kazakhstan. In this regard, an integrated approach to solving the problems of utilization of various wastes has become relevant, including ash and slag.

Each year, a huge amount of ash and slag wastes are generated at the thermal power station, and the largest producers are China, the United States and India (table 1) [1].

The current global annual production of ash and slag is approximately 750 million tons [2], and in the near future, this amount of waste is expected to grow. This fact is one of the serious environmental problems associated with the threat to public health and environmental safety (damage to soil, plants, atmosphere). Fly ash can even get into the soil and contaminate groundwater with heavy metals [3, 4]. In this regard, there is a necessary need for the utilization and processing of ash [5].

As the Head of State N. Nazarbayev noted in his message to the people of Kazakhstan on January 10, 2018: "It is important to increase the requirements for energy efficiency and energy saving of enterprises, as well as the environmental friendliness and efficiency of the energy producers themselves.

Table 1 - Annual production of coal ash in the world (2013)

Country	Ash production (mln. tons)
China	385
USA	118
India	105
Europe	52,6
Middle East and Africa	32,6
Russia	26,6
Asia	16,7
Australia	13,1
Japan	11,1
Canada	6,8

At present 500 million tons of ash and slag waste has accumulated in the Kazakhstan, and this volume is growing by 19 million tons per year. At the same time, ash dumps occupy large areas, and their construction requires significant capital expenditures from power plants, which ultimately affect the cost of production of energy (according to the Kazakhstan Electric Power Association)..

From ash-and-slag wastes from coal produced by CHP, about 8% of ash is processed in Kazakhstan (less than 1.9 million tons). If the use of ash remains at this level, by 2020 the amount of accumulated waste will exceed 650 million tons, and by 2030 - 1 billion tons [6].

In this context, global processing of ash not only contributes to the improvement of the ecological state of the environment, which is a priority, but additionally (except for energy) will significantly improve the efficiency of coal processing with the production of high added value products.

Ash-and-slag wastes have specific properties that determine the possibility of their effective use in various industries. A wide application of processing of ash and slag wastes was found in the developed countries of the West, where about 65-70% of ash and slag (formed by heat and power plants) are processed, mainly in the production of building materials (as additives in cement, concrete, bricks, etc.). In Germany, Denmark, China, up to 100% of the annual output of ash and slag materials is used in the production of building materials. In Germany, it is currently forbidden to build coal-fired power plants and ash-and-slag-dumps without the technology of 100% processing into other goods. Changes in Indian law led to an increase in the use (utilization) of ash from 30% of the annual output to 53%, which is about 70 million tons/year [6].

At the same time, in addition to building materials, various valuable metals can be obtained from ash and slag wastes. Many rare elements found in ashes are in demand and are intensively used, for example: yttrium - for the production of new structural and high-temperature superconducting ceramics and phosphors; scandium - in military technology, for the manufacture of halogen lamps; Lithium - for the production of aluminum-lithium alloys for aircraft missile technology; gallium - for the production of laser diodes for fiber-optic communication and ultra-high-frequency radar equipment; beryllium - in electrical engineering and electronics, in aerospace engineering, in the automotive industry; germanium - for the production of infrared technology, fiber optics, in pharmaceuticals, in metallurgy.

Chemical composition of ash-and-slag wastes

The composition of ash and slag wastes is determined by the mineral composition of the coals, which depends on the deposit, the depth of the beds, methods of extraction and enrichment, and the ash content of the coal is constantly increasing.

The chemical properties of ash and slag waste vary greatly depending on the type of coal, combustion temperature, combustion technology, air/fuel ratio and coal particle size. The main part (up to 98-99%) of ash and slag wastes are compounds of ash-forming macroelements (Si, Al, Fe, O, Ca, Ti, Mg, S, K, Na). The remaining elements (microelements) are present in the ash at a level of 0.1% or less. Some of the trace elements (Sr, Ba, Sc, Y, La, Ti, Zr, etc.) are contained in the slag. Other elements (Ga, In, Tl, Ge, Sn, Pb, etc.) at temperatures above 1000 0C are removed from the high temperature zone and condense in cyclones, electrostatic precipitators (at 110-120 0C) [7].

Alkali and alkaline-earth metals (Na, K, Ca, Mg, etc.) occupying the position between macro and micro components are in the form of organomineral components, and also form inorganic compounds (calcite, dolomite, gypsum).

All elements of ash can be a part of both the mineral part of the coals (i.e., form minerals) and in the form of compounds with organic matter of coals, forming so-called organomineral components, which are the least studied forms. These include: salts of humic acids (K, Na, Ca, Mg, etc.), complex humates characterized by a cyclic system of bonds, as well as elementorganic compound compounds (ie, with a bond C-E, where E - S, Si etc.).

Phase-mineralogical composition of ash is determined by compounds of inorganic components in coal, as well as by physicochemical processes occurring during coal combustion. The main quantity of inorganic elements is concentrated in the form of quartz, minerals of the kaolinite group, siderite (FeCO_3). As admixtures there are hydromicas, feldspars, calcium carbonates (aragonite CaCO_3 and calcite CaCO_3), magnesium (magnesite MgCO_3), pyrite (FeS_2). The content of iron varies considerably in coals, the main compounds of which are siderite and pyrite, which sometimes form quite large concretions.

The problems of the origin and distribution of basic inorganic components in coals and their processing products are described in works [8, 9].

In some coal deposits (as in ores), there are elevated concentrations of valuable metals - vanadium, germanium, titanium, tungsten, zirconium, gallium, niobium and some others. Thus, up to 40-67% of titanium, 45-77% of beryllium, 70-87% of copper, 50-81% of manganese, 74-84% of arsenic, 48-60% of vanadium and 62-83% of gallium are extracted from ash-and-slag wastes of brown coal.

Thus, a significant accumulation of ash and slag wastes due to burning of coals is the reason for special attention to the study of the chemical composition of coals with the further development of technologies for extracting valuable elements from ash. We will briefly review the physicochemical composition of the coals most used in Kazakhstan and attractive from the point of view of extracting valuable substances from them (data are taken from [10]).

The Karaganda basin (hard coal). The coal ash is refractory (melting point 1250-1500 ° C). In separate layers (Dolinskaya and Tentekskaya suites), the yttrium content reaches 40-54 g/t ash, scandium up to 43 g / t ash.

Karaganda basin (brown coal). Low-sulfur coals (0.5-0.8%), medium phosphorus (0.01-0.08%). Coals of the Dubov suite are characterized by increased concentrations of yttrium (up to 180 g/t of ash), scandium (up to 90 g/t) and other impurity elements (beryllium, vanadium, chromium, cobalt).

Ekibastuzsky basin. It is one of the coals most used at CHP. The actual average ash content of coal is 39%. The ash of the top three layers is refractory (1610-1690 ° C), highly abrasive. Coals are low-sulfur (0.4-1.0% S total, with predominantly organic sulfur), polyphosphorous. A peculiar feature of the ash of Ekibastuz coals is the increased content of alumina (26-30%). In heavy fractions with a density of more than 1.7 g/cm³, zinc, copper, lead, and also silver, scandium and other elements are concentrated to a few hundredths of a percent. Calculations showed that from the ash yield of about 30 million tons, with the creation of the appropriate technology, it is possible to extract 70,000 tons of titanium, 24,000 tons of zinc, 12,000 tons of lead, 9,000 tons of tin, 3,000 tons of copper, 180 tons scandium, 30 tons of silver and other elements (vanadium, manganese, zirconium). Considering the huge reserves of ash and slag waste obtained from the burning of Ekibastuz coals at the CHP, the issue of extracting valuable components from them can become an important economic problem. Then, ash waste can be used as raw material for building materials.

Maykubensky basin. Coals of the basin are humus, brown with a high degree of coalification, medium-ash. The ash is refractory, with a high content of Al_2O_3 (up to 30%). Coals are low-sulfur (0.5-1.0%) and polyphosphorous (0.1%).

In addition, elevated scandium concentrations (up to 0.05%, an average of 7 clarkes), yttrium (up to 0.03%), ytterbium (up to 0.005%, an average of 10 clarkes), gallium and zirconium (up to 0.06%) are in the coal ashes of the Shoptykol suite. High concentrations are characteristic for copper, zinc and lead. The titanium content reaches 1%. It is noted up to 100 g of beryllium per 1 t of ash, 1-30 g/t of silver.

The ashes of Maykubensky coals with a high Al₂O₃ content can be a good raw material for alumina production. In addition, the ash from the coals of the Shoptkykol suite is a complex raw material not only for the production of aluminum, but also for titanium, scandium, rare earth elements and other valuable impurity elements. In addition, the presence of biostimulants (phosphorus, boron, zinc, etc.) in the ashes allows them to be used as microfertilizers.

The Borlydeposit. Coals are humus, stone, high-ash (32-40% and more), low-sulfur. Ash is characterized by a high content of alumina (an average of 26.8%). The elevated Al₂O₃ contents (38-39%) are characteristic in particular of the coals and rock layers of the lower coal horizon. The same coals are characterized by fairly high concentrations of titanium (3400 g/t in coal and 8,500 g/t in ash), zirconium (209 and 520 g/t in coal and ash, respectively), yttrium (25 and 62 g/t), ytterbium (2.5 and 6.5 g/t) and scandium (209 and 520 g/t).

The Kara-Zhyradeposit (the old name is Yubileynoye). Coals belong to the brown (B3) high-metamorphosed, transitional to the stone long-flame, humic with an ash content of 14-19% (average 16.3%), low-sulfur (average sulfur 0.48%). Coal ash, in addition to titanium, is enriched with scandium (46-95 g / t ash), yttrium (66-79 g / t ash), beryllium (more than 10 to 50 g / t ash), copper (the vast part contains 100-300 grams / t ash) and other elements-impurities. On a large area of coal seams, the concentrations of these elements are maximal. Taking this into account, the coals of the deposit should be considered as a potential source of rare-earth-scandium raw materials and more detailed additional research is needed.

Some basic indicators of the chemical composition of the above coals are summarized in Table 2 (the gold-forming organic and mineral macroelements C, H, S, P, Si, Al, Fe, O, Ca, Ti, Mg, K, N are given in units of mass% microelements Ti, Zr, Sc, Y, Yb are given in units of - g/t ash, A^r- ash content of coal, W_t^r- coal moisture, T_m - melting temperature of ash).

Table 2 – Chemical composition of Kazakhstan coal [10]

The Karaganda basin (hard coal)											
A ^r	T _m ²		SiO ₂	Al ₂ O ₃	CaO	MgO	SO ₄				
от 10-15 до 25-40	1250-1500 °C		51	35	7	1	4				
The Karaganda basin (brown coal)											
W _t ^r	A ^r	S	P		C	H	Y		Sc		
17-25	16-21	0,5-0,8	0,01-0,08		71	5,4	до 180		до 90		
Ekibastuz Basin											
A ^r	T _m	SiO ₂	Al ₂ O ₃	Fe ₂ O ₃	CaO	MgO	N ₂ O	K ₂ O	Ti	Zr	Y
39	1610-1690°C	62,9	28,6	3,8	1,1	0,3	2,4	0,2	до 10000	до 10000	30
Maykubensky Basin											
A ^r	S	P	Al ₂ O ₃	Sc	Y	Yb	Zr	Ti	Be	Ag	
25-28	0,5-1,0	0,1	до 30	до 0,05	до 0,03	до 500	0,06	до 10000	100	1-30	
The Borly deposit											
A ^r	Al ₂ O ₃	Ti	Zr	Y	Yb	Sc					
32-40	38-39	8500	520	62	6,5	520					
The Kara-Zhyra											
A ^r	S	SiO ₂	Al ₂ O ₃	Fe ₂ O ₃	CaO	TiO ₂	MgO	SO ₃	Sc	Y	Be
14-19	0,48	45,7	29,8	8,25	5,01	1,2	2,06	5,63	46-95	66-79	10-50

Methods of extraction the elements from ash and slag wastes

– In studies devoted to the study of the leaching of trace minerals, the experiments differ in both the set of elements studied (depending on the qualitative composition of the ash), the choice of the reaction medium for leaching, and the temperature and time treatment regimes. Analysis of literature data on how to extract trace minerals allows them to be divided into three main groups:

– acid methods. For the extraction of microelements of basic and amphoteric character, solutions of strong mineral acids (H₂SO₄, HCl, HNO₃) [11-13], acetic acid [13] are used;

- alkali methods. Alkaline solutions (NaOH, Na₂CO₃, NaHCO₃, NH₄OH) [12], Ca(OH)₂ are used to extract microelements of acidic and amphoteric character [14].
- extraction in harsh process conditions (increased pressure, temperature) [15] or with use of aggressive media (oxidation-reduction or chlorinating calcination) [16], fusion with chlorides, sublimation [17];
- biotechnology of metal leaching (using bacteria) [18].

In addition, recently, the fluoride methods of processing mineral raw materials have been increasingly developing. Previously, fluorides were used, mainly, for the production of uranium hexafluoride in the nuclear industry. Fluoride technologies allow expanding the range and depth of extraction of elements. The condition for the profitability of fluoride technologies is the use of fluorine and hydrogen fluoride in pure form, or in the form of more technological fluoride and ammonium bifluoride [19]. The method of fluoride processing of ash consists in the fact that hydrogen fluoride interacts with the ash and transfers silicon (contained in the ashes) to the gaseous compound - tetrafluorosilane. This separates the silicon compound from the bulk of the substances. Tetrafluorosilane is absorbed with a solution of ammonium fluoride, which is then treated with an excess of ammonia to isolate the highly dispersed residue. The physicochemical basis of this process with the use of ammonium fluorides is the difference in the properties of ammonium fluorometallates. For the complete extraction of components from the ash, optimal process conditions are determined by varying the difference in the physicochemical properties of ammonium fluorides and fluorometallates [20].

Prior to direct leaching of valuable components from ash, unburned coal (undersized) and iron-containing fractions are usually recovered. Unburned (content in ash is 5-15%) is separated from the ash usually by the froth flotation method (on flotation machines). With regard to trace elements, separation of coal will further increase their content in the solid residue. The most common method of magnetic separation is used to separate the iron-containing fraction from the ash. In addition, there is an additional stabilization of the composition of macrocomponents.

The complex processing of fly ash from the Ekibastuz Basin is proposed in the work [21], the technological scheme of which is shown in Figure 1. Such processing includes sulfuric acid leaching of rare-earth and radioactive metals, followed by alkaline extraction of gallium and amorphous silicon oxide.

Aluminium extraction

In accordance with the reagents used, the sintering processes can be separated into lime or calcination agglomerate, the Kalsinter process and other agglomeration processes. The agglomeration processes include a high temperature reaction of coal fly ash with powdered sintering agents to form soluble alumina compounds. The agglomerate is then leached (to separate aluminum) and the resulting solution is treated to produce high purity alumina.

In the agglomeration process, the ash reacts with lime (added as limestone) at an elevated temperature (> 1100 °C) to form calcium aluminate (soluble in the extractant) and calcium silicate insoluble in the same solution. The extraction of alumina from the agglomerate is carried out by dissolving the alumina in the extractant and precipitating the calcium silicate as a solid residue. Conventional extractants include water and dilute alkaline solutions, such as Na₂CO₃ and NaOH [22]. After leaching, aluminum precipitates as Al(OH)₃ by contacting the solution with CO₂. The next step is calcining the precipitate to produce the final product of α- or γ-alumina.

The first method of agglomeration with calcareous soda was developed by Kaiser A. in 1902 to separate alumina from silica. It is known that the reaction of a mixture of lime and soda with fly ash forms soluble sodium aluminate and insoluble calcium silicate. At high temperatures (usually 1100-1400°C), the formation of other compounds is inevitable, depending on the type of fly ash and sintering conditions. As in lime agglomeration, the sintered product is leached with water, caustic soda or sodium carbonate solution. Therefore, the agglomeration process with calcareous soda also includes a purification step of the solution. The resulting suspension is filtered and the solution is treated with Ca(OH)₂ suspensions to precipitate the dissolved silica at a high temperature and pressure, which is then decomposed in the same manner as in the Bayer process, or treated with CO₂ to precipitate the hydrated alumina. Al(OH)₃ is separated and converted to alumina by calcinations.

Wang and co-authors [23] extracted aluminum by pre-precipitation of fly ash, agglomeration with lime and soda, dissolution and carbonization. The degree of recovery reached 40%, and the Al_2O_3/SiO_2 molar ratio increased after preliminary precipitation. The rate of extraction of alumina from the agglomerate reached 91%.

Bai and co-authors [24] extracted alumina from the precipitated fly ash by the agglomeration process with lime and soda. The extraction rate reached 90% under optimal conditions. Bai and co-authors [25] obtained aluminum from fly ash by dilution with alkali and carbonization to convert amorphous silica to a product of amorphous nanoparticles. In this process, fly ash is mixed and sintered with gypsum and limestone at a temperature of about 1000-1200°C. The agglomerate is then leached with dilute acid. The solid waste particles are removed by filtration, and the metal residues are recovered from the filtrate.

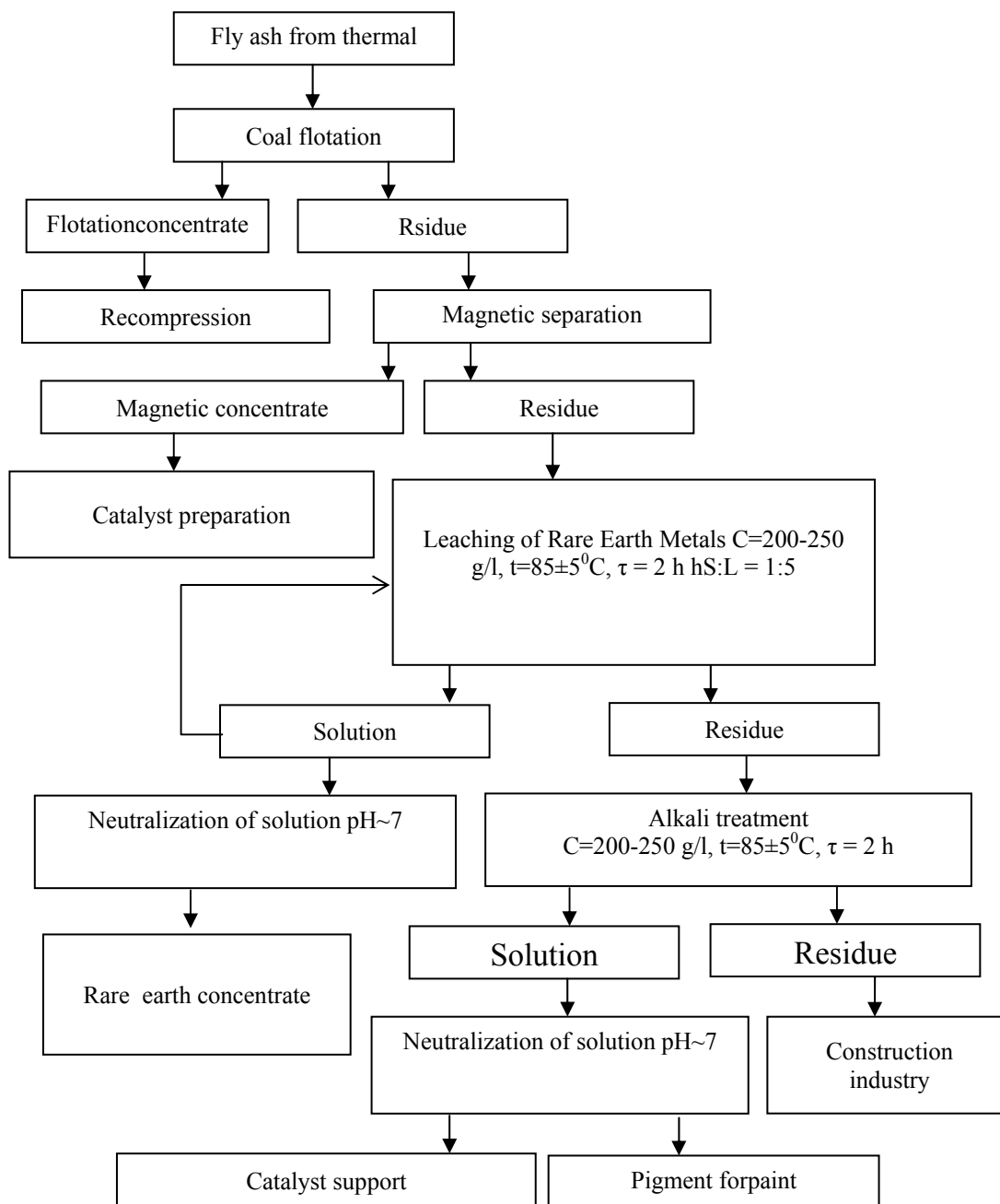


Figure 1 – Technological scheme of complex processing of fly ash from the Ekibastuz basin

In the patent [26], fly ash was sintered with a mixture of NaCl and Na₂CO₃ at temperatures of 700-900°C. The agglomerate was then leached with nitric or sulfuric acid, recovering 90-99% aluminum. The careful separation of aluminum from silicon can be achieved by a direct acid leaching process. Usually, sulfuric, hydrochloric and nitric acid is used to leach fly ash. An aqueous suspension of 20% (w/v) fly ash is prepared using 16 mol/l HNO₃ and 36 mol/l H₂SO₄, which will dissolve no more than 10% of the total amount of aluminum at ambient temperature for 72 hours. A greater amount of aluminum is recovered by leaching under reflux conditions for a long period of time; and even then not more than half of the aluminum is dissolved in the acid filtrate.

Wu et al. [27] extracted aluminum from fly ash by acid pressure leaching. The optimum conditions were determined: sulfuric acid concentration 50% and reaction temperature 180 ° C for 4 hours. Under optimal conditions, the extraction efficiency reached 82.4%. In comparison with traditional heating processes, microwave heating has its advantages, since it can be selective, controlled and effective.

In [28, 29], alumina was extracted using the acid sintering leaching process. A mixture of fly ash and concentrated sulfuric acid was calcined to convert most of the aluminum to aluminum sulphate, which can be extracted with hot water. The degree of extraction of aluminum oxide reaches 70-90% with a relatively lower processing temperature and a smaller amount of solid residue.

In [30], fly ash was calcinated with soda at 900 ° C to obtain soluble aluminates. The agglomerate was then leached with sulfuric acid to produce a solution containing aluminum. The recovery efficiency reached above 98%.

In [31], high-temperature chlorination of fly ash was studied using a reactor with a gas-liquid layer. In the presence of carbon and carbon monoxide present as reducing agents, about 25% of the alumina in the ash was chlorinated for 2 hours at a temperature above 900 ° C.

Извлечение Sc, Y, La

In [32] scandium, yttrium and lanthanum were leached from the ash. An aqueous solution was prepared in a ratio of solid and liquid phases of 1:10 (10 g of ash and 90 ml of distilled water). The following acids were used: sulfuric acid H₂SO₄ - 93.6-95.6% by weight. (GOST 4204-77); nitric acid HNO₃ - 65% by weight (GOST 4461-77); Hydrochloric acid HCl - 35% by weight (GOST 3118-77). After acid addition, the samples were placed in a shaker for 0.5 hours, or 2.5 hours at 80 ° C and 250 rpm. As a result, it was found that the optimal leaching conditions are as follows: for lanthanum - 25 g HNO₃, T = 80 ° C, t = 2.5 hours (average leaching value 49.5%); for yttrium - 5 g H₂SO₄, T = 80 ° C, t = 2.5 hours (average leaching value 45.33%); for scandium - 5 g H₂SO₄, T = 80 ° C, t = 2.5 hours (average leaching value 75%). It can be seen that the most effective treatment is sulfuric acid treatment and leaching at 80 ° C for 2.5 hours.

The authors of work [33] extracted yttrium and scandium from the ash of brown coals with hydrochloric acid solutions. The optimal leaching conditions were established: T = 40-50 °C, the initial concentration of HCl was 2.5-3.2 mol/l, the ratio of T: F = 1: 4-1: 5, the duration of the process was 30-60 min. At the same time, 95-96% of yttrium and 85-90% of scandium pass into the solution, which is a rather high index.

Extraction of aluminum and titanium

The method for reducing Al and Ti involves leaching fly ash by acid / alkaline leaching, followed by precipitation, solvent extraction or recrystallization [34-36].

An acid pressure leaching method was demonstrated in [37], in which high extraction (82.4%) of Al was obtained by reducing the size of fly ash (74 μm) and increasing the acid concentration (50%). However, in this method, non-target metals were easily leached into the acid, which led to contamination.

Extraction of vanadium

In the patent [38] used an acid solution for the recovery of vanadium V. Extraction was carried out by precipitation of vanadium pentoxide as a result of increasing the pH by adding calcium hydroxide, lime or calcium carbonate to the acid solution. After precipitation of vanadium V, the solid was separated by filtration or centrifugation. The recovery percentage of V from the acidic solution was ≥ 98%.

An acid leaching process using large volumes of sulfuric acid was also described in ref. [39], where the recovery of vanadium V was up to 95.8% from the filtrate.

Extraction of silicon and gallium

In the hydro-alkali treatment of fly ash from Ekibastuz coal, silicon and gallium were recovered [40]. Under optimum conditions ($T = 85 \pm 5 \text{ }^\circ\text{C}$, $t = 1 \text{ h}$, $C_w = 200\text{-}250 \text{ g/l}$, $T: F = 1: 4\text{-}6$), the recovery of silicon (based on SiO_2) is 49.3%, aluminum - 5.5%, gallium - 56%. The leaching solution is characterized by the following parameters: SiO_2 - 60 g/l, Ga - 5 mg/l. For the subsequent extraction of gallium, known schemes can be used, including extraction or ion exchange. Amorphous silicon dioxide can be isolated from the solution and used as a raw material for the chemical industry, for example, to obtain a silicate matrix of catalysts, paint and varnish, white soot.

Extraction of gallium and germanium

After the combustion of coal at the power plant, the fly ash is enriched with gallium Ga and germanium Ge in comparison with the initial coal [41].

The extraction of Ge and Ga from the ash was carried out using various extractants in a wide range of extraction conditions (acidic, alkaline, complex, reducing and oxidizing) [42]. High extraction yields of Ge (up to 90%) and Ga (up to 82%) were obtained using weak solutions of oxalic and sulfuric acids, respectively, for 1-2 hours of the extraction period.

In order to extract Ge germanium from solution, an ion flotation method using various complexing agents (pyrogallol, catechol, hydroquinone and resorcinol) in the pH range 4-7 was developed in Ref. [43]. It was found that when dodecylamine is used as a surfactant and pyrogallol or catechin as a complexing agent at pH values of 4-7, germanium can almost completely be recovered in 30 minutes. The use of catechol as a complexing agent for the extraction of Ge (from filtrates) was also noted in [44].

Extraction of aluminum, gallium and germanium

A special place is occupied by works connected with bacterial leaching of microcomponents from ash [45,18]. The basis of this process is the oxidation of sulfide minerals, which are contained in rocks. Thionic bacteria oxidize the sulphides of iron, copper, zinc, etc. At the same time, metals from an insoluble sulphide form transform into sulphates that dissolve well in water. From sulfate solutions, metals are extracted by extraction, sedimentation, sorption.

Monograph [18] developed a schematic diagram of bacterial (biochemical) leaching of aluminum, gallium, and germanium by Thion bacteria Th. Ferrooxidans by the method of biochemical heap leaching from the coal mine dump. The process of metal extraction consists of such operations: selection of an industrial site and its preparation for heap leaching; preparation of waterproofing base; ore preparation; installation of pipelines, sump, sedimentation tanks and collectors; delivery and storage of the rock; irrigation of ore dumps with ready-made bacterial solutions; directly the process of bacterial leaching of metals; drainage of the solutions through a heap pile; accumulation of metal solutions in sedimentation tanks and reservoirs; delivery through the pipeline system of the formed solution with metals to the processing complex for processing the obtained solutions and obtaining the chemical concentrate of the extracted metal.

Extraction of cerium, gallium, vanadium

In the works of the Department of Inorganic Chemistry, Omsk State University, the possibility of extracting rare and rare-earth elements from the ash of Ekibastuz coals was studied [46]. When the ash is treated with sulfuric acid ($C = 200 \text{ g/l}$, $t = 2 \text{ h}$, $T: L = 1: 5$), the recovery rates of rare metals are small: Ce - 0.35%, Ga - 1.2%, V - 4, 6%. Increasing the temperature to 85°C increases the recovery of these metals to 82; 16.3; 5.8% respectively. An effective method is the addition of NaCl. The use of a sulfuric acid solution ($C = 200 \text{ g/l}$) with a NaCl concentration of 50 g/l at $85 \text{ }^\circ\text{C}$ makes it possible to extract 90% of Ce from the ash, while Ga extraction was 25.6%, V = 7%. When coal ash is treated with sulfuric acid, radioactive elements - uranium and thorium - also leach out of it. Under these conditions, the recovery rate is 87% for uranium, 86% for thorium. Increase the recovery of rare earth elements from ash in the sulfuric acid medium by electrochemical leaching.

The extraction of REE

The elements of rare earth metals include light REE (Sc, La, Ce, Pr, Nd and Pm), average REE (Sm, Eu and Gd) and heavy REE (Tb, Dy, Ho, Er, Tm, Yb, Lu and Y), which are mainly used for various industrial purposes, such as fuel cells, high capacity accumulators, magnets for wind generation[47-49].

There are several methods developed to extract rare elements from ash. The method of chlorination is preferable because of its selectivity and high reactivity, but this method is expensive. This method can be used to recovery only some rare elements, where other complex recovery processes are not suitable.

The patent [50] describes the reduction of REE from ash. In this method, the ash samples were first treated with mineral acid (HNO₃) at 90 ° C to form a more concentrated mineral acid solution. This solution was mixed with an organic solution (tributyl phosphate and kerosene), which includes salts of rare earth metals. The organic solution was mixed with water to form an aqueous solution of REE and the REE was recovered using an ion exchange process.

Conclusions

The methods of extracting useful components from ash and slag wastes considered in this paper are mainly used in laboratory conditions. Therefore, the commercialization of these methods and their introduction on an industrial scale is one of the most important technological and environmental problems in Kazakhstan. A processing of ash in construction materials and valuable components, for example, near (in the territory) CHP, as well as numerous boiler houses, can significantly increase the efficiency of their operation, as a result, it will significantly reduce the cost of produced heat and / or electricity. In addition, the industrial production of these products (in addition to increasing local workplaces) will lead to a significant reduction (or lack, depending on the volume of production) of the volume of the corresponding imported products.

The present work was carried out within the framework of the scientific and technical program No. IRN BR05236359 on the topic: "Scientific and technological support of coal processing and production of high-conversion products of carbon chemistry", funded by the Science Committee of the Ministry of Education and Science of the Republic of Kazakhstan.

REFERENCES

- [1] Heidrich C., Feuerborn H.J., Weir A. (2013) Coal combustion products: a global perspective. World of coal ash (WOCA) Conference, *Lexington*.
- [2] Yao Z.T., Ji X.S., Sarker P.K., Tang J.H., Ge L.Q., Xia M.S., Xi Y.Q. (2015) A comprehensive review on the applications of coal fly ash, *Earth Sci Rev*, 141:105–121. DOI: [10.1016/j.earscirev.2014.11.016](https://doi.org/10.1016/j.earscirev.2014.11.016) (in Eng).
- [3] Prasad B., Mondal K.K. (2009) Environmental impact of manganese due to its leaching from coal fly ash, *Journal of Environmental Science & Engineering*, 51(1):27–32 (in Eng).
- [4] Ramya S.S., Deshmukh V.U., Khanderkar V.J., Padmakar C., SuriNaidu L., Mahore P.K., Pujari P.R., Panaskar D. et al (2013) Assessment of impact of ash ponds on groundwater quality: a case study from Koradi in Central India, *Environ Earth Sci*, 69: 2437–2450 (in Eng).
- [5] Ilic M., Cheeseman C., Sollars C., Knight J. (2003) Mineralogy of microstructure of sintered lignite coal fly ash, *Fuel*, 82(3): 331–336. DOI:[10.1016/S0016-2361\(02\)00272-7](https://doi.org/10.1016/S0016-2361(02)00272-7) (in Eng).
- [6] Maria Umarova. Achieving 100% processing of ash waste is proposed in Kazakhstan. Available at: <http://agmpportal.kz/dobitsya-stoprotsentnoj-pererabotki-zolotohodov-predlagayut-v-kazahstane/> (accessed 19.08.2016).
- [7] Adeeva L.N., Borbat V.F. (2009) *Bulletin of Omsk University* [Vestnik Omskogo universitetata] 2: 141-151 (In Russian).
- [8] ShiprtM.Ya., Kler V.R., Perzikov I.Z. (1990) Inorganic components of solid fuels. *Chemistry*, Moscow, ISBN 5-7245-0578-9.
- [9] Korobeckiy I.A., ShpirtM.Ya. (1988) Genesis and properties of mineral components of coals. *Science*, Sibir department, Novosibirsk. ISBN 5-02-028678-8.
- [10] Directory (1997) Basins and deposits of coal and oil shale in Kazakhstan. *Mineral Resources of Kazakhstan*, Almaty.
- [11] Sandhu S.S., Mills G.L. (1989) Kinetics of mobilization of trace elements from impounded coal ashes. III 197 th ACS Nat. Meet., Dallas, Tex., Apr. 9-14. Abstr. Pap., Washington. P. 315.
- [12] Suslova E.P., Pertsikov I.Z. (1990) *Solid fuel chemistry* [Khimiya tverdogo topliva] 5: 104-106. (in Russian).
- [13] Karuppiah MaKesh, Gupton Gian (1998) Toxicity of metals in coal combustion ash leachate, *Hazardous Materials*, 56(1-2): 53-58 (in Eng). DOI: [10.1016/S0304-3894\(97\)00034-4](https://doi.org/10.1016/S0304-3894(97)00034-4).
- [14] Guzhelev E.P., Usman U.T. (1998) Rational use of ash from CHP: Results of scientific and practical research. *State University*, Omsk, Russia. P. 238.
- [15] Lisowj B. (1987) Method of extraction of gallium and germanium from coal ash-entrainment. Patent US 4678647.

- [16] Clements J.L. (1985) Recovery of metals from coal fly ash, *Recycle and Secondary Recovery Metals*. Proc. Int. Symp. And Fall Ext. And Process Met. Meet., Fort Landerdale, Fla, *Warrendale*. Pa, P. 747-769.
- [17] Lisowyi Bohdan, Hitchcock David (1987) Benefication of gallium in fly ash. Patent US 4686031.
- [18] Zubova L.G., Zubov A.R. (2012) Vereh-Belousova K.I., Oleinik N.V. Obtaining metals from the waste pits of the Donbass coal mines. Monograph, publishing house of East Ukrainian National University named after V. Dal, Lugansk. ISBN 978-966-590-946-0.
- [19] Andreev A.A., Dyachenko A.N. (2009) Fluorammonium technologies in the processing of mineral raw materials. Fluoride technologies: The collection of theses and reports of the all-Russian scientific and practical conference, TSU, Tomsk. P. 87.
- [20] Andreev A.A., Dyachenko A.N., Kraidenko RI (2009) Ammonium fluorides in the technology of processing of mineral raw materials. Fluoride technologies: The collection of theses and reports of the all-Russian scientific and practical conference, TSU, Tomsk. P. 15.
- [21] Mikhailov Yu. L. Fiziko-khimicheskie issledovaniya processov vyshhelachivaniya mikrokomponentov zoly ot szhiganiya uglei Ekibastuzskogo basseina. Avtoref. diss. kand. khim. nauk [Physicochemical studies of the processes of leaching of ash microcomponents from the combustion of Ekibastuz Basin Coal. The abstract of the dissertation of the Candidate of Chemical Science. Omsk, 2001]. Omsk, 2001. 20 p.
- [22] Padil R., Sohn H.Y. (1985) Sintering kinetics and alumina yield in lime-soda sinter process for alumina from coal wastes, *Metallurg Mater Trans B*, 16(2): 385–395 (in Eng).
- [23] Wang M.W., Yang J., Ma H.W., Shen J., Li J.H., Guo F. (2012) Extraction of aluminum hydroxide from coal fly ash by pre-desilication and calcination methods. *Advanced Materials Research*, 396-398: 706-10. DOI: [10.4028/www.scientific.net/AMR.396-398.706](https://doi.org/10.4028/www.scientific.net/AMR.396-398.706) (in Eng).
- [24] Bai G., Teng W., Wang X.G., Qin J.G., Xu P., Li P.C. (2010) Alkali desilicated coal fly ash as substitute of bauxite in lime-soda sintering process for aluminum production, *Trans. Nonferrous Met. Soc. China*, 20: 169-175. DOI: [10.1016/S1003-6326\(10\)60034-9](https://doi.org/10.1016/S1003-6326(10)60034-9) (in Eng).
- [25] Bai G.H., Teng W., Wang X.G., Zhang H., Xu P. (2010) Processing and kinetics studies on the alumina enrichment of coal fly ash by fractionating silicon dioxide as nano particles, *Fuel Process. Technol.*, 91(2): 175-84 (in Eng). DOI: [10.1016/j.fuproc.2009.09.010](https://doi.org/10.1016/j.fuproc.2009.09.010) (in Eng).
- [26] McDowell W.J., Seeley F.G. (1981) Salt-soda sinter process for recovering aluminum from fly ash. Patent US4254088.
- [27] Wu C.Y., Yu H.F., Zhang H.F. (2012) Extraction of aluminum by pressure acid-leaching method from coal fly ash, *Trans. Nonferrous Met. Soc. China*, 22: 2282-8. DOI: [10.1016/S1003-6326\(11\)61461-1](https://doi.org/10.1016/S1003-6326(11)61461-1) (in Eng).
- [28] Liu K., Xue J.L., Zhu J. (2012) Extracting Alumina from fly ash using acid sintering-leaching process, In: Light Metals, Suarez CE, (Ed.), *John Wiley & Sons Inc*, 6: 201 (in Eng).
- [29] Bai G.H., Qiao Y.H., Shen B., Chen S.L. (2011) Thermal decomposition of coal fly ash by concentrated sulfuric acid and alumina extraction process based on it, *Fuel Process. Technol.*, 92: 1213-1219 (in Eng).
- [30] Ji H.M., Lu H.X., Hao X.G., Wu P. (2007) High purity alumina powders extracted from fly ash by the calcining-leaching process, *J. Chinese Ceram. Soc.*, 35: 1657-1660 (in Eng).
- [31] Mehrotra A.K., Behle L.A., Raj Blshol P., Svrcek W.Y. (1982) High-temperature chlorination of coal ash in a fluidized bed, *Ind. Eng. Chem. Process Des. Dev.*, 21(1): 44-50. DOI: [10.1021/i200016a009](https://doi.org/10.1021/i200016a009) (in Eng).
- [32] Ksenofontov B.S., Kozodayev A.S., Taranov R.A., Vinogradov M.S., Butorova I.A., Senik Ye.V., Voropaeva A.A. (2014) *Engineering Bulletin* [Inzhenernyi vestnik] 11: 112-121 (in Russian)
- [33] Kontsevoi A.A., Mikhnev, G.L. Pashkov, Kolmakova L.P. (1995) *Journal of Applied Chemistry* [Zhurnal prikladnoi khimii] 7: 68. (in Russian).
- [34] Matjie R.H., Bunt J.R., Heerden JHP (2005) Extraction of alumina from coal fly ash generated from a selected low rank bituminous South African coal, *Miner Eng.*, 18: 299–310. DOI: [10.1016/j.mineng.2004.06.013](https://doi.org/10.1016/j.mineng.2004.06.013) (in Eng).
- [35] Halina M., Ramesha S., Yarmob M.A., Kamarudin R.A. (2007) Non-hydrothermal synthesis of mesoporous materials using sodium silicate from coal fly ash, *Mater Chem. Phys.*, 101:344–351. DOI: [10.1016/j.matchemphys.2006.06.007](https://doi.org/10.1016/j.matchemphys.2006.06.007) (in Eng).
- [36] Li L., Wu Y., Liu Y., Zhai Y. (2011) Extraction of alumina from coal fly ash with sulfuric acid leaching method, *Chin J Process Eng.*, 11(2): 254–258 (in Eng).
- [37] Wu C., Yu H., Zhang H. (2012) Extraction of aluminium by pressure acid-leaching method from fly ash. *Trans Nonferr Met Soc China*, 22: 2282–2288 (in Eng). DOI: [10.1016/S1003-6326\(11\)61461-1](https://doi.org/10.1016/S1003-6326(11)61461-1).
- [38] Scharifker B. et al. (2009) Process to recovery vanadium contained in acid solutions. Patent US 7498007B2.
- [39] Xiang-Yang C., Xin-zhe L., Qui-li Z., Hong-zhou M.A., Hin Z. (2010) Leaching vanadium by high concentration sulfuric acid from stone coal, *Trans Nonferr Met Soc China*, 20: 123–126. DOI: [10.1016/S1003-6326\(09\)60108-4](https://doi.org/10.1016/S1003-6326(09)60108-4) (in Eng).
- [40] Borbat V.F., Mikhailov Y.L., Adeeva L.N., Golovanova O.A. (2000) Chemistry and Chemical Technology [Khimiya I khimicheskayatechnologiya] 1: 102–105 (In Russian).
- [41] Querol X., Fernández-Turiel J., López-Soler A. (1995) Trace elements in coal and their behavior during combustion in a large power station, *Fuel*, 74:331–343. DOI: [10.1016/0016-2361\(95\)93464-O](https://doi.org/10.1016/0016-2361(95)93464-O) (in Eng).

- [42] Arroyo F., Font O., Chimenos J.M., Pereira C.F., Querol X., Coca P. (2014) IGCC fly ash valorisation. Optimisation of Ge and Ga recovery for an industrial application, *Fuel Process Technol.*, 124: 222–227. DOI: [10.1016/j.fuproc.2014.03.004](https://doi.org/10.1016/j.fuproc.2014.03.004) (in Eng).
- [43] Hernandez-Exposito A., Chimenos J.M., Fernandez A.I., Font O., Querol X., Coca P., Garcia P.F. (2006) Ion flotation of germanium from fly ash aqueous leachates, *Chemical Engineering journal*, 118: 69–75. DOI: [10.1016/j.cej.2006.01.012](https://doi.org/10.1016/j.cej.2006.01.012) (in Eng).
- [44] Torralvo F.A., Fernández-pereira C. (2011) Recovery of germanium from real fly ash leachates by ion-exchange extraction, *Miner Eng.*, 24: 35–41. DOI: [10.1016/j.mineng.2010.09.004](https://doi.org/10.1016/j.mineng.2010.09.004) (in Eng).
- [45] Tatarinov A.V., Yalovik L.I., Danilova E.V. (2007) The role of microorganisms in the hypergenic transformation of polymetallic ores and the formation of biogeochemical anomalies of precious metals in the deposits of Transbaikalia, *Reports of the Academy of Sciences of the Russian Federation*, 414(5): 651–655 (In Russian). <https://doi.org/10.32014/2018.2518-1491>
- [46] Borbat M.F., Adeeva L.N., Mikhailov Y.L. (2009) *Chemistry and Chemical Technology* [Khimiya i khimicheskaya tekhnologiya] 2: 23–27. (In Russian).
- [47] Chen Z. (2011) Global rare earth resources and scenarios of future rare earth industry, *J Rare Earths*, 29: 1–6. DOI: [10.1016/S1002-0721\(10\)60401-2](https://doi.org/10.1016/S1002-0721(10)60401-2) (in Eng).
- [48] Hoenderdal S., Espinoza L.T., Marscheider-Weidemann F., Grus W. (2013) Can a dysprosium shortage threaten green energy technologies, *Energy*, 49: 344–355. DOI: [10.1016/j.energy.2012.10.043](https://doi.org/10.1016/j.energy.2012.10.043) (in Eng).
- [49] Franus W., Wiatros-Motyka M.M., Wdowin M. (2015) Coal fly ash as a resource for rare Earth elements, *Environ Sci Pollut Int*, 22: 9464–9474. DOI: [10.1007/s11356-015-4111-9](https://doi.org/10.1007/s11356-015-4111-9) (in Eng).
- [50] Chandrashekar S. (2010) Process for obtaining treated coal and silica from coal containing fly ash. Patent US 2010/0287827A1.
- [51] Malyshev VP (2000) К определению ошibки эксперимента, адекватности и доверительного интервала аппроксимированных функций. *Bulletin NAS RK*. 4:22-30 <https://doi.org/10.32014/2018.2518-1467> (In Russian)

**Б.Т. Ермагамбет¹, Н.У. Нурғалиев¹, Л.Д. Абылғазина¹,
Н.А. Маслов¹, Ж.М. Касенова¹, Б.К. Касенов²**

¹«Көмір химиясы және технология институты» ЖШС, Астана қ, Қазақстан;

²Ж. Әбішев атындағы Химия-металлургиялық институты, Қарағанды

КӨМІР ШЛАК ҚАЛДЫҚТАРЫНЫҢ ӨНІМДЕРІНЕН БАҒАЛЫ КОМПОНЕНТТЕР АЛУДЫҢ ӘДІСТЕРІ

Аннотация. Мақалада ЖЭС да көмірді жағу барысында шығатын күл шлак қалдықтарын (КШК) қайта өңдеу мәселелері қарастырылды. Шлак қалдықтарының жалпы химиялық құрамы, құрамындағы бағалы қоспалардың сонымен қатар Қазақстандағы меңгерілген және пайдаланылатын кен орындарында бағалы заттарды алу жайлы мәліметтер берілді. Осындай кен орындар ретінде Қарағанды бассейні, Экібастұз бассейні, Майкұбы бассейні, Борлы кен орыны, Қара-Жыра кен орындары таңдалды.

Көмір шлак өнімдерінен элементтерді шаймалау жайлы жасалған әдеби шолуда іс жүргізу жағдайы және де қажетті рективтерді таңдау көмір күлінің бастапқы дайындау дәрежесі мен құрамына байланысты, ал басты құрамдас факторы болып алынатын компоненттің концентрациясы болып табылатыны анықталды.

Көмір шлак қалдықтарының күлінен пайдалы компоненттерін алуды жүзеге асыру үшін көбінесе таралған және тиімді әдістер ретінде қышқылдық және сілтілік шаймалау болып табылады. Бірақта мұндай қымбат реагенттерді осы өнімдерді шығару барысында қолдану мұқият қажетті технологияларды әзірлеуді талап етеді, сонымен қоса реагенттерді қалпына келтіру мүмкіндігі де болуы қажет. Микроэлементтерді алынудың жоғарғы деңгейіне қарамастан өз кемшіліктері де бар, қышқылдық шаймалау қымбат қышқылға төзімді технологиялармен байланысты қондырғыларды қолдану, кремнийлі шлақты тұз қышқыл ерітінділерінен ажырату және алюминий тұзынан темірді тазарту сияқты қиыншылықтары бар.

Шлак қалдықтарының күлінен бағалы компоненттерді алу үшін келешегі бар технология болып биохимиялық үйме шаймалау болып табылатын Th. Ferrooxidans тиондық бактериялар, фторлық технология (фтор және фторсутекті немесе фторид және аммоний бифторидін) қолдануға болады.

Түйін сөздер: көмір, күл, шаймалау, қышқыл, сілті, металлдар, қайта қалпына келтіру, макроэлементы, микроэлементы.

Б.Т. Ермагамбет¹, Н.У. Нурғалиев¹, Л.Д. Абылғазина¹,
Н.А. Маслов¹, Ж.М. Касенова¹, Б.К. Касенов²

¹ТОО «Институт химии угля и технологии», г.Астана, Казахстан;
²Химико-металлургический институт имени Ж. Абишева, Караганда

МЕТОДЫ ИЗВЛЕЧЕНИЯ ЦЕННЫХ КОМПОНЕНТОВ ИЗ ЗОЛОШЛАКОВЫХ ОТХОДОВ УГЛЕЙ

Аннотация. В статье рассмотрены проблемы переработки золошлаковых отходов (ЗШО), образующихся от сжигания угля в ТЭЦ. Приведены общие сведения о химическом составе золошлаковых отходов и содержании в них ценных компонентов некоторых наиболее освоенных и используемых в Казахстане месторождений и привлекательных с точки зрения извлечения из них ценных веществ. Среди таких месторождений выбраны Карагандинский бассейн, Экибастузский бассейн, Майкубенский бассейн, месторождение Борлы, месторождение Кара-Жыра.

Проведенный литературный обзор методов выщелачивания элементов из золошлаковых отходов из углей показал, что условия ведения процесса и подбор необходимых реактивов зависят от состава и степени подготовки исходной угольной золы, а важным составляющим фактором является концентрация извлекаемого компонента.

Наиболее распространенными и эффективными методами извлечения ценных компонентов из ЗШО является выщелачивание кислотами и щелочами. Однако использование таких дорогостоящих реагентов уже в самом производстве данных продуктов требует тщательной разработки соответствующей технологии (по все цепочке процессов), где имеется возможность еще и восстановления реагентов. Кроме того, несмотря на относительно высокую степень извлечения микроэлементов кислотное выщелачивание имеет недостатки, связанные с применением дорогостоящего кислотоустойчивого технологического оборудования сложностью отделения кремнеземистого шлама от кислых растворов солей и трудностью очистки солей алюминия от железа.

Перспективными технологиями извлечения ценных компонентов из ЗШО является биохимическое кучное выщелачивание с применением тионовых бактерий *Th. Ferrooxidans*, фторидная технология (с использованием фтора и фтороводорода, или фторида и бифторида аммония).

Ключевые слова: уголь, зола, выщелачивание, кислота, щелочь, металлы, восстановление, макроэлементы, микроэлементы

Information about the authors:

Yermagambet Bolat Toleukhanuly – Doctor of Chemical Science, Professor, Director of LLP "Institute of Coal Chemistry and Technology", Astana, Kazakhstan, e-mail: bake.yer@mail.ru

Nurgaliyev Nurken Uteuovich – Candidate of Chemical Science, Leading Researcher of LLP "Institute of Coal Chemistry and Technology", Astana, Kazakhstan, e-mail: nurgaliyev_nao@mail.ru

Abylgazina Leila Dauletovna – Master of Engineering Sciences, Junior Researcher of LLP "Institute of Coal Chemistry and Technology", Astana, Kazakhstan, e-mail: lelya_1501@mail.ru

Maslov Nikolay Alexandrovich – Chief Specialist for Energy and Automation of LLP "Institute of Coal Chemistry and Technology", Astana, Kazakhstan, Akzhol 26, office 308, phone 8(7172)48-77-20, mob. 8-775-861-6484, e-mail: nike.6484@mail.ru

Kassenova Zhanar Muratbekovna – Master of Chemical Sciences and Technology, Deputy Director of LLP "Institute of Coal Chemistry and Technology", Astana, Kazakhstan, e-mail: zhanar_k_68@mail.ru

Kasenov Bulat Kunurovich – Head of laboratory of thermochemical processes "Chemical and Metallurgical Institute named after Zh. Abisheva" (Karaganda), e-mail: kasenov1946@mail.ru

NEWS

OF THE NATIONAL ACADEMY OF SCIENCES OF THE REPUBLIC OF KAZAKHSTAN

SERIES CHEMISTRY AND TECHNOLOGY

ISSN 2224-5286

<https://doi.org/10.32014/2018.2518-1491.29>

Volume 6, Number 432 (2018), 79 – 86

UDC 577.4:550.41:66.097:661(004.8)

Zh.K. Shomanova¹, R.Z. Safarov², A.S. Zhumakanova³,
Yu.G. Nosenko⁴, A.T. Zhanibekova¹, N.L. Shapekova², D. Lorant⁵

¹Pavlodar State Pedagogical Institute, Pavlodar, Kazakhstan

²L.N. Gumilyov Eurasian National University, Astana, Kazakhstan

³D.V.Sokolsky Institute of Fuel, Catalysis and Electrochemistry, Almaty, Kazakhstan

⁴Innovative University of Eurasia, Pavlodar, Kazakhstan

⁵Eötvös Loránd University, Budapest-Szombathely, Hungary

e-mail: ruslanbox@yandex.ru

ELECTRON MICROSCOPY SURFACE STUDY OF CATALYSTS BASED ON FERROALLOY PRODUCTION WASTE

Abstract: In the paper results of electron microscopy study of catalysts based on ferroalloy production waste from ash-slime storage of Aksu ferroalloy plant (Aksu, Kazakhstan). The surface morphology of catalyst granules as well pattern of surface distribution of crystallites of catalytically active metals (Fe, Cr and Mn) were described. It was shown, that during the process of catalyst obtaining, uniform porous surfaces without visible large agglomerates of metal crystallites were obtained. Distribution of metallic components was equable, particles were fine disperse, sizes of the crystallites were of one order.

Keywords: catalyst, waste, ferroalloy production, electron microscopy, surface.

Introduction

In result of activity of a ferroalloy plant various types of waste form. The main of them are slime and dust from gas cleaning equipment [1–3]. The waste is accumulated in slime storages. Usually the waste are dumped under the layer of water in artificial ponds. These materials are very disperse and unusable for remelting of ferroalloy, that is, they unusable for direct use in metallurgy [4]. However, earlier, it was shown that their elemental and phase content as well as surface structure make it possible to use them as catalysts for various chemical processes, in particular, in the processes of oil chemistry and oil refining [5].

Earlier we studied waste dumped in ash-slime storage of Aksu ferroalloy plant (Aksu, Kazakhstan) [6–8]. We investigated elemental content, phase content, structure of the surface with ammonia thermoprogrammed desorption and electron microscopy. A series of granulated catalyst was prepared based on obtained waste. In the paper, we are presenting electron micrographs of obtained catalyst samples. The aim of the study is to reveal morphological peculiar surface properties of catalyst samples prepared from samples of waste picked up from different locations of the ash-slime storage.

Methods

Catalyst preparation

For catalyst preparation ferroalloy production waste samples were picked up from the territory of ash-slime storage of Aksu ferroalloy plant according to GOST «17.4.3.01-83 Soils. General Sampling Requirements». Totally 80 samples from 16 locations were taken. From every location we took 5 samples using the method of «envelope» and well mixed them for obtaining of joint sample. So, we have obtained

16 joint samples. Each sample was assigned a serial number. Catalysts were named using serial number of joint sample used for preparing of it. In the research we used according names of catalysts Kt-1, Kt-2 ... Kt-16. For preparing of catalysts obtained ash-slime mass was washed by distilled water in order to separate small organic particles. Then the washed mass was dried on airtight petridishes to obtain a pasty mass. Laboratory extruder molded mass to obtain cylindrical granules with diameter of 3-4 mm and length 10-15 mm. After that granules were dried at 100-150 °C for 5 hours at the rate of temperature rise 25-30 °C per hour, then it was calcinated at 200 °C for 1 hour, 300 °C - 1 hour, 400 °C - 1 hour, 500 °C - 5 hours.

Electron microscopy

For studying of structure and surface of researched materials scanning electron microscope with thermionic cathode (LaB6) JSM-6610LV ("JOEL", Japan) was used. The device was kitted with the system of energy dispersive microanalysis, wave dispersion microanalysis system, backscattered electron diffraction analysis system using a reflected electron detector, Everhart-Thornley Secondary Electron Detector, secondary electron detector for low vacuum mode and equipment for sample preparation. The research was carried out at x1000 and x3000 magnifications.

Results and discussion

The broadness of the application of the method of electron microscopy is associated with its high informativity and versatility, as well as the simplicity and convenience of equipment managing [9]. Scanning electron microscopy has several advantages over other methods. For example, compared with traditional light microscopy, it is characterized by a significantly higher resolution and depth of sharpness; relative ease of interpretation of the images due to their three-dimensional representation; the ability to connect additional devices for analysis in the micro-range with sufficient ease of adaptation and control of these devices [10]. It is also necessary to note the relatively low requirements for sample preparation. Compared with scanning probe microscopy scanning electron microscopy allows you to explore significantly large areas of the surface; work with highly relief surfaces; use a much wider range of magnifications; obtain information not only about the surface, but also about the adjacent to the surface "subsurface" layers [11, 12].

We have obtained micrographs of cross sections and side surfaces of granules of catalysts Ct-2, Ct-3, Ct-4, Ct-5, Ct-15 at magnifications $\times 1000$ and $\times 3000$ (Fig. 1-20).

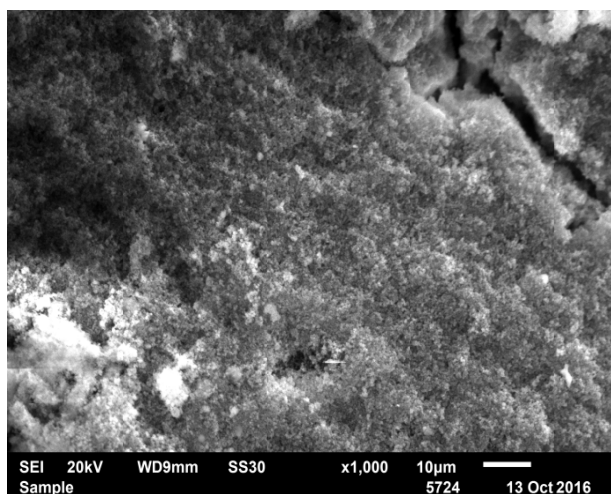


Figure 1 – Micrograph of cross section of catalyst Ct-2 granule ($\times 1000$)

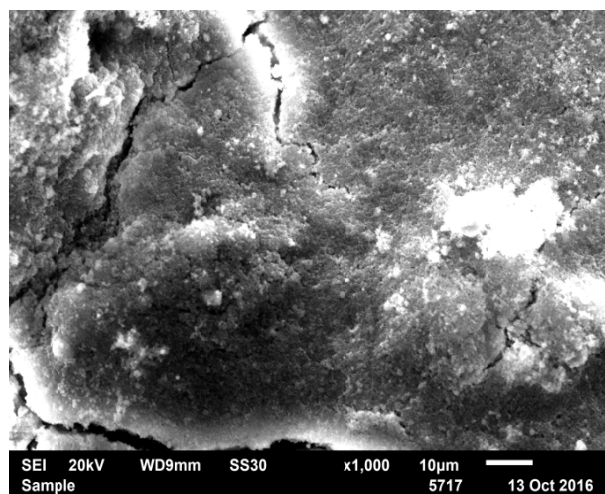


Figure 2 - Micrograph of side surface of catalyst Ct-2 granule ($\times 1000$)

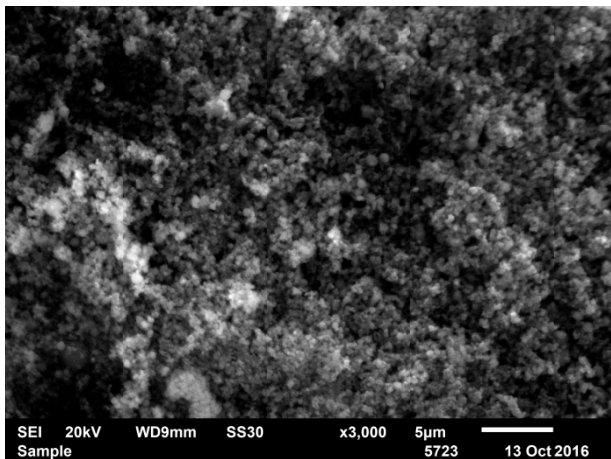


Figure3 –Micrographof cross section of catalyst Ct-2 granule(×3000)

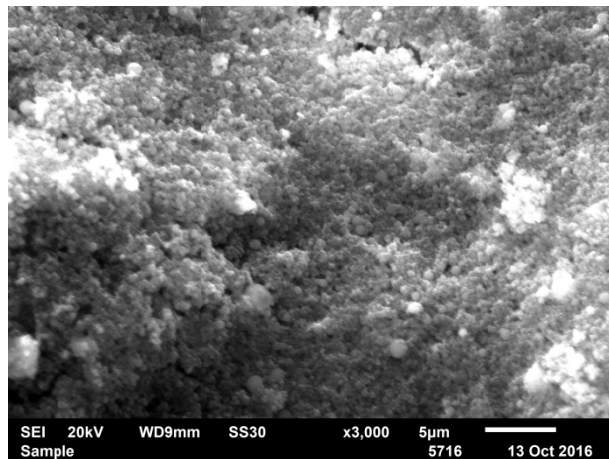


Figure4 - Micrographofside surface of catalyst Ct-2granule(×3000)

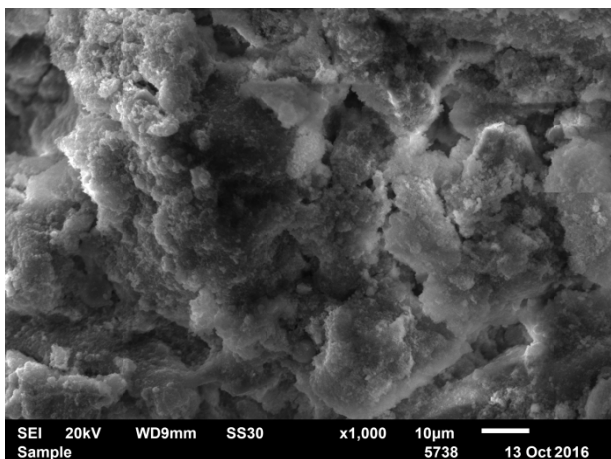


Figure5 –Micrographof cross section of catalyst Ct-3 granule(×1000)

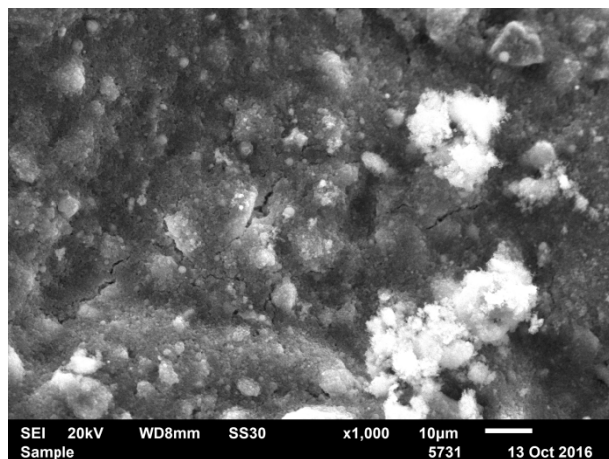


Figure6 - Micrographofside surface of catalyst Ct-3granule(×1000)

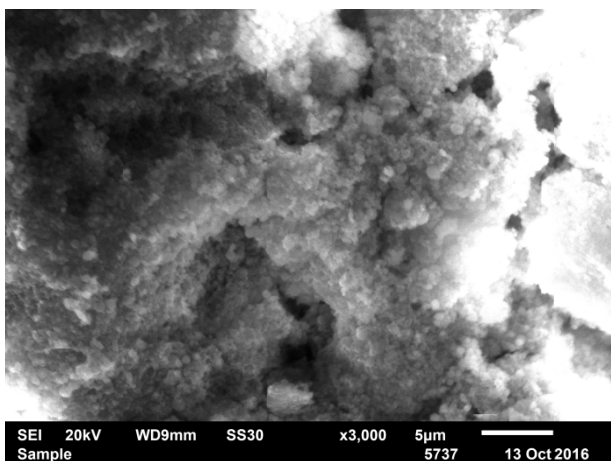


Figure7 –Micrographofcross section of catalyst Ct-3 granule(×3000)

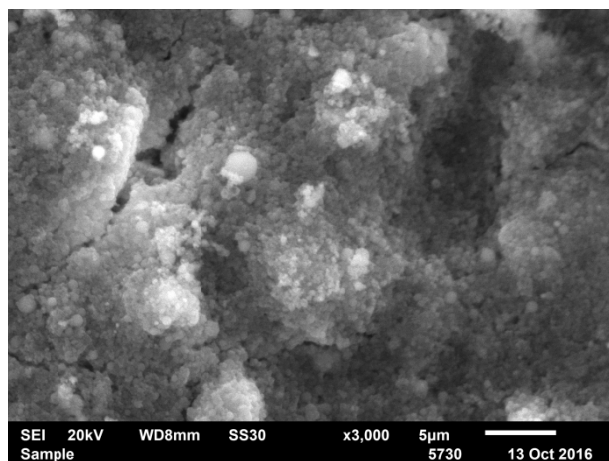


Figure8 - Micrographofside surface of catalyst Ct-3 granule(×3000)

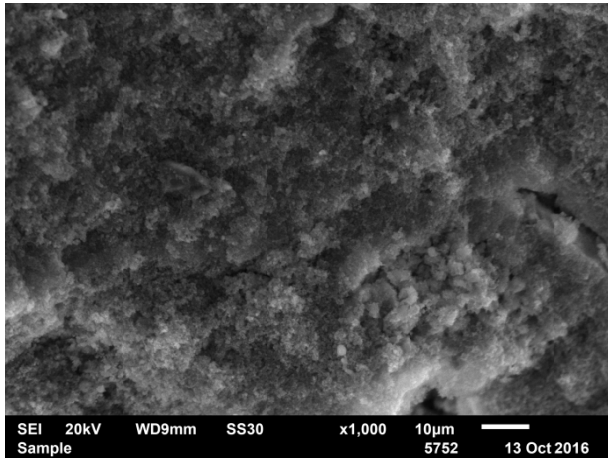


Figure9 - Micrograph of cross section of catalyst Ct-4 granule (×1000)

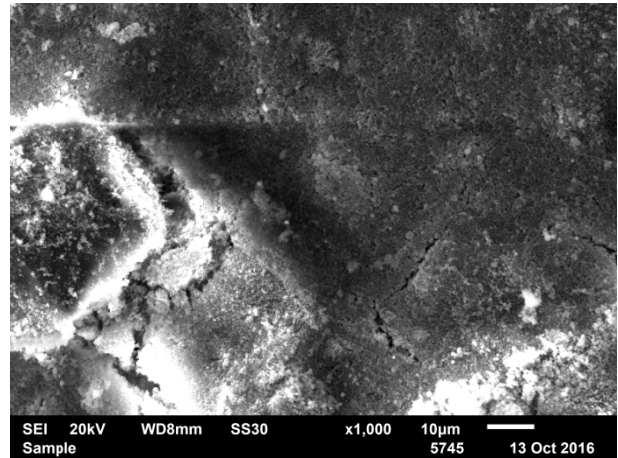


Figure10 - Micrograph of side surface of catalyst Ct-4 granule (×1000)

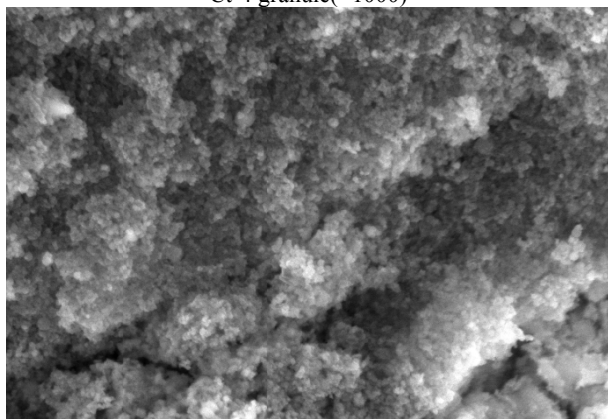


Figure11 - Micrograph of cross section of catalyst Ct-4 granule (×3000)

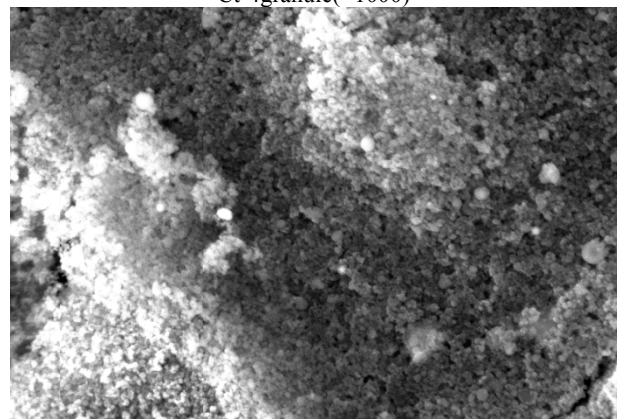


Figure12 - Micrograph of side surface of catalyst Ct-4 granule (×3000)

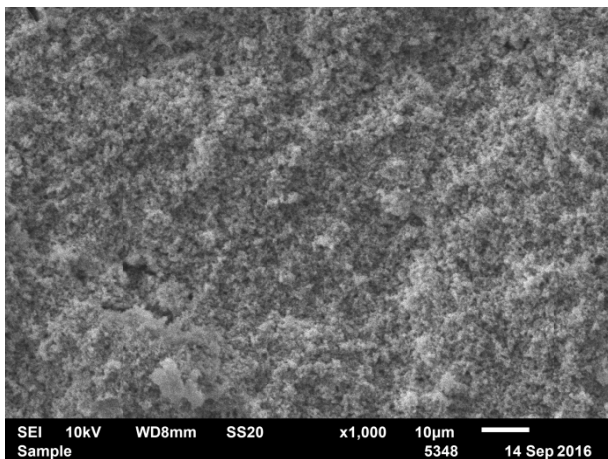


Figure13 - Micrograph of cross section of catalyst Ct-5 granule (×1000)

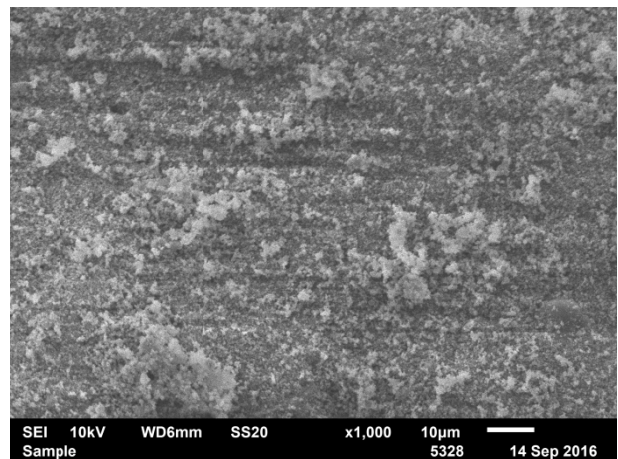


Figure14 - Micrograph of side surface of catalyst Ct-5 granule (×1000)

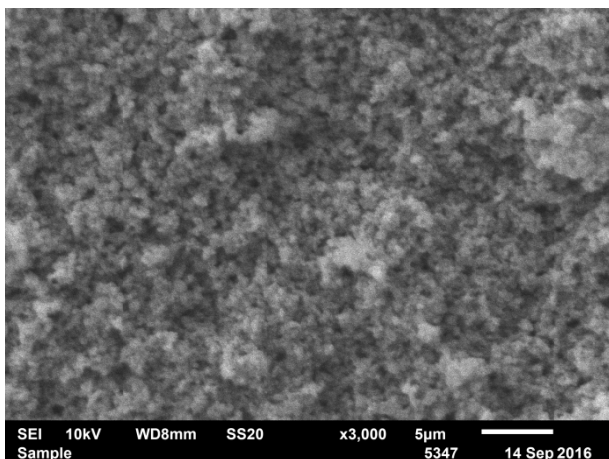


Figure15 –Micrograph of cross section of catalyst Ct-5 granule($\times 3000$)

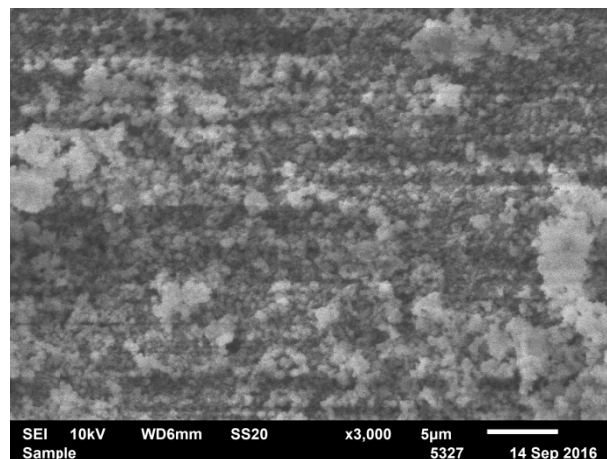


Figure16 - Micrograph of side surface of catalyst Ct-5 granule($\times 3000$)

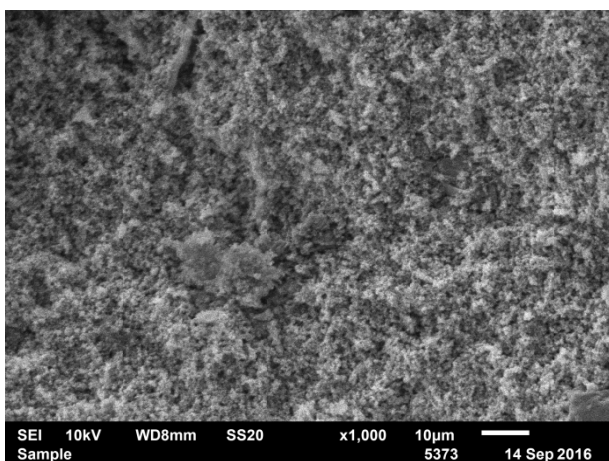


Figure17 –Micrograph of cross section of catalyst Ct-15 granule($\times 1000$)

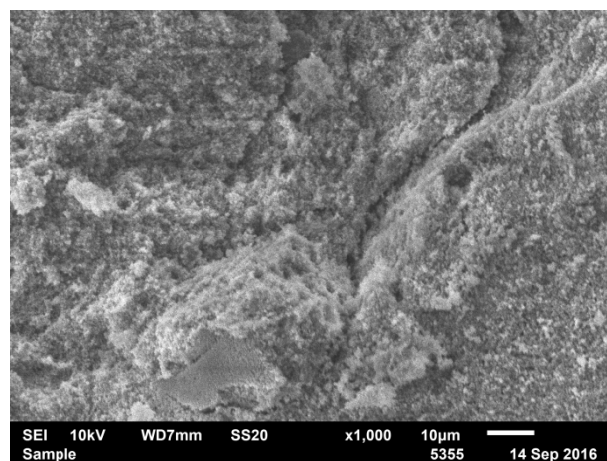


Figure18 - Micrograph of side surface of catalyst Ct-15 granule($\times 1000$)

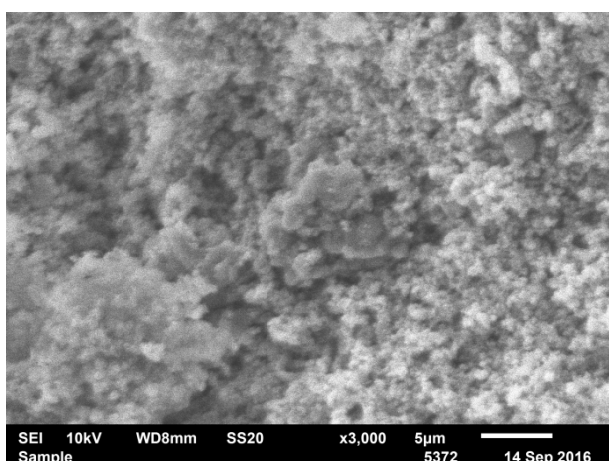


Figure19 –Micrograph of cross section of catalyst Ct-15 granule($\times 3000$)

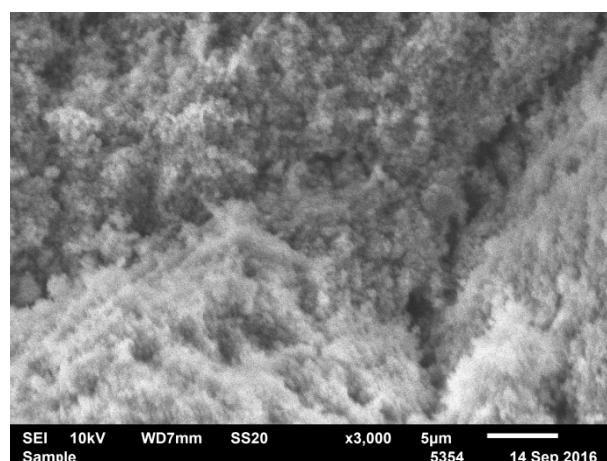


Figure20 –Micrograph of side surface of catalyst Ct-15 granule($\times 3000$)

Analysis of electronic micrographs allows us to establish that at magnification for 1000 times the lateral surfaces of the granules is more uniform than the cross-section surfaces. That is obvious due to the fact that formation of granules was performed with laboratory extruder, which forms more or less smooth surface of granules. The same time at magnification for 3000 times the difference in cross section surface and side surface morphology practically unnoticeable. The surface is finely porous, represented by fine

granular particles. Porous surface can be formed during the process of high temperature treatment as a result of elimination of volatile components.

In figures 21-23 micrographs of side surfaces of catalyst Ct-15 granules in the mode of frequencies filtration are represented. That allows to reveal distribution of crystallites of metallic components on surface. On presented micrographs it is visible, that metal components distribution is uniform, particles are finely dispersed, sizes of crystallites are of one order.

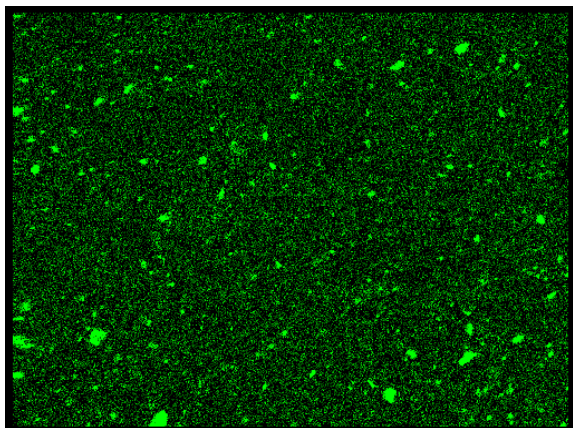


Figure 21 - Micrograph of side surface of catalyst Ct-15 granule with representation of Cr crystallites distribution

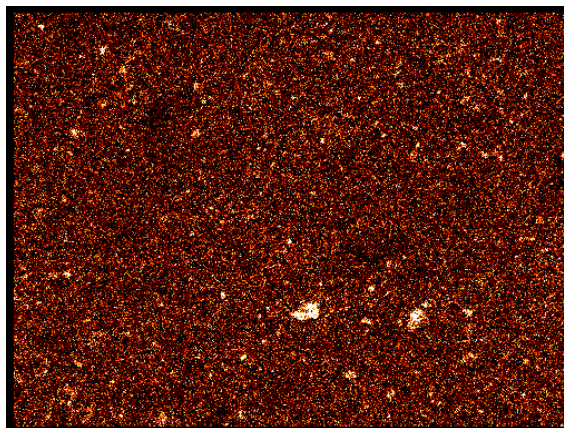


Figure 22 - Micrograph of side surface of catalyst Ct-15 granule with representation of Mn crystallites distribution

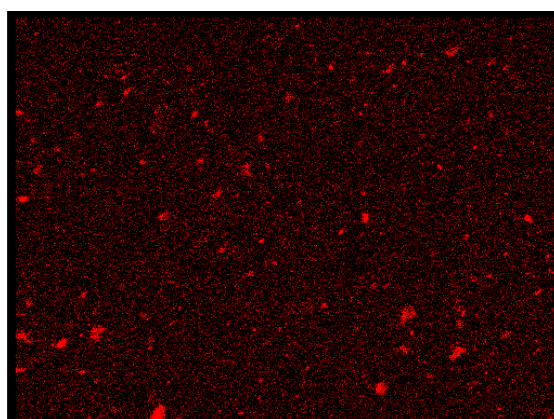


Figure 23 - Micrograph of side surface of catalyst Ct-15 granule with representation of Fe crystallites distribution

Conclusion

Thus, as a result of catalyst preparation, uniform, porous surface without visible large agglomerates of metal (or of metal compounds) crystallites was obtained. Taking into account characteristic content of ferroalloy production waste with increased concentration of catalytically active elements – Fe, Cr, Mn, specific for heterogeneous catalysts surface morphology [13,14], trend of distribution and degree of dispersity of metal crystallites on catalyst surface [15], it can be concluded that obtained materials can be used as heterogeneous nanosized catalysts for various processes of hydrocarbon-containing raw materials refining.

Important conclusion of electron microanalysis is the fact that morphology of surfaces of catalysts Ct-2, Ct-3, Ct-4, Ct-5, Ct-15 is practically the same. This fact allows indirectly confirm possibility of using of ash-slime storage as secondary source for mining of raw material for obtaining of catalyst. The same surface morphology of waste taken from different locations of ash-slime storage is the consequence of the fact that the waste was accumulated during many years of performing of regular processes of ferroalloys melting with strict adherence to regulations. In the other words, conditions of these wastes are constant and are controlled during the melting process. The spread of waste over the area of the ash-

slimestorage lake occurs as a result of hydrodynamic processes of mass transfer, diffusion. Waste material does not mix with ground, the presence of flora on the perimeter of the lake storage is minimal.

Based on the data obtained, it can be concluded that the catalysts obtained are promising materials and can be used in various processes of processing of hydrocarbon-containing raw materials, in particular, in the processes of cracking, hydrogenation, oxidation.

REFERENCES

- [1] Acharya P.K., Patro S.K. (2016) Use of ferrochrome ash (FCA) and lime dust in concrete preparation, *Journal of Cleaner Production*, 131:237–246. <https://doi.org/10.1016/j.jclepro.2016.05.042> (in Eng)
- [2] Ordiales M. et al. (2016) Cold Agglomeration of Ultrafine Oxidized Dust (UOD) from Ferromanganese and Silicomanganese Industrial Process, *Metals (Basel)*, 6(9):203. <https://doi.org/10.3390/met6090203> (in Eng)
- [3] Zhdanov A. V. et al. (2015) Problems with Waste Generation and Recycling in the Ferroalloys Industry, *Metallurgist*, 581(11–12):1064–1070. <https://doi.org/10.1007/s11015-015-0041-5> (in Eng)
- [4] Ferreira W.L., Reis É.L., Lima R.M.F. (2015) Incorporation of residues from the minero-metallurgical industry in the production of clay–lime brick, *Journal of Cleaner Production*, 87:505–510. <https://doi.org/10.1016/j.jclepro.2014.09.013> (in Eng)
- [5] Shomanova Z.K. et al. (2017) Study of composition of waste from metallurgy production aimed in use them as active phases of catalysts for hydrocarbon raw materials refining, *News of the National Academy of Sciences of the Republic of Kazakhstan. Series of geology and technologysciences*, 6(426):195–200. <https://doi.org/10.32014/2018.2518-170X> (in Eng)
- [6] Shomanova Z.K. et al. (2016) Structure and Activity Research of Hydrocarbons Refining Catalysts Based on Wastes of Ferroalloy Production, *International Journal of Chemical, Molecular, Nuclear, Materials and Metallurgical Engineering*, 10(10):1148–1152 (in Eng)
- [7] Shomanova Z.K. et al. (2015) Investigation of adsorption properties of waste from gas cleaning system of ferroalloy production using the BET method [Исследование адсорбционных свойств отходов системы газоочистки ферросплавного производства методом BET], *News of the National Academy of Sciences of the Republic of Kazakhstan. Series of chemistry and technology*, 414(6):17–21. <https://doi.org/10.32014/2018.2518-1491> (in Russian)
- [8] Shomanova Z.K. et al. (2017) Study of Composite Catalysts Containing Sludge of Ferroalloy Production in the Process of Cyclohexane Oxidation, *News of the National Academy of Sciences of the Republic of Kazakhstan. Series of chemistry and technology*, 426(6):55–61. <https://doi.org/10.32014/2018.2518-1491> (in Eng)
- [9] Cossio R. et al. (2018) Innovative unattended SEM-EDS analysis for asbestos fiber quantification, *Talanta* 190:158–166. <https://doi.org/10.1016/j.talanta.2018.07.083> (in Eng)
- [10] Seki T., Ikuhara Y., Shibata N. (2018) Theoretical framework of statistical noise in scanning transmission electron microscopy, *Ultramicroscopy*, 193:118–125. <https://doi.org/10.1016/j.ultramicro.2018.06.014> (in Eng)
- [11] Jasnikov I.S. et al. (2013) Scanning electron microscopy as a method of research of microscopic objects of electrolytic origin [Skanirovushhaja jelektronnamikroskopija kak metod izuchenija mikroskopicheskikh objektov jelektroliticheskogo proishozhdenija], *Fundamental researches [Fundamental'nye issledovaniya]*, 1:758–764 (in Russian)
- [12] Song Z., Xie Z.-H. (2018) A literature review of in situ transmission electron microscopy technique in corrosion studies, *Micron*, 112:69–83. <https://doi.org/10.1016/j.micron.2018.04.011> (in Eng)
- [13] Pompe C.E. et al. (2018) Impact of heterogeneities in silica-supported copper catalysts on their stability for methanol synthesis, *Journal of Catalysis*, 365:1–9. <https://doi.org/10.1016/j.jcat.2018.06.014> (in Eng)
- [14] Zhu Y., Xu M., Zhou W. (2018) High-resolution electron microscopy for heterogeneous catalysis research, *Chinese Physics B*, 27(5):056804. <https://doi.org/10.1088/1674-1056/27/5/056804> (in Eng)
- [15] Campelo J.M. et al. (2009) Sustainable Preparation of Supported Metal Nanoparticles and Their Applications in Catalysis, *ChemSusChem*, 2(1): 18–45. <https://doi.org/10.1002/cssc.200800227> (in Eng)

УДК 577.4:550.41:66.097:661(004.8)

**Ж.К. Шоманова¹, Р.З. Сафаров², А.С. Жумаканова³,
Ю.Г. Носенко⁴, А.Т. Жанибекова¹, Н.Л. Шапекова², Д. Лорант⁵**

¹Павлодар мемлекеттік педагогикалық университеті, Павлодар, Қазақстан;

²Л.Н. Гумилев атындағы Еуразиялық ұлттық университеті, Астана, Қазақстан;

³Д.В. Сокольский атындағы жанармай, катализ және электрохимия институты, Алматы, Қазақстан;

⁴Инновациялық еуразия университеті, Павлодар, Қазақстан;

⁵Eötvös Loránd University, Будапешт - Сомбатхей, Венгрия

ФЕРРО ҚОРЫТПАНЫ ӨНДЕУ ҚАЛДЫҚТАРЫ НЕГІЗІНДЕ АЛЫНҒАН КАТАЛИЗАТОРЛАР БЕТІН ЭЛЕКТРОНДЫҚ МИКРОСКОПИЯ ӘДІСІМЕН ЗЕРТТЕУ

Аннотация. Мақалада Ақсу ферроқорытпа зауытының күлшлам қалдықтарынан ферроқорытпа өндірісі қалдықтары негізінде алынған катализаторлардың электронды - микроскопиялық зерттеулерінің нәтижелері келтірілген. Катализатор түйіршіктер бетінің морфологиясы мен каталитикалық белсенді Fe, Сг және Mn

металдар кристаллиттерінің беткі таралуы сипатталған. Катализаторды дайындау барысында металл кристаллиттерінің ірі агломераттарының көрінбейтін біркелкі, кеуекті беті алынғаны, металл компоненттері құрамдас бөліктерінің біркелкі болуы, кристаллиттердің өлшемі бірдей екендігі, бөлшектердің ұсақ дисперстілігі көрсетілді.

Түйін сөздер: катализаторлар, қалдықтар, феррокорытпаны өңдеу, электронды микроскопия, бет.

УДК 577.4:550.41:66.097:661(004.8)

**Ж.К. Шоманова¹, Р.З. Сафаров², А.С. Жумаканова³,
Ю.Г. Носенко⁴, А.Т. Жанибекова¹, Н.Л. Шапекова², Д. Лорант⁵**

¹Павлодарский государственный педагогический университет, Павлодар, Казахстан;

²Евразийский национальный университет им. Л.Н. Гумилева, Астана, Казахстан;

³Институт теплообмена, катализа и электрохимии им. Д.В. Сокольского, Алматы, Казахстан;

⁴Инновационный евразийский университет, Павлодар, Казахстан;

⁵EötvösLorándUniversity, Будапешт - Сомбатхей, Венгрия

ИССЛЕДОВАНИЕ МЕТОДОМ ЭЛЕКТРОННОЙ МИКРОСКОПИИ ПОВЕРХНОСТИ КАТАЛИЗАТОРОВ, ПОЛУЧЕННЫХ НА ОСНОВЕ ОТХОДОВ ФЕРРОСПЛАВНОГО ПРОИЗВОДСТВА

Аннотация. В статье приведены результаты исследования методом электронной микроскопии катализаторов, полученных на основе отходов ферросплавного производства с золошламонакопителя Аксуского ферросплавного завода. Описана морфология поверхности гранул катализатора, а также характер поверхностного распределения кристаллитов каталитически активных металлов Fe, Cr и Mn. Показано, что в ходе приготовления катализатора, получена равномерная, пористая поверхность без видимых крупных агломератов кристаллитов металлов, распределение металлических компонентов является равномерным, частицы мелкодисперсные, размеры кристаллитов одного порядка.

Ключевые слова: катализаторы, отходы, производство ферросплавов, электронная микроскопия, поверхность.

Information about authors:

Zhanat Kairollinovna Shomanova – doctor of technical sciences, professor of the Geography and chemistry department, Pavlodar state pedagogical institute, zshoman@yandex.ru, <https://orcid.org/0000-0001-8346-9688>

Ruslan Zairovich Safarov – candidate of chemical sciences, the Acting Associate Professor of the Department of Chemistry, vice-dean in science at Natural Sciences Faculty, L.N. Gumilyov Eurasian national university, ruslanbox@yandex.ru, <https://orcid.org/0000-0003-2158-6330>

Ardak Sydykovna Zhumakanova – candidate of chemical sciences, scientist secretary, D.V. Sokolsky Institute of Fuel, Catalysis and Electrochemistry, a.jumakanova@ifce.kz, <https://orcid.org/0000-0003-4983-4199>

Yuri Gennadievich Nosenko – Candidate of Chemical Sciences, acting Associate Professor of the Department of Chemical and Biological Technologies, Innovative University of Eurasia, nosenko1980@yandex.ru, <https://orcid.org/0000-0002-2491-7337>

Aisulu Talgatovna Zhanibekova – bachelor of environmental science, zshoman@yandex.ru, <https://orcid.org/0000-0002-5739-6267>

Nelya Lukpanovna Shapekova – doctor of medical sciences, professor of the Department of Biotechnology and microbiology, Dean of Natural Sciences Faculty, L.N. Gumilyov Eurasian national university, shapekova_nl@enu.kz, <https://orcid.org/0000-0003-2534-7951>

Dr. habil. habil. habil. Dávid Lóránt Dénes – full-professor, Jean Monnet Professor, PhD, EötvösLorándUniversity, davidlo@ektf.hu, <https://orcid.org/0000-0001-7880-9860>

NEWS

OF THE NATIONAL ACADEMY OF SCIENCES OF THE REPUBLIC OF KAZAKHSTAN

SERIES CHEMISTRY AND TECHNOLOGY

ISSN 2224-5286

<https://doi.org/10.32014/2018.2518-1491.30>

Volume 6, Number 432 (2018), 87 – 95

A. Bayeshov¹, T.E. Gaipov¹, A.K. Bayeshova², A.V. Kolesnikov³¹Institute of Fuel, Catalysis and Electrochemistry named after DV Sokolsky, Almaty, Kazakhstan;²Kazakh National University named after al-Farabi, Almaty, Kazakhstan;³D.Mendeleyev University of Chemical Technology of Russia, Moscow, Russiabayeshov@mail.ru, tulkinjon.gaipov@gmail.com, azhar_b@bk.ru, artkoles@list.ru**SYNTHESIS OF NANO- AND ULTRADISPERSE
COPPER POWDERS BY CEMENTATION OF COPPER (II) IONS
BY THREE-VALENT TITANIUM IONS**

Abstract. The process of cementation of copper (II) ions by tri-valent titanium ions is considered. The consistent patterns of the formation of nano- and ultra-disperse copper powders as a result of the interaction of copper (II) ions with titanium (III) ions have been established. It was demonstrated that during the reaction atomic copper is formed, the particles of which are combined with the formation of fine aggregates of certain sizes, which are stabilized in the form of spheres.

In the course of the research, the possibility of obtaining titanium (III) sulfate, which is necessary for carrying out the cementation of copper (II) ions, is shown in an inexpensive, simplified way and the results of studying the influence of various parameters on this process are presented. The possibility of regeneration of tetra-valent titanium ions formed as a result of the reaction using an electrolyzer equipped with an anion exchange membrane is demonstrated.

The effect of the initial concentration of copper ions (II) and titanium ions (III) on the formation of copper powder was studied. The shapes and sizes of the obtained copper powders were determined using an electron microscope. The constant of the reversible oxidation-reduction reaction was calculated and it was established that copper (II) ions contained in the solution are almost completely formed as nano-scale copper powders.

A schematic diagram of the technology for the production of fine copper powders, corresponding to the requirements of modernity, is proposed.

Key words: titanium ions, copper, powders, cementation, electrolysis, alternating current, electrolyte, reduction.

Introduction. The formation of metal powder is one of the spheres of metallurgical engineering. Metallic powder is widely used in mechanical engineering, and metallurgical engineering chemistry. Metal powder also has its place in the field of metallurgical engineering [1-9].

If in a nutshell we turn our attention on the information on the use of metal powder: it is widely used in the manufacture of complex shapes parts in mechanical engineering. It turns out that it is possible to easily manufacture parts of very complex shapes by placing the metal powder in a certain shape and exposing high pressure at high temperatures. With this heat treatment, the temperature of the medium must be below the melting point of the metal produced. It is known that obtaining of complex shapes parts by planing and cutting hard metal costs more than 100 times or more in comparison with powder technology [6].

Along with powder metallurgy, flat dispersed metal powders are used as catalysts in chemical production (iron, nickel, copper, etc.), in oxygen-flux welding, magnetic defectoscopy (iron), in the manufacture of products from polymer materials, in the production of lacquers (zinc, lead, iron, nickel), in the production of batteries (lead), in the production of pyrophores. Powders of flat disperse iron, copper, nickel increase the mechanical strength of products when forming them from plastic, rubber, nylon. If irons, zinc, bismuth powders, are added to the rubber glue, the quality of rubber products will improve. In hydrometallurgy, zinc powder is used in the production of zinc, in the separation from solutions

containing copper and cadmium ions, by cementation; however such plants are widely used to separate gold from cyanide solutions [8-11].

If we talk about copper powder, in the ancient period copper powder was widely used as decorative cosmetics. It is impossible to imagine ceramics and fine arts without copper powder. Today, the use of copper powder becomes wider with every passing day.

Copper powders in an active form are widely used by powder metallurgy in the manufacture of mechanisms and for other purposes, mainly in electrical engineering, instrument making, mechanical engineering and aviation production, chemical manufacturing, nanotechnology. Also used in the manufacture of anti-wear agents, in the manufacture of automobile tires and many other areas [1-3, 16].

Recently, copper powders in the form of ultra-disperse spheres are used in the implementing of 3D technology, in reducing the friction force and wear of machine parts [16].

Copper powders can be obtained by electrochemistry and cementation. It should be noted that more than 90% of the copper powder currently produce is obtained only by the electrochemistry methods. In laboratory environment, copper powder is obtained by cementation of its ions with zinc powder. The standard copper potential is $E_{\text{Cu}/\text{Cu}^{2+}}^0 = 0.34\text{V}$, and the zinc potential is $E_{\text{Zn}/\text{Zn}^{2+}}^0 = -0.76\text{V}$. Since the potential difference value ($\Delta E = 0.34 - (-0.76) = 1.2\text{V}$) is very large, the size of the formed copper powder is 30-50 microns [17]. In the proposed article, we examined the process of cementation of copper (II) ions with tri-valent titanium ions. Preliminary studies have shown the formation of very flat, ultra-disperse copper powders. If comes to think of it, obtaining copper powder by cementation with titanium ions (III) has a promising future. Because copper powders in the form of a dispersed sphere are in great demand. But unfortunately, sulphate compounds of tri-valent titanium ions are not produced in a great volume and the cost of such compounds is very high. For this reason, we, in this proposed work, together with the study of the process of cementation of copper ions (II) with titanium ions (III), also considered the possibility of obtaining titanium sulfate (III) by simple affordable means.

Procedure of work execution. The study of the formation of copper powders by cementing copper ions (II) with tri-valent titanium ions was carried out in a 200 ml beaker. During the reaction, the solution was stirred with a magnetic stirrer. To carry out laboratory work, we used "chemically pure" copper sulfate ($\text{CuSO}_4 \cdot 5\text{H}_2\text{O}$). The sulphate of trivalent titanium required for investigation was obtained by polarization of two titanium electrodes by a 50-Hz alternating current in a solution of sulfuric acid. In this paper, the regularity of the formation of titanium sulphate (III) is examined, the effect of various electrochemical processes on it is studied, and their results are presented. The main investigations were carried out under atmospheric conditions at room temperature. The purity of titanium electrodes used to obtain titanium sulfate (III): Ti – 97.65%.

The effect of the initial concentration of copper (II) ions and titanium (III) ions on the formation of copper powder was investigated. The shapes and sizes of the obtained copper powders were evaluated through an electron microscope.

Theoretical. When the solution is combined with copper ions and the ions of trivalent titanium, the following reaction is obtained:



According to the literature $\text{Cu}^{2+} \rightleftharpoons \text{Cu}^0$, $\text{Ti}^{4+} \rightleftharpoons \text{Ti}^{3+}$ the potential values of corrosion-recovery electrode systems [17]: $E_{\text{Cu}^{2+}/\text{Cu}^0}^0 = 0,34\text{V}$, $E_{\text{Ti}^{4+}/\text{Ti}^{3+}}^0 = 0,04\text{V}$.

In order to calculate the constant (K) of the above (1) recurrent redox reaction (red-ox), we determined lgK by the following formula [18]:

$$\lg K_{\text{red-ox}} = \frac{n(E_1^0 - E_2^0)}{0,059} \quad (2)$$

Further, the value of K (n=2) is set for the reaction (1):

$$K = 10^{\frac{(E_1^0 - E_2^0)n}{0,059}} \quad (3)$$

(2) by the equation:

$$\lg K_{Cu^{2+}/Ti^{3+}} = \frac{2(0,34 - 0,04)}{0,059} = 10,2$$

As a result, the value of the «red-ox» reaction constant (1):

$$K \approx 10^{10}$$

This value of «K» proves that reaction (1) moves completely from the left to the right and that this is a complete, irreversible reaction. Consequently, this shows that repeated interaction of the formed copper powders with four-valence titanium ions, and a new formation of copper (II) and titanium (III) ions are impossible. In other words, reaction (1) will be equal only when the product of $[Cu^0] \cdot [Ti^{3+}]$ ions is larger by 10^{10} products of $[Cu^{2+}] \cdot [Ti^{3+}]$ ions.

In previous studies [15, 20-22], we demonstrated the formation of ultra-disperse copper powders on the cathode-anode area, and in the size of the electrolyte. And in this article, we propose the regularities of the formation of copper powders by cementing copper ions (II) with ions (III) titanium.

Experimental. The solution containing copper (II) ions was poured into a beaker, stirred and gradually added to a solution with tri-valent titanium sulfate. The solution of titanium sulphate (III) was added to the decoloration of copper (II) sulphate of blue color. At that time an interesting phenomenon was observed. As indicated above, a solution of copper (II) sulfate is blue, and a solution of sulphate of tri-valent titanium is violet. When the two solutions are combined, the electrolyte is discolored. It is known that a solution of four-valent titanium is colorless. When the concentration of copper ions in the solution is 1 g/l, within two to three minutes the formation of copper powders is not visible by eyes. Only after four to five minutes, you can observe the formation of copper powders of colloidal light yellow color throughout the electrolyte. Consequently, copper (II) ions are reduced to very dispersed metal powders and a colloidal copper solution is formed.

At a certain point in the electrolyte the formation of copper powders becomes not visible by eyes, it can be assumed that this is due to the formation of atomic copper. Only after a certain time, the copper atoms begin to connect with each other, and a light yellow-colored colloidal metal solution is formed. After a couple of hours, these copper particles are even more connected and precipitated. We believe that the dimensions observed through the microscope are not their exact dimensions, but only their combined forms.

The table below shows the values of copper powders formed by combining the solution with different copper (II) ions and titanium (III) ions.

Table 1 - The impact of the initial concentration of copper (II) ions on the formed copper powders: V = 100 ml

Concentration of copper (II) ions in solution, g / l	The value of copper in solution, g	Mass of the formed copper powder, g
1,0	0,1	0,098
2,5	0,25	0,225
5,0	0,5	0,480
7,5	0,75	0,710
10	1,0	0,930
20	2,0	1,920

The results of the study showed that during the reaction, the copper (II) ions completely transform into the form of nano-sized copper powders.

Copper powders obtained on the basis of cementation, filtered, rinsed, dried in an inert medium (box).

In figures 1-4, microphotographs of copper powders formed at different initial concentrations (1 g/l, 5 g/l, 10 g/l) of copper (II) ions in solution are presented.

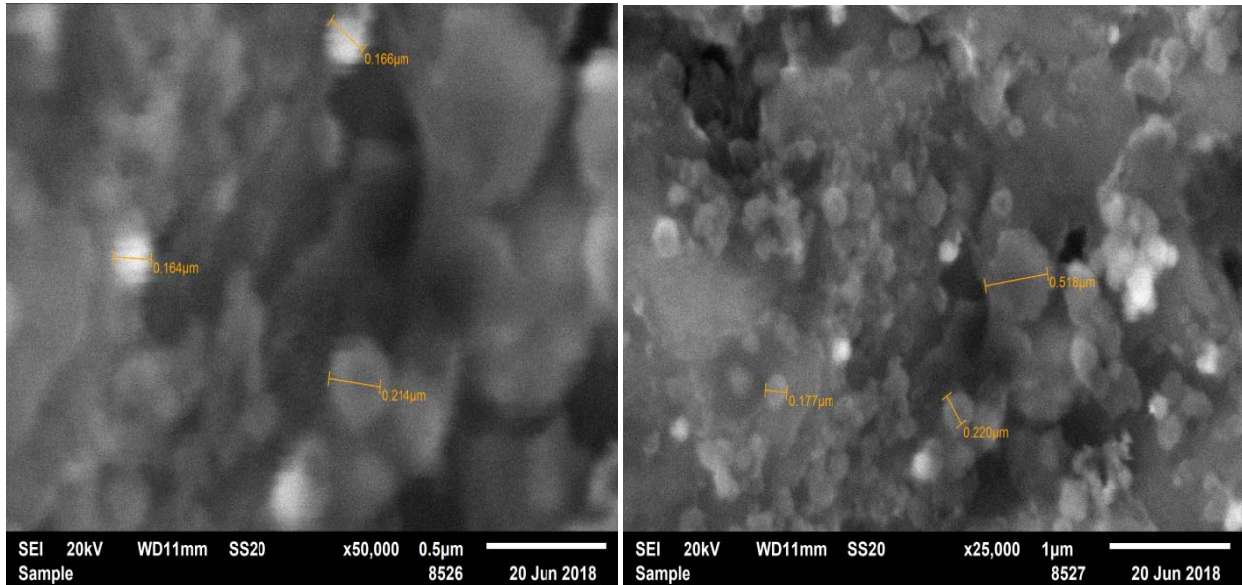


Figure 1 - Microphotograph of copper powders with the initial concentration of copper (II) ions in a solution of 1 g/l: the average size of copper powders is 0.1 - 0.4 μm.

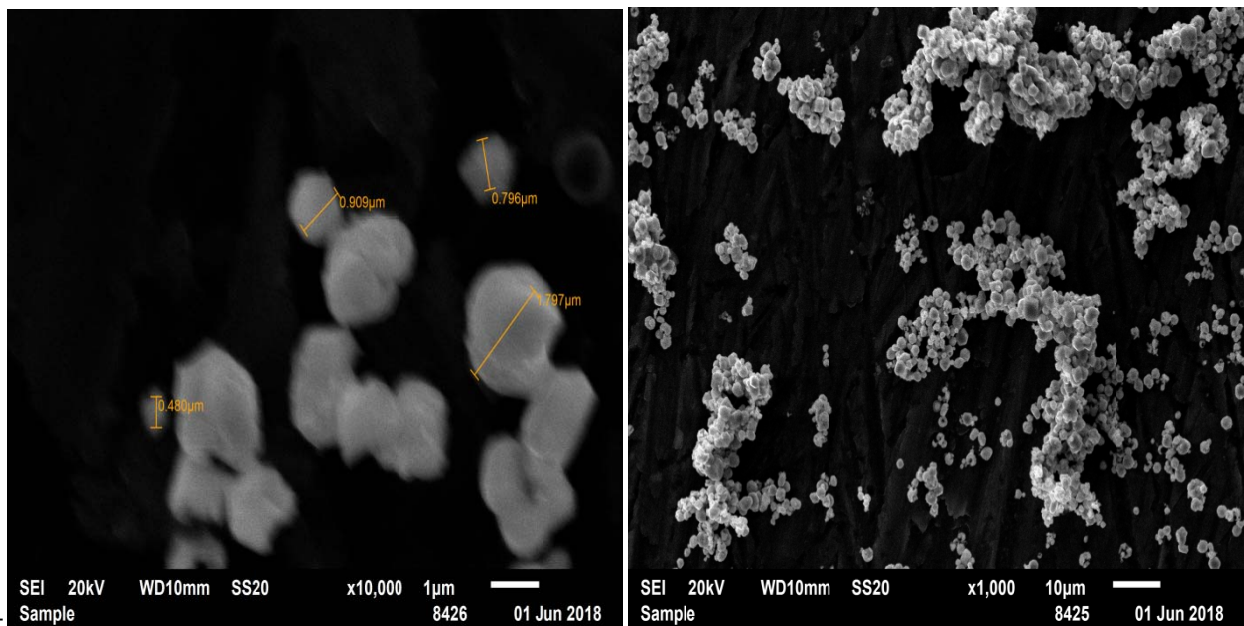


Figure 2. Microphotograph of copper powders with the initial concentration of copper (II) ions in a solution of 5 g/l: the average size of copper powders is 0.4-0.9 μm.

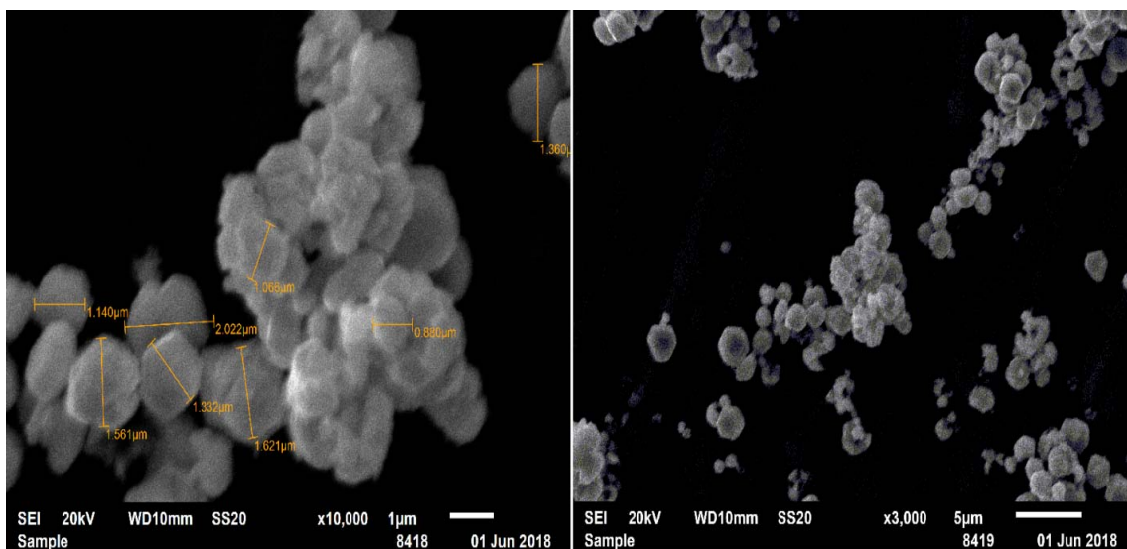


Figure 3. Microphotograph of copper powders with the initial concentration of copper (II) ions in a solution of 10 g/l: the average size of copper powders is 0.8 - 2 μm .

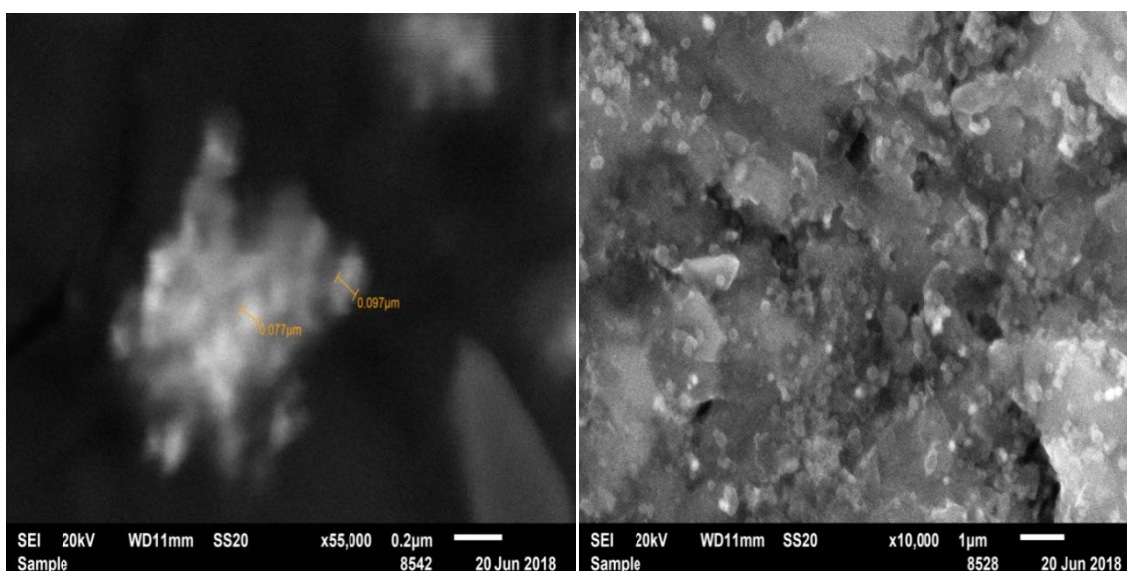


Figure 4 - Microphotography of copper powders with the initial concentration of copper (II) ions in a solution of 1 g/l: the average size of copper powders is 0.077-0.097 μm .

According to the results of the electron microscope examination, it was observed that with an increase in the initial concentration of copper (II) ions, the sizes of copper powders increased from 0.1 μm to 2 μm . In general, this is not the formation of copper powders in a large volume with a high initial concentration of copper (II) ions, we assume, that with an increase in the initial concentration of copper (II) ions it depends on the increase in the rate of the process of aggregation of copper atoms with each other. Because the sequential results of the study showed that copper powders have nanoscale form in a colloidal solution (Figure 4).

In order to make full use of the aforementioned method for producing a copper powder, it is necessary to create a simple method for preparing a tri-valent sulfate compound. The compounds of tri-valent ions are not constant, they are easily and rapidly oxidized to tetra-valent states. Therefore, this connection must be used immediately after receipt.

The influence of various parameters in the process of obtaining titanium (III) sulphate by the alternating current polarization of titanium electrodes in a solution of sulfuric acid is studied below.

The Figure 5 shows the effect of the current density in the electrodes on the current consumption of the dissolution of the formed $Ti_2(SO_4)_3$ compound in a 300 g/l sulfuric acid solution of the titanium electrode. When the current density is polarized with an alternating current of up to $200 A/m^2$, dissolution of the titanium electrodes is not observed. After that, at $600 A/m^2$ the dissolution rate by the current of titanium electrodes increases to 30%, and up to $1000 A/m^2$ reaches the same value.

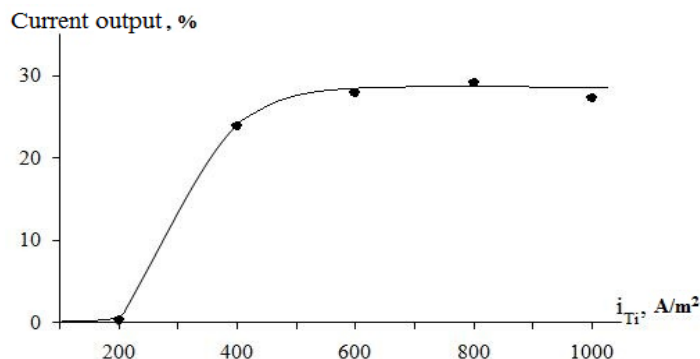


Figure 5 - The effect of the current density in the electrodes on the current consumption of the dissolution of the formed titanium (III) sulfate compound in a solution of sulfuric acid of titanium electrodes polarized by the industrial alternating current: $H_2SO_4 = 300 g/l$; $\tau = 0,5$ hours; $t = 25^0C$.

Dissolution during the polarization of titanium electrodes by alternating current can be explained by the fact that in connection with the oxidation in the cathode half-period of the oxide film on the surface and anodic dissolution during the anode period. With prolonged electrolysis, it is possible to observe the precipitate of crystals of titanium (III) sulphate in the form of needles at the bottom of the electrolyzer.

The increase in the concentration of sulfuric acid in the solution increases the current consumption rate by the dissolution of titanium (Figure 6). This phenomenon can be explained by a decrease in the constancy of the titanium oxide layer on the surface of titanium electrodes due to the increase in the concentration of sulfuric acid.

We present the scheme of a new technology for obtaining ultra-disperse copper powder based on the above laboratory studies (Figure 7). Into electrolysis process, where two (2) titanium electrodes are located, a solution of sulfuric acid (3) is poured and alternating current in a certain volume is directed through the LAVD along the chain. At that time, tri-valent titanium sulfate is formed in the electrolysis. This electrolyte is directed to the reactor (4) with copper (II) sulfuric acid sulfate. In the reactor, ultra-disperse copper powders (1) are formed in reaction. After a certain time, precipitating dispersed copper powders are decanted, then filtered, washed, dried, as the result we have a very dispersed copper powder. The electrolyte released from the decantation, the electrode core, is sent to the cathode cavity of the electrolysis, separated by an anionite membrane, ions of tetra-valent titanium are oxidized-regenerated in the cathode of titanium to the state of tri-valence, and sent to the reactor (4) to obtain copper powders.

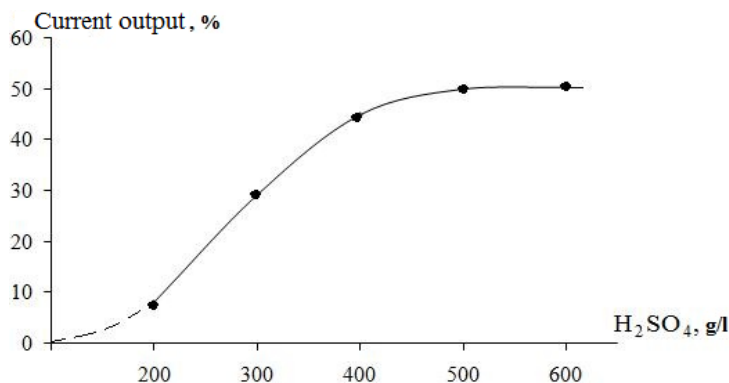


Figure 6 - The effect of the concentration of sulfuric acid in the solution on the dissolution of titanium electrodes: $i_{Ti} = 800 A/m^2$; $\tau = 0,5$ hours; $t = 25^0C$.

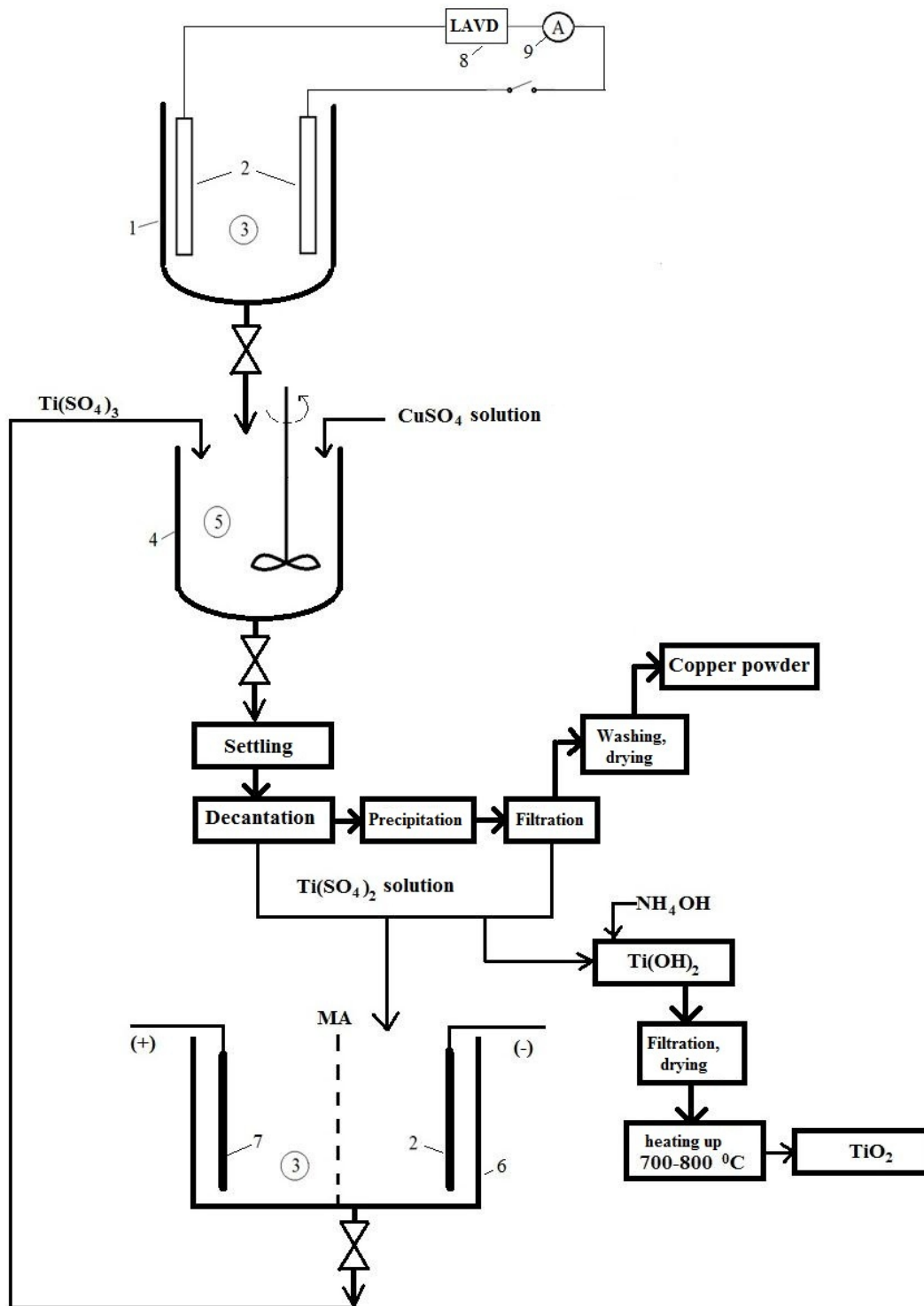


Figure 7 - Scheme of the principle technology of obtaining ultra-disperse copper powder by cementing a solution of copper (II) sulfate with titanium(III) ions: 1 - electrolyzer; 2 - titanium electrodes; 3 - solution of sulfuric acid; 4 - the reactor forming ultra-disperse copper powders; 5 - stirrer; 6 - electrolyzer designed to produce tri-valent titanium ions, separating the cores of the electrodes by an anionite membrane; 7 - lead electrode; 8 - LAVD; 9 - ampere-meter.

From the excess amount of tetra-valent titanium sulfate, as shown in the flow chart, by the addition of ammonia, it is possible to obtain the titanium (III) hydroxide, then the titanium dioxide (IV). It should be noted that the titanium (III) hydroxide is a very good sorbent, and its dioxide is the necessary pigment for obtaining a white color.

In conclusion, as a result of thorough comprehensive studies, the interaction of copper (II) and titanium (III) ions was studied, the patterns of formation of nano- and ultra-dispersed copper powders were established. During the reaction, the formation of atomic copper is established, their particles are connected to each other and flat dispersed aggregates are formed, stabilized in a certain volume in the form of a sphere. It has been shown that it is possible to obtain, in a simple and easy way, the tri-valent titanium compounds necessary for the preparation of the powder and to regenerate the tetra-valent titanium ions formed by the reaction using anionite membranes. A scheme of complex technology is presented in accordance with modern requirements for the preparation of dispersed copper powder.

REFERENCES

- [1] Kiparisov S.S., Libenson G.A (1972) Poroshkovaja metallurgija. M., 528. (in Russian)
- [2] Dzhons V.D (1965) Osnovy poroshkovej metallurgii. Svoystva i primeneniye poroshkovykh materialov. M., 392. (in Russian)
- [3] Libenson G.A (1975) Osnovy poroshkovej metallurgii. M., Metallurgija, 200. (in Russian)
- [4] Nomberg M.I (1971) Proizvodstvo mednogo poroshka jelektroliticheskim sposobom. M., Metallurgija, 134. (in Russian)
- [5] Fedorchenko I.M., Andrievskij R.A (1952) Osnovy poroshkovej metallurgii. Kiev, 144. (in Russian)
- [6] Ajzenkol' F. (1969) Uspehi poroshkovej metallurgii. M., 542. (in Russian)
- [7] Kudra O.K., Gitman E.B (1952) Jelektroliticheskoe poluchenie metallicheskikh poroshkov. Kiev, 144. (in Russian)
- [8] Sobol' S.I., Vinogradov G.A., Konov A.V, Ogajan R.A (1966) Proizvodstvo mednykh poroshkov i prokata (obzor otechestvennogo i zarubeznogo opyta). M., Ch.1. 83. (in Russian)
- [9] Pomosov A.V., Kalugin V.D (1963) O vlijanii materiala katoda na jelektroosazhdenie poroshkovej medi. Zhurn.prikl.him., T.36. № 9. 1969. (in Russian)
- [10] Gusev A.I (2005) Nanomaterialy, nanostruktura, nanotehnologija. M., Fizmatlit, 416.
- [11] Klimnik A.B., Ostrazhkova E.Ju (2012) Jelektrohimicheskij sintez nanodispersnykh poroshkov oksidov metallov. Izd. TTTU, Tambov, 144.
- [12] Klimov B.N., Shtykov S.N., Gorin D.A (2009) Fiziko-himija nanostruktirovannykh materialov. Uchebnoe posobie, Saratov, (in Russian)
- [13] F.Miomandr, S.Sadki, P.Odeber, R.Mealle-Reno (2008) Jelektrohimija. Perevod s francuzskogo V.N. Grasevicha pod redakciej d.h.n. Ju.D.Gamburga, d.h.n. V.A.Safonova. Moskva, tehnosfera, 360. (in Russian)
- [14] Il'in A.P., Korshunov A.V., Perevezenceva D.O., Tolbanova L.O (2009) Nanoporoshki metallov kak metastabil'nye sistemy: problemy diagnostiki. Fundamental'nye issledovaniya, №2, 102-102. (in Russian)
- [15] Baeshov A.B., Kozhakov B.E., Buketov E.A (17.07.1982) Sposob poluchenija poroshka medi, A.S. SSSR № 1082066, (ne podlezhit publikacii v otkrytoj pečhati). (in Russian)
- [16] Konjushaja Ju.P (1988) Otkrytija sovetских uchenyh, chast' I. M. Moskovskij Universitet, 477. (in Russian)
- [17] Suhotin A.M (1981) Spravochnik po jelektrohimii. L., Himija, 488. (in Russian)
- [18] Kreshkov A.P (1970) Osnovy analiticheskoy himii. Himija, 2 tom, 456. (in Russian)
- [19] Baeshov A.B., Dauletbaev A.S., Baeshova A.K (2010) Jelektrohimicheskij sposob poluchenija mednogo poroshka. Innovacionnyj patent RK №22669, Bjul. №7. (in Russian)
- [20] Baeshov A.B., Baeshova A.K., Baeshov K.A (2014) Jelektrohimicheskij sposob poluchenija mednogo poroshka. Innovacionnyj patent RK №28225, Bjul. №7. (in Russian)
- [21] Baeshov A., Baeshova A.K., Abduvalieva U.A. Jelektrorefinacijalau kezinde mys untaktarynyn tuziluine kuproindardyn aseri. KR UGA Habarlary. 2018. № 4. S.43-51. <https://doi.org/10.32014/2018.2518-1491> (in Kazakh)
- [22] Baeshov A., Baeshova A.K., Baeshova S.A (2014) Jelektrohimija, Qazaq universiteti, Almaty, 316. (in Kazakh)

ӨОЖ 541.13/ 621.762

А. Баешов¹, Т.Э. Гаипов¹, А.К. Баешова², А.В. Колесников³

¹Д.В.Сокольский атындағы Жанармай, катализ және электрохимия институты, Алматы, Қазақстан

²Әл-Фараби атындағы Қазақ ұлттық университеті, Алматы, Қазақстан

³Д.И. Менделеев атындағы Ресей химия-технологиялық университеті, Мәскеу, Ресей

МЫС (II) ИОНДАРЫН ҮШ ВАЛЕНТТІ ТИТАН ИОНДАРЫМЕН ЦЕМЕНТАЦИЯЛАУ АРҚЫЛЫ НАНО – ЖӘНЕ УЛЬТРАДИСПЕРСТІ МЫС ҰНТАҚТАРЫН АЛУ

Аннотация. Мыс (II) иондарын үш валентті титан иондарымен цементациялау процесі қарастырылды. Мыс (II) иондары мен титан (III) иондарының әсерлесуі зерттеліп, нано- және ультрадисперсті мыс ұнтақтарының түзілу заңдылықтары анықталды. Реакция кезінде атомарлы мыстың түзіліп, оның бөлшектері бір – бірімен белгілі өлшемдегі майда дисперсті агрегаттарға бірігіп, сфера формасында тұрақтанатыны айқындалды.

Зерттеу барысында мыс (II) иондарын цементациялауға қажетті титан (III) сульфатын қарапайым арзан жолмен алу мүмкіндігі қарастырылып, осы процеске әртүрлі параметрлердің әсерін зерттеу нәтижелері келтірілді. Реакция нәтижесінде түзілген титанның төрт валентті иондарын анионитті мембранасы бар электролизерді қолданып, регенерациялауға болатындығы көрсетілді.

Мыс ұнтағының түзілуіне мыс (II) иондарының және титан (III) иондарының бастапқы концентрацияларының әсері зерттелді. Алынған мыс ұнтақтарының формасы мен өлшемдері электрондық микроскоп арқылы сарапталды. Қайтымды тотығу-тотықсыздану реакциясының константасы есептеліп, ерітіндідегі мыс (II) иондары түгел дерлік наноразмерлі мыс ұнтақтары түріне өтетіндігі анықталды.

Өте дисперсті мыс ұнтағын алудың қазіргі заманның талабына сай кешенді технологиясының принципалды сызба-нұсқасы ұсынылды.

Түйін сөздер: титан иондары, мыс, ұнтақ, цементация, электролиз, айнымалы ток, электролит, тотықсыздану.

УДК 541.13/ 621.762

А.Башов¹, Т.Э.Гаипов¹, А.К.Башова², А.В. Колесников³

¹Институт топлива, электрохимии и катализа имени Д.В.Сокольского, Алматы, Казахстан;

²Казахский Национальный университет имени аль-Фараби, Алматы, Казахстан;

³Российский химико-технологический университет имени Д. И. Менделеева, Москва, Россия

ПОЛУЧЕНИЕ НАНО- И УЛЬТРАДИСПЕРСНЫХ ПОРОШКОВ МЕДИ ЦЕМЕНТАЦИЕЙ ИОНОВ МЕДИ (II) ИОНАМИ ТРЕХВАЛЕНТНОГО ТИТАНА

Аннотация. Рассмотрен процесс цементации ионов меди(II) ионами трехвалентного титана. Установлены закономерности формирования нано- и ультрадисперсных порошков меди в результате взаимодействия ионов меди (II) с ионами титана (III). Показано, что в процессе реакции образуется атомарная медь, частицы которой объединяются с формированием мелкодисперсных агрегатов определенных размеров, которые стабилизируются в виде сфер.

В процессе исследования показана возможность получения недорогостоящим, упрощенным способом сульфата титана (III), необходимого для проведения реакции цементации ионов меди (II) и приведены результаты изучения влияния различных параметров на данный процесс. Показана возможность регенерации четырехвалентных ионов титана, образующихся в результате реакции, с использованием электролизера, снабженного анионитовой мембраной.

Исследовано влияние исходной концентрации ионов меди (II) и ионов титана (III) на формирование порошка меди. Формы и размеры полученных порошков меди установлены с помощью электронного микроскопа. Рассчитана константа обратимой окислительно-восстановительной реакции и установлено, что ионы меди (II), содержащиеся в растворе, практически полностью формируются в виде наноразмерных порошков меди.

Предложена принципиальная схема технологии получения мелкодисперсных порошков меди, соответствующая требованиям современности.

Ключевые слова: ионы титана, медь, порошки, цементация, электролиз, переменный ток, электролит, восстановление.

Information about the authors:

Bayeshov A. - Chief Researcher, Doctor of Chemical Sciences, Laboratory of electrochemical technology, JSC "D.V. Sokolsky Institute of Fuel, Catalysis and Electrochemistry", Institute of Fuel, Electrochemistry and Catalysis named after DV Sokolsky, Almaty, Kazakhstan. Tel: 87017605635, e-mail: bayeshov@mail.ru, orcid: 0000-0003-0745-039X

Bayeshova A.K. - Doctor of Chemical Sciences, Al-Farabi Kazakh National University, Almaty, Kazakhstan. Tel: 87017605625, e-mail: azhar_b@bk.ru, orcid: 0000-0002-9076-8130

Gaipov T.E. - Senior Researcher, Candidate of Chemical Sciences, Laboratory of electrochemical technology, JSC "D.V. Sokolsky Institute of Fuel, Catalysis and Electrochemistry", Institute of Fuel, Electrochemistry and Catalysis named after DV Sokolsky, Almaty, Kazakhstan. Tel: 87024962449, e-mail: tulkinjon.gaipov@gmail.com, orcid: 0000-0002-9723-3745

Kolesnikov A. - Candidate of technical Sciences, D.Mendeleev University of Chemical Technology of Russia, Moscow, Russia, Tel: 8 985 243 46 46, e-mail: artkoles@list.ru, orcid: 0000-0002-4586-6612

NEWS

OF THE NATIONAL ACADEMY OF SCIENCES OF THE REPUBLIC OF KAZAKHSTAN

SERIES CHEMISTRY AND TECHNOLOGY

ISSN 2224-5286

<https://doi.org/10.32014/2018.2518-1491.31>

Volume 6, Number 432 (2018), 96 – 101

A.B. Bayeshov¹, B.E. Myrzabekov¹, A.V. Kolesnikov²

¹Institute of Fuel, Catalysis and Electrochemistry named after DV Sokolsky, Almaty, Kazakhstan;

²D.Mendeleev University of Chemical Technology of Russia, Moscow, Russia

E-mail: bayeshov@mail.ru, myrzabekbegzat@mail.ru, artkoles@list.ru

PATTERNS OF FORMATION OF DISPERSED COPPER POWDERS IN THE BODY OF ELECTROLYTE DURING THE USE OF COPPER ANODE IN SULFURIC ACID SOLUTION ALONG WITH TITANIUM (IV) IONS

Abstract. For the first time it was shown that when a copper-titanium pair of electrodes is polarized in a solution of sulfuric acid with titanium (IV) ions, copper powders are formed between the holes of the electrodes.

The mechanism of formation of copper powders during electrolysis is investigated. It was shown that during the polarization of copper and titanium electrodes in a solution of sulfuric acid with Ti (IV) ions, copper anodes dissolve, forming copper (II) ions, and in the cathode titanium (IV) ions are oxidized to the tri-valent state. At this time, the color of the electrolyte at the cathode is purple, and at the anode it turns blue. It was established that the formed copper (II) and Ti (III) ions are found in the main gap of the electrodes, as a result of which nano-scale copper powders are formed.

It was shown that the resulting tetra-valent titanium ions in the cathode are again oxidized to the tri-valent state, interacting with copper (II) ions. Copper powders form again between the electrodes, and these processes are repeated cyclically. It was shown that during the electrolysis between the electrodes colloidal copper powders are first formed, and then they are combined and are precipitated.

Key words: titanium ions, copper, powders, electrolysis, electrolyte, reduction.

Introduction. Dispersed copper powders have a special property. Therefore, copper powders are used in various fields of production. Electrochemical methods have been widely used in the preparation of copper powders. The patterns of the formation of copper powders during cathodic polarization have been studied in detail [1-18].

In our previous research, we were the first in the world to show that when electrolysis is performed using copper electrodes in a solution of sulfuric acid with four-valent titanium ions, copper powders are formed between the electrodes and the discovery was protected by the patent of the Republic of Kazakhstan [17].

This article describes the impact of current density, sulfuric acid in solution, concentrations of titanium (IV) ions and the duration of electrolysis on the current consumption (CC) of the formation of dispersed copper powders. Copper was used as the anode electrodes, and titanium plates as the cathode. The area of the electrodes is equal to 3 cm², the distance between them is 6 cm. A solution of sulfuric acid was used as the electrolyte. It stands to mention that the electrolyte contains no copper ions. The principal variant of the electrolyzer and the reactions taking place in it is shown in Figure 1.

Theoretical. During electrolysis, the formation of copper powders is carried out by the following mechanism: when polarizing copper and titanium electrodes in a solution of sulfuric acid with Ti (IV) ions, the copper anode dissolves forming copper (II) ions:



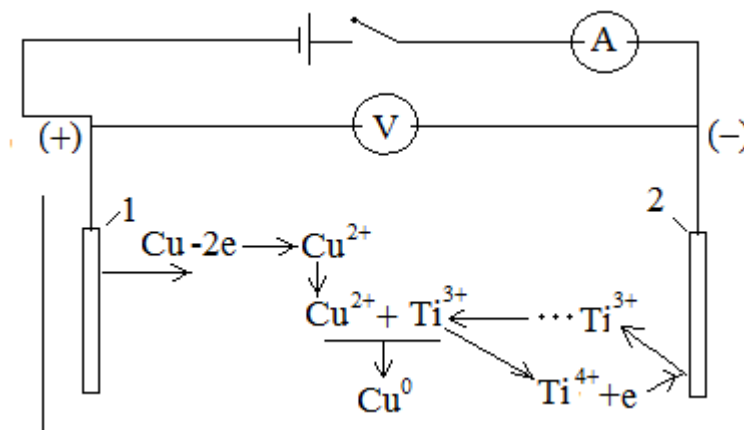
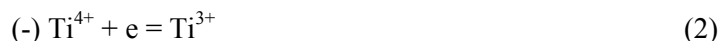


Figure 1 - Schematic diagram of the electrolyzer. 1 - copper electrode; 2 - titanium electrode; electrolyte composition: Ti(IV) + H₂SO₄

In the cathode, titanium (IV) ions are oxidized to the tri-valent state.:



Copper (II) and Ti (III) ions, formed during reactions (1) and (2), are found among the electrodes and, as a result, nano-scale copper powders are formed.



As it is shown in Figure 1, tetra-valent titanium ions formed as a result of reaction (3) in the cathode are again oxidized to the trivalent state during reaction (2), interacting with copper (II) ions between the electrodes and the formation of copper powders is again based on the reaction (3). These processes are cyclically repeated. The objective of the research is to study the effect of various parameters on the formation of copper powders by the mentioned mechanism..

Experimental. The formation of copper powders was investigated when exposed to a current density in the electrodes in the range of 50–1,200 A/m². Within the current density range in the electrodes, 50-150 A/m², the formation of copper powders is 100%. It should be noted that on the basis of reaction (3) a very dispersed colloidal copper is formed. Only after an hour they connect and increase, then precipitated. Increasing the current density in the electrodes reduces the current consumption of the formation of copper powders. This phenomenon can be explained by the course of an additional reaction in the electrodes at a high current density. At this time, copper powders are still formed on the surface of the cathode. In the cathode, in addition to the main oxidation reaction of titanium (IV) ions in the 2nd reaction, the oxidation reaction of other hydrogen ions also takes place:



As a result, the current consumption of titanium (IV) ion oxidation decreases and the formation of copper powders is reduced during the reaction (3).

It stands to mention that when electrolysis is carried out in a low current density of 100-150 A/m², without involving of titanium (IV) ions, ionization of copper electrodes is observed in the first reaction (1) and after some time oxidation of copper (II) ions on the cathode surface.



The distance between the anode and cathode electrodes is 4-6 cm or more, also in the presence of titanium (IV) ions in the solution, the oxidation of copper ions to copper powders is not carried out immediately, but after a certain time between the electrodes.

The impact of sulfuric acid on the formation of copper powders in the range of 50-250 g/L (Table 1) was investigated. There is a decrease in the current consumption for the formation of copper powders after the increase in acid concentration. This phenomenon can be explained by a slight dissolution of the formed dispersed powders in sulfuric acid. Since electrolysis is carried out in the open air, the following reaction can take place:



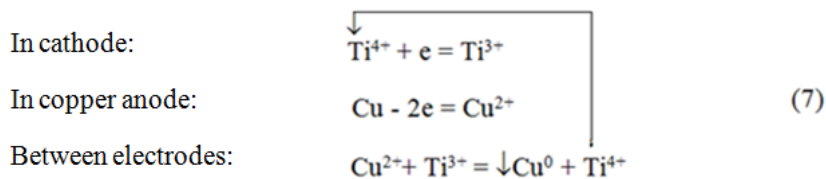
Table 1 - The impact of acid concentration on the current consumption of the formation of copper powders:
Ti(IV) = 8 g/L, $i = 150 \text{ A/m}^2$, $\tau = 30 \text{ minutes}$, $t = 25 \text{ }^\circ\text{C}$

H ₂ SO ₄ , g/L	50	100	150	200	250
CO, %	109,2	110,0	111,1	104,5	95,3

The impact of the concentration of tetra-valent titanium ions on the formation of copper powders in the range of 1–16 g/L during electrolysis was studied. In the absence of titanium (IV) ions in the solution between the electrodes, the formation of copper powders is not observed. The results of the study showed that, depending on the increase in the concentration of titanium (IV) ions in solution, the current consumption of the formation of copper powders increases..

With an increase in the concentration of titanium (IV) ions in the solution, the current consumption of their oxidation to the tri-valent state in the cathode increases, and the rate of formation of copper powder increases according to reaction (3). As a result, we can say that the current consumption of the copper powders formation is growing..

When conducting electrolysis using copper and titanium electrodes in a solution of sulfuric acid with titanium (IV) ions, the following cyclic mechanism took place: copper (II) ions $\text{Cu} - 2e = \text{Cu}^{2+}$ are formed in the anode, at this time the electrolyte color in the anode area begins to acquire blue shade, in the cathode, tetra-valent titanium ions are oxidized to the tri-valent state and in this area of the electrode the color of the electrolyte turns purple. Further, these ions collide between the electrodes and as a result of reaction (3) dispersed copper powders are formed. At this time, the formed tetra-valent titanium ions are diffused towards the cathode and are oxidized again to the tri-valent state on the surface of the cathode. This reaction is repeated cyclically. This process can be shown as a general diagram as follows:



As can be seen from reaction (7), under the above conditions, the titanium (IV) - titanium (III) scheme acts as a catalyst system, these processes are repeated cyclically.

It should be noted that with a smaller distance between the anode and cathode, as well as a high current density in the electrodes, the dissolution current consumption of copper will be 100%, and the oxidation current consumption of titanium (IV) ions will decrease dramatically. In this case, an excess of copper (II) ions formed in the anode is oxidized forming copper powders under the conditions of a current density limited in the cathode. At this time, the formation of copper powders takes place both between the electrodes and on the surface of the cathode.

Microphotographs of copper powders obtained under various electrolysis conditions were taken and studies were carried out. An electron microscope of the JSM6610W model was used in these studies.

It is established that in the electrode area very dispersed sphere-shaped powders are formed. Figure 3 shows a microphotograph of copper powders formed between the electrodes at a current density 150 A/m^2 in the electrodes. The average size of copper particles $0.1\text{-}0.2 \text{ }\mu\text{m}$.

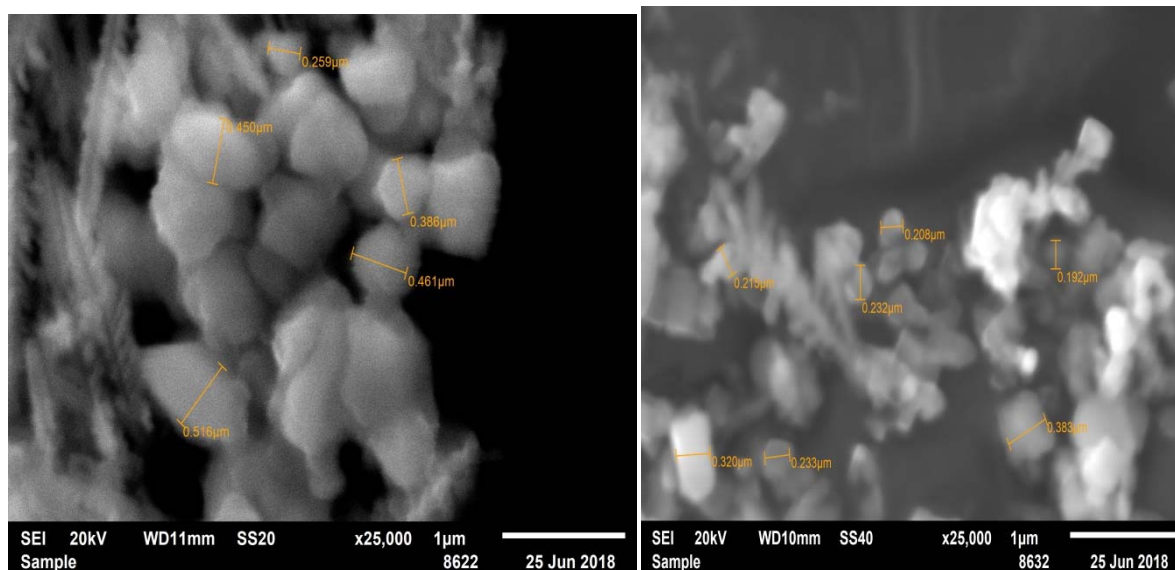


Figure 4 - Microphotograph of copper powders, formed between electrodes $i=150 \text{ A/m}^2$, $\text{Ti(IV)} = 8 \text{ g/L}$, $t = 25 \text{ }^\circ\text{C}$

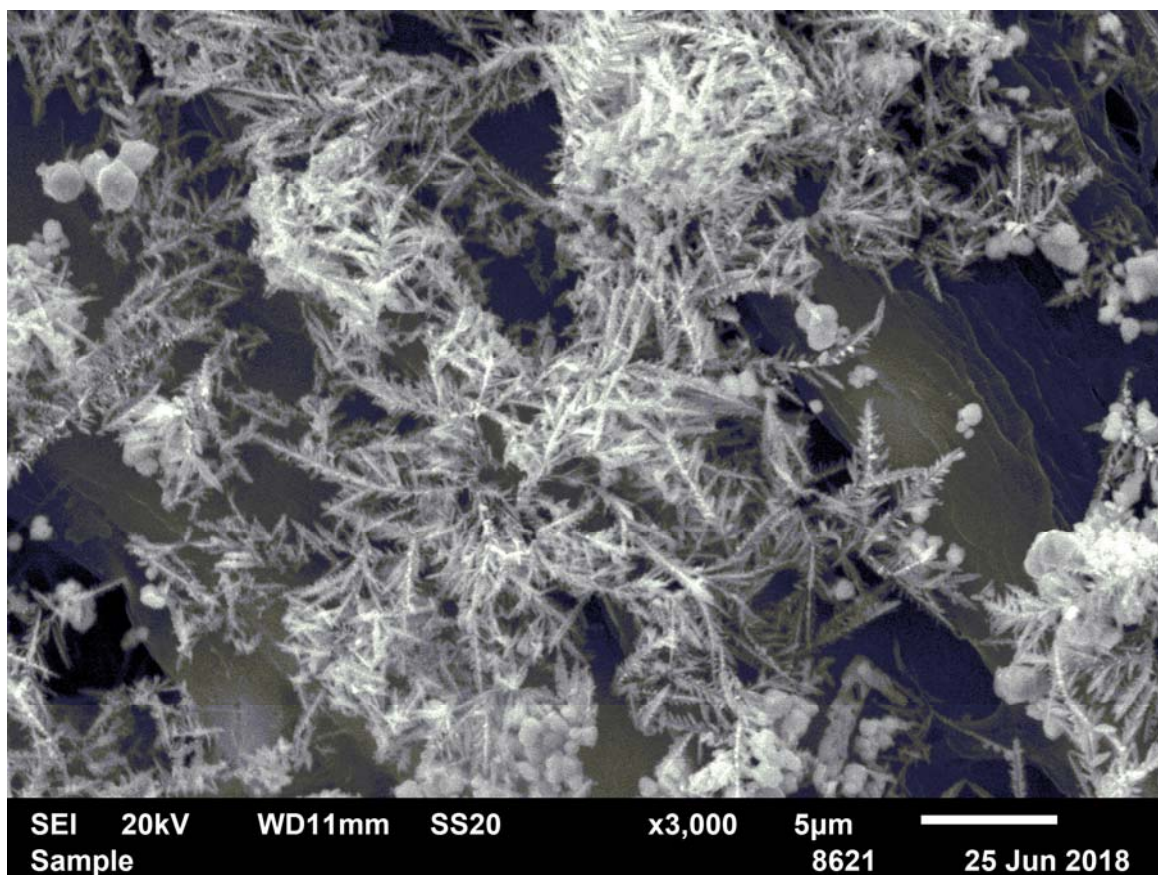


Figure 5 - Microphotograph of copper powders, formed on the surface of cathode $i=1200 \text{ A/m}^2$, $t = 25 \text{ }^\circ\text{C}$

Figure 5 shows microphotographs of copper powders formed on the surface of the cathode at a current density 1200 A/m^2 in the electrodes. In this case, it was found that copper powders in the form of threads are formed on the cathode surface.

In conclusion, for the first time when using the copper anode in a sulfuric acid solution with titanium (IV) ions, when using a copper anode between the electrodes under certain conditions, a very dispersed

copper powder is formed, the impact of various parameters on this process is investigated. It has been established that between the electrodes copper particles are formed in the sphere shape with an average size of 0.1-0.2.

REFERENCES

- [1] Libenson G.A. (1975) Fundamentals of powder metallurgy. M., Metallurgy, 200p.(in Russian).
- [2] Nomberg M.I. (1971) Copper powder production by electrolytic method. M., Metallurgy, 134 p.(in Russian).
- [3] Kiparissov S.S., Libenson G.A. (1972) Powder metallurgy. M., 528 p.(in Russian).
- [4] Jones V.D. (1965) Fundamentals of powder metallurgy. Properties and application of powder materials. M.,392 p. (in Russian).
- [5] Fedorchenko I.M., Andriyevskiy R.A. (1952) Fundamentals of powder metallurgy. Kyiv, 144 p.(in Russian).
- [6] Aizenkolb F. (1969) Advances in Powder Metallurgy. M., 542 p.(in Russian).
- [7] Kudra O.K., Ghitman Ye.B. (1952) Electrolytic production of metal powders. Kyiv, 144 p.(in Russian).
- [8] Sobol S.I., Vinogradov G.A., Konov A.V., Ogayan R.A. (1966) Manufacture of copper powders and rolled products (review of domestic and foreign experience). M., Part 1. 83 p.(in Russian).
- [9] Pomosov A.V., Kalugin V.D. (1969) On the influence of the cathode material on the electrodeposition of powder copper. Journal of Applied Chemistry. 1963. Vol. 36. № 9 p. (in Russian).
- [10] F. Miomandre, S.Sadki, P.Odebere, R.Mealles-Reno. (2008) Electrochemistry. Translation from French by V.N. Grasevich, edited by Dr. of Sc. Yu.D.Gamburg, Doctor of chemical sciences V.A. Safonov. Moscow, Техносфера Publishing house, 360 p.(in Russian).
- [11] Ilyin A.P., Korshunov A.V., Perevezentseva D.O., Tolbanova L.O. (2009) Nanopowders of metals as metastable systems: problems of diagnostics. Basic research. №2. P.102.(in Russian).
- [12] Ilyin A.P., Korshunov A.V., Perevezentseva D.O., Tolbanova L.O.(2009) Diagnostics of nanopowders and nanomaterials: tutorial. Tomsk: TPU publishing house, 249 p.(in Russian).
- [13] Bayeshov A.B.(1990) Electrochemical methods of extraction of copper, chalcogenes and synthesis of their compounds, Nauka KazSSR, 108 p.(in Russian).
- [14] Bayeshov A.B., Bayeshova A.K., Bayeshova S.A. (2014) Electrochemistry, Almaty, 326 p.(in Russian).
- [15] Bayeshov A.B., Kozhakov B.E., Buketov E.A. (1982) The method of copper powder producing, A.C. USSR № 1082066 (Not subject to publication in public media).(in Russian).
- [16] Konyushaya Yu.P. (1988) Discoveries of Soviet scientists, part I. M. Moscow University, . 477 p.(in Russian).
- [17] Baeshov A., Baeshova A.K., Abduvalieva U.A. Jelektorrafinaçijalau kezinde mysuntaktarynyn tuziluine kuproindardyn aseri. KRUGAHabarlary. 2018. № 4. S.43-51. <https://doi.org/10.32014/2018.2518-1491> (inKazakh).
- [18] Bayeshov A.B, Bayeshova A.K., Bayeshov K.A. (2014) Electrochemical method of obtaining a copper powder. Innovative patent RK №28225, Bull. №7, (in Russian).

ӨОЖ 541.13/ 621.762

А.Б. Баяшов¹, Б.Э. Мырзабеков¹, А.В. Колесников²

¹Д.В.Сокольский атындағы Жанармай, катализ және электрохимия институты, Алматы, Қазақстан;

²Д.И. Менделеев атындағы Ресей химия-технологиялық университеті, Мәскеу, Ресей

ҚҰРАМЫНДА ТИТАН (IV) ИОНДАРЫ БАР КҮКІРТ ҚЫШҚЫЛЫ ЕРІТІНДІСІНДЕ МЫС АНОДЫН ҚОЛДАНУ КЕЗІНДЕ ЭЛЕКТРОЛИТ КӨЛЕМІНДЕ ДИСПЕРСТІ МЫС ҰНТАҚТАРЫНЫҢ ТҮЗІЛУ ЗАҢДЫЛЫҚТАРЫ

Аннотация. Құрамында титан (IV) иондары бар күкірт қышқылы ерітіндісінде “мыс-титан” жұбы электродын поляризациялау кезінде электродтар кеңістіктері аралығында дисперсті мыс ұнтақтарының түзілетіндігі алғаш рет көрсетілді.

Электролиз кезінде мыс ұнтақтарының түзілуі механизмі зерттелді. Мыс және титан электродтарын Ti(IV) иондары бар күкірт қышқылды ерітіндіге салып поляризацияланған кезде, мыс аноды мыс(II) иондарын түзе еріп, ал катодта титан (IV) иондары үш валентті күйге дейін тотықсызданатындығы көрсетілді. Бұл кезде катод аумағындағы электролиттің түсі – күлгін, ал анод аумағында – көк түске өтеді. Түзілген мыс (II) және Ti (III) иондары электродтар аралығында бір-бірімен кездесіп, нәтижесінде наноразмерлі мыс ұнтағы түзілетіндігі анықталды.

Реакция нәтижесінде түзілген төрт валентті титан иондары катодта қайтадан үш валентті күйге дейін тотықсызданып, ол электродтар аралығында мыс (II) иондарымен әрекеттесіп қайтадан мыс ұнтағының түзілетіндігі және бұл процестер цикілді түрде қайталанып тұратындығы көрсетілді. Электролиз кезінде электродтар аралығында алғашқыда коллоидты мыс ұнтақтарының түзілетіні және олардың бір-бірімен бірігіп содан кейін тұнбаға түсетіндігі көрсетілді.

Түйін сөздер: титан иондары, мыс, ұнтақ, электролиз, электролит, тотықсыздану

А.Б. Баяшов¹, Б.Е. Мырзабеков¹, А.В. Колесников²

¹Институт топлива, электрохимии и катализа имени Д.В.Сокольского, Алматы, Казахстан;

²Российский химико-технологический университет имени Д. И. Менделеева, Москва, Россия

**ЗАКОНОМЕРНОСТИ ОБРАЗОВАНИЯ ДИСПЕРСНЫХ МЕДНЫХ ПОРОШКОВ
В ОБЪЕМЕ ЭЛЕКТРОЛИТА ПРИ ИСПОЛЬЗОВАНИИ МЕДНОГО АНОДА
В РАСТВОРЕ СЕРНОЙ КИСЛОТЫ, СОДЕРЖАЩЕЙ ИОНЫ ТИТАНА (IV)**

Аннотация. Впервые показано, что при поляризации пары электродов «медь-титан» в растворе серной кислоты, содержащей ионы титана (IV) в межэлектродном пространстве образуются медные порошки.

Исследован механизм образования медных порошков при электролизе. Показано, что при поляризации электродов меди и титана в растворе серной кислоты, содержащей ионы титана (IV), аноды меди растворяются, образуя ионы меди (II), а на катоде ионы титана (IV) восстанавливаются до трехвалентного состояния. В это время цвет электролита на катоде – фиолетовый, а на аноде – переходит в синий цвет. Установлено, что образованные ионы меди (II) и Ti (III) взаимодействуют в объеме раствора между электродами, в результате образуются наноразмерные медные порошки.

Показано, что четырехвалентные ионы титана, образованные в результате реакции снова восстанавливаются на катоде до трехвалентного состояния в свою очередь в межэлектродном пространстве они снова взаимодействуют с ионами меди (II), образуя медные порошки и эти процессы циклично повторяются. Показано, что при электролизе между электродами сначала образуются коллоидные медные порошки, затем они соединяются и оседают.

Ключевые слова: ионы титана, медь, порошки, электролиз, электролит, восстановление.

Information about authors:

Bayeshov A. - Chief Researcher, Doctor of Chemical Sciences, Laboratory of electrochemical technology, JSC “D.V. Sokolsky Institute of Fuel, Catalysis and Electrochemistry”, Almaty, Kazakhstan. Tel: +77017605635, e-mail: bayeshov@mail.ru. ORCID 0000-0003-0745-039X;

Myrzabekov B. - Senior Researcher, PhD, Laboratory of electrochemical technology, JSC “D.V. Sokolsky Institute of Fuel, Catalysis and Electrochemistry”, Almaty, Kazakhstan. [Tel:+77782170085](tel:+77782170085), e-mail: myrzabekbegzat@mail.ru. ORCID0000-0001-7321-2782;

Kolesnikov A. - Candidate of technical Sciences, D.Mendeleev University of Chemical Technology of Russia, Moscow, Russia, Tel: 8 985 243 46 46, e-mail: artkoles@list.ru, orcid: 0000-0002-4586-6612

NEWS

OF THE NATIONAL ACADEMY OF SCIENCES OF THE REPUBLIC OF KAZAKHSTAN

SERIES CHEMISTRY AND TECHNOLOGY

ISSN 2224-5286

<https://doi.org/10.32014/2018.2518-1491.32>

Volume 6, Number 432 (2018), 102 – 108

D.I. Chyrkun¹, A.E. Leudanski¹, V.G. Golubev², D. Sarsenbekuly², S.A. Kumisbekov²

¹Belorussian State Technological University, Minsk, Belarus;

²M. Auezov South Kazakhstan State University, Shymkent, Kazakhstan

email: alex_levdansky@mail.ru nii_mm@mail.ru alex_levdansky@mail.ru serik_argin@mail.ru

ANALYSIS OF INDUSTRIAL DRUM MILLS' OPERATION AND WAYS OF THEIR IMPROVEMENT

Abstract. There has been done the analysis of existing industrial drum mills, which has permitted to reveal their design imperfection. In order to increase the intensity of heterogeneous processes, it is proposed to aim at increasing the surface of contacting phases, involved in the process. For this purpose, it is necessary to combine such processes as grinding, activation, classification, mixing and chemical synthesis in the grinding device, which enables to intensify the subsequent operations for processing of dispersed compositions. The efficiency of mill operation in a closed cycle can be further improved, if to provide a highly efficient classification of ground products, removed from the mill. It is proposed to divide the whole drum of the mill along its length by lattice partitions into a large number of chambers, with a certain distance between the chambers of about $1,5 \div 2$ meters; to install two lattice partitions between the chambers, with a distances of $0,25 \div 0,4$ meters between the partitions; to fix the blades to the drum wall in the space between the partitions, similar to the drum dryer. It is recommended that in order to reduce energy costs, there should be provided a rational organization of the grinding process with optimal process conditions for industrial mills, applied in cement milling, with the air speed in the free drum space having to be within $0,7 \div 1,4$ m/sec.

Keywords: industrial drum mills, continuous classification of ground products, particles, process intensification, material cooling energy, specific energy costs, designs.

Introduction. Improving production efficiency is an essential part of the economic strategy of the country and, finally, is shown in increasing the output of high quality products at lowest costs. This is achieved through technical re-equipment, wide introduction of advanced technologies and equipment.

To increase the intensity of heterogeneous processes, it is necessary to aim at increasing the surface of contacting phases, involved in the process. Therefore, at present, many products for most industries are obtained in a fine-disperse state, with the requirements for powder dispersity continuously growing.

The modern direction in the development of technological production equipment is a combination of technological processes. The combination of such processes as grinding, activation, classification, mixing and chemical synthesis in the grinding device enables to intensify the subsequent operations for processing of dispersed compositions.

Grinding of various materials to the particles of less than a tenth of a millimeter is the most important technological process in the production of cement, lime, ceramic products, ore dressing, etc. [1-4].

Methods of research. To carry out the research, there were used analytical and numerical methods with the computers applied.

Results of research. As is known, the main drawback of the milling process is high energy intensity, although directly on the material grinding there is spent a small part of the energy, consumed by the machine.

In modern large-tonnage production there are mainly used drum mills for grinding. However, a very low-efficiency coefficient of these mills forces the researchers to work on their improvement, as well as to develop and apply mills of other designs. Such mills as medium-speed, impact, impact-centrifugal and others are beginning to find more and more application in the processes of fine grinding [5,6].

Drum mills are hollow rotating drums, in which there are grinding bodies (in most cases, steel balls), and just here the material is fed for grinding. Grinding is carried out by impact, crushing and attrition. These mills have been used in industry since the beginning of the twentieth century. The reason for such a long life of this mill is in reliability and simplicity of its design, and due to these characteristics, being very important for production, it is still out of competition in comparison with other designs. Therefore, it is necessary to remember that the newly created designs of mills can move from the development phase to the implementation phase only when they will be comparable by reliability to the drum ones. During the long period of their application, the drum mills have undergone some design changes that have enabled slightly to reduce energy losses, but they still remain very high.

In paper [7, p.17-18] there is given an approximate balance of power consumption items in the drum ball mill:

1. Formation of new surfaces	– 0,6%
2. Losses in the transformation of electricity into the kinetic energy of ball lifting	– 12,3%
3. Heating of the drum	– 6,4%
4. Heating of the medium	– 31%
5. Heating of the material	– 47,6%
6. Other losses	– 2,1%

The balance shows that the main energy losses are related to heating of the material, the medium and the drum itself. Heat in the mill is released as a result of friction between the particles, the friction of the particles on the grinding bodies and the drum wall, as well as due to the volumetric and plastic deformations. Often, high specific energy consumption in fine grinding is explained only by strength change. The smaller the particles, the smaller the internal defects in the material, the stronger they are and, therefore, their grinding requires more energy costs. This explanation is true, but far from being exhaustive. In grinding, part of the particles, having reached the desired size, remaining in the whole mass of the material, take over them the part of acting forces, dissipate them, are over-ground and slow down sharply the process in the right direction. With increasing the dispersity of particles, the effect of interaction of the particles between each other also increases. As a result, there is observed the formation of very small particles' coagulation structures, the destruction of which consumes a significant portion of the energy, supplied to the particle.

The main ways of reducing the energy losses and improving the efficiency of grinding in a drum mill are as follows. By grinding method, the drum mills can be dry and wet grinding. Wet grinding is used in those cases, when the material to be ground is further processed in the form of suspensions, for example, in mineral processing by flotation or extraction of certain components by chemical means.

The advantages of wet grinding, compared to dry grinding, are as follows:

1. less energy consumption per 1 ton of the material;
2. higher grinding capacity of the mill (approximately by 15%), absence of dust and, accordingly, aspiration ventilation and air purification systems;
3. facilitation of transportation and distribution of the material: the hydraulic transport can be used;
4. wet classification is more effective than air classification

The energy consumption reduction in wet grinding and the growth of mill capacity are explained by the fact that the liquid penetrates into cracks and causes tensile stresses that contribute to the destruction of the material, in addition, the friction force between the particles of the ground material decreases.

However, if after grinding the material, the further technology requires its use in a dry form, the dry grinding appears to be more feasible economically due to the large heat consumption for drying.

By operation principle, the drum mills are subdivided into batch and continuous. Batch mills are working by wet method. These mills are not used for operation by dry method because of great difficulties, arising in their discharge. A major drawback of batch mills is a large loss of energy to the mill operation at the end of the grinding cycle, when a very small amount of underground material is left in it. Batch mills are operated very much at the enterprises of the Republic and in order to reduce energy costs they are to be replaced by continuous mills.

To improve the process and to reduce energy costs per unit of the ground material in long drum mills, for example, tube ones, is possible by dividing them along the length into several chambers by installing

lattice partitions. Since the size of the material to be crushed is decreasing while it is moving from the charging spout to the discharge one, in accordance with this, each chamber should be charged with grinding bodies, the size of which corresponds to the size of the material to be crushed. The largest bodies will be in the first chamber and the smallest bodies - in the last one.

To increase the grinding capacity and to reduce the energy costs substantially when grinding in a drum mill is possible by converting its operation from an open cycle to a closed one.

The open cycle operation circuit, when all the material to be crushed is passed through the drum once, is simpler. In this operation circuit there are no devices, providing the finished product selection, and therefore all the material is in the mill until it is completely crushed, as a result of which there will be observed the finished product grinding heterogeneity, part of the material will be over-ground. Naturally, in the open cycle operation there will be low grinding capacity and high specific energy consumption for grinding. However, it should be noted that the mills, working by open method, are simple in design and are not difficult to operate, which ensures their application up to the present time.

In a closed grinding cycle there is no aim to bring the whole material to the desired grinding fineness, and at the exit of the mill it is sent for separation to the separator, when using a dry grinding method, and to the screens or hydrocyclones, when using wet grinding. After separation, the fine fraction as a finished product is removed from the circuit, and the coarse fraction is sent again to the mill for re-grinding. The fresh and underground material is charged into the mill through the second hollow spout or the finished product - through the hollow spout, while the underground material is charged through a special hole in the middle part of the drum wall. Andreyev S. Ye. [8, p. 330-338] proved theoretically that grinding capacity of the mill, working in a closed cycle with a classifier is proportional to the content of coarse size grains in it. At the same time, it is easy to prove that the content of coarse size grains in the mill is directly proportional to the frequency rate of the circulating load. However, the increasing frequency rate of circulation results in the increased energy costs at the stage of classification and transportation of the material under the scheme: mill → classifier → mill. The conditions are considered to be optimal, when the material makes three to six passes through the mill [9, p. 94-95]. The mill's grinding capacity here increases, in comparison with the open cycle, by 20%, with a decrease in energy costs by $15 \div 20\%$; in addition, the specific consumption of grinding bodies is reduced and the service life of the lining is extended.

Taking into account the advantages of a closed grinding cycle, in most countries in cement production and other large-tonnage industries the drum mills are converted to a closed cycle of operation, and only in recent years, such reconstruction has begun to be carried out at some enterprises of our Republic.

The efficiency of closed cycle mills can be further improved, if to provide a highly efficient classification of ground products, removed from the mill. Many researchers, on the basis of evaluation of the existing industrial separators [10, p.130-135; 11, p.42-43], note that the applied designs have low separation efficiency and about $40 \div 70\%$ of the finished finely ground material, having not separated in separators, return again to the mill. The use of screens and hydrocyclones in the wet grinding method also does not provide a high-quality classification, since these devices can work well on low-concentrated suspensions [10, p. 34-35].

Thus, the classification problems in grinding are very acute and need to be solved.

Practice [12, p. 3-6] and studies [13, p. 12-16; 14] show that the air blowing of a drum mill has a positive effect on the grinding process by dry method. Moreover, it was found that with increasing intensity of aspiration to a certain limit, the mill's grinding capacity increases substantially. Thus, monograph [7] gives the graphic dependence, obtained on the basis of the drum mill's industrial testing, which shows that due to active blowing it is possible to increase the mill's grinding capacity by 25%.

The increase of the mill's grinding capacity when blowing it with air can be explained by several factors, the degree of influence of each of which on the process has not yet been determined. Some researchers [13, p. 12- 16; 14; 15, p. 6-8] believe that the improvement of tube mills' grinding capacity with their intense aspiration occurs due to removal of the crushed material's fine fraction from the grinding area, which results in the increase of the coarse fraction portion and the increase of the relative grinding velocity.

It is also known that in fine grinding there are observed aggregation and sticking of small particles on grinding bodies and lining, which has a negative influence on the process. Examination of industrial mills in clinker grinding shows that with increasing the intensity of aspiration, the temperature in the mill is reducing by $35 \div 40^{\circ}\text{C}$, the aggregation and sticking of fines fractions of the material to the grinding bodies and lining are reducing, and in milling a relatively cold clinker ($60 \div 70^{\circ}\text{C}$) there is no sticking at all. The particle sticking occurs due to the action of electrostatic charges on the surface of particles. Water vapors, contained in the air, washing the small particles of the material, form temporary "bridges", which are a kind of conductors, through which the neutralization of electrostatic charges is carried out. Thus, aggregation and sticking are eliminated and due to this the grinding process is intensified.

The grinding degree increase with increasing air speed in the mill is explained by some researchers [16, p. 38-45] not only by the removal of fine fractions of the material from the grinding zone, but also by the influence of the environment on the grinding process. Adsorption of water vapors, which in this case are surface-active substances, from the air, passing through the mill, facilitates the deformation and destruction of the solid body. The effect of adsorption strength reduction is determined primarily by the fact that surface-active substances, reducing the material's surface energy, contribute to the development of various defects at lower stresses. To adsorption influence there are primarily exposed the surface defects of structure – weak points that are always present in any solid body and even in the most well-formed crystals. Into the defects of structure - the micro-cracks, being present in a solid body and appearing in the process of its exposure to the grinding media, with air, there penetrate the water vapors, covering the surface, available to them inside the deformed body, with a uniform adsorption layer. When the liquid comes to the mouth of a micro-crack, its molecules are distributed on both surfaces of the micro-crack up to the narrowest places, where their further penetration is prevented by the size of the molecules themselves. The adsorption layer of water molecules prevents the closure of the micro-cracks and thus reduces the hardness of the material to be ground.

Thus, the air purging of the drum mill chamber can have a positive effect on the grinding process for the following reasons:

1. Due to continuous removal of a fine fraction from the grinding zone;
2. Due to removal of electrostatic charges from the surface of very fine particles and thus, reduction of their aggregation and prevention of sticking to the grinding media and lining;
3. Due to adsorption effect of the air moisture on the particle defective structures and thus, reduction of the material's strength.

All these factors, undoubtedly, have a positive influence on the grinding process, and it is very difficult to give preference to any of them. One thing is clear that the closer contact will be in the mill between the air and the particles of the crushed material, the more effective will be the influence of these factors on grinding.

If we consider the movement of flows in the drum mill in the cross section, we shall see that in the operating state all the grinding bodies and the material occupy a little more than 50% of the section (the bottom and side part along the way of the mill's movement).

If we supply air to the mill, it will move in its free space without a sufficiently good contact with the material. Of course, during the rise and fall of the grinding media and the material there will be their intensive mixing and, naturally, a certain part of the fine-disperse material will be thrown into the free space, where the fine particles will be picked up by the air flow and carried away to the separator. However, there will be no good air purge of the whole mass of the material in the existing structural design and therefore the bulk of the crushed material will be in the general flow.

When solving the problem of a close contact between the material and air in a drum mill, it is necessary to take into account the recommendations of Andreyev S. Ye. and Sidenko P. M. [16, p.337; 16, p.26-41], who repeatedly note that in a drum mill it is not advisable to conduct a process with a high degree of grinding in one chamber. It is more economical to conduct it in several serially mounted chambers with the necessary intermediate selection of fractions that do not need grinding in the next chamber. It is also important that to the grinding chamber there came the material with a narrow size range, and the frequency rate of destruction in it was minimal. So, Andreev S.Ye. notes that, from the theoretical point of view, the perfect one there would be a method of grinding in a series of ball mills, each

operating in a closed cycle with a classifier and so short that the material, passing through the mill, would be subjected to a limited number of ball impacts and all the resulting finished product would be immediately removed from the classification cycle.

On the basis of the above, we offer a more perfect version of the drum mill. The whole drum of the mill along its length should be divided by lattice partitions into a large number of chambers, with a distance between the chambers, being, for example, $1,5 \div 2$ meters; to set not one lattice partition between the chambers, but two, with a distance of $0,25 \div 0,4$ meters between the partitions; to fix blades to the drum wall in the space between the partitions, similar to the drum dryer, as shown in Fig. 1.

In this case, the material is crushed in the chamber, passes through the first lattice partition and, falling on the blades, rises up and falls down from above. Since there are many blades, the falling particles will fill almost the whole cross section of the mill. The air, moving in the longitudinal direction, will enter the flow of falling particles, cool them and, depending on the speed, will pick up the particles of certain sizes and carry them away with it. This separation process will be observed after each chamber. The air velocity must be such that the near-mesh size particles, picked up by the air flow before they settle, could fly over the whole length of the chamber.

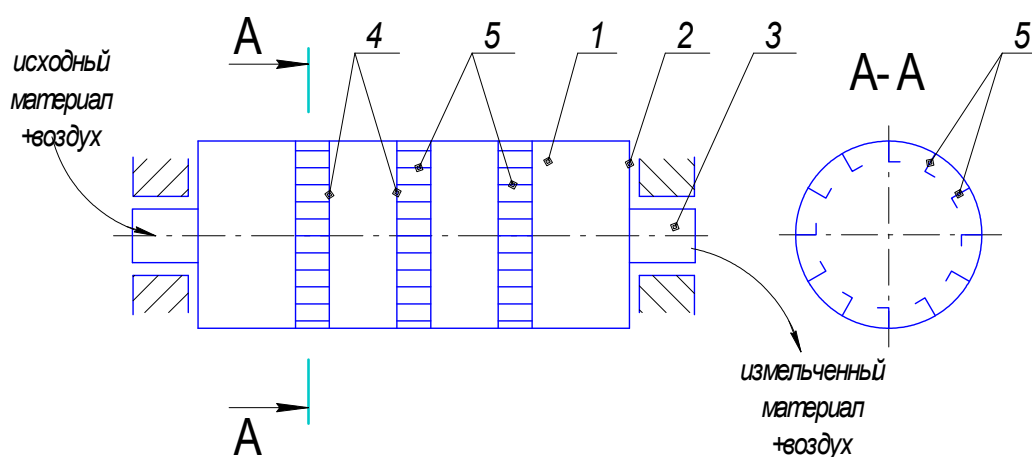


Figure 1. The scheme of reconstruction of the drum mill
1 – the drum; 2 – the end covers; 3 – the spouts; 4 – the lattice partitions; 5 – the blades.

To calculate the air velocity in the chamber, it is necessary to calculate the settling velocity of near-mesh size particles in the drum, using the Stokes formula. Knowing the particle settling velocity and the mill diameter, we determine the particle settling time. During this time, the particle should manage to pass the whole length of the chamber in the horizontal direction. Knowing the length of the chamber and the settling time, we determine the air velocity in the chamber. According to our approximate calculations, for industrial mills, used for cement milling, the air velocity in the free space of the drum should be within $0,7 \div 1,4$ m/sec. [16].

Conclusions. Thus, with the help of such reconstruction, there will be carried out continuously almost complete removal of crushed particles from the mill, there will be intensified the processes of cooling the material and the adsorption of moisture on its surface, which will significantly increase the grinding capacity of the mill, with reducing its energy costs.

However, at the exit of the mill, the ground material must be subjected to a highly efficient classification, so that the finished product could be almost completely removed from the system, and only the underground particles returned back for re-grinding. It is known that there are used medium-speed mills, having much lower energy consumption due to a highly organized grinding process, but having a much more complicated design.

REFERENCES

- [1] Bobrova N. V. Influence of the wear of impact elements of crushers on their performance characteristics. //International scientific conference "Actual problems and prospects of the agro-industrial complex development", Ivanovo, 2007. P. 124-125.
- [2] Lapshin V. B., Abalikhin A. M., Bobrova N. V., Bogorodskiy A.V., Kolobov M. Yu. Ways of improving the durability of the centrifugal-impact grinders' operating elements // Repair. Reconstruction.Modernization.No. 8.M.; Science and technology, 2008. - P. 41-44.
- [3] Abalikhin A. M., Bobrova N. V., Subbotin K. V. Ways of improving the durability of the impact- centrifugal grinders' operating elements. // Proceedings of the international scientific and methodical conference " Modern problems of the agro-industrial complex development in the works of young scientists and students of the FSEI HPE (Federal State Educational Institution of Higher Professional Education) "Ivanovo SAA (State Agricultural Academy) named after academician D. K. Belyaev"", Ivanovo, 2008. P. 203-204.
- [4] Verigin Yu. A., Tolstenev S. V. Synergetic bases of processes and technologies. Barnaul: AltSTU, 2007. 172 p.
- [5] Gridchin A. M., Sevostyanov V. S., Lesovik V. S., Gorlov A., Perelygin D. N., Romanovich A. A., Kolesnikov A.V. Energy saving complexes of fine and ultrafine grinding of the materials// IzvestiyaVUZov. Construction, 2006. №11. P. 60-67.
- [6] Baranov V. F., Weisberg L. A. Trends in the development of technology and technique of ore preparation // "Modern methods of technological mineralogy in the processes of complex and deep processing of mineral raw materials".- Proceedings of the international meeting "Plaksinsky readings – 2012", Petrozavodsk, September 10-14, 2012. p. 12 - 16.
- [7] Lowrison G. Crushing and grinding. London, Butterworth's, 1974, V.1.
- [8] Andreyev S. Ye., Perov V. A., Zverevich V. V. Crushing, grinding and screening of minerals. Moscow: Nedra, 1980. 415 p.
- [9] Sapozhnikov M. Ya. Mechanical equipment of the enterprises of building materials, products and structures. Moscow: Higher school, 1971. - 382 p.
- [10] Dешко Yu. I., Kramer, M. B., Krykhtin G. S. Grinding of materials in cement industry. M.: Ed. liter. on construction, 1966. 274 p.
- [11] The trend of development of hammer mills with separators. Review.Power engineering, 1976. - 62 p.
- [12] Cherep I. L., Belkoskiy G. V. Increase of the cement mills' capacity. Cement № 3, 1956. P. 13-14.
- [13] Krykhtin G. S. Influence of ventilation on the main indices of tubular cement mills' operation. / Proceedings of NIICement, Issue 12, 1959. 86 p.
- [14] Apimakh Ye.V. and etc. Promising directions of reducing specific energy costs in grinding // News of the academy of sciences of the Republic of Kazakhstan. Series chemistry and technology, No5 (431), 2018. P.32-41. <https://doi.org/10.32014/2018.2518-1491>
- [15] Tovarov V. V. Ways to improve the grinding capacity of mills.// Cement № 2, 1962. P. 16-17.
- [16] Khodakov G. S. Physics of grinding. - Moscow: Science, 1972. 256 p.
- [17] Levdanskiy A. E. Scientific and practical bases of applying the flowing currents for intensification of classification and grinding processes: dis. ... Dr. Techn. Sciences: 05.17.08 / A. E. Levdanskiy. Minsk, 2004. 272 p.

Д. И. Чиркун¹, А. Э. Левданский¹, В.Г. Голубев², Д. Сарсенбекулы², С.А. Кумисбеков²

¹ Белорусский государственный технологический университет, г. Минск, Беларусь;

² М.Әуезов атындағы Оңтүстік Қазақстан мемлекеттік университеті, Шымкент, Қазақстан

ӨНЕРКӘСІПТІК БАРАБАНДЫ ДИІРМЕНДЕР ЖҰМЫСЫН САРАПТАЛАУ ЖӘНЕ ОЛАРДЫ ЖЕТІЛДІРУ ЖОЛДАРЫ

Аннотация. Олардың конструкциялық жетілдірілмегендігін анықтауға мүмкіндік берген қолданыстағы өнеркәсіптік барабанды диірмендердің жұмысына сараптама жүргізілді. Гетерогендік процесстердің қарқындылығын жоғарылату мақсатында процеске қатысатын түйісуші фазалардың беттерін ұлғайтуға ұмтылу ұсынылады. Бұл үшін дисперсті композицияларды өңдеу бойынша кейінгі операцияларды қарқындыруға мүмкіндік беретін ұсақтау, активация, классификация, жылжыту және аппараттағы химиялық синтез сияқты процесстерді біріктіру қажет. Егер диірменнен шығарылатын ұсақтау өнімдерін жоғары тиімді классификацияды қамтамасыз ететін болса тұйық цикл бойынша диірмен жұмысының тиімділігін тағы көбірек жоғарлатуға болады.

Диірмен барабанын ұзына бойы торлы қалқалар мен үлкен камераларға белгілі бірарақашықтықта камералар арасы шамамен 1,5÷2 метр бөлу ұсынылды. Камералар арасына қалқалар арасының қашықтығы 0,25÷0,4 м болатын екі торлық алқалар орнатылсын. Қалқалар арасындағы кеңістікте барабан қабырғасына барабанды кептіргіштегідей күрекшелерді орнату. Энергия шығындарын төмендету үшін цементті ұнтақтауда қолданылатын өнеркәсіптік диірмендер үшін процесс өтуінің оңтайлы шарттарымен ұсақтау процесін ұтымды ұйымдастыруды қамтамасыз ету ұсынылады, барабанның еркін кеңістігіндегі ауа жылдамдығы шамамен 0,7÷1,4 м/с болуы қажет.

Түйін сөздер: Өнеркәсіптік барабанды диірмендер, ұсақтағыш өнімдердің үздіксіз классификациясы, бөлшектер, процесті қарқындастыру, материалды салқындату энергиясы, меншікті энергия шығындар, конструкциялар.

УДК 621.926.4

Д. И. Чиркун ¹, А. Э. Левданский ¹, В.Г. Голубев ², Д. Сарсенбекулы ², С.А. Кумисбеков ²

¹Белорусский государственный технологический университет, г.Минск, Беларусь;

²Южно-Казахстанский государственный университет им.М.Ауэзова, г.Шымкент, Казахстан

АНАЛИЗ РАБОТЫ БАРАБАННЫХ ПРОМЫШЛЕННЫХ МЕЛЬНИЦ И ПУТИ ИХ УСОВЕРШЕНСТВОВАНИЯ

Аннотация. Выполнен анализ работы существующих барабанных промышленных мельниц, который позволил определить их конструктивное несовершенство. С целью повышения интенсивности гетерогенных процессов предлагается стремиться к увеличению поверхности контактирующих фаз, участвующих в процессе. Для этого необходимо объединение таких процессов, как измельчение, активация, классификация, смешение и химический синтез в аппарате – измельчителе, позволяет интенсифицировать последующие операции по обработке дисперсных композиций. Эффективность работы мельниц по замкнутому циклу можно еще более повысить, если обеспечить высокоэффективную классификацию продуктов измельчения, выводимых из мельницы.

Предложено весь барабан мельницы по длине разделить решетчатыми перегородками на большое количество камер, с определенным расстоянием между камерами, порядка 1,5÷2 метра. Между камерами установить две решетчатые перегородки с расстояниями между перегородками 0,25÷0,4. В пространстве между перегородками к стенке барабана закрепить лопасти, аналогично как в барабанной сушилке. Рекомендовано, что для снижения энергозатрат должна обеспечиваться рациональная организация процесса измельчения с оптимальными условиями протекания процесса для промышленных мельниц, применяемых для помола цемента, скорость воздуха в свободном пространстве барабана должна быть в пределах 0,7÷1,4.

Ключевые слова: барабанные промышленные мельницы, непрерывная классификация продуктов измельчения, частицы, интенсификация процесса, энергия охлаждения материала, удельные энергозатраты, конструкции.

Information about the authors:

Chyrkun Dzmitry Ivanovich - Candidate of Technical Sciences, teacher of the Department "Processes and Apparatuses of Chemical Production", Belorussian State Technological University, e-mail: alex_levdansky@mail.ru

ORCID: 0000-0003-0195-2575;

Leudanski Aliaksandr Eduardovich - Doctor of Technical Sciences, Associate Professor of the Department "Processes and Apparatuses of Chemical Production", Belorussian State Technological University, e-mail: alex_levdansky@mail.ru

ORCID: 0000-0003-2684-7771;

Golubev Vladimir Grigorievich - Doctor of Technical Sciences, Professor of the Department of Oil & Gas Business, M.Auezov South Kazakhstan State University, e-mail: nii_mm@mail.ru

ORCID: 0000-0001-7370-3872;

Sarsenbekuly Didar - PhD, teacher of the Department of Technological Machines and Equipment, M.Auezov South Kazakhstan State University, e-mail: nii_mm@mail.ru

ORCID: 0000-0003-0595-4375;

Kumisbekov Serik Arginbaevich - Candidate of Technical Sciences, Associate Professor of the Department of Technological Machines and Equipment, M.Auezov South Kazakhstan State University, e-mail: serik_argin@mail.ru

ORCID: 0000-0003-4440-5520.

NEWS

OF THE NATIONAL ACADEMY OF SCIENCES OF THE REPUBLIC OF KAZAKHSTAN

SERIES CHEMISTRY AND TECHNOLOGY

ISSN 2224-5286

<https://doi.org/10.32014/2018.2518-1491.33>

Volume 6, Number 432 (2018), 109 – 119

UDC 539.19;541.128.13;544.14;544.46

**A.R. Brodskiy, V.P. Grigor'eva, L.V. Komashko, Y.Y. Nurmakanov,
I.S. Chansheva, A.A. Shapovalov, I.A. Shlygina, V.I. Yaskevich**

"D.V. Sokolsky Institute of Fuel, Electrochemistry and Catalysis" JSC, Almaty, Kazakhstan
albrod@list.ru

**INTERACTION OF THE Fe/ γ -Al₂O₃ CATALYTIC SYSTEM
WITH PROBE MOLECULES I. RESEARCH OF THE γ -Al₂O₃
AND THE Fe/ γ -Al₂O₃ INITIAL SYSTEM**

Abstract. The work is the first part of the studies devoted to the interaction of a heterogeneous catalytic system with adsorbed molecules. It presents the results for the initial oxide γ -Al₂O₃ and Fe/ γ -Al₂O₃ system with an iron content of 0.5; 3; 13% by weight, obtained with a wide range of physicochemical methods. The Fe/ γ -Al₂O₃ system was chosen as the object of the study, since it exhibits catalytic activity in many chemical processes and can later be used as a model.

The performed work showed that during the preparation of the Fe/ γ -Al₂O₃ system by impregnation, the structure of the support can be modified. The nature of the filling of the support surface with the iron-containing phase depends substantially on its percentage and can be multilayered.

It is established that the Fe/ γ -Al₂O₃ system contains iron in the form of Fe³⁺. Depending on the iron content, iron-containing aggregates of various sizes may be present in it, both in the paramagnetic and in the magnetically ordered states.

Key words: heterogeneous catalysis, physicochemical methods of investigation.

Introduction

This work is the beginning of a series of studies devoted to the interaction of a heterogeneous catalytic system with adsorbed molecules. This formulation of the problem is topical, since, in heterogeneous catalysis, the most important stage is the adsorption stage [1, 2].

The iron-containing Fe/ γ -Al₂O₃ (γ -Al₂O₃-support) system was chosen as the object of research because it exhibits catalytic activity in many chemical processes, such as the production of ammonia [3-5] and carbon nanotubes [6, 7], in CO hydrogenation reactions (Fischer-Tropsch synthesis) [8, 9], in the oxidation of hydrogen sulphide to elemental sulfur [1], deep processing of solid fossil and renewable organic raw materials [10], in gasoline reforming reactions [11], and many other reactions [12]. Thus, the catalytic system Fe/ γ -Al₂O₃ being practically multifunctional, in the future, can be used as a model system.

Experimental

The Fe/ γ -Al₂O₃ system with an iron content of 0.5; 3; 13 wt.% was prepared by impregnation [1, 13, 14] of the initial γ -Al₂O₃ oxide with an aqueous solution of iron acetate, followed by drying and calcination in air.

A wide range of physicochemical methods during the research was used.

X-ray diffractometry. The X-ray diffractometer Dron-4-07 with cobalt anode tube was used.

Mode:

- speed 2 deg/min;

- working parameters of the tube: 30 kV, 20 mA.

Transmission electron microscopy. Equipment - EM-125K, accelerating voltage of 75 kV.

Scanning electron microscopy. JSM 6610 LV, JEOL, Japan is a scanning low-vacuum electron microscope. Accelerating voltage 20 kV.

BET method (low-temperature nitrogen adsorption). Equipment -AccuSorb, Micromeritics, USA. The standard procedure. Calcination of the sample at 230-250° C for 3 hours with evacuation. The relative error in determining the specific surface area is $\pm 5\%$.

Mossbauer spectroscopy. Equipment - MS 1104Em, Russia. The source was cobalt 57 in a chromium matrix with an activity of 100 μCi . The spectra were processed on a PC by the "least squares" method. The isomeric shifts are given in terms of $\alpha\text{-Fe}$. The temperature of the spectra is 23°C. The shooting mode is "on the skylight". The error in determining the isomer shift (IS) is $\Delta\text{IS} = \pm 0.03$ mm/s; quadrupole splitting (QS) $\Delta\text{QS} = \pm 0.03$ mm/s; relative content (S) $\Delta\text{S} = \pm 2\%$.

Results and Discussion

The study of $\gamma\text{-Al}_2\text{O}_3$ oxide and Fe/ $\gamma\text{-Al}_2\text{O}_3$ system was carried out.

X-ray diffractometry.

X-ray diffraction patterns (Fig. 1) of $\gamma\text{-Al}_2\text{O}_3$ oxide and Fe/ $\gamma\text{-Al}_2\text{O}_3$ system with various iron contents were obtained.

Following results were obtained:

- Initial $\gamma\text{-Al}_2\text{O}_3$:

Reflexes at 4.5641; 2.7959; 2.3981; 2.2883; 1.9767; 1.5258; 1.3950 Å - $\gamma\text{-Al}_2\text{O}_3$ phase (ASTM 10-424);

- 0.5% Fe/ $\gamma\text{-Al}_2\text{O}_3$ system:

Reflexes at 4.5641; 2.8032; 2.3815; 2.2891; 1.9781; 1.5210; 1.3994 Å - $\gamma\text{-Al}_2\text{O}_3$ phase (ASTM 10-424);

Reflexes at 4.8524; 4.3735; 4.3158; 3.3285; 2.4580; 2.3815; 1.8017; 1.7475 Å - gibbsite phase of $\text{Al}(\text{OH})_3$ (ASTM 33-18);

Reflexes at 4.1784; 2.6891; 2.4580 Å - $\alpha\text{-FeO}(\text{OH})$ (goethite) phase (ASTM 29 - 713);

- 3% Fe/ $\gamma\text{-Al}_2\text{O}_3$ system:

Reflexes at 4.5562; 2.8003; 2.3898; 2.2807; 1.9829; 1.5214; 1.3976 Å - phase $\gamma\text{-Al}_2\text{O}_3$ (ASTM 10-424);

Reflexes at 4.8579; 4.3698; 4.3230; 3.3264; 2.4580; 2.3898; 1.7978; 1.7501 Å - gibbsite phase of $\text{Al}(\text{OH})_3$ (ASTM 33-18);

Reflexes at 4.1784; 2.6904; 2.4580 Å - $\alpha\text{-FeO}(\text{OH})$ (goethite) phase (ASTM 29 - 713)

- 13% Fe/ $\gamma\text{-Al}_2\text{O}_3$ system:

Reflexes at 4.5681; 2.7974; 2.3908; 2.2853; 1.9733; 1.5217; 1.3994 Å - $\gamma\text{-Al}_2\text{O}_3$ phase (ASTM 10-424);

Reflexes at 4.8434; 4.3771; 4.3158; 3.3161; 2.4481; 2.3908 Å - gibbsite phase of $\text{Al}(\text{OH})_3$ (ASTM 33-18);

Reflexes at 4.1817; 2.6837; 2.4481 Å - $\alpha\text{-FeO}(\text{OH})$ (goethite) phase (ASTM 29-713).

The data obtained indicate that the original alumina is indeed $\gamma\text{-Al}_2\text{O}_3$. Partial hydrolysis of aluminum oxide occurs during the synthesis of the Fe/ $\gamma\text{-Al}_2\text{O}_3$ system, resulting in the formation of aluminum hydroxide in the form of gibbsite. It should be noted that the highest degree of hydrolysis is observed for the Fe/ $\gamma\text{-Al}_2\text{O}_3$ system with the lowest iron content and it decreases monotonically with its growth (Fig. 1). This is probably due to the fact that as the concentration of iron acetate increases, in the solution there is an ever-decreasing amount of free water capable of causing hydrolysis of aluminum oxide [15].

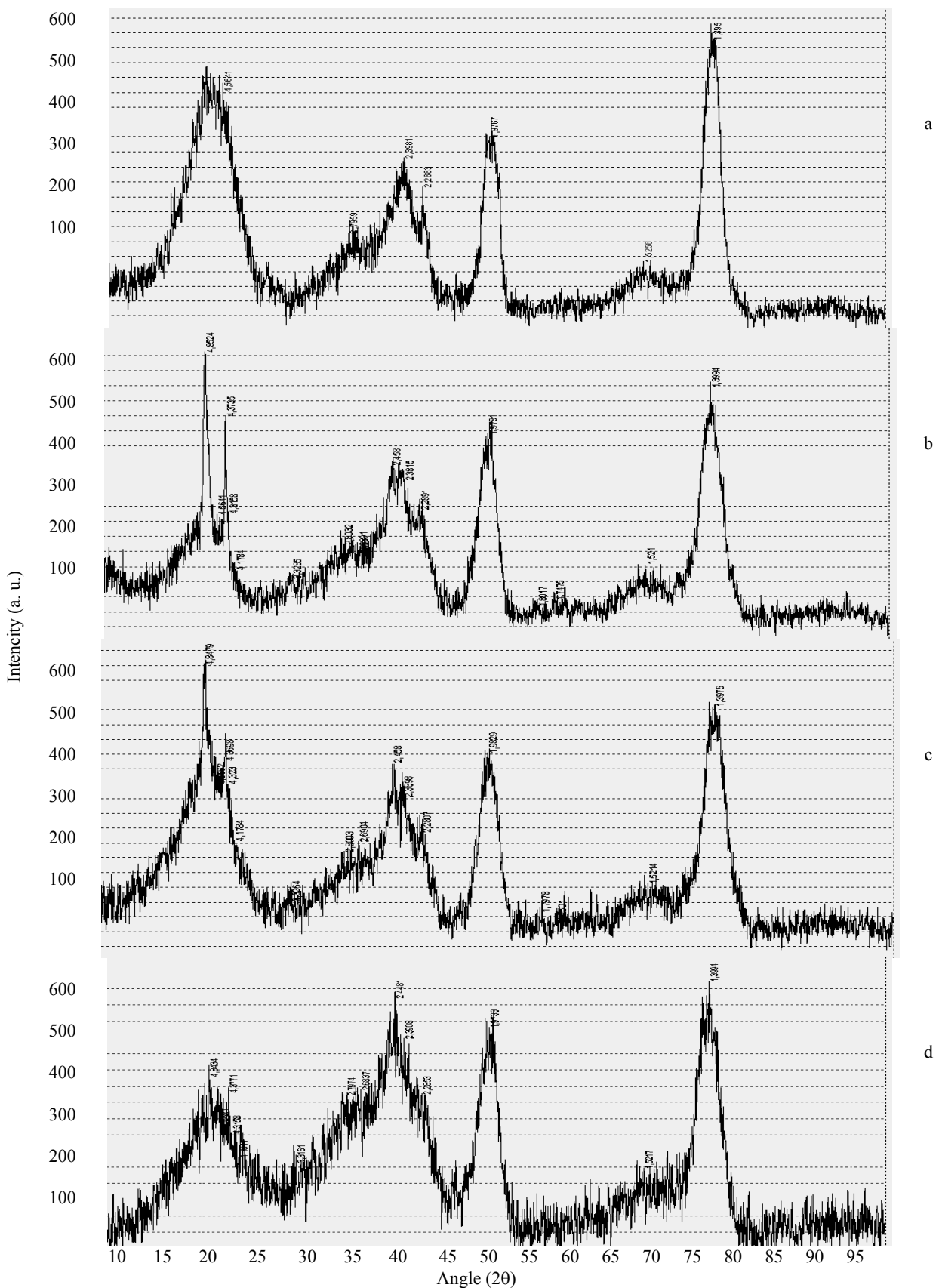


Figure 1 – Diffraction patterns of γ -Al₂O₃ oxide and Fe/ γ -Al₂O₃ system
 a - γ -Al₂O₃; b - 0.5% Fe/ γ -Al₂O₃; c - 3% Fe/ γ -Al₂O₃; d - 13% Fe/ γ -Al₂O₃

Transmission electron microscopy.

Microphotographs of the initial aluminum oxide $\gamma\text{-Al}_2\text{O}_3$ and the $\text{Fe}/\gamma\text{-Al}_2\text{O}_3$ system with different iron contents are shown in Fig. 2.

There are two kinds of particles in $\gamma\text{-Al}_2\text{O}_3$ sample. The first type is characterized by aggregates of large, semitransparent, plate-like particles with a hexagonal facets (the (111) plane of $\alpha\text{-Al}_2\text{O}_3$ crystallites) reaching almost micron sizes (400-800 nm) (Fig. 2a).

The second type of particles is small transparent plates of elongated rectangular shape (planes (001), (111) of $\gamma\text{-Al}_2\text{O}_3$ crystallites) which in the width are 5-10nm (Fig. 2b). Microdiffraction was taken from various parts of the sample. The pictures show reflexes that are located on the rings. They correspond to $\gamma\text{-Al}_2\text{O}_3$ (JCPDS, 10-425). A trace amount of $\delta\text{-Al}_2\text{O}_3$ (JCPDS, 16-394), $\text{Al}(\text{OH})_3$ gibbsite (JCPDS, 7-324) and $\theta\text{-Al}_2\text{O}_3$ (JCPDS, 11-517) also were observed.

Micrograph of the 0.5% $\text{Fe}/\gamma\text{-Al}_2\text{O}_3$ system is shown in Fig. 2c. It has large particles with signs of faceting ranging in size from 200 to 1000 nm. Microdiffraction produces symmetrical and individual reflexes, which correspond to $\gamma\text{-Al}_2\text{O}_3$ (JCPDS, 10-425). A large 200nm in size particle of a pointed shape and small aggregates made up of particles of 10-40 nm in size are shown in Fig. 2d. Microdiffraction gives a large number of symmetrical and individual reflexes, which can be attributed to a mixture of phases: gibbsite (JCPDS, 7-324), $\beta\text{-AlO}(\text{OH})$ Diaspore (JCPDS, 5-355), $\gamma\text{-AlOOH}$ Boehmite (JCPDS, 21-1301), with a significant predominance of the former.

Only phases of aluminum oxides and hydroxides in the sample were found. The low iron content in the system did not allow the detection of iron-containing phases because of a small amount they did not reach the field of view of the microscope.

The microphotographs of the 3% $\text{Fe}/\gamma\text{-Al}_2\text{O}_3$ system have many dense aggregates; also large particles of lamellar type of medium transparency are present in the sample, which is shown in Fig. 2e. A conglomerate of transparent particles of lamellar type of micron size, surrounded by small aggregates of small dense particles 5-10 nm in size is shown in Fig. 2e. Microdiffraction gives a large set of reflexes that are located along a distorted hexagonal view, and individual reflexes, which can be attributed to a mixture of the phases $\gamma\text{-FeO}(\text{OH})$ - goethite (JCPDS, 29-713), FeOOH (JCPDS, 26-792), $\text{Al}(\text{OH})_3$ - gibbsite (JCPDS, 29-41), $\gamma\text{-Al}_2\text{O}_3$ (JCPDS, 10-425).

There is an aggregate of transparent particles of lamellar type ~ 0.5 micron in size for a 13% $\text{Fe}/\gamma\text{-Al}_2\text{O}_3$ system in Fig. 2g. Microdiffraction gives reflexes located on a distorted hexagonal view, which can be referred to $\delta\text{-FeOOH}$ (JCPDS, 13-87). In addition, this micrograph has round-shaped particles with dimensions of 10-30nm. Microdiffraction gives reflexes (rings) related to FeOOH (JCPDS, 26-792). In Fig. 2h, the particles are larger, for them microdiffraction shows a large set of reflections of the following phases: Fe_2O_3 (JCPDS, 32-469) and $\gamma\text{-Al}_2\text{O}_3$ (JCPDS, 10-425).

Scanning electron microscopy

Microphotographs of the initial aluminum oxide $\gamma\text{-Al}_2\text{O}_3$ and the $\text{Fe}/\gamma\text{-Al}_2\text{O}_3$ system with different iron content are shown in Fig. 3.

From microphotographs it follows that aggregates of various sizes (Fig. 3a, b, c) are present on the surface of the support $\gamma\text{-Al}_2\text{O}_3$, from tens to micrometers. Porous structure of the support surface is clearly visible when the magnification is large (Fig. 3c).

The relief of the support is "smoothed" when the acetate of iron is deposited on $\gamma\text{-Al}_2\text{O}_3$ (Figure 3), and the effect is most pronounced at 13% iron content. It can be assumed that an iron-containing film (crust) is formed on the surface of the support, and this, in fact, leads to a visible "smoothing" effect of the relief. In the case of the $\text{Fe}/\gamma\text{-Al}_2\text{O}_3$ system with 0.5% iron content (Fig. 3d, e, f), the complete surface coverage of the $\gamma\text{-Al}_2\text{O}_3$ support by the iron-containing component is not noticeable, apparently due to its small amount. On the contrary, it can be assumed that for a system with 13% iron content (Fig. 3 j, k, l), the coating is multilayer.

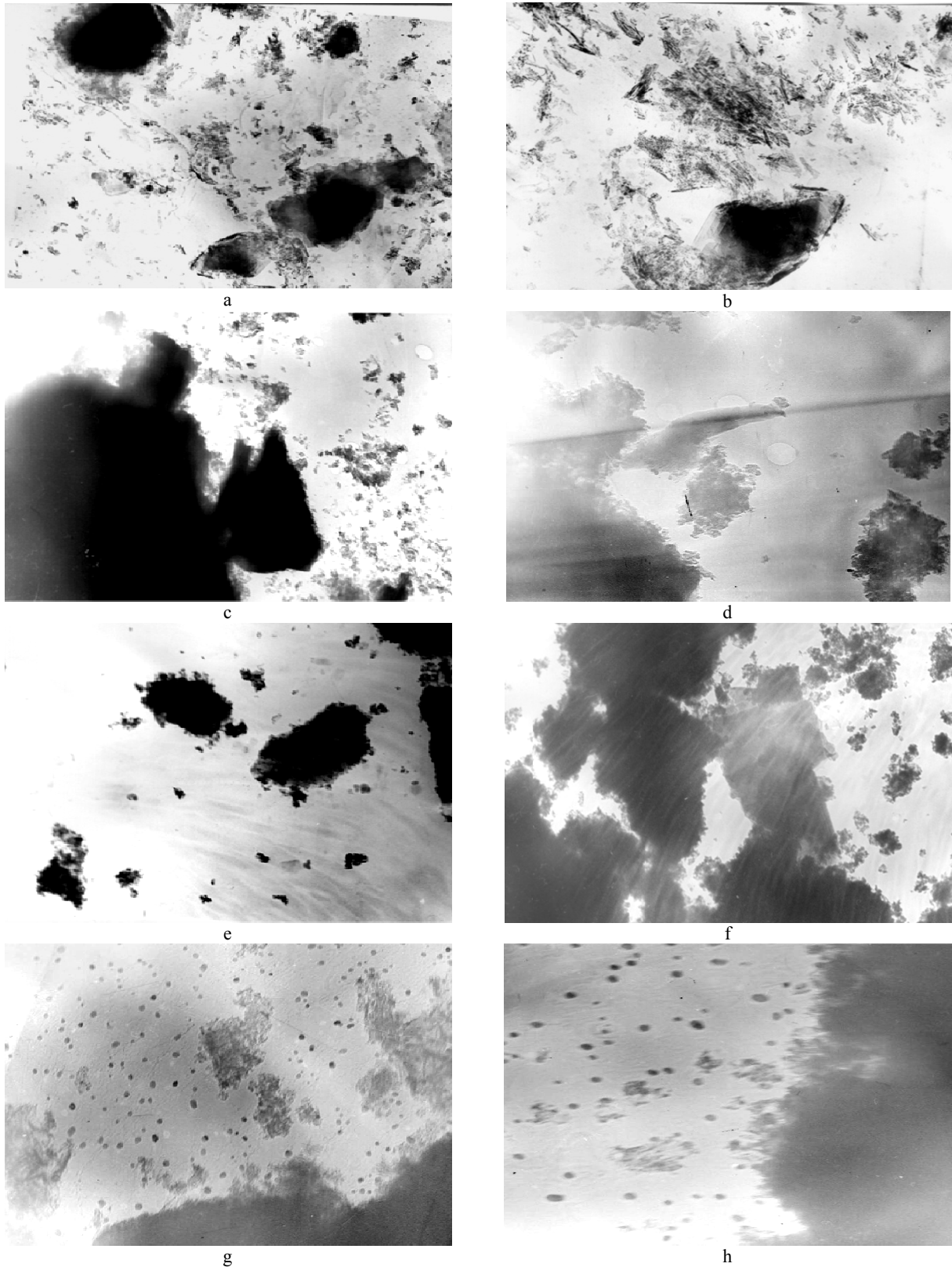


Figure 2 - Micrographs of the initial aluminum oxide γ - Al_2O_3 and the Fe/ γ - Al_2O_3 system with an iron content of 0.5; 3 and 13%
a, b - initial γ - Al_2O_3 oxide; c, d - 0.5%Fe/ γ - Al_2O_3 system; e, f - 3%Fe/ γ - Al_2O_3 system; g, h - 13%Fe/ γ - Al_2O_3 system.
Magnification: a, c, e, f - 24000 times; b, d, g, h - 50000 times

BET method

Specific surface area and its texture (porosity) for $\gamma\text{-Al}_2\text{O}_3$ oxide and $\text{Fe}/\gamma\text{-Al}_2\text{O}_3$ system with different iron content are determined. The results are shown in Table 1 and are shown in Fig. 4. The data for $\gamma\text{-Al}_2\text{O}_3$ in agreement with the results of [16].

Table 1 – The specific surface area of the $\gamma\text{-Al}_2\text{O}_3$ oxide and the $\text{Fe}/\gamma\text{-Al}_2\text{O}_3$ system

Sample	Parameter		
	SW, m^2/g	V_{ADSmax} , mL/g	V_{true} , mL/g
$\gamma\text{-Al}_2\text{O}_3$	214	180	0,28
0.5%Fe/ $\gamma\text{-Al}_2\text{O}_3$	211	196	0,31
3%Fe/ $\gamma\text{-Al}_2\text{O}_3$	190	115	0,18
13%Fe/ $\gamma\text{-Al}_2\text{O}_3$	173	101	0,16

Note: SW - specific surface area, m^2/g ;
 V_{ADSmax} - total pore volume with gas filling, mL/g;
 V_{true} - total true pore volume, mL/g

From Table 1 it follows that when the iron is precipitated to the support, as the content thereof increases, the value of the specific surface tends to decrease, indicating the filling of the surface.

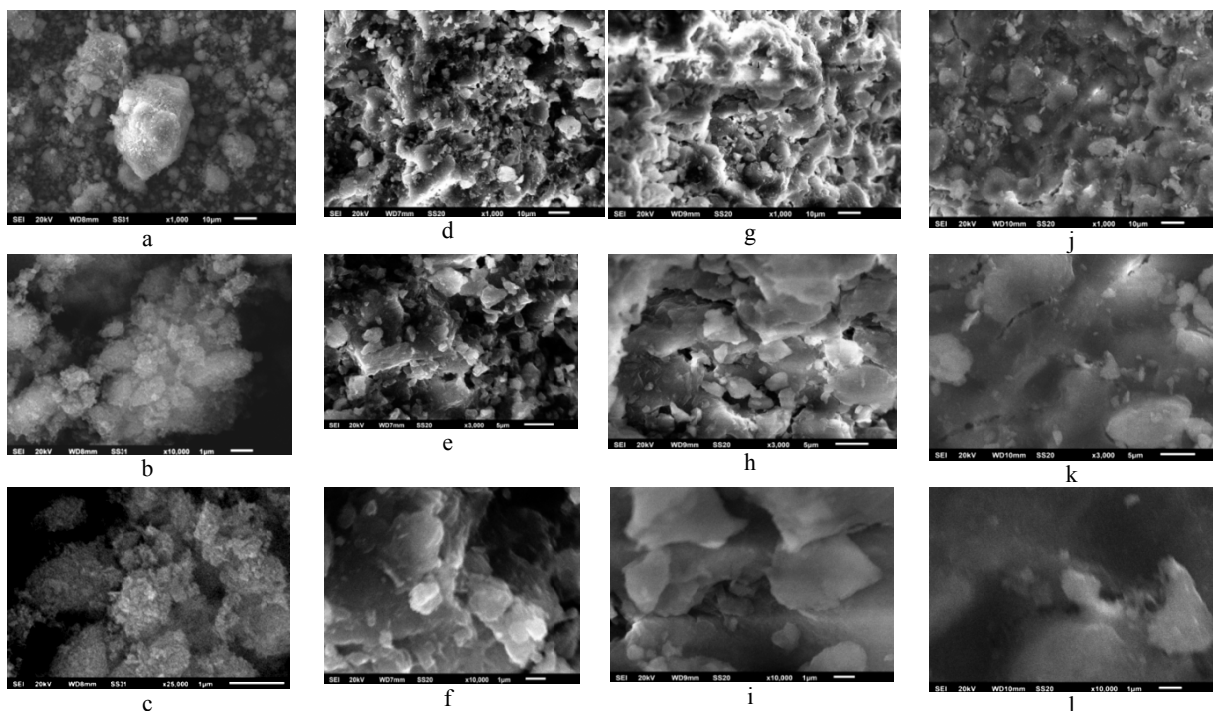


Figure 3 - Microphotographs of aluminum $\gamma\text{-Al}_2\text{O}_3$ and $\text{Fe}/\gamma\text{-Al}_2\text{O}_3$ systems with different iron content
 $\gamma\text{-Al}_2\text{O}_3$ - (a, b, c); 0.5%Fe/ $\gamma\text{-Al}_2\text{O}_3$ (d, e, f); 3%Fe/ $\gamma\text{-Al}_2\text{O}_3$ (g, h, i); 13%Fe/ $\gamma\text{-Al}_2\text{O}_3$ (j, k, l).
Magnification: (a, d, g, j) – 1000 times; (e, h, k) – 3000 times; (b, f, i, l) – 10000 times; (c) – 25000 times

At the same time, the pore volume has a maximum at the point for the system of 0.5%Fe/ $\gamma\text{-Al}_2\text{O}_3$. The presence of an extremum can probably be explained by the hydrolysis of $\gamma\text{-Al}_2\text{O}_3$ and the transition of a part of aluminum oxide to the hydroxide, which was discussed above. In aluminum hydroxide, the total pore volume is noticeably higher than that of $\gamma\text{-Al}_2\text{O}_3$ [17]. Since the iron-containing component does not completely cover the support surface in the 0.5%Fe/ $\gamma\text{-Al}_2\text{O}_3$ system (Fig. 3d, e, f), therefore, at least some of the pores of the hydroxide are accessible.

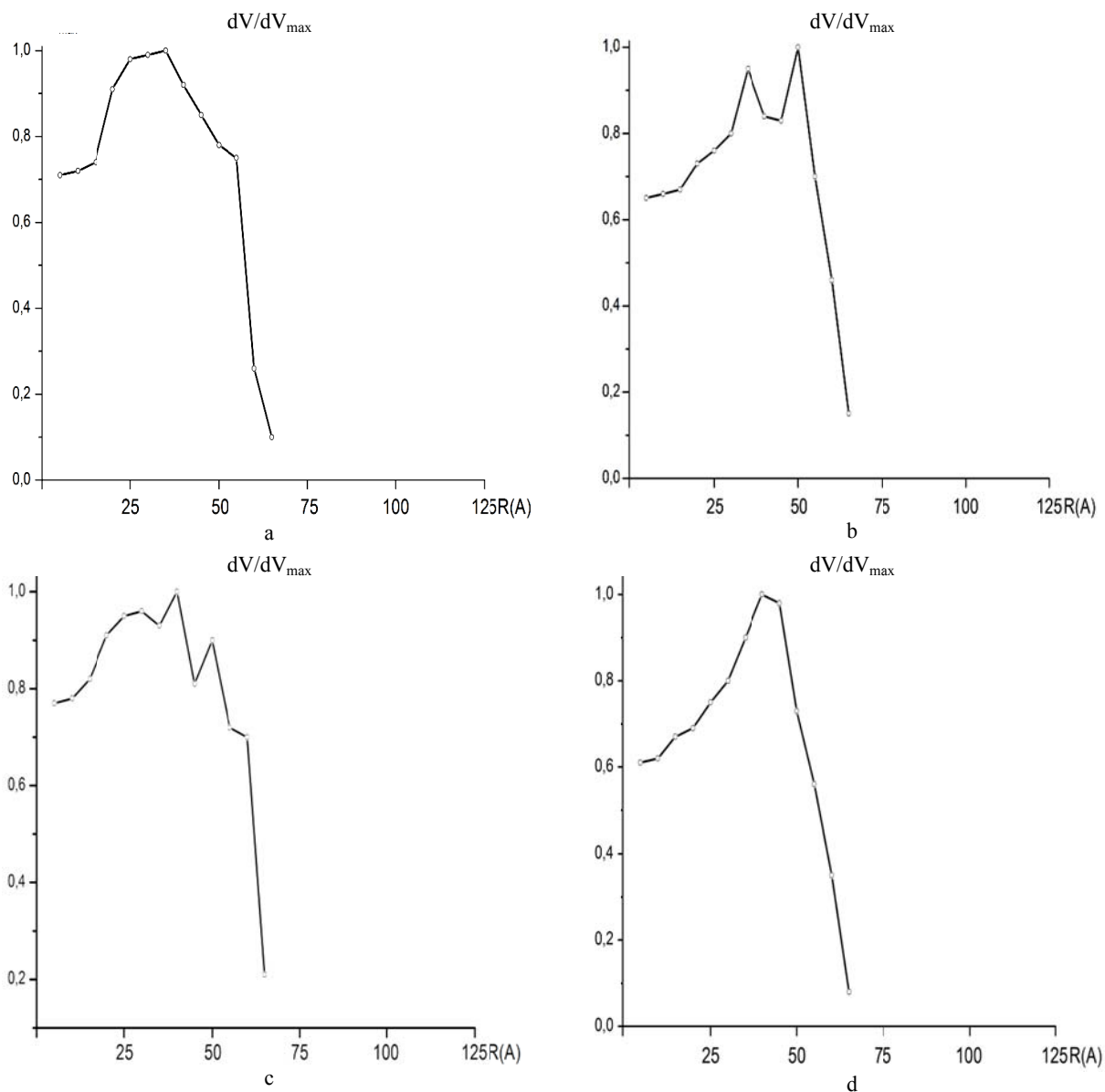


Figure 4 - Pore size distribution in γ - Al_2O_3 and in the Fe/γ - Al_2O_3 system with different iron content

a - γ - Al_2O_3 ; b - 0.5% Fe/γ - Al_2O_3 ; c - 3% Fe/γ - Al_2O_3 ; d - 13% Fe/γ - Al_2O_3

$R(\text{\AA})$ is the pore radius in angstroms (\AA); dV/dV_{max} the ratio of the pore volume of a given radius to the maximum volume

The combination of these factors may lead to an increase in the total pore volume for the 0.5% Fe/γ - Al_2O_3 system.

With an increase in the iron content the total pore volume decreases which on one side may indicate their possible filling, and on the other hand, the difficulty of accessing the probe gas (nitrogen). The latter can be indicated by scanning electron microscopy data (Figure 3), from which it follows that with a high content of iron in the system, the support surface is almost completely closed.

In Fig. 4 - pore size distribution for γ - Al_2O_3 and Fe/γ - Al_2O_3 . The pore size for γ - Al_2O_3 and the Fe/γ - Al_2O_3 system fits within a narrow range of values and their radius does not exceed 65-70 \AA (Fig. 4). When the iron-containing component is applied to alumina, the pore size distribution in comparison with γ - Al_2O_3 (Fig. 4a) varies, for 0.5% Fe/γ - Al_2O_3 , a "dip" is observed in the 40-45 \AA region (Fig. 4b), it follows that in the first place pores of this size are filled. For the 3% Fe/γ - Al_2O_3 system, this "gap" is retained, although the shape of the distribution varies (Fig. 4c), which is apparently related to the filling of the surface with

an iron-containing component. For a system of 13%Fe/ γ -Al₂O₃, due to the filling of the surface, the access of the probe gas to the pores of small size is essentially limited and the pore size distribution shows the presence of basically larger pores (Fig. 4d). All this occurs against the background of a decrease in the total volume of pores (Table 1).

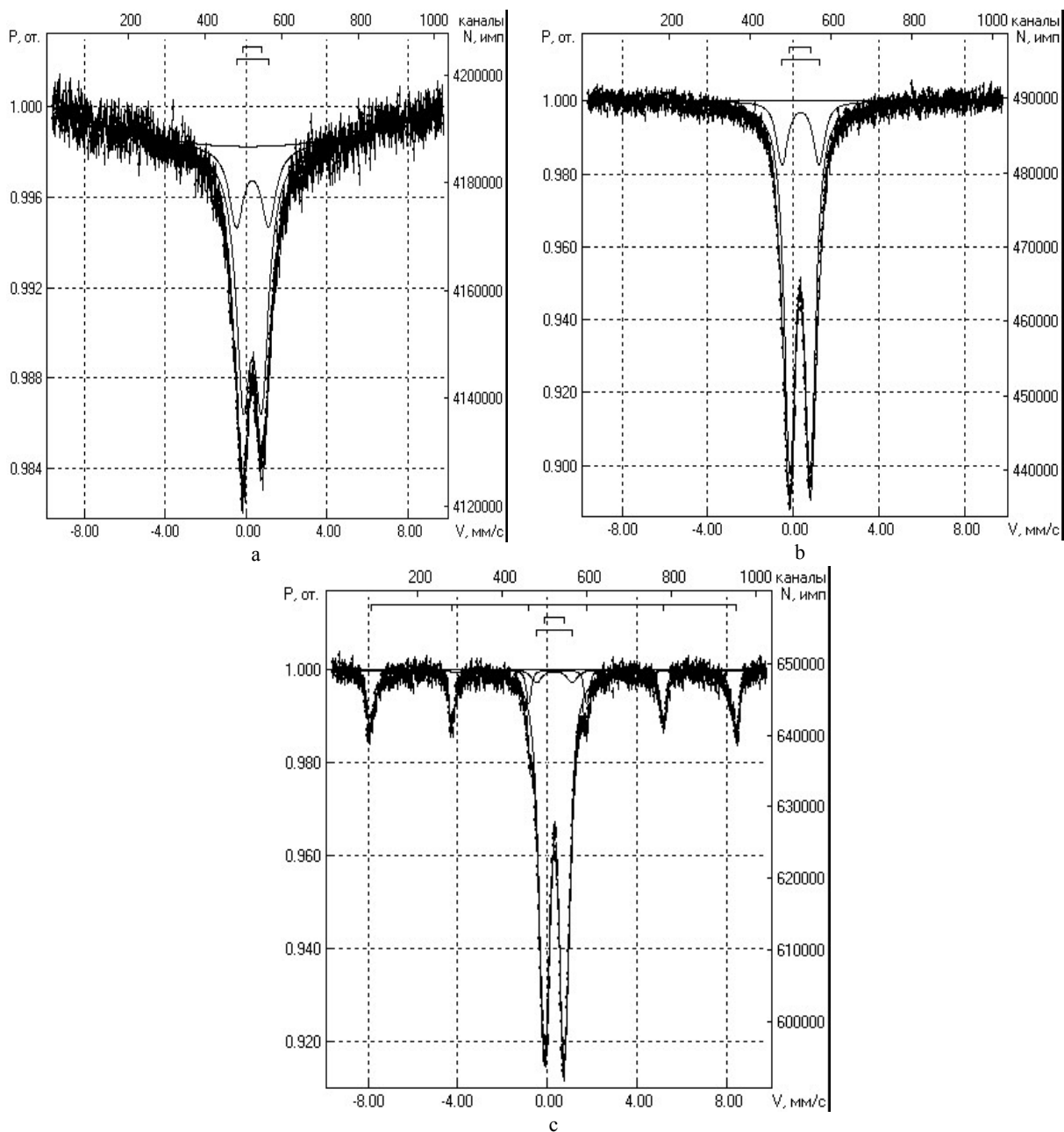


Figure 5 - Mössbauer spectra of the Fe/ γ -Al₂O₃ system with different iron content
 a – 0,5%Fe/ γ -Al₂O₃; b – 3%Fe/ γ -Al₂O₃; c – 13%Fe/ γ -Al₂O₃

Mössbauer spectroscopy

Mössbauer spectra of the Fe/ γ -Al₂O₃ system with different iron contents are shown in Figure 5. The spectra showed that the system, based on the values of isomeric shifts, contains various forms of Fe³⁺ both in the paramagnetic state and in the magnetically ordered one.

The following iron forms are present in the system:

0.5%Fe/ γ -Al₂O₃

Fe₁³⁺ form - IS = 0.32 mm•s⁻¹; QS = 0.95 mm•s⁻¹; S = 62%

Fe_2^{3+} form - IS = 0.32 mm•s⁻¹; QS = 1.59 mm•s⁻¹; S = 38%

3%Fe/ γ -Al₂O₃

Fe_1^{3+} form - IS = 0.31 mm•s⁻¹; QS = 0.98 mm•s⁻¹; S = 70%

Fe_2^{3+} form - IS = 0.32 mm•s⁻¹; QS = 1.62 mm•s⁻¹; S = 30%

13%Fe/ γ -Al₂O₃

Fe_1^{3+} form - IS = 0.32 mm•s⁻¹; QS = 0.93 mm•s⁻¹; S = 77%

Fe_2^{3+} form - IS = 0.31 mm•s⁻¹; QS = 1.59 mm•s⁻¹; S = 3%

α -Fe₂O₃ - IS = 0.37 mm•s⁻¹; QS = - 0.21 mm•s⁻¹; H_{eff} = 506 kOe; S = 20%

(H_{eff} is the Zeeman hyperfine magnetic splitting)

The forms of Fe_1^{3+} and Fe_2^{3+} , irrespective of the iron content in the Fe/ γ -Al₂O₃ system, have similar parameters and are paramagnetic. At the same time, having almost identical IS, they differ significantly in QS. The shape of Fe_2^{3+} with a large value of QS can be attributed to iron on the surface of the support, and the form of Fe_1^{3+} with smaller QS - to a more deeply located [18, 19].

It should be noted that with an increase in the iron content in the system, a gradual increase in the relative content of the more deeply located form of Fe_1^{3+} takes place, which agrees with the BET data.

There is also a magnetically ordered phase that corresponds to α -Fe₂O₃ in the 13% Fe/ γ -Al₂O₃ system, in addition to the Fe_1^{3+} and Fe_2^{3+} forms [20]. A somewhat smaller value of H_{eff} (should be 515-517 kOe) indicates that the particles giving in the Mössbauer spectrum of the Zeeman hyperfine magnetic splitting are of the order of 8-12 nm [21]. At such particle sizes, H_{eff} has a smaller value than for bulk samples.

Conclusion

The performed work has shown that during the preparation of the Fe/ γ -Al₂O₃ system by impregnation, the structure of the support can be modified. The nature of the filling of the support surface with the iron-containing phase depends substantially on its percentage and can be multilayered.

It has been established that the Fe/ γ -Al₂O₃ system contains iron in the form of Fe^{3+} . Depending on the iron content, iron-containing aggregates of various sizes can be present in the system, both in the paramagnetic and magnetically ordered states.

Acknowledgments

The work was supported by the Ministry of Education and Science of the Republic of Kazakhstan (AP05130654).

REFERENCES

- [1] Krylov O.V. Heterogennyi kataliz. M.: IKTs «Akademkniga». **2004**. 663 p. (ISBN 5-94628-141-0) (in Russian).
- [2] Goncharuk V.V., Kamalov G.L., Kovtun G.A., Rudakov Ye.S., Yatsimirskii V.K. Kataliz: mekhanizmy gomogenogo i heterogennogo kataliza, klasternyye podhody. Kiyev, Naukova Dumka, **2002**, 543 p. (in Russian).
- [3] Semenov V.P. Proizvodstvo ammiaka. V. Khimiya. **1985**. 368 p. (in Russian).
- [4] Sibileva S.V., Nefyodova N.V. Razrabotka metoda prigotovleniya osazhdennykh zheleznykh katalizatorov sinteza ammiaka. Uspekhi v khimii i khimicheskoi tekhnologii: sb. nauchn. trudov. V.22, № 10 (90). M., Rkhtu im. D.I. Mendeleeva, **2008**. P. 9-13. (in Russian).
- [5] Sibileva S.V., Nefyodova N.V., Mikhailichenko A.I. Polucheniye nanorazmernogo promotirovannogo magnetita - prekursora katalizatora sinteza ammiaka. Khimicheskaya promyshlennost segodnya. **2011**. № 6. P. 14-20. (in Russian).
- [6] Tsareva S.Yu., Zharikov Ye.V., Anoshkin I.V., Kovalenko A.N. Obrazovaniye uglerodnykh nanotrubok pri kataliticheskom pirolize uglevodorodov s zhelezosoderzhashim katalizatorom. Izvestiya vuzov. Elektronika. **2003**. № 1. P. 20-24. (in Russian).
- [7] Mischenko S.V., Tkachev A.G. Uglerodnye nanomaterialy. Proizvodstvo, svoystva, pimeneniye. 2008. 320 p. (in Russian)
- [8] Khadzhiev S.N., Lyadov A.S., Krylova M.V. Sintez Fishera-Tropscha v trekhfaznoi sisteme s nanorazmernymi chastitsami zheleznoy katalizatora. Neftekhimiya. **2011**. V. 51. № 1. P. 25-32. (in Russian).
- [9] Sai P., Jong W.B., Ki-Won J. Fischer-Tropsch Synthesis by Carbon Dioxide Hydrogenation on Fe-Based Catalysts. Catalysis Surveys from Asia. **2008**. V.12. № 3. P.170-183. (<https://doi.org/10.1007/s10563-008-9049-1>).
- [10] Sharypov V.I., Kuznetsov P.N., Krichko A.A., Yulin M.K., Boldyrev V.V., Beregovtsova N.G. Patent RF 2036950 or 09.06.1995. (in Russian).

- [11] Khatmullina D.D. Katalizatory reforminga. Molodoi uchenyi. **2014.** № 1. P. 136-138. (in Russian).
12. Kobotayeva N.S., Skorohodova T.S., Sirotkina Ye.Ye. Ispolzovaniye oksidirovannogo zheleza v kachestve katalizatora oksileniya uglevodorodov. Neftepererabotka i neftekhimiya. **2010.** № 2. P. 18-23. (in Russian).
- [13] Radchenko Ye.D., Nefyodov B.K., Aliyev R.R. Promyshlennye katalizatory gidrogenizatsionnykh processov neftepererabotki. M.: Khimiya. **1987.** 224 p. (in Russian).
- [14] Ramanovskii B.V. Osnovy kataliza. M.: Binom. **2014.** 175 p. (in Russian).
- [15] Shirai T., Watanabe H., Fuji M., Takahashi M. Structural Properties and Surface Characteristics on Aluminum Oxide Powders. Annual report of the Ceramics Research Laboratory, Nagoya Institute of Technology. 2009. V.9. P.23-31.
- [16] Samaina L., Jaworski A., Edén M., Ladd D.M., Seo D.K., Garcia-Garcia F.J., Häussermann U. Structural analysis of highly porous γ -Al₂O₃. *Journal of Solid State Chemistry*. **2014.** V.217. P.1-8. (<https://doi.org/10.1016/j.jssc.2014.05.004>).
- [17] Stails E.B. Nositeli i nanesennyye katalizatory. Teoriya i praktika. M.: Khimiya. **1991.** 230 p.
- [18] Zakumbayeva G.D., Brodskiy A.R., Zhumbekova A.K., Gazizova A.D., Yaskevich V.I., Komashko L.V. Vliyanie molibdena na svoystva zhelezo-platinovykh nanesennykh katalizatorov. Izvestiya NAN RK, seriya khimicheskaya. **2006.** № 5. P. 11-16. (<https://doi.org/10.32014/2018.2518-1726>) (in Russian).
- [19] Bukhtiyarova G.A., Martyanov O.N., Yakushin S.S., Shuvayeva M.A., Baiukov O.A. Sostoyaniye zheleza v nanochastitsah, poluchennykh metodom propitki silikagelya i oksida aliuminiya rastvorom FeSO₄. Fizika tverdogo tela. **2010,** V.52, P. 771-781.(in Russian).
- [20] Brooks J.S. Thorpe S. A Method for the Study of the Surface Corrosion Beneath Protective Layers. Hyperfine Interaction. **1989.** V.47. P.159-178. (<https://doi.org/10.1007/BF02351606>).
- [21] Shipilin A.M., Zakharova I.N., Bachurin V.I. Messbauyevovskie isledovaniya chastits magnetita issledovaniy. Zh. Poverhnost, Rentgenovskiy, Sinhotronnyy i neitronnyy isledovaniya. **2014.** №6. P. 45-50. (in Russian).

**А.Р. Бродский, В.П. Григорьева, Л.В. Комашко, Е.Е. Нурмаканов,
И.С. Чанышева, А.А. Шаповалов, И.А. Шлыгина, В.И. Яскевич**

«Д.В. Сокольский атындағы Жанармай, Катализ және электрохимия институты» АҚ, Алматы, Қазақстан

МОЛЕКУЛА ЗОНДЫ БАР Fe/ γ -Al₂O₃ КАТАЛИЗДІК ЖҮЙЕНІҢ ӨЗАРА ӘРЕКЕТТЕСТІГІ I. γ -Al₂O₃ ЖӘНЕ Fe/ γ -Al₂O₃ БАСТАПҚЫ ЖҮЙЕНІҢ ЗЕРТТЕЛУІ

Бұл жұмыс адсорбцияланған молекулаға ие гетерогенді катализдік жүйенің өзара әрекеттестігіне арналған зерттеудің бірінші бөлігі болып табылады. Оған бастапқы γ -Al₂O₃ тотығы және 0,5; 3; 13 вес.% темір мөлшері бар Fe/ γ -Al₂O₃ жүйесі бойынша кең ауқымды физика-химиялық әдістер жиынтығы көмегімен алынған нәтижелер ұсынылған. Көптеген химиялық процестерде катализдік белсенділік көрсетіп, келешекте модельдік ретінде қолдану мүмкіндігі болғандықтан Fe/ γ -Al₂O₃ жүйесі зерттеу нысаны болып таңдалған болатын.

Жүргізілген жұмыс сіңіру әдісімен Fe/ γ -Al₂O₃ жүйесін дайындау процесінде тасығыш құрылымының модификациясы мүмкін екендігін көрсетті. Темірқұрамды фазамен тасығыш бетінің толтырылу сипаты айтарлықтай оның пайыздық мөлшеріне тәуелді және көп қабатты болуы мүмкін.

Fe/ γ -Al₂O₃ жүйесі Fe³⁺ формалы темір құрайтындығы анықталды. Темірдің мөлшеріне байланысты оған әртүрлі пішіндегі, яғни парамагнитті және магнит тәртіпті күйдегі темірқұрамды агрегаттар қатысуы мүмкін.

УДК 539.19;541.128.13;544.14;544.46

**А.Р. Бродский, В.П. Григорьева, Л.В. Комашко, Е.Е. Нурмаканов,
И.С. Чанышева, А.А. Шаповалов, И.А. Шлыгина, В.И. Яскевич**

АО «Институт топлива, катализа и электрохимии им. Д.В.Сокольского», Алматы, Казахстан

ВЗАИМОДЕЙСТВИЕ КАТАЛИТИЧЕСКОЙ СИСТЕМЫ Fe/ γ -Al₂O₃ С МОЛЕКУЛАМИ-ЗОНДАМИ I. ИССЛЕДОВАНИЕ γ -Al₂O₃ И ИСХОДНОЙ СИСТЕМЫ Fe/ γ -Al₂O₃

Аннотация. Работа является первой частью исследований, посвящённых взаимодействию гетерогенной каталитической системы с адсорбированными молекулами. В ней представлены результаты по исходному

оксиду $\gamma\text{-Al}_2\text{O}_3$ и системе $\text{Fe}/\gamma\text{-Al}_2\text{O}_3$ с содержанием железа 0,5; 3; 13 вес.%, полученные с помощью широкого набора физико-химических методов. Система $\text{Fe}/\gamma\text{-Al}_2\text{O}_3$ была выбрана объектом исследования, поскольку она проявляет каталитическую активность во многих химических процессах и в дальнейшем может быть использована как модельная.

Проведённая работа показала, что в процессе приготовления системы $\text{Fe}/\gamma\text{-Al}_2\text{O}_3$ методом пропитки возможна модификация структуры носителя. Характер заполнения поверхности носителя железосодержащей фазой существенно зависит от её процентного содержания и может быть многослойным.

Установлено, что система $\text{Fe}/\gamma\text{-Al}_2\text{O}_3$ содержит железо в форме Fe^{3+} . В зависимости от содержания железа, в ней могут присутствовать железосодержащие агрегаты различного размера, как в парамагнитном, так и в магнитоупорядоченном состояниях.

Ключевые слова: гетерогенный катализ, физико-химические методы исследования.

Information about authors:

Brodsky Alexander Rafaelevich-Ph. D., Assoc. Professor, head of the laboratory. Institute of fuel, catalysis and electrochemistry. D. In Sokolsky, Almaty. albrod@list.ru, <https://orcid.org/0000-0001-6216-4738>;

Grigorieva Valentina Petrovna - researcher, Institute of fuel, catalysis and electrochemistry. D. In Sokolsky, Almaty. grig1944@inbox.ru, <https://orcid.org/0000-0002-1807-8530>;

Komashko Larisa Vladimirovna - researcher, Institute of fuel, catalysis and electrochemistry. D. In Sokolsky, Almaty. komashko535@mail.ru, <https://orcid.org/0000-0003-0031-2816>;

Nurmakhanov Aslambekovich Yerzhan – PhD, senior researcher, Institute of fuel, catalysis and electrochemistry. D. In Sokolsky, Almaty. yerzhan.nurmakanov@gmail.com, <https://orcid.org/0000-0002-0404-1833>;

Irina S. Chanyшева - researcher, Institute of fuel, catalysis and electrochemistry. D. In Sokolsky, Almaty. chanyшева37@mail.ru, <https://orcid.org/0000-0002-7286-6036>;

Anatoly Shapovalov-Ph. D., Assoc. Professor, senior researcher, Institute of fuel, catalysis and electrochemistry. D. In Sokolsky, Almaty. shapov1937@mail.ru, <https://orcid.org/0000-0003-0386-5838>;

Slugina Irina artyomovna – Ph. D., leading researcher, Institute of fuel, catalysis and electrochemistry. D. In Sokolsky, Almaty. iashlygina@mail.ru, <https://orcid.org/0000-0002-0883-1007>;

Yaskevich Vladimir Ivanovich - researcher, Institute of fuel, catalysis and electrochemistry. D. In Sokolsky, Almaty. yaskevich46@mail.ru, <https://orcid.org/0000-0001-9342-8337>

NEWS

OF THE NATIONAL ACADEMY OF SCIENCES OF THE REPUBLIC OF KAZAKHSTAN

SERIES CHEMISTRY AND TECHNOLOGY

ISSN 2224-5286

<https://doi.org/10.32014/2018.2518-1491.34>

Volume 6, Number 432 (2018), 120 – 129

UDC 539.19;541.128.13;544.14;544.46

A.R. Brodskiy, V.P. Grigor'eva, L.V. Komashko, Y.Y. Nurmakanov,
I.S. Chanysheva, A.A. Shapovalov, I.A. Shlygina, V.I. Yaskevich

“D.V. Sokolsky Institute of Fuel, Catalysis and Electrochemistry” JSC, Almaty, Kazakhstan

albrod@list.ru

INTERACTION OF THE CATALYTIC Fe/ γ -Al₂O₃ SYSTEM WITH PROBE MOLECULES II. STUDY OF γ -Al₂O₃ SUPPORT AND Fe/ γ -Al₂O₃ SYSTEM AFTER INTERACTION WITH HYDROGEN AND AMMONIA

Abstract. In this work, studies of the Fe/ γ -Al₂O₃ system after its interaction with hydrogen and ammonia using X-ray diffractometry, electron microscopy (transmission and scanning), BET on low-temperature nitrogen adsorption and Mössbauer spectroscopy were carried out. The obtained results showed that the Fe/ γ -Al₂O₃ system is multiphase.

It contains aluminum and iron oxide, hydroxide phases. In addition, the iron-containing components can be partially reduced to Fe²⁺ and be in two forms, differing in their location relative to the surface.

It was established that in the process of interaction with hydrogen and ammonia, there is a specific surface excursion of the system and its texture. The nature of these changes depends on both the percentage iron phase, and the reagent nature, hydrogen or ammonia.

Key words: heterogeneous catalysis, physicochemical research methods, adsorbed molecules.

Introduction

A unified theory of the selection of catalysts does not currently exist. Many abundantly used catalysts are selected empirically. Theoretical ideas about the catalysis mechanism determine the principles of creating catalysts suitable for individual types of reactions, both in homogeneous and heterogeneous conditions, and / or associated with the type of catalyst (metallic; oxide; metals deposited on an oxide substrate; metals associated with polymeric molecules and others).

The catalytic activity [1 - 6] is determined through various catalyst characteristics: the number of d-electrons per cation orbital (for simple oxides); lattice parameter; electrical conductivity; ion charge and radius; chemical bond energy; acidity; assembly effect (which is determined by the catalyst atoms number which one molecule of the reactant interacts); for structures that can be regarded as periodic, by the energy spectrum nature and the Fermi level position in it, as well as by the periodic localization of particles chemisorbed on the surface and participating in the reaction, affecting the energy spectrum.

In heterogeneous catalysis, the most important stage is adsorption (chemisorption) [1, 4]. When constructing the corresponding models, it is necessary to study the surface state — its structure, adsorption complexes formed by active surface centers and reagent molecules. The active center can combine the adsorption and catalytic centers, for heterogeneous catalysts, they, as a rule, coincide.

The catalyst may contain more than one type of active centers, which allows it to participate in several chemical reactions in parallel. At the same time, a systematic study of various centers on the crystal surfaces of metal-coated oxides, active in the adsorption of various probe molecules, was not carried out.

From this, it follows the relevance of an experimental study of the gases interaction (adsorption) with a heterogeneous catalytic system. This work is a continuation [7] of the Fe/ γ -Al₂O₃ catalytic system study with adsorbed molecules and is devoted to the study of the γ -Al₂O₃ support and the Fe/ γ -Al₂O₃ system after interaction with hydrogen and ammonia.

As noted in [7], the choice of the Fe/ γ -Al₂O₃ system as a model is due to its actual multifunctionality, since it exhibits catalytic activity in many chemical processes [1, 3, 8 - 16].

Experimental

The Fe/ γ -Al₂O₃ system with different iron contents was prepared similarly to [7] by the impregnation method [1, 6, 17] of the starting γ -Al₂O₃ oxide with an aqueous iron acetate solution, followed by drying and calcination in air. The interaction of γ -Al₂O₃ oxide and the Fe/ γ -Al₂O₃ system with hydrogen and ammonia was carried out at 500 °C.

Due to the difficulty of detecting iron-containing phases in the system with 0.5 weight. %, iron (0.5% Fe/ γ -Al₂O₃), due to its low content [7], studies were mainly conducted on systems 3%Fe/ γ -Al₂O₃ and 13%Fe/ γ -Al₂O₃.

During the research, the same set of physicochemical methods was used as in [7].

X-ray diffractometry. The device X-ray diffractometer Dron-4-07. Cobalt anode tube.

Mode:

- speed 2 deg/min;

- working parameters of the tube: 30 kV, 20 mA

Transmission electron microscopy. The device is an EM 125K, accelerating voltage of 75 kV.

Scanning electron microscopy. Equipment is a scanning low-vacuum electron microscope JSM 6610 LV, JEOL, Japan. Accelerating voltage of 20 kV.

BET method (low-temperature nitrogen adsorption). Equipment is AccuSorb, Micromeritics, USA. Standard technique. Calcination of the sample at 230 - 250 °C for 3 hours with vacuum. The relative error in determining the specific surface area is $\pm 5\%$.

Mössbauer spectroscopy. Equipment - MS 1104Em, Russia. The source was cobalt 57 in the chromium matrix, with an activity of 100 mCi. The spectra were processed on a PC using the "least squares" method. The isomeric shifts values are given relative to α -Fe. The spectra were taken in air at a temperature of 23 °C. Shooting mode - "on the light." The error in determining the isomeric shift (IS)

$\Delta IS = \pm 0,03$ mm / s; quadrupole splitting (QS) $\Delta QS = \pm 0,03$ mm/s; content ratio (S) $\Delta S = \pm 2\%$.

Results and Discussion

A study of γ -Al₂O₃ oxide and Fe/ γ -Al₂O₃ system after their interaction with hydrogen and ammonia was carried out.

X-ray diffractometry

From the obtained results after the interaction of γ -Al₂O₃ with hydrogen and ammonia, it follows that the oxide structure does not change and the obtained diffractograms coincide with the diffractogram of the original γ -Al₂O₃, which is given in [7].

In fig. 1 shows the diffraction patterns of the systems 3%Fe/ γ -Al₂O₃, 13%Fe/ γ -Al₂O₃ after their interaction with hydrogen and ammonia.

Processing of diffractograms gave the following results:

3%Fe/ γ -Al₂O₃ system

- after interaction with hydrogen

Reflexes 4.1817; 2.6971; 2.4503 Å - phase O(OH) (goethite) (ASTM 29 - 713)

Reflexes 4.5681; 2.8046; 2.3856; 2.2863; 1.9781; 1.5261; 1.3985 Å - γ -Al₂O₃ phase (ASTM 10-424);

Reflexes 4.8569; 4.3088; 2.4503; 2.3856; 1.9781 Å - gibbsite phase Al(OH)₃ (ASTM 33-18);

Reflexes 3.6768; 2.6971; 2.5154; 2.2863 Å - α -Fe₂O₃ phase (maghemite) (ASTM 33-664);

Reflexes; 2.5154; 2.4903; 2.1518; 1.5261 Å - FeO phase (wustite) (ASTM 6-615)

- after interaction with ammonia

Reflexes 4.1750; 2.6997,4449 Å - α -FeO(OH) phase (ASTM 29 - 713)

Reflexes 4.5641; 2.8090; 2.3754; 2.2910; 1.9788; 1.5261; 1.3985 Å - γ -Al₂O₃ phase (ASTM 10-424);

Reflexes 4.8569; 4.3158; 3.1854 2.4449; 2.3754; 1.9788 Å - Al(OH)₃ phase(ASTM 33-18);

Reflexes 3.6794; 2.6997; 2.5282; 2.2910 Å - α -Fe₂O₃ phase(ASTM 33-664);

Reflexes 2.4903; 2.1592; 1.5261 Å - FeO phase(ASTM 6-615)

13%Fe/ γ -Al₂O₃ system

- after interaction with hydrogen

Reflexes 4.1784; 2.7001; 2.4514 Å - α -FeO(OH) phase(ASM 29 - 713)

Reflexes 4.5602; 2.7988; 2.3754; 2.2986; 1.9863; 1.5280; 1.3982 Å - γ -Al₂O₃ phase(ASM 10-424);

Reflexes 4.8569; 4.3265; 2.4514; 2.3754; 1.9863 Å - Al(OH)₃ phase(ASM 33-18);

Reflexes 3.6615; 2.7001; 2.5178; 2.2986 Å - α -Fe₂O₃ phase(ASM 33-664);

reflexes: 2.5178; 2.1452; 1.5280 Å - FeO (ASM 6-615)

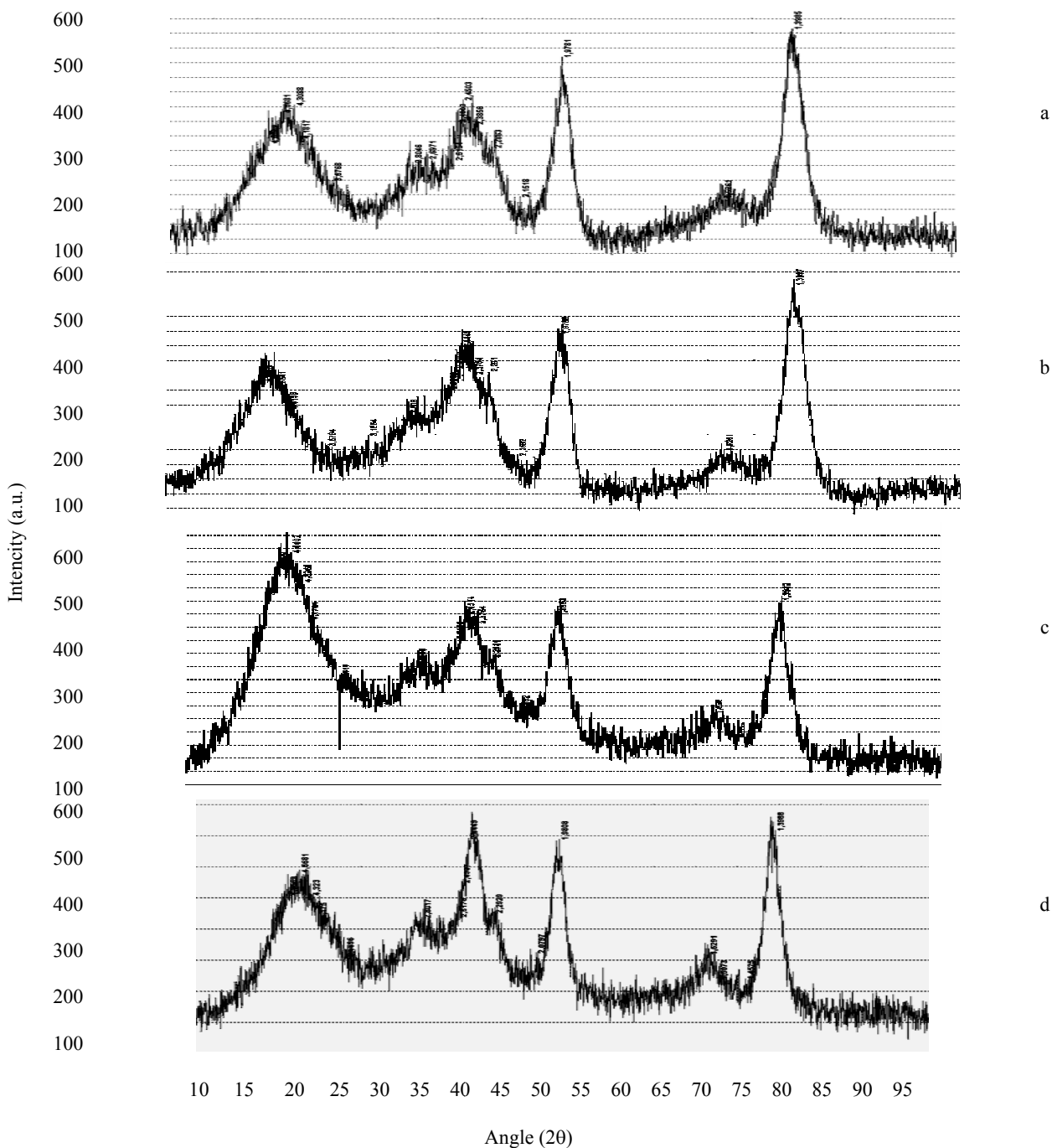


Figure 1 - Diffraction patterns of systems 3%Fe/ γ -Al₂O₃ and 13%Fe/ γ -Al₂O₃ after their interaction with hydrogen and ammonia a, b - 3%Fe/ γ -Al₂O₃ system; c, d 13%Fe/ γ -Al₂O₃ system; a, c - after interaction with hydrogen; b, d- after interaction with ammonia

Processing of diffractograms gave the following results:

3%Fe/ γ -Al₂O₃ system

- after interaction with ammonia

Reflexes 4.1750; 2.7001; 2.4514 Å - phase α -FeO(OH) phase (ASTM 29 - 713)

Reflexes 4.5681; 2.8017; 2.2929; 1.9808; 1.5291; 1.3988 Å - γ -Al₂O₃ phase (ASTM 10-424);

Reflexes 4.8569; 4.3230; 2.4449; 1.9808 Å - Al(OH)₃ phase (ASTM 33-18);

Reflexes 3.6896; 2.7101; 2.5178; 2.2929 Å - α -Fe₂O₃ phase (ASTM 33-664);

Reflexes: 2.5178; 2.4937; 2.0797; 1.5291; 1.5073; 1.4550 Å - phase mixture

FeO (ASTM 6-615) and Fe_{0,98}O (ASTM39-1088)

The obtained data show the presence of Fe/ γ -Al₂O₃ oxide γ -Al₂O₃, Al(OH)₃ hydroxide (gibbsite) and several iron-containing phases, including iron, reduced to the state of Fe²⁺ in the system.

Transmission electron microscopy

In fig. 2 shows micrographs of the Fe/ γ -Al₂O₃ system with different iron content after interaction with hydrogen and ammonia, obtained using transmission electron microscopy.

3%Fe/Al₂O₃ system

- after hydrogen interaction

In fig. 2a, (magnification of 24,000 times) aggregates of particles up to 10 nm in size, which are located at the edges of large, dense particles of micron size. Microdiffraction gives a set of symmetric and separate reflexes and can be attributed to γ -Al₂O₃ (JCPDS, 10-425).

In fig. 2b (magnification of 50,000 times) a large particle of the plate type is shown, on which seals from 5 to 40 nm are observed. Microdiffraction shows a set of symmetric, separate intense and weak reflections, which can be attributed to a mixture of phases of aluminum oxides with a predominance of γ -Al₂O₃ (JCPDS, 10-425) and iron hydroxides α -FeO (OH) - getit (JCPDS, 29-713), Fe (OH)₂ (JCPDS, 13-89).

In fig. 2c (magnification of 50,000 times), the edges of the aggregates composed of their fine, dense particles 5 to 10 nm in size. Microdiffraction gives a small set of weak diffuse rings, which can be attributed to a mixture of phases Al (OH)₃ - gibbsite (JCPDS, 7-324) and Fe₂O₃ (JCPDS, 32-469).

- after ammonia interaction

In fig. 2d (magnification of 24,000 times) is an aggregate of translucent particles ranging in size from 150 to 300 nm. Microdiffraction gives symmetrical reflexes, which can be attributed to the phase of FeO - wustite (JCPDS, 6-615).

In fig. 2e (magnification of 24,000 times), a dense aggregate is shown, with translucent particles ranging in size from 150 to 200 nm along its edge. Microdiffraction shows symmetrical reflexes that can respond to Fe₂O₃ (JCPDS, 32-469).

In fig. 2f there is a small aggregate, on the edge of which there are semitransparent particles with a size of 20-40 nm. Microdiffraction gives symmetric reflections, they can be attributed to a mixture of phases γ -Al₂O₃ (JCPDS, 10-425), Al (OH)₃ (JCPDS, 7-324).

13% Fe/Al₂O₃ system

- after hydrogen interaction

In fig. 2g (magnification of 24,000 times) aggregate of large particles ranging in size from 70 to 200 nm. Microdiffraction shows a large set of reflections and can be attributed to the mixture of phases of hydroxides Fe (OH)₂ (JCPDS, 13-89) and α -FeO (OH) (JCPDS, 29-713).

In fig. 2h (magnification of 24,000 times) is an aggregate of large dense particles ranging in size from 70 to 500 nm and translucent rectangular crystals, reaching 150 to 200 nm in diameter. Microdiffraction gives a large set of reflexes. They can be attributed to the mixture of phases FeOOH (JCPDS, 26-792), γ -FeO (OH) (JCPDS, 8-98), Fe₂O₃ (JCPDS, 32-469), α -FeO (OH) (JCPDS, 29-713).

- after ammonia interaction

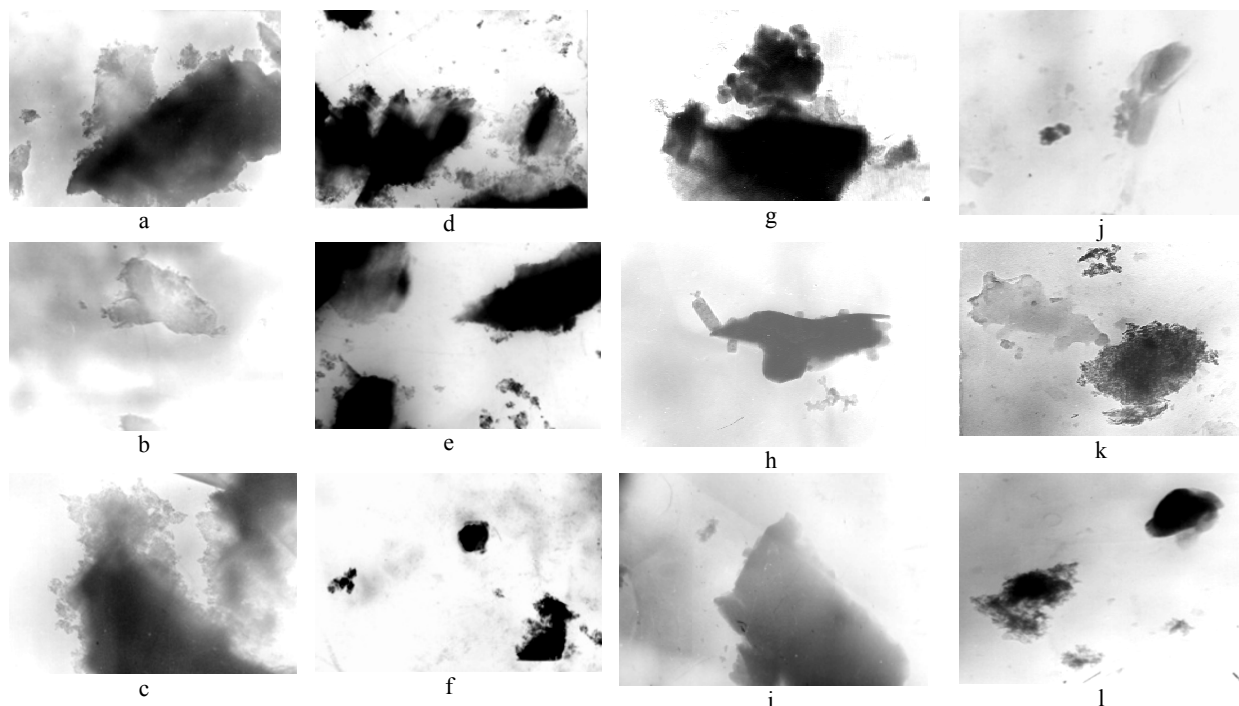


Figure 2 - Micrographs of the Fe/ γ -Al₂O₃ system with different iron content after interaction with hydrogen and ammonia
(a, b, c, d, e, f) - 3%Fe/Al₂O₃; (g, h, i, j, k, l) - 13%Fe/Al₂O₃;
(a, b, c, g, h, i) - after hydrogen interaction; (d, e, f, g, h, i) - after ammonia interaction

In fig. 2i (magnification of 50,000 times) a small aggregate of dense particles 40–60 nm in size is shown. Microdiffraction gives a small set of reflexes that can be attributed to Fe₂O₃ (JCPDS, 32-469).

In fig. 2j (an increase of 24,000 times) an aggregate of translucent particles of plate-like type with a size of 100–200 nm and small aggregates with a size of up to 10 nm. Microdiffraction gives a large set of reflections that can be attributed to a mixture of phases Fe(OH)₂ (JCPDS, 13-89), δ -FeOOH (JCPDS, 13-87), Al(OH)₃ (JCPDS, 29-41) and FeO (JCPDS, 6-615)

In fig. 2k aggregate of particles with a size of 70 - 100 nm. Microdiffraction shows a large set of reflections that can be attributed to a mixture of Fe₂O₃ (JCPDS, 32-469), γ -FeO (OH) (JCPDS, 8-98), Al(OH)₃ (JCPDS, 7-324), γ -Al₂O₃ (JCPDS, 10-425).

Thus, the results obtained using transmission electron microscopy in diffraction mode show that the system Fe/Al₂O₃, after interaction with hydrogen and ammonia, has a complex composition. It contains oxide and hydroxide phases of aluminum, as well as iron, including phases containing Fe²⁺. This result is in good agreement with the X-ray diffractometry data.

Scanning electron microscopy

In fig. 3 shows micrographs of the Fe/ γ -Al₂O₃ system with different iron contents after interaction with hydrogen and ammonia, obtained using scanning electron microscopy.

A comparison of the microphotographs of the initial Fe/ γ -Al₂O₃ system [7] with the microphotographs in fig. 3 shows that after interaction with hydrogen and ammonia, the surface relief of the system becomes smoother, with the most significant in the case of ammonia, which is especially noticeable for 3%Fe/ γ -Al₂O₃. Perhaps this effect is associated with the formation of some surface compounds, with the result that the iron-containing component is more evenly distributed over the support surface.

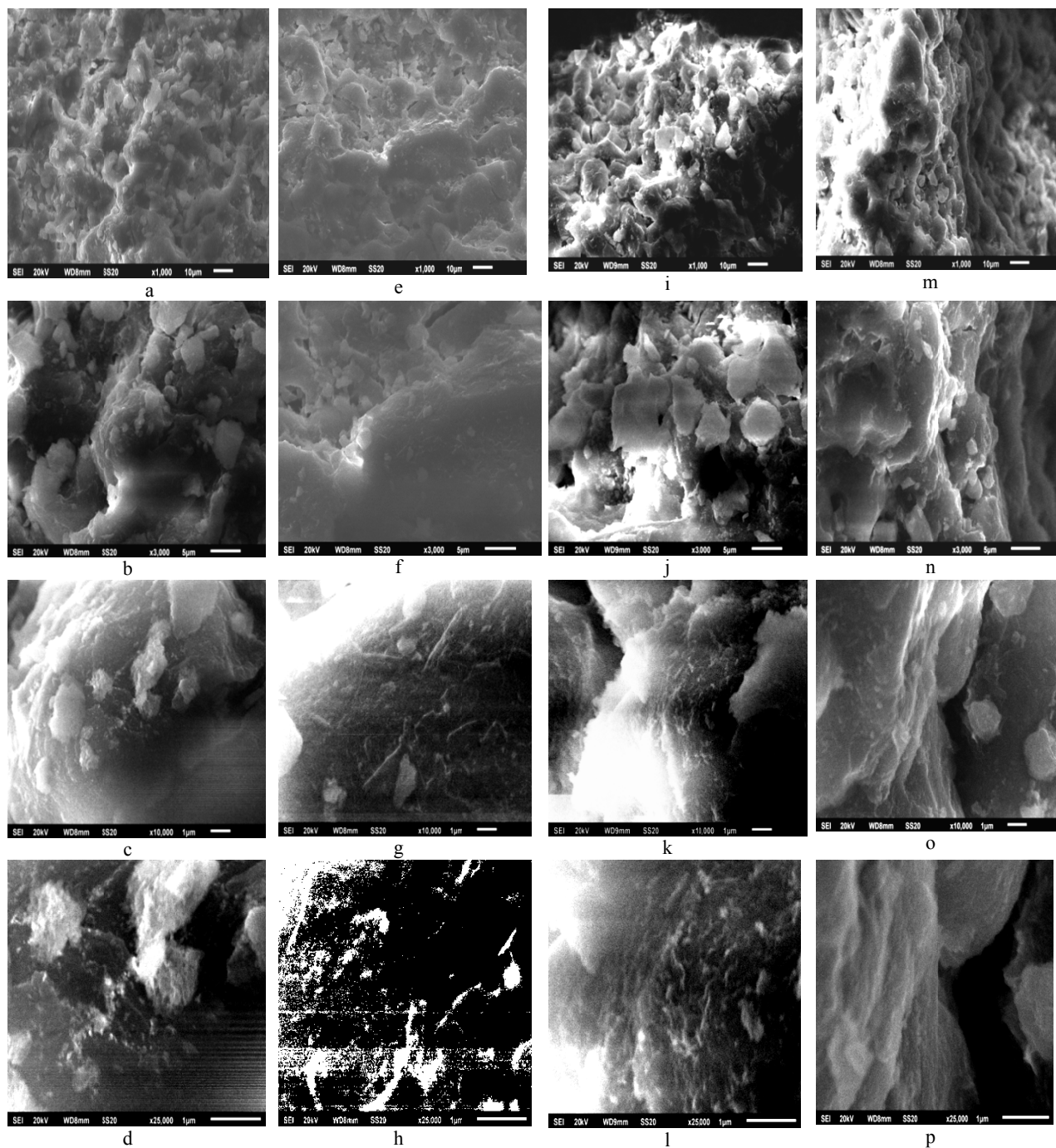


Figure 3 - Microphotographs of the system $\text{Fe}/\gamma\text{-Al}_2\text{O}_3$, obtained using scanning electron microscopy, with different iron content after hydrogen and ammonia interaction (a, b, c, d, e, f, g, h) - 3% $\text{Fe}/\text{Al}_2\text{O}_3$; (i, j, k, l, m, n, o, p) - 13% $\text{Fe}/\text{Al}_2\text{O}_3$; (a, b, c, d, i, j, k, l) - after hydrogen interaction; (d, f, g, h, m, n, o, p) - after ammonia interaction; magnification: (a, e, i, m) - 1000 times; (b, f, j, n) - 3000 times; (c, g, k, o) - 10000 times; (d, h, l, p) - 25000 times

BET method

The specific surface area and its texture (porosity) for the $\text{Fe}/\gamma\text{-Al}_2\text{O}_3$ system with different iron content after interaction with hydrogen and ammonia are determined. The results are shown in table 1 and shown in figure 4.

Table 1 - The specific surface of the Fe/ γ -Al₂O₃ system after hydrogen and ammonia interaction

Sample	Parameter		
	SW, m ² /g	V _{ADSmax} , mL/g	V _{true} , mL/g
γ -Al ₂ O ₃ *	214	180	0,28
γ -Al ₂ O ₃ - hydrogen interaction	168	236	0,37
γ -Al ₂ O ₃ - ammonia interaction	171	249	0,39
0,5%Fe/ γ -Al ₂ O ₃ *	211	196	0,31
0,5%Fe/ γ -Al ₂ O ₃ - hydrogen interaction	202	253	0,39
0,5%Fe/ γ -Al ₂ O ₃ - ammonia interaction	209	268	0,42
3%Fe/ γ -Al ₂ O ₃ *	190	115	0,18
3%Fe/ γ -Al ₂ O ₃ - hydrogen interaction	186	225	0,35
3%Fe/ γ -Al ₂ O ₃ - ammonia interaction	188	233	0,36
13%Fe/ γ -Al ₂ O ₃ *	173	101	0,16
13%Fe/ γ -Al ₂ O ₃ - - hydrogen interaction	158	189	0,29
13%Fe/ γ -Al ₂ O ₃ - ammonia interaction	139	194	0,39

Note: SW - specific surface area, m² / g;
V_{ADSmax} - total pore volume with gas filling, mL / g;
V_{true} - total true pore volume, mL / g
* - data from work [7]

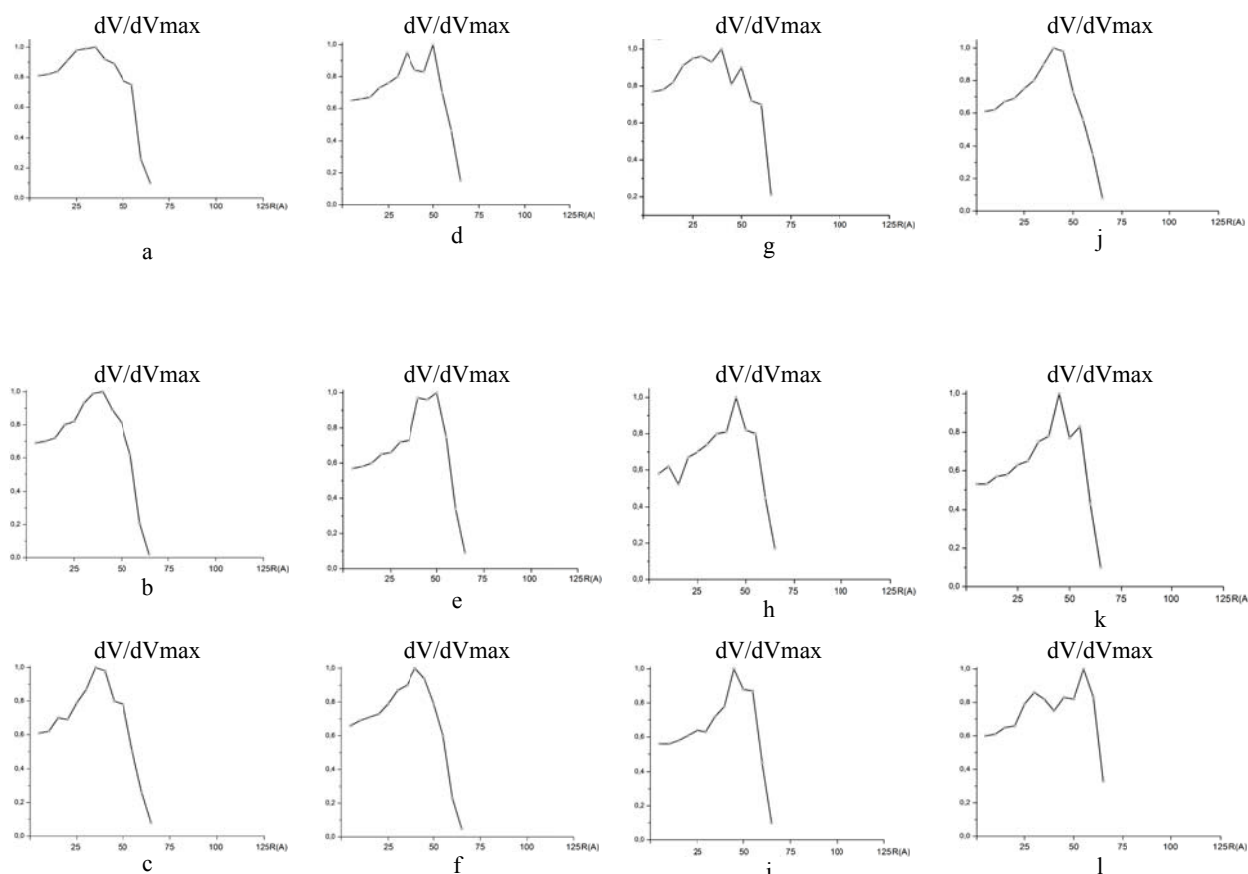


Figure 4 - The distribution of pore sizes in γ -Al₂O₃ and in Fe/ γ -Al₂O₃ after hydrogen and ammonia interaction (a*, b, c) - γ -Al₂O₃; (d*, e, f) - 0,5%Fe/ γ -Al₂O₃; (g*, h, i) - 3%Fe/ γ -Al₂O₃; (j*, k, l) - 13%Fe/ γ -Al₂O₃; (a, b, g, j) – initial states; (b, e, g, k) – after hydrogen interaction; (c, f, i, l) – after ammonia interaction; * - data from work [7]; R(A) – pore radius in angstroms (Å); dV/dVmax the ratio of the pore volume of a given radius to the maximum volume

From the results of table 1, it follows that the interaction of the γ - Al_2O_3 oxide, of the $\text{Fe}/\gamma\text{-Al}_2\text{O}_3$ system with hydrogen and ammonia leads to a decrease in the specific surface area and an increase in the total pore volume. It should be noted that it is possible there is a tendency for a larger increase in the value of the total pore volume in the case of interaction with ammonia.

The data presented in fig. 4 shows that the interaction of $\gamma\text{-Al}_2\text{O}_3$ oxide of the $\text{Fe}/\gamma\text{-Al}_2\text{O}_3$ system with hydrogen and ammonia leads to a change in the size distribution of the pores. For oxide $\gamma\text{-Al}_2\text{O}_3$, the relative content of pores with a diameter of up to 25 Å decreases (fig. 4 (a, b, c)).

In the case of a 00,5% $\text{Fe}/\gamma\text{-Al}_2\text{O}_3$ system, the relative content of pores with a diameter in the range of 27–40 Å decreases and there is an extremum in the graphs in the range of 40–50 Å (fig. 4 (d, e, f)). The situation is similar for 3% $\text{Fe}/\gamma\text{-Al}_2\text{O}_3$, but with the formation of a “sharp” maximum at a distribution in the region of ~ 45 Å (fig. 4 (f, h, i)). In the case of a system of 13% Al_2O_3 during its interaction with hydrogen, a “sharp” maximum is also observed at ~ 45 Å. When interacting with ammonia, the relative intensity of this maximum decreases and the other two appear with a center of distribution at ~ 28 –30 and 55 Å (fig. 4 (k, l, m)).

Mössbauer spectroscopy

In fig. 5 shows the Mössbauer spectra of the 3% $\text{Fe}/\gamma\text{-Al}_2\text{O}_3$ system after hydrogen and ammonia interaction.

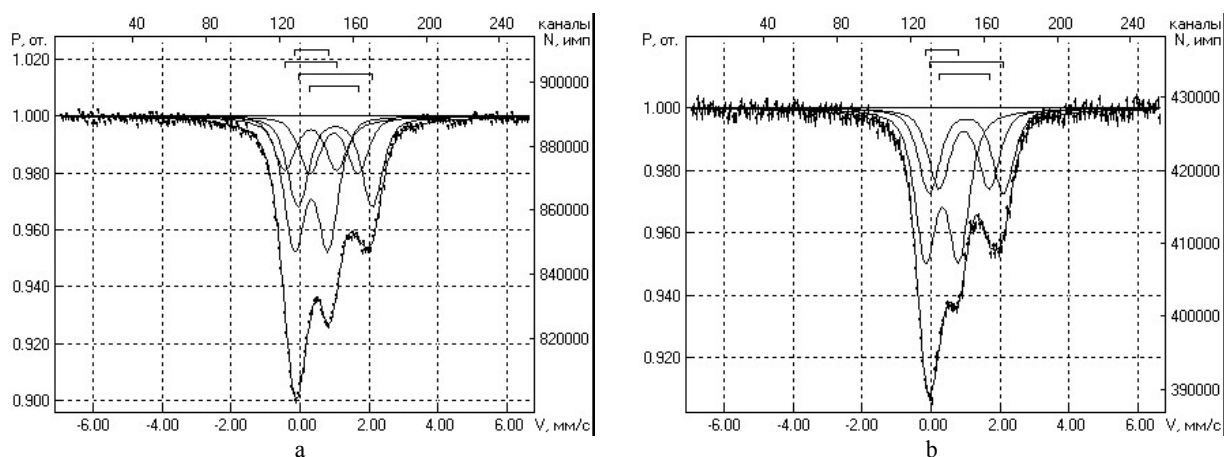


Figure 5 - Mössbauer spectra of the system 3% $\text{Fe}/\gamma\text{-Al}_2\text{O}_3$ after interaction with hydrogen (a) and ammonia (b)

The processing of the spectra showed that the system, based on the values of the Mössbauer parameters, contains various forms of Fe^{3+} and Fe^{2+} in the paramagnetic state [18].

The following iron forms are present in the 3% $\text{Fe}/\gamma\text{-Al}_2\text{O}_3$ system:

- after interaction with hydrogen

Fe_1^{3+} form - IS = 0,33 $\text{mm}\cdot\text{s}^{-1}$; QS = 0,97 $\text{mm}\cdot\text{s}^{-1}$; S = 39%

Fe_2^{3+} form - IS = 0,32 $\text{mm}\cdot\text{s}^{-1}$; QS = 1,51 $\text{mm}\cdot\text{s}^{-1}$; S = 16%

Form

Fe_1^{2+} form - IS = 1,02 $\text{mm}\cdot\text{s}^{-1}$; QS = 2,15 $\text{mm}\cdot\text{s}^{-1}$; S = 28%

Fe_2^{2+} form - IS = 0,98 $\text{mm}\cdot\text{s}^{-1}$; QS = 1,40 $\text{mm}\cdot\text{s}^{-1}$; S = 17%

- after ammonia interaction

Fe_1^{3+} form - IS = 0,32 $\text{mm}\cdot\text{s}^{-1}$; QS = 0,96 $\text{mm}\cdot\text{s}^{-1}$; S = 47%

Fe_1^{2+} form - IS = 1,02 $\text{mm}\cdot\text{s}^{-1}$; QS = 2,15 $\text{mm}\cdot\text{s}^{-1}$; S = 27%

Fe_2^{2+} form - IS = 0,95 $\text{mm}\cdot\text{s}^{-1}$; QS = 1,46 $\text{mm}\cdot\text{s}^{-1}$; S = 26%

The forms Fe_1^{3+} and Fe_2^{3+} after the interaction of the system with hydrogen have almost identical IS values, at the same time, they differ significantly in QS. In [7], based on the data of [19-21], the form Fe_2^{3+} with a large QS value was attributed to iron on the support surface, and the form Fe_1^{3+} with a smaller QS to the more deeply located one. It should be noted that after interaction with ammonia, only one form of Fe_1^{3+} is present in the system.

The corresponding reduced forms of iron (Fe_1^{2+} and Fe_2^{2+}), after interaction with hydrogen and ammonia, have close Mössbauer parameters. It should be noted that in the case of ammonia, the total relative content of the forms of Fe_2^{2+} in the system is noticeably higher, in addition, there is no form of Fe_2^{3+} , which, presumably, is located closer to the surface, and therefore must be restored first. Regarding the forms Fe_1^{2+} and Fe_2^{2+} , it can be assumed that each of them has a corresponding form of Fe^{3+} as its predecessor.

Conclusion

Studies of $\text{Fe}/\gamma\text{-Al}_2\text{O}_3$ system after its hydrogen and ammonia interaction using X-ray diffractometry, electron microscopy (transmission and scanning), BET on low-temperature nitrogen adsorption, and Mössbauer spectroscopy were carried out. The results showed that the system $\text{Fe}/\gamma\text{-Al}_2\text{O}_3$ is multiphase. It contains oxide, hydroxide phases of aluminum and iron. In addition, the iron-containing components can be partially reduced to Fe^{2+} and can be in two forms, differing by their location relative to the surface.

It was established that in the process of interaction with hydrogen and ammonia, there is a change in the value of the specific surface of the system and its texture. The nature of these changes depends on both the percentage of the iron-containing phase and the nature of the reagent, hydrogen or ammonia.

Acknowledgements

The work was supported by the Ministry of Education and Science of the Republic of Kazakhstan (AP05130654).

REFERENCES

- [1] Kryilov O.V. Geterogennyiy kataliz. M. IKTs «Akademkniga». **2004**. P. 663. ISBN 5-946281-41-0. (in Russian)
- [2] Geterogennyiy kataliz Boreskov G.K. Izdatelstvo: Nauka. **1986**. 305 p. (in Russian).
- [3] Balandin A.A. Multiplernaya teoriya kataliza. M.: Izd-vo MGU, ch. I, **1963**; ch. II, 1964; ch. III, 1970. (in Russian)
- [4] Goncharuk V.V., Kamalov G.L., Kovtun G.A., Rudakov E.S., Yatsimirskiy V.K. Kataliz: mehanizmyi gomogennoy i geterogennoy kataliza, klasternyye podhodyi. Kiev, Naukova Dumka. **2002**. 543 p. (in Russian).
- [5] Volkenshteyn F.F. Elektronnyie protsessy na poverhnosti poluprovodnikov pri hemosorbtsii M.: Nauka. Gl. red. fiz.-mat. lit. **1987**. 432 p. (in Russian).
- [6] Ramanovskiy B.V. Osnovy kataliza. M.: Binom. **2014**. 175 p. (in Russian).
- [7] Brodskiy A.R., Grigor'eva V.P., Komashko L.V., Nurmakanov Y.Y., Chanysheva I.S., Shapovalov A.A., Shlygina I.A., Yasevich V.I. Vzaimodejstvie kataliticheskoy sistemy $\text{Fe}/\gamma\text{-Al}_2\text{O}_3$ s molekulami-zondami. I. Issledovanie $\gamma\text{-Al}_2\text{O}_3$ i iskhodnoj sistemy $\text{Fe}/\gamma\text{-Al}_2\text{O}_3$. Izvestiya NAN RK, seriya himii i tekhnologii. **2018**. № 6 (in press). (<https://doi.org/10.32014/2018.2518-1726>) (in Russian).
- [8] Semenov V.P. Proizvodstvo ammiaka. M. Himiya. **1985**. 368 p. (in Russ.).
- [9] Sibileva S.V., Nefedova N.V. Razrabotka metoda prigotovleniya osazhdennyih zheleznyih katalizatorov sinteza ammiaka. Uspehi v himii i himicheskoy tekhnologii: sb. nauchn. trudov. T.22, № 10 (90). M., RHTU im. D.I.Mendeleeva. **2008**. P. 9-13. (in Russian).
- [10] Sibileva S.V., Nefedova N.V., Mihaylichenko A.I. Poluchenie nanorazmernogo promotirovannogo magnetita – prekursora katalizatora sinteza ammiaka. Himicheskaya promyshlennost segodnya. **2011**. № 6. P. 14-20. (in Russian).
- [11] Tsareva S.Yu., Zharikov E.V., Anoshkin I.V., Kovalenko A.N. Obrazovanie uglerodnyih nanotrubok pri kataliticheskom pirolize uglevodorodov s zhelezosoderzhaschim katalizatorom. Izvestiya vuzov. Elektronika. **2003**. № 1. P. 20-24. ISBN 978-5-94275-407-5. (in Russian).
- [12] Mischenko S.V., Tkachev A.G. Uglerodnyie nanomaterialyi. Proizvodstvo, svoystva, primenenie. M.: Mashinostroenie. **2008**. 320 p. (in Russian).
- [13] Hadzhiev S.N., Lyadov A.S., Kryilova M.V. Sintez Fishera-Tropscha v trehfaznoy sisteme s nanorazmernymi chastitsami zheleznoy katalizatora. Neftehimiya. **2011**. V. 51. № 1. P. 25-32. (in Russian).
- [14] Sai P., Jong W.B., Ki-Won J. Fischer-Tropsch Synthesis by Carbon Dioxide Hydrogenation on Fe-Based Catalysts. Catalysis Surveys from Asia. **2008**. V.12. № 3. P. 170-183. DOI 10.1007/s10563-008-9049-1.
- [15] Sharyipov V.I., Kuznetsov P.N., Krichko A.A., Yulin M.K., Boldyrev V.V., Beregovtsova N.G. Patent RF 2036950 ot 09.06.1995. (in Russian).
- [16] Hatmullina D.D. Katalizatoryi riforminga. Molodoy uchenyy. **2014**. № 1. P. 136-138. (in Russian).
- [17] Radchenko E.D., NefYodov B.K., Aliev R.R. Promyshlennyye katalizatoryi gidrogenizatsionnyih protsessov neftepererabotki. M.: Himiya. **1987**. 224 p. (in Russian).
- [18] Suzdalev I.P. Dinamicheskie efektyi v gamma-rezonansnoy spektroskopii. M.: Atomizdat. **1979**. 192 p. (in Russian)
- [19] Bukhtiyarova G.A., Martyanov O.N., Yakushin S.S., Shuvayeva M.A., Baiukov O.A. Sostoyanie zheleza v nanochastitsah, poluchennyh metodom propitki silikagelya i oksida aliuminiya rastvorom FeSO_4 . Fizika tverdogo tela. **2010**. V.52. P. 771-781. (in Russian).
- [20] Brooks J.S., Thorpe S. A Method for the Study of the Surface Corrosion Beneath Protective Layers. Hyperfine Interaction. **1989**. V.47. P.159-178. doi:10.1007/bf02351606.
- [21] Shipilin A.M., Zaharova I.N., Bachurin V.I. Messbauerovskie issledovaniya chastits magnetita. Zh. Poverhnost, Rentgenovskie, Sinhrotronnyie i neytronnyie issledovaniya. **2014**. № 6. P. 45-50. (in Russian).

**А.Р. Бродский, В.П. Григорьева, Л.В. Комашко, Е.Е. Нурмаканов,
И.С. Чанышева, А.А. Шаповалов, И.А. Шлыгина, В.И. Яскевич**

«Д.В. Сокольский атындағы Жанармай, Катализ және электрохимия институты» АҚ, Алматы, Қазақстан

**МОЛЕКУЛА ЗОНДЫ БАР $Fe/\gamma-Al_2O_3$ КАТАЛИЗДІК ЖҮЙЕНІҢ ӘРЕКЕТТЕСТІГІ
II. СУТЕГІ МЕН АММИАКПЕН ӘРЕКЕТТЕСУІНЕН KEЙІНГІ $\gamma-Al_2O_3$ ТАСУШЫ МЕН $Fe/\gamma-Al_2O_3$
ЖҮЙЕНІҢ ЗЕРТТЕУІ**

Аннотация. Бұл жұмыста $Fe/\gamma-Al_2O_3$ жүйенің оның сутегі мен аммиакпен әрекеттесуінен кейінгі рентгендік дифрактометрия, электронды микроскопия (жарықтық және сканерлеуші), төменгі температуралы азоттың адсорбциясы арқылы БЭТ пен мессбауэрлік спектроскопия әдістерінің зерттеулері көрсетілген. Алынған нәтижелер $Fe/\gamma-Al_2O_3$ жүйенің көпфазалы екенін анықтады. Бұл фаза алюминий мен темірдің оксидті, гидроксидті фазасынан тұрады. Одан басқа, темірқұрамды компоненттер Fe^{2+} дейін жартылай тотықсызданады және беттік қабатының орналасуының айырмашылығымен екі түрде орналасуы мүмкін.

Сутегі мен аммиакпен әрекеттесуі кезінде жүйенің және оның текстурасының меншікті бет шамасының өзгеруі болатыны анықталды. Бұл өзгерістердің ерекшелігі темірқұрамды фазаның пайыздық құрамы мен реагент табиғатына да – сутегі мен аммиак тәуелді.

Түйін сөздер: гетерогенді катализ, зерттеудің физикалық-химиялық әдістері, адсорбталған молекулалар

УДК 539.19;541.128.13;544.14;544.46

**А.Р. Бродский, В.П. Григорьева, Л.В. Комашко, Е.Е. Нурмаканов,
И.С. Чанышева, А.А. Шаповалов, И.А. Шлыгина, В.И. Яскевич**

АО «Институт топлива, катализа и электрохимии им. Д.В.Сокольского», Алматы, Казахстан

**ВЗАИМОДЕЙСТВИЕ КАТАЛИТИЧЕСКОЙ СИСТЕМЫ $Fe/\gamma-Al_2O_3$
С МОЛЕКУЛАМИ-ЗОНДАМИ II. ИССЛЕДОВАНИЕ НОСИТЕЛЯ $\gamma-Al_2O_3$
И СИСТЕМЫ $Fe/\gamma-Al_2O_3$ ПОСЛЕ ВЗАИМОДЕЙСТВИЯ С ВОДОРОДОМ И АММИАКОМ**

Аннотация. В работе проведены исследования системы $Fe/\gamma-Al_2O_3$ после её взаимодействия с водородом и аммиаком методами рентгеновской дифрактометрии, электронной микроскопии (просвечивающей и сканирующей), БЭТ по низкотемпературной адсорбции азота и мессбауэровской спектроскопии. Полученные результаты показали, что система $Fe/\gamma-Al_2O_3$ является многофазной. Она содержит оксидные, гидроксидные фазы алюминия и железа. Кроме того, железосодержащие компоненты могут частично восстанавливаться до Fe^{2+} и находиться в двух формах, различаясь расположением относительно поверхности.

Установлено, что в процессе взаимодействия с водородом и аммиаком, происходит изменение величины удельной поверхности системы и её текстуры. Характер этих изменений зависит как от процентного содержания железосодержащей фазы, так и от природы реагента - водорода или аммиака.

Ключевые слова: гетерогенный катализ, физико-химические методы исследования, адсорбированные молекулы

Information about authors:

Brodsky Alexander Rafaelevich-Ph. D., Assoc. Professor, head of the laboratory. Institute of fuel, catalysis and electrochemistry. D. In Sokolsky, Almaty. albrod@list.ru;

Grigorieva Valentina Petrovna - researcher. Institute of fuel, catalysis and electrochemistry. D. In Sokolsky, Almaty. grig1944@inbox.ru;

Komashko L. V. – researcher. Institute of fuel, catalysis and electrochemistry. D. In Sokolsky, Almaty. komashko535@mail.ru;

Nurmakanov Aslambekovich Yerzhan – PhD, senior researcher. Institute of fuel, catalysis and electrochemistry. D. In Sokolsky, Almaty. yerzhan.nurmakanov@gmail.com;

Chanysheva Irina Sergeevna-researcher. Institute of fuel, catalysis and electrochemistry. D. In Sokolsky, Almaty. chanysheva37@mail.ru;

Anatoly Shapovalov-Ph. D., Assoc. Professor, senior researcher. Institute of fuel, catalysis and electrochemistry. D. In Sokolsky, Almaty. shapov1937@mail.ru;

Slugina Irina artyomovna – Ph. D., leading researcher. Institute of fuel, catalysis and electrochemistry. D. In Sokolsky, Almaty. iashlygina@mail.ru;

Yaskevich Vladimir Ivanovich - researcher. Institute of fuel, catalysis and electrochemistry. D. In Sokolsky, Almaty. yaskevich46@mail.ru

NEWS

OF THE NATIONAL ACADEMY OF SCIENCES OF THE REPUBLIC OF KAZAKHSTAN

SERIES CHEMISTRY AND TECHNOLOGY

ISSN 2224-5286

<https://doi.org/10.32014/2018.2518-1491.35>

Volume 6, Number 432 (2018), 130 – 137

UDC 541.13:546.19

M.M. Dospaev¹, A. Bayeshov², A.S. Zhumakanova²,
D.M. Dospaev³, B.B. Syzdykova¹, K.S. Kakenov⁴, G.A. Esenbaeva⁴

¹ Chemical and Metallurgical Institute named after Zh. Abishev, Karagandy, Kazakhstan;

² Sokolsky Institute of Fuel, Catalysis and Electrochemistry, Almaty, Kazakhstan;

³ Karaganda State Technical University, Karagandy, Kazakhstan;

⁴ Karaganda Economic University of Kazpotreboyz, Karagandy, Kazakhstan

E-mail: manten.mur@mail.ru, elhimproc@mail.ru

MECHANISM OF FORMING NANODISPERSE COPPER SILICATE POWDER DURING ANODIC POLARIZATION OF COPPER ELECTRODE IN POTASSIUM SILICATE SOLUTION

Abstract. The main advantage of the known electrochemical methods is the possibility of obtaining powders with a smaller particle size, which eliminates the additional stage of its processing, i.e. regrinding. The works aimed at obtaining nanodimensional powders of copper oxide compounds that are widely used in the production of antibacterial materials, solar batteries, gas sensors, photovoltaic cells, in semiconductor technology, as well as a catalyst for the oxygen electrode of a fuel cell with a solid electrolyte, are now of ever-greater interest.

In this paper by the method of voltammetry there has been for the first time studied the mechanism of forming copper silicate powder nanoparticles during anodic polarization of a copper electrode in a slightly alkaline solution of potassium silicate. Based on the results obtained, using the method of mathematical planning of the experiment, there has been studied the effect of the current density, the concentration of potassium silicate, the temperature of the electrolyte, the duration of electrolysis on the current yield of the nanosized copper silicate powder. The optimal parameters of electrolysis in galvanostatic conditions have been determined. The chemical analytical method has established the compliance of the electrolysis-produced copper silicate with the formula $\text{CuSiO}_3 \cdot 3.8\text{H}_2\text{O}$. There have been performed the electronic microscopic studies of the synthesized copper silicate powder and the particle sizes have been determined in the region of 50 nm.

Key words: nanoparticle, silicate copper powder, potassium silicate, voltammetry, electrolysis, electronic microscopy.

Introduction. The unique properties of oxidized copper compounds due to the presence of a developed surface are widely used in a lot of branches of engineering and production [1]. Of ever-greater interest are the works aimed at obtaining powders of copper oxide compounds that are widely used in the production of antibacterial materials, solar batteries, gas sensors, photovoltaic cells, semiconductor technology, as well as a catalyst for the oxygen electrode of a fuel cell with a solid electrolyte.

There is no information of obtaining pure copper silicate in literature, only various reference data on the chemical methods of synthesizing other silicate compounds are encountered. For example, the authors of Ref. [2] describe the Cu/SiO_2 -catalysts that contain slaty copper silicate, it has been shown that owing to forming highly disperse copper phyllosilicates, these compounds are effective catalysts for converting ethanol to ethyl acetate. Similarly to [2], the authors of [3] describe the good catalytic activity of the Cu/SiO_2 -catalyst due to the presence of finely dispersed copper slaty silicate. The difference between the works [2] and [3] is that the Cu/SiO_2 -catalyst was obtained by the sol-gel method. However, in [4], although the Cu/SiO_2 -catalyst is also obtained and its structural properties are studied, good catalytic properties are attributed to the presence of copper nanoparticles in the silica gel.

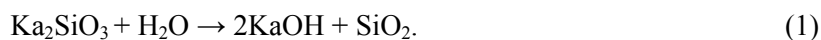
Electrode reactions, in particular anodic copper oxidation processes in silicic acid solutions, are practically unexplored areas in electrochemistry of copper. Our research tasks include studying the anodic behavior of copper in the solution of potassium silicate and identifying the possibility of synthesizing the nanosized copper silicate powder.

Experiment methodology. Voltammetric studies have been carried out by the method of taking polarization curves in the solution of potassium silicate. Polarization curves have been taken using a clamping electrode of special design [5]. In contrast to the known electrodes, the advantage of the clamping electrode design is the ability to polarize powders due to the direct contact with the electroconductive surface of the electrode. The anode curves have been plotted using a copper electrode at the temperatures of 20-800 °C, the potential sweep rate of 10 mV / s, and the electrolyte concentration of 0.6-7.5 g/l.

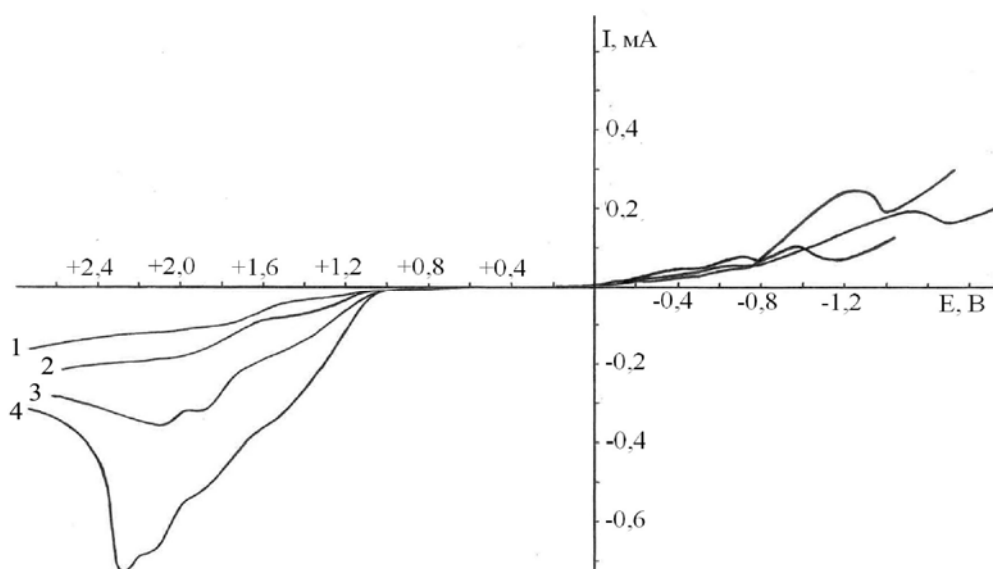
The electrolysis has been performed in a 300 ml thermostated electrolyzer, the electrodes have been made of cathodic copper. To prepare the electrolyte, distilled water and potassium silicate reagent (K_2SiO_3) have been used. The method of multifactorial mathematical planning of the experiment has been used to study the possibility of obtaining a nanosized copper silicate powder by electrolysis in galvanostatic conditions. The effect of the current density, the potassium silicic acid concentrations, the electrolyte temperature and the duration of electrolysis has been studied. The duration of the experiments has been 15-240 minutes. The precipitate formed by nanosized copper silicate formed during electrolysis has been subjected to washing with distilled water, filtration and dried in a special chamber. The obtained product has been studied by chemical and electronic microscopic methods of analyzing.

Discussing results. The electrode reactions, in particular anodic copper oxidation processes in silicic acid solutions, are practically unexplored areas in electrochemistry of copper. The tasks of our researchers have included studying the anodic behavior of copper in the solution of potassium silicate and revealing the possibility of synthesizing the nanosized copper silicate powder.

It is known [6] that when dissolved in water, potassium silicate is hydrolyzed and its solution has an alkaline reaction:



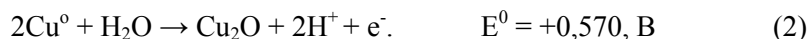
On the anodic polarization curve of the copper electrode (Figure 1) there are observed two waves.



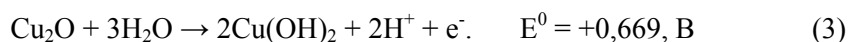
1- 0.5; 2 - 1.0; 3 - 2.5; 4 - 5.0 g/l, $t = 25^\circ C$

Figure 1 – Cyclic anodic-cathodic polarization curve of the copper electrode in potassium silicate solutions

The first weakly manifested wave corresponds to the process of forming cuprous copper oxide:



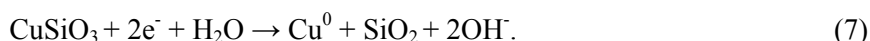
The second wave corresponds to the process of the active transition of cuprous copper oxide into copper hydroxide:



Copper hydroxide formed [7] reacts with potassium silicate and forms a new phase, i.e. copper silicate:



On cathodic voltammetric curves there are observed three waves that probably correspond to the following reactions:



Based on the above-mentioned electrochemical studies, the present work has shown for the first time the possibility of obtaining a nanosized copper silicate powder by the electrolytic method [8].

In a sequential study of the factors, the effect of the current density, the concentration of potassium silicate, the temperature and the duration of electrolysis on the current yield of the nanosized copper silicate powder has been studied by the method of mathematical planning of the experiment [9]. Point dependences have been constructed for the current yield of a nanosized copper silicate powder (Figure 2). The approximating function has been selected taking into account the physical meaning of the dependence being studied.

The adequacy of the private dependences for the current yield of a nanosized copper silicate powder and pH changing in the solution has been determined from the correlation coefficient R and its relevance t_R .

The essence of the processes that occur during electrolysis is that when passing direct current through the solution of potassium metasilicate (K_2SiO_3) on copper electrodes there take place the following processes:

- on the cathode there released hydrogen:

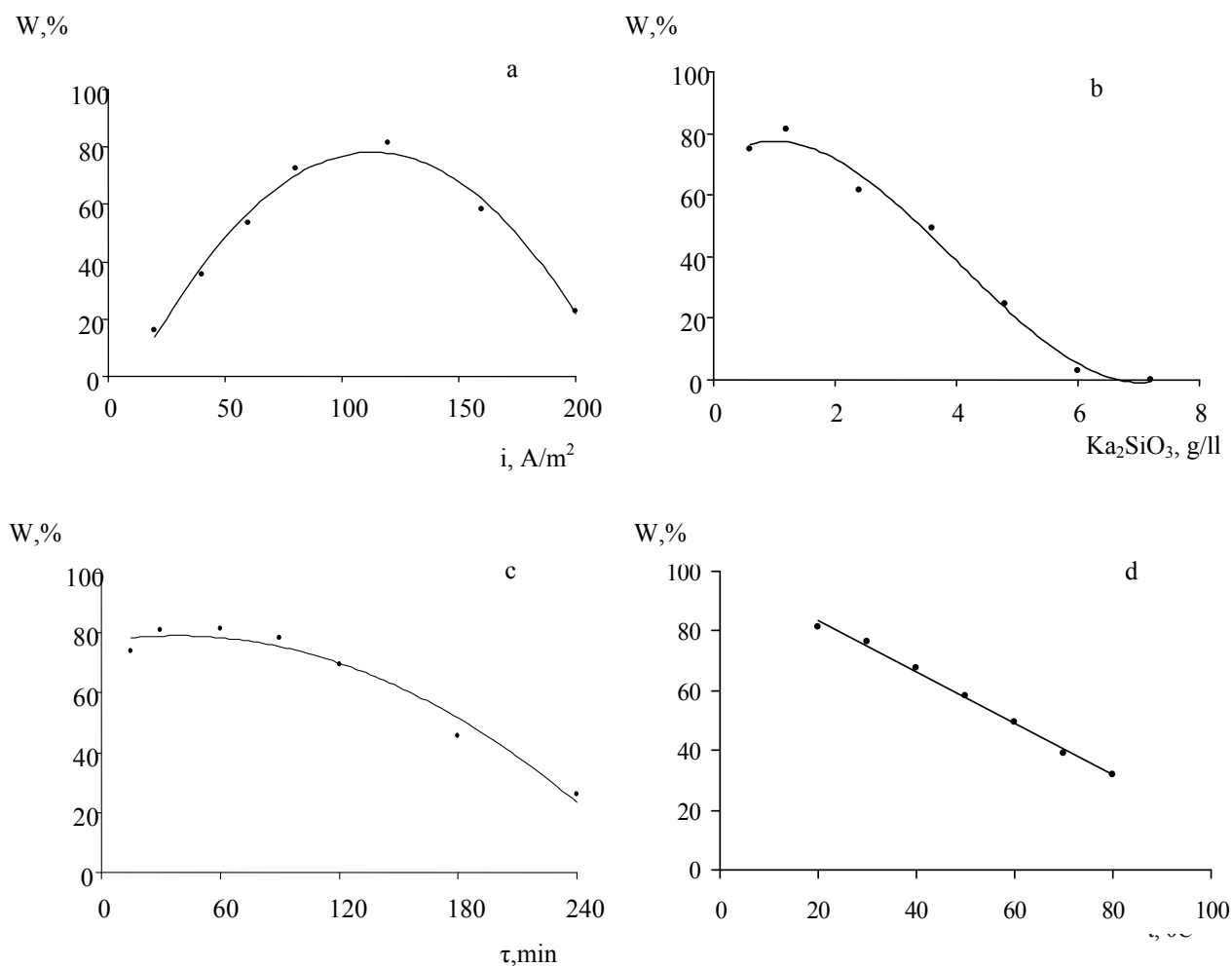


- on the anode there is observed copper electrode dissolution according reactions (2, 3).

Copper hydroxide formed by reaction (3) reacts with the potassium silicate present in the solution and forms by reaction (4) copper silicate of bright blue color.

From the experimental data (Figure 2) it is seen that with gradual increasing the current density in the range of 20-120 A/m², the current yield increases from 16.2 to 81.5 %, respectively.

Increasing the current density above 120 A/m² leads to significant decreasing the current yield of a nanosized copper silicate powder [10].



a – current density; b – potassium silicate concentration; c – electrolysis duration; d – temperature points: experimental data; line – approximating function

Figure 2 – the effect of preset factors on the current yield of the copper silicate nanosized powder

The initial concentration of potassium silicate has a significant effect on the current yield of the synthesized product. The nanosized copper silicate powder is formed only at strict concentration limits from 0 to 6 g/l. The maximum value of the current yield of 81.5 % is reached even at the concentration of potassium silicate of 1.2 g/l (Figure 2, b) [12]. Increasing the concentration of the latter above 6 g/l leads to a sharp cessation of copper silicate formation, the current yield in this case is reduced to zero.

With increasing the temperature in the range of 20–80 °C the current yield of the nanosized copper silicate powder gradually decreases [13].

With increasing the duration of electrolysis (Figure 2, c) in the range of 15-60 minutes, the current yield of the nanosized copper silicate powder reaches the maximum value of 81.5 %. Further increasing the duration leads to decreasing the current yield [14].

Decreasing the current yield of the nanosized copper silicate powder with increasing the current density, the concentration of potassium metasilicate, the temperature of the solution and the duration of electrolysis is higher than their optimal values due to the simultaneous increasing the solution pH for the above parameters (Figure 2,a).

Due to pH increasing in the solution, a competitive reaction occurs to form copper (II) oxide on the surface of the copper anode, which leads to passivation of the electrode and contamination of the resulting product [11]:



It follows that in order to ensure purity and to achieve relatively high current yield results of the nanosized copper silicate powder, the optimal pH of the potassium metasilicate solution in electrolysis should correspond to 10-11.

The adequacy of the private dependences for the current yield of the nanosized copper silicate powder has been determined from the correlation coefficient R and its relevance t_R (Table 1).

Table 1 – Coefficient of correlation R, its value t_R for private functions of the current yield of the nanosized copper silicate powder

Equation	R	Condition $t_R > 2$	Relevance
$y = -0,0075i^2 + 1,6873i - 17,253$	0.9891	101.8 > 2	relevant
$y = 0,7124C^3 - 8,5771C^2 + 14,946C + 70,455$	0.9944	199.1 > 2	relevant
$y = -0,0014\tau^2 + 0,1057\tau + 76,995$	0.9795	54.07 > 2	relevant
$y = -0,8629t + 100,74$	0.9316	14.10 > 2	relevant

The obtained equations for the current yield of the nanosized copper silicate powder taking into account relevant functions are generalized by the dependence in the form of their product [15, 16]:

$$BT = \frac{(-0,0075i^2 + 1,6873i - 17,253) \cdot (0,7124C^3 - 8,5771C^2 + 14,946C + 70,455)}{79,2203^3 \left[(-0,0014\tau^2 + 0,1057\tau + 76,995) \cdot (-0,8629t + 100,74) \right]^{-1}} \quad (10)$$

When comparing the results of the experiment and calculation, we find the values $R = 0.97$ and $t_R = 4279 > 2$, $R = 0.986$ and $t_R = 114,3 > 2$, which confirms the adequacy of describing the experimental data by equation (10), respectively. The confidence interval calculated through t_R [17] is 1.89 %.

Electron-microscopic studies of particles of a nanosized copper silicate powder on a transmission scanning electron microscope were performed. It is established that the particle size of the copper silicate powder synthesized by us lies in the region of 50 nm (Fig. 3).

There have been carried out electronic microscopic studies of the nanosized copper silicate powder particles on the transmission scanning electronic microscope. It has been established that the sized of the powder synthesized lies in the region of 50 nm (Figure 3).

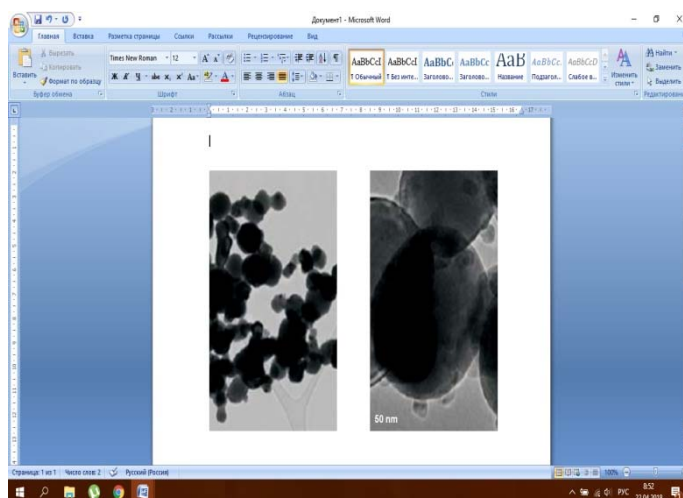


Figure 3 – Photomicrograph of copper silicate nanopowder on the transmission scanning electronic microscope

The chemical analysis of synthesized nanodisperse copper silicate has been carried out for copper and silica according to the well-known methods [18]. According to the results of the analysis, the copper content in the precipitate is 44.81 %, and silicon 20.13 %; when converted to copper silicate $\text{CuSiO}_3 \cdot n\text{H}_2\text{O}$ there has been established compliance with the formula $\text{CuSiO}_3 \cdot 3,8\text{H}_2\text{O}$.

Conclusions. It has been established that two waves are observed on the anodic polarization curve of the copper electrode in the solution of potassium silicate. The first weakly manifested wave is referred to the process of forming cuprous copper oxide, the second wave corresponds to the process of active transition of cuprous oxide to hydroxide that reacts with potassium silicate and forms a new phase, i.e. copper silicate.

Based on the carried out electrochemical studies, it has been shown for the first time that it is possible to obtain a nanosized copper silicate powder by electrolysis from the aqueous solution of potassium silicate. Using the method of mathematical planning of the experiment, the effect of the current density, the potassium silicate concentration, the solution temperature and the duration of electrolysis on the current yield of the nanosized copper silicate powder has been studied. The highest values of the current yield of the nanosized copper silicate powder have been achieved under the following conditions of electrolysis: the current density 120A/m^2 , the duration of electrolysis 60 min., $\text{pH}=11.0$, $t=20^\circ\text{C}$, the potassium silicate concentration 1.2 g/l, above 6 g/l leads to a sharp cessation of forming the nanoscale copper silicate powder.

The electronic microscopic method has been used to determine the particle sizes of the nanosized copper silicate powder synthesized that lie in the region of 50 nm.

REFERENCES

- [1] Dausheva MR, Songina OA (1973) Povedenie suspensii trudnorastvorimykh veshchestv na elektrodakh. *Uspekhi khimii*, 2:323-342. (In Russian).
- [2] Xue Yu, Shubo Zhai, Wanchun Zhu, Shuang Gao, Jianbiao Yan, and others. (2014) The direct transformation of ethanol to ethyl acetate over Cu/SiO_2 catalysts that contain copper phyllosilicate. *Journal of Chemical Sciences*. 126:4:1013–1020. DOI: 10.1007/s12039-014-0659-z (In Eng).
- [3] Liming He, Xiaochun Chen, Jingsheng Ma, Hailong He, Wei Wang (2010) Characterization and catalytic performance of sol-gel derived Cu/SiO_2 catalysts for hydrogenolysis of diethyl oxalate to ethylene glycol. *Journal of Sol-Gel Science and Technology*. 55:3:285–292. DOI: 10.1007/s10971-010-2247-0 (In Eng).
- [4] Tongmei Ding, Hengshui Tian, Bingqin Zhao. (2016) Synthesis of 1,3-propanediol through diethyl malonate hydrogenation on Cu/SiO_2 nanoparticles. *Reaction Kinetics, Mechanisms and Catalysis*. 118:2:497–508. DOI:10.1007/s11144-016-1008-7 (In Eng).
- [5] Baeshova AK, Baeshov A, Ugorets MZ, Buketov EA (1980) Katodnaia poliarizatsiia dispersnogo selena v rastvorakh gidrookisi natriia na tverdykh elektrodakh. *ZhPKh*. 53:2:2122-2125. (In Russian).
- [6] Brauer G (1956) Rukovodstvo po preparativnoi neorganicheskoi khimii. Leningrad, Izdatel'stvo Leningrad. (In Russian)
- [7] Naumov IuI, Molvina LI, Korolev GV (1979) *Elektrokhimii*. 15:4:597. (In Russian).
- [8] Dospaev MM, Lisova IV, Lu NIu (1998) Issledovanie fiziko-khimicheskikh zakonov obrazovaniia khrizokolly v kremnievokislykh rastvorakh. *Tez. dokl. Mezhd. nauchno-prakt. konf. «Kompleksnoe ispol'zovanie mineral'nykh resursov Kazakhstana»*. P. 221. (In Russian).
- [9] Dospaev MM, Lisova IV, Lu NIu (1998) Fiziko-khimicheskii metod sinteza khrizokolly iz rastvora kremnievokislogo natriia. *Sb. tr. Mezhd. nauchnoi konf. «Nauka i obrazovanie – vedushchii faktor strategii Kazakhstan-2030»*. P. 99-101. (In Russian).
- [10] Dospaev MM, Figurine IV, Baeshov A (2007) Elektrokhimicheskii metod polucheniia silikata medi. *Mezhd. konf. po khimii i khimicheskoi tekhnologii, posv. 50-letiiu osnovaniia Instituta Obshchei i Neorganicheskoi Khimii im. akademika NAN RA Manveliana M.G.* P. 215-216. (In Russian).
- [11] Miliutin NN (1978) Elektrokhimicheskoe povedenie medi v shchelochnykh rastvorakh. *ZhPKh*. 12:426-429. (In Russian).
- [12] Dospaev MM (2008) Obrazovanie silikata medi pri elektrokhimicheskoi poliarizatsii mednogo elektroda v rastvorakh metasilikata kaliia. *Vestnik KarGU, ser. khim.* 1:26-29. (In Russian).
- [13] Dospaev MM, Baeshova AK, Dospaev DM, Ivanskaia LA (2008) Mekhanizm elektroliticheskogo polucheniia kremnii soderzhashchikh soedinenii medi. *Tr. VI mezhd. Beremzhanovskogo s'ezda po khimii i khimicheskoi tekhnologii*. P. 103-106. (In Russian).
- [14] Dospaev MM, Baeshov A, Karimova LM, Dospaev DM (2009) Izuchenie vlianiia razlichnykh parametrov elektroliza na obrazovanie silikata medi. *Promyshlennost' Kazakhstana*. 4:584-86. (In Russian).

[15] Malyshev VP (1978) Matematicheskoe opisanie rezul'tatov mnogofaktornogo eksperimenta, provedennogo po metodu Zeidelia-Gaussa. *Vestnik AN Kaz SSR*. 4:31-38. (In Russian).

[16] Malyshev VP (2008) Kineticheskii i tekhnologicheskii analiz obobshchaiushchikh matematicheskikh modelei khimiko-metallurgicheskikh protsessov. Reports of the national academy of sciences of the republic of kazakhstan. 2:13-18. <https://doi.org/10.32014/2018.%202518-1483> (In Russian).

[17] Malyshev VP (2000) K opredeleniiu oshibki eksperimenta, adekvatnosti i doveritel'nogo intervala approksimiruiushchikh funktsii. *Bulletin NAS RK*. 4:22-30 <https://doi.org/10.32014/2018.2518-1467> (In Russian).

[18] Fainberg Slu (1958) Analiz mineral'nogo syr'ia. –Moskva, Goskhimizdat. (In Russian).

**М. М. Доспаев¹, А.Башов², А.С. Жумақанова²,
Д.М.Доспаев², Б.Б.Сыздыкова¹, К.С. Какенов³, Г.А.Есенбаева³**

¹Ж. Әбішев атындағы Химия-металлургия институты, Қарағанды, Қазақстан,

²Д.В. Сокольский атындағы Жанармай, катализ және электрохимия институты, Алматы, Қазақстан,

³Қарағанды мемлекеттік техникалық университеті, Қарағанды, Қазақстан,

⁴Қазтұтынуодағы Қарағанды экономикалық университет, Қарағанды, Қазақстан.

КАЛИЙ МЕТАСИЛИКАТЫ ЕРТІНДІСІНДЕ МЫС АНОДЫН ПОЛЯРИЗАЦИЯЛАУ КЕЗІНДЕГІ НАНОДИСПЕРСТІ МЫС СИЛИКАТЫ ҰНТАҒЫНЫҢ ТҮЗІЛУ МЕХАНИЗМІ

Аннотация. Белгілі электрохимиялық әдістердің негізгі артықшылығы төмен өлшемді ұнтақ бөлшектерін алу болып табылады, ол қосымша ұнтақтау кезеңін жояды. Қазіргі кезде наноөлшемді тотыққан мыс қоспаларын алуға бағытталған жұмыстар қызығушылық тудыруда, өйткені олар жартылай өткізгіш техникасында, фотогальваникалық ұяшықтарда, газдық сенсорларда, күн батареяларда және антибактериалдық материалдар өндірісінде кең қолданыс тапқан.

Бұл жұмыста вольтамперометрия әдісімен алғаш рет төмен сілтілі калий метасиликаты ертіндісінде мыс анодын поляризациялау кезінде мыс силикаты ұнтағы нанобөлшектерінің түзілу механизмі зерттелді. Алынған нәтижелер негізінде экспериментті математикалық жоспарлау әдісін пайдалана отырып наноөлшемді мыс силикаты ұнтағының шығымына тоқ тығыздығының, калий метасиликаты концентрациясының, электролит температурасының, электролиз ұзақтығының әсері зерттелді. Гальваностатикалық жағдайдағы электролиздің тиімді параметрлері анықталды. Химиялық анализ әдісімен электролиз арқылы алынған мыс силикатының $\text{CuSiO}_3 \cdot 3,8\text{H}_2\text{O}$ формуласына сәйкестегі дәлелденді. Синтезделген мыс силикаты ұнтағына электронды микроскопиялық зерттеулер жүргізілді және оның бөлшектерінің өлшемі анықталды, олар 50нм өлшем аймағында.

Түйін сөздер: нанобөлшек, мыс силикаты ұнтағы, калий метасиликаты, вольтамперометрия, электролиз, электрондық микроскопия.

**М. М. Доспаев¹, А.Башов², А.С. Жумақанова²,
Д.М.Доспаев³, Б.Б.Сыздыкова¹, К.С. Какенов⁴, Г.А.Есенбаева⁴**

¹Химико-металлургический институт им. Ж.Абишева, Караганда, Казахстан;

²Институт топлива, катализа и электрохимии им. Д.В.Сокольского, Алматы, Казахстан;

³Карагандинский государственный технический университет, Караганда, Казахстан;

⁴Карагандинский экономический университет казпотребсоюза, Караганда, Казахстан

МЕХАНИЗМ ОБРАЗОВАНИЯ НАНОДИСПЕРСНОГО ПОРОШКА СИЛИКАТА МЕДИ В РАСТВОРЕ МЕТАСИЛИКАТА КАЛИЯ

Аннотация. Основным преимуществом известных электрохимических методов является возможность получения порошков с меньшим размером частиц, что исключает дополнительную стадию его обработки – доизмельчение. Все больший интерес вызывают работы направленные на получение наноразмерных порошков оксидных соединений меди, которые находят широкое применение в производстве антибактериальных материалов, солнечных батарей, газовых сенсоров, фотогальванических ячеек, а также в технике полупроводников в качестве катализатора для кислородного электрода топливного элемента с твердым электролитом.

В данной работе методом вольтамперометрии впервые исследован механизм образования наночастиц порошка силиката меди при анодной поляризации медного электрода в слабощелочном растворе метасиликата калия. На основании полученных результатов с использованием метода математического планирования эксперимента изучено влияние плотности тока, концентрации метасиликата калия, температуры электролита, продолжительности электролиза на выход по току наноразмерного порошка силиката меди. Определены оптимальные параметры электролиза в гальваностатических условиях. Химическим методом анализа установлено соответствие полученного электролизом силиката меди формуле $\text{CuSiO}_3 \cdot 3,8\text{H}_2\text{O}$. Проведены электронно-микроскопические исследования синтезированного порошка силиката меди и определены размеры его частиц, которые лежат в области 50 нм.

Ключевые слова: наночастица, порошок силиката меди, метасиликат калия, вольтамперометрия, электролиз, электронная микроскопия.

Information of the authors:

Dospaev M.M. - Doctor of Engineering, Head of the Laboratory of Electrochemical Processes of the Chemistry and Metallurgical Institute named after Zh.Abishev, manten.mur@mail.ru. ORCID ID: 0000-0001-9602-8099

Bayeshov A. - academic NAS RK, Doctor of Chemistry, Sokolsky Institute of Fuel, Catalysis and Electrochemistry, bayeshov@mail.ru. ORCID ID: 0000-0003-0745-039X;

Zhumakanova A.S. - Candidate of Technical Sciences, Sokolsky Institute of Fuel, Catalysis and Electrochemistry, zhumakanova62@mail.ru. ORCID ID: 0000-0003-4983-4199;

Dospaev D.M. - Master of Engineering, Leading Engineer of the International Material Science Center of Karaganda State Technical University, dospaev_dar@mail.ru. ORCID ID: 0000-0002-8276-093X;

Syzdykova B.B. – Master of Engineering, junior researcher of the Chemical and Metallurgical Institute named after Zh.Abishev, syzdykova.b@gmail.com. ORCID ID: 0000-0003-4497-6366;

Kakenov K.S. - Candidate of Technical Sciences, Head of the Certification and Standardization of Consumer Goods Department of Karaganda Economic University of Kazpotrebsoyuz, sattu55@mail.ru. ORCID ID: 0000-0003-2314-4595;

Esenbaeva G.A. - Doctor of Education, senior lecturer of the Certification and Standardization of Consumer Goods Department of Karaganda Economic University of Kazpotrebsoyuz, esenbaeva_keu@mail.ru. ORCID ID: 0000-0002-1561-0026

NEWS

OF THE NATIONAL ACADEMY OF SCIENCES OF THE REPUBLIC OF KAZAKHSTAN

SERIES CHEMISTRY AND TECHNOLOGY

ISSN 2224-5286

<https://doi.org/10.32014/2018.2518-1491.36>

Volume 6, Number 432 (2018), 138 – 149

UDC 621.43:532.582.7

MRNTI 55.42.01

**K.S. Nadirov, G.V. Cherkaev, E.A. Chikhonadskikh,
N.A. Makkaveeva, A.S. Sadyrbaeva, G.E. Orymbetova**

^{1,5,6}M.Auezov South-Kazakhstan State University, Shymkent, Kazakhstan;

²⁻⁴St. Petersburg State Marine Technical University, St. Petersburg, Russia

**ANALYSIS OF INFLUENCE OF EMISSIONS OF HARMFUL
SUBSTANCES WITH EXHAUST GASES OF MARINE DUAL FUEL
INTERNAL COMBUSTION ENGINE ON THE ENVIRONMENT AND
HUMAN HEALTH**

Abstract. Due to the low cost of gas and the expediency of its use for power generation, especially in the areas of its production, as well as on ships-gas carriers, a number of engine companies began to upgrade their engines to adapt them to work on gas fuel. Modernization goes on in two directions: on transfer of the diesel to work on Otto cycle with use of carburetors and spark plugs similar to the carburettor gasoline engine and preservation of the diesel cycle with injection of a small amount of diesel fuel for ignition of a mixture of gas and fuel. In the case of necessity is not excluded by the operation of the engine only on diesel fuels – dual fuel engines. The purpose of the work is to study the use of two-fuel internal combustion engines on ships and formed suspended particles during its combustion. The relevance of the topic lies in the fact that most ships use as fuel oil, gasoline and diesel fuel, which adversely affects human health and the environment, especially marine. Therefore, the solution to this situation was the introduction of two-fuel internal combustion engines, which at times reduce emissions from ships to the marine and air environment.

Key words: emissions of harmful substances, exhaust gases of marine internal combustion engines, environment, public health, liquefied natural gas, atmospheric diffusion calculation models.

Introduction

The level of air pollution largely depends on the conditions of dispersion of impurities in atmosphere. Under certain meteorological conditions, the concentration of impurities in air increases, and can reach dangerous values. Prevention of such cases on the basis of their advance forecast is essential for improving state of the air basin.

The main and auxiliary engines of power plants are the main source of marine pollution of environmental pollution. The most common are diesel engines. Diesel engines have the highest fuel economy (their efficiency exceeds 50%); Stable operate on various types of gaseous and liquid fuels, including heavy with a viscosity of 700 cSt (the value of viscosity measurement) and sulfur content of 5%; best suited to automation, ensuring unobstructed management and maintenance. They have a significant resource and always ready for operation.

The exhaust gases (EG) of marine diesel engines are complex gas mixture. Their composition has more than 200 components and largely depends on the type of used fuel, type of mixture formation, nature of the combustion process, parameters of operating cycle. The components of complete combustion (carbon dioxide CO₂ and water H₂O), residual oxygen O₂ and nitrogen of air N₂ constitute 99-99.9% of the volume of exhaust gases, are non-toxic. The remaining 0.1-1% of gases constitute harmful components,

which determine the ecological level of internal combustion engine (ICE), i.e. its negative impact on the environment and public health. The most toxic of these are nitrogen oxides NO_x , carbon oxide CO, total hydrocarbons CH_x and sulfur oxides SO_x (Table 1) [1-5].

Table 1 - The average composition of exhaust gases of marine diesel engines [1]

Component EG	Concentration in exhaust gas		
	%	g/m^3	$\text{g}/(\text{kW}\cdot\text{h})$
Nitrogen (N_2)	74.0–78.0	–	–
Oxygen (O_2)	2.0–18.0	–	–
Water vapor (H_2O)	0.5–9.0	15–100	–
Carbon dioxide (CO_2)	1.0–12	40–240	–
Nitric oxide (NO)	0.004–0.5	1.0–4.5	6–18
Nitrogen dioxide (NO_2)	0.00013–0.0130	0.1–0.8	0.5–2.0
Carbon oxide (CO)	0.005–0.4	0.25–2.5	1.5–12.0
Hydrocarbons (CH_x)	0.009–0.3	0.25–2.0	1.5–8.0
Sulphur dioxide (SO_2)	0.0018–0.02	1.0–0.5	0.4–2.5
Carbon black (Soot)(C)	–	0.05–0.5	0.25–0.5

In the Gothenburg Protocol until 2020 contain commitments to reduce emissions of finely dispersed suspended particles ($\text{PM}_{2.5}$). In the new edition, black carbon or soot appears as an important component of $\text{PM}_{2.5}$. Black carbon is a pollutant that has a negative impact on human health and contributes to climate change [2,4].

Currently considered, that negative impact on human health is due to the action of many PM components associated with black carbon. So polycyclic aromatic hydrocarbons (PAHs) have their carcinogenic and direct toxic effects on cells. The International Agency for Research on Cancer has classified exhaust gases from diesel engines consisting of solid particles, as carcinogenic to humans. According to the American expert M. Jacobson, 15-30% of global warming is due to the emission of soot particles. In the air, soot absorbs solar energy and emits infrared (thermal) radiation, contributing to its additional warming up of the Earth [3-5].

When burning raw materials in power-generating installations, tens of millions of tons of harmful toxic components are formed, that are ejected annually into the environment.

Emissions of exhaust gases become the main global problems of ecology, i.e. lead to the formation of "greenhouse effect", the degradation of ozone layer and formation of acid rain.

Emissions of harmful substances that included in the composition of exhaust gases of internal combustion engines, the criteria for their normalization and hazard class are presented in Table 2.

As can be seen from the presented table, many harmful substances belong to the 1st class of danger. So benzopyrene has a good penetrating ability in cells of living organisms. A person gets it through skin, airways and with food. In the body, benzopyrene is oxidized to phenolic and quinone type having mutagenic activity, and partially excreted from body in an unchanged form.

The average annual concentration of benzopyrene in atmospheric air is $0.001 \mu\text{g}/\text{m}^3$ (according to the World Health Organization (WHO)), above which adverse on human health are observed, causing cancer.

The degree of danger of air pollution is determined by maximum permissible concentration of pollutants (MPC).

The MPC does not take into account regional climatic conditions, does not reflect the toxicological load on the ecosystem as whole, since it does not take into account the processes of substance accumulation in biological objects [4-7].

To determine criteria for real hazard of harmful substances, standard GOST 12.1.007-76 "Classification and general safety requirements" is set, taking into account the following characteristics of the hazard class definition (Table 3).

Table 2 - Harmful substances emitted into atmosphere from internal combustion engines and criteria for their normalization

Code	Ingredient name	Hazard Class	$MPC_{m.p.}$	$MPC_{e.c.}$
0110	di-vanadium pentoxide (Vanadium pentoxide)	1	—	0,0020
0183	Mercury (Mercury metal)	1	—	0,0003
0184	Lead and its inorganic compounds (in recount of lead)	1	—	0,0003
0185	Lead sulfite (Sulfur lead (in recount of lead))	1	—	0,0017
0192	Tetraethyl lead	1	0,0001	0,00004
0203	Chromium hexavalent (in recount of chromium trioxide)	1	—	0,0015
0301	Nitrogen dioxide	3	0,20	0,04
0304	Nitrogen oxide	3	0,40	0,06
0326	Ozone	1	0,16	0,03
0328	Carbon (Soot)	3	0,15	0,05
0329	Selenium dioxide (in recount of selenium)	1	0,0001	0,00005
0330	Sulfur dioxide (Sulphurous anhydride)	3	0,50	0,05
0332	di sulfur dichloride (Sulfur chloride)	—	—	—
0333	Dihydrogen sulfide (Hydrogen sulfide)	2	0,008	—
0334	Carbon disulphide	2	0,03	0,005
0337	Carbon oxide	4	5,0	3,0
0602	Benzene	2	0,3	0,1
0616	Dimethylbenzene (Xylene)	3	0,2	—
0621	Methylbenzene (Toluene)	3	0,6	—
0703	Benz (a) pyrene (3,4-Benzopyrene)	1	—	0,000001
1071	Hydroxybenzene (Phenol)	2	0,01	0,006
1325	Formaldehyde	2	0,05	0,01

Table 3 - Classification of the risk of air pollution [1]

Air pollution hazard category	Signs of human exposure
Extremely dangerous	Acute death defeats. Increase in specific mortality
Highly dangerous	Toxic lesions of the respiratory system and other organs. Chronic
Dangerous	Physiological changes outside the norm. Signs of the disease
Moderately dangerous	Changes within the physiological norm
Safe (allowable)	No change

Safe and permissible pollution is considered, which for any duration of exposure, have not directly or indirectly affected the human body. Moderately hazardous are one-time concentrations exceeding 2-2.5 times the MPC, are able to subjectively deteriorate person's state due to odor and cause short-term changes in the body within physiological norms without complications and diseases. Air pollution at the level of more than 10 MPC has a more pronounced effect on the body. At such contamination, increase in the number of visits to the doctor and general morbidity is observed. The main symptoms of the disease are irritation of mucous membranes of eyes, nosepharynx, respiratory failure, reduction of working ability. This level of pollution belongs to hazardous category. A higher level of air pollution, depending on type and concentration of toxic agents, can increase mortality and morbidity of population. Such an effect on humans refers to cases of extremely dangerous air pollution.

At determining the criteria for real danger of pollution, one of the main tasks is the establishment of dependencies of adverse effects from amount of harmful substances. Based on these dependencies, the level of environmental safety of ships is normalized.

The International Marine Organization (IMO) develops requirements for the environmental safety of ships. These requirements in the form of IMO standards, applications and protocols of the MARPOL 73/78 convention regulate the technical, organizational and legal issues of environmental protection at sea. The technical requirements determine the means and necessary equipment for cleaning harmful emissions, specify the maximum levels of waste toxicity. Organizational requirements provide for periodic certification of ships for their compliance with the provisions of the Convention MARPOL.

In Russia, standards for the regulation of harmful emissions from exhaust gases of diesel engines were introduced in 1980-1981. The introduction of these standards allowed to streamline the ecological control over produced diesel engines. For 30 years, these standards have been repeatedly revised and significantly changed. As rule, changes concerned list of controlled parameters, their values, test methods and calculations. At present, the main national documents limiting harmful emissions of ship internal combustion engines are:

–GOST R 51250-99. Diesel ships, diesel and industrial. Smoke of exhaust gases. Norms and methods of measurement;

–GOST R 51249-99. Reciprocating internal combustion engines. Emissions of harmful substances with exhaust gases. Norms and methods of measurement;

–GOST R 52408-2014. Reciprocating internal combustion engines. Emissions of harmful substances with exhaust gases. Measurement in operating conditions.

The toxicity and smoke emissions of exhaust gases are largely regulated by the requirements of Russian and international standards.

The toxicity and smokiness of the exhaust gases are assessed by analyzing sample of gas taken from the exhaust manifold. In order to gas sample was representative, the gas sampler must be located in exhaust gas flow. For cleaner experiment, samples are sometimes taken directly from the diesel cylinder using stroboscopic umbrella. The following requirements are imposed on the gas sampling system:

–the identity of the gas composition in sample selection and in the combustion chamber of the diesel engine;

–unchanged gas composition of gas sample during sampling and during storage until analysis;

–the sampling tube should be short to maintain the temperature of sample gas at 150-200 ° C and thereby eliminate condensation of water vapor.

In order to fulfill the first requirement and obtain gas sample corresponding to this operating mode of the engine, recommended taking gas after special mixer. Such mixer allows averaging the values of the sample, since the harmful substances in composition of the exhaust gases of multi-cylinder diesel are distributed unevenly. This is due to the uneven cyclic fuel flow through the cylinders and, as consequence, the exhaust gases from each cylinder have different chemical composition.

Another feature of measurements is that gaseous toxic components have chemical selectivity, i.e. the direction of action on one or other component, in this connection measurement results depend on the selected chemical analysis. For this reason, in existing normative documents strictly specify the components and methods for measuring them.

The aim of this work is to study the use of bi-fuel internal combustion engines on ships and formed suspended particles during its combustion.

Objects and methods of research

In this paper, the following methods and techniques were taken into account in the calculation of the characteristics of dual-fuel internal combustion engines:

1) Method for selecting the flow characteristic of the injector;

2) Method for selecting the static and dynamic fuel consumption of an electromagnetic injector;

3) Method for specifying the flow characteristic of an electromagnetic injector in the electronic control unit of a two-fuel internal combustion engine;

4) Method for calculating the electromagnetic nozzle for a spark-ignited internal-combustion gas engine;

5) The method of using the energy of the gas differential pressure at the injector to improve the filling of the cylinders with the gas-air mixture;

6) Procedure for processing the parameters of electromagnetic nozzles after testing at a non-motorized stand;

7) Method for controlling the start-up and warm-up of a dual-fuel gas-fueled internal combustion engine;

8) The method of controlling the gas feed at stationary conditions;

9) The method of control of gas supply in transient modes;

10) The method of controlling the ignition timing for operation on one and two types of fuel;

11) Control methods for ignition misfires;

- 12) Correction method for cyclic feed depending on pressure pulsations in the gas train of injectors;
- 13) Method of adaptation to various gas fuel compositions;
- 14) Methods of diagnostics of elements of gas-cylinder equipment during the operation of the vehicle;
- 15) Methods of diagnostics of measuring devices of gas-cylinder equipment;
- 16) Methods of diagnostics of executive devices of gas-cylinder equipment;
- 17) Methods for controlling the operation of a dual-fuel internal combustion engine on standby modes in the event of failure of gas-cylinder equipment;
- 18) Methods of adapting the control system of a gas internal combustion engine;
- 19) Methods for reducing fuel consumption when working on gas fuel [6-10].

Results and discussion

The study of the mechanism of formation of normalized harmful components in combustion chamber of diesel engine allows to purposefully look for ways and means to reduce them. This approach makes it possible to justify the principles of influence on the processes of fuel mixture formation and combustion in order to reduce the formation of toxic substances and soot. These methods do not lead to an increase in fuel consumption.

In the combustion chamber of an internal combustion engine, the chemical reaction of oxidizing the fuel by air oxygen occurs at variable rate depending on the physical processes of mixing the fuel by air, formation of a fuel-air mixture, its heating, ignition and combustion. The main provisions of these processes, formulated in 1927, by N.N. Semenov, made up the theory of chain oxidative reactions. According to this theory, active molecules determine beginning of chain reaction. As they collide, thermal energy is released, which is expended on heating the reacting substances and the formation of new active molecules. Depending on the conditions in the combustion chamber, the reaction can be unbranched (linear) or branched. In the first case, instead of one active molecule, one new molecule is formed, and reaction proceeds until chain breaks. In the second case, several new molecules form from one active molecule, as result of which the oxidation reaction self-disperses, accumulation of active molecules takes place, in result a fuel ignition source appears. At branched chain reaction, the reaction rate can increase to infinity, but this does not occur for two reasons. First, part of the branches in the reaction terminates, reaching relatively cold walls of the combustion chamber, and, secondly, number of active molecules decreases as reactants. Having reached the maximum value, the reaction rate will begin to decrease.

The considered theory of ignition and combustion due to chain reactions is valid for homogeneous combustible mixtures, i.e. such mixtures, in which reactants of the reaction are in the same aggregate state and pre-mixed together [1,5-9].

A special place in a row of marine engines is occupied by L32DF (Dual-Fuel) engine, which represents the two-fuel version of the Wärtsilä L32 engine (Figure 1), which operates on a diesel cycle using both diesel fuel and gaseous fuel with an effective efficiency of 44%. The transfer of engine from one type of fuel to another is automatic and, practically, instantaneously, regardless of the mode in which it operates.

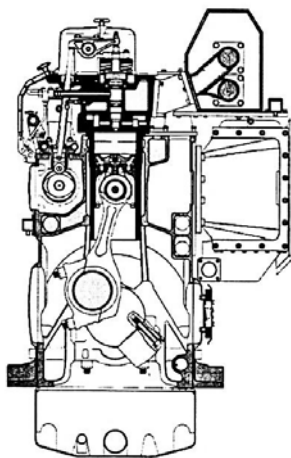


Fig. 1 - Cross section of the engine of Wärtsilä L32

An important feature of the engine (Figure 2) is that it operates on poor gas mixtures, air in the cylinder is roughly twice as large as required for complete combustion. Therefore, a large amount of heat is expended on heating air, and this, contributes to significant reduction in the peak values of combustion temperatures and sharp decrease in formation of NO_x .

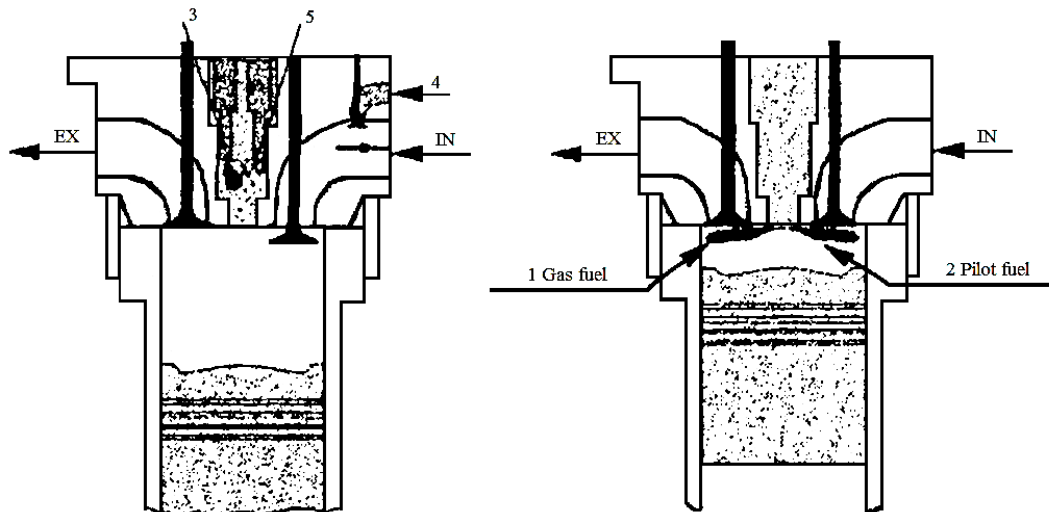


Fig.2 - Supply of gas and fuels

The excessively large values of detonation (explosive combustion) lead to characteristic for gas engines skip flares in cylinders. Therefore, for all loads and speed conditions, excess air ratio should lie in relatively narrow range. Adjustment of “air-gas” ratio (Figure 3) is carried out automatically in all modes by changing the turbocharger output, by bypassing exhaust gases, some of them are directed past the gas turbine plant.

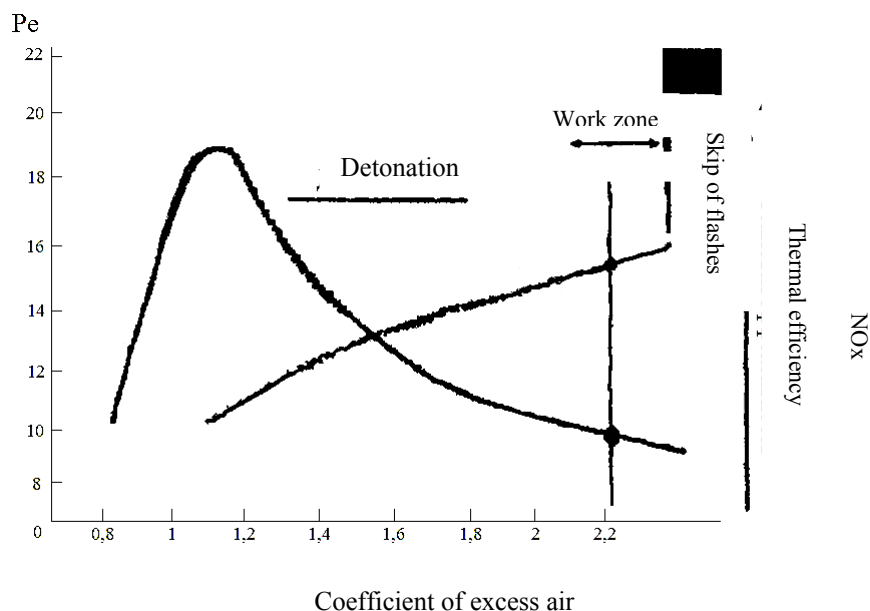


Fig. 3 - Operating range of air-gas ratio

Before engine, the gas is filtered, compressed depending on the engine load to pressures (3.5 bar at full load). The magnitude of the pressure depends on the engine condition. Then gas is directed to main inlet valve, which installed on cover of each cylinder. Control impulses to valves are fed from the

electronic control unit, which receives information from the load-sensing sensors, pressure and charge air temperature and combustion control sensor in each cylinder.

The main gas valve opens and closes at specified times. Delivers the required amount of gas to the inlet of the cylinder cover.

The gas enters cylinder during its filling by air. Feeding is carried out through main hydraulically controlled valve, installed in inlet pipe of cylinder. The valve is opened by oil, compressed to 370 bar. The opening and closing phases of the valve are determined by electronic control unit, which drops the current to solenoid valve.

The ignition of lean air-gas mixture is initiated by flame that occurs at small amount fuel into the combustion chamber is ignited at self-ignition. The supply of diesel fuel to the engine is carried out in two ways. The fuel for pre-injection is compressed by a separate scaled pump to 1000 bar and sent to battery in which constant pressure is maintained. From the accumulator fuel arrives to atomizers. Each nozzle has two nozzles and two needles. A small needle is designed for preliminary fuel injection, and large - for the main supply during engine operation marine diesel (MDO). The time for opening a small needle is determined by opening and closing the solenoid-operated valve in nozzle. The current to the solenoid comes from common electronic control unit. The large needle is controlled hydrodynamically, advance angle and amount of fuel supplied are set by high-pressure fuel pump (HPFP) in its usual version for diesel engines. The consumption of diesel fuel for pre-injection does not exceed 1 g/kW per hour.

The main advantage of dual-fuel engines is that they operate on cheap gas fuels and use them rationally on gas carrier ships and onshore power plants in gas fields. In the event of interruptions in the supply of gas, engine can continue to operate on marine diesel fuel (MDO) [5-8,11-15].

To model the processes of air pollution and build concentration fields at small and medium distances from the source of emissions, there are two approaches - based on Gaussian dispersion, which involves estimating the distribution of pollutant concentrations along the coordinate axes and based on the mass transfer theory (the so-called "gradient" models or K-models, based on solution of turbulent diffusion equations).

Various versions of Gaussian models are widely used abroad. Such models include the American models HIWAY-2, CALINE-4 (California Line Source Model), GM (General Motors), GFLSM (General Finite Line Source Model), the Finnish model - CAR-FMI (Contaminants in the Air from a road, By the Finnish Meteorological Institute). In the HIWAY-2 and CALINE-4 models, concentrations are calculated for a finite linear source with an arbitrary wind direction; in calculation process the source is divided into series of elements from which concentrations are calculated, which are then summed. The GFLSM model is based on formulas for an infinite linear source.

The basis for modeling distribution of pollutants on basis of statistical description of processes of turbulence was laid down by works of Setton, Pasquill, Gifford. The models are constructed on assumption that trail of suspended solids has a Gaussian distribution and concentration at given point along wind direction can be calculated using the generalized Gauss equation. Such models are widely used due to the simplicity and the obtaining of results consistent with experiment. Gaussian models are officially recommended by European Economic Commission, meteorological services of several countries.

The basic model for the case of constant wind speed and absence of chemical transformation is represented by formula:

$$C = \frac{M}{2\pi u \delta_y \delta_z} \exp\left(-\frac{y^2}{2\delta_y^2}\right) \left(\exp\left(-\frac{(z-H)^2}{\delta_z^2}\right) + k \exp\left(-\frac{(z+H)^2}{\delta_z^2}\right) \right), \quad (1)$$

where: C - concentration of suspended substances, g/m³; M - emission power, g/s; u - wind speed at height H, m/s; δ_y , δ_z - parameters of horizontal and vertical dispersion, m; y - distance from the center line of plume, m; z - height above ground, m; k - reflection coefficient ($0 \leq k \leq 1$); H - final height of plume, m.

Equation (1) is valid for concentrations averaged over time for several minutes, that for time interval for which values of scattering parameters and wind speed are representative. The merits of model, thanks

to which it found greatest application in calculating atmospheric pollution in most countries of the world, is as follows:

–the field of concentration from one or several emission sources is described by algebraic relationships, so the machine implementations of this model are characterized by high speed and do not require large amounts of memory;

–the Gaussian scattering approximation allows to take into account a multitude of factors that influence on levels of impurity concentrations in the near-Earth atmosphere. Among these factors are meteorological conditions (wind speed and atmospheric stability), reflection of the impurity from the underlying surface and raised inversions, removal of impurities from atmosphere by precipitation, due to dry deposition and chemical transformation;

– the results of calculations for the model and numerous experimental observations carried out by research teams, showed a good correspondence between themselves: the errors in calculations for the model are estimated at several tens of percent. In some cases, the differences can reach 2-3 times. Estimates of atmospheric pollution within these errors satisfy most practical problems.

The main causes leading to differences in the comparison of measured and calculated concentrations are associated with inaccurate determination of emission of harmful substances from sources of pollution, uncertainty in the choice of the category of atmospheric stability, measurement errors of meteorological parameters.

The main disadvantage of the Gaussian model is that it treats the initial state of the atmosphere as unperturbed, and the distribution of temperature, pressure, inversion, air humidity and other physical parameters along the height leads to the correspondence with the model of the International Standard Atmosphere, which in real conditions is never observed. As known from numerous studies, meteorological conditions are one of the most important factors affecting the dispersion and distribution of concentrations of harmful substances in the atmosphere. The model allows to predict the spatiotemporal picture of atmospheric pollution without taking into account specifically to terrain and meteorological conditions of the territory.

The Gaussian approach is empirical, which hinders the generalization of its results in number of practically important cases. It does not take into account the dependence of diffusion coefficients on height of source, therefore it allows to describe the surface field of impurity concentrations from source of only fixed height.

Models based on the K-theory are based on equations of turbulent diffusion and are the most elaborated theoretically. Russia occupies leading place in the world in these models. In Russia was widespread model M.E. Berland.

In accordance with this approach, the degree of air pollution by emissions of harmful substances from continuously operating sources is determined by the largest calculated value of the single surface concentration (C_M), which is set at certain distance (x_M) from the emission site under unfavorable meteorological conditions, when wind speed reaches dangerous value (u_M) and an intense turbulent exchange occurs in surface layer.

According to this method, the process of transport of harmful substances is described by equations of turbulent diffusion in atmosphere. Then applying averaging techniques from diffusion equations for instantaneous concentrations go to equation of turbulent diffusion for mean values of the concentrations.

The approach of M.E. Berland is applicable only under the condition that dimension of the emission cloud is greater than size of dominant turbulence. In general, all models constructed on the solution of the turbulent diffusion equation are most applicable to describing vertical diffusion near the earth's surface for distance of no more than 10 km from the source.

Models based on the equations of turbulent diffusion possible to solve a variety of practical problems on unified basis and at the same time: take into account development, terrain, averaging time (one-time, annual), photochemical reactions, meteorological conditions (normally unfavorable and anomalously unfavorable). It is also possible to consider various types of sources: point, linear, area.

It can be concluded that the transfer process according to the model of M.E. Berland is applicable to insufficiently powerful sources, since it is not designed for strong overheating of gases in source zone and presence of powerful turbulent mixing as result of overheating. Theoretical patterns of distribution and spatial-temporal distribution of contaminants in the atmosphere are determined by solving the equation of

atmospheric diffusion. This partial differential equation (2), in fact, represents mathematical formalization of fundamental physical law of the conservation of flow of matter and in this sense gives universal description of the regularities of distribution of atmospheric impurities:

$$\frac{\partial q}{\partial t} + \sum_{i=1}^3 u_i \frac{\partial q}{\partial x_i} = \sum_{i=1}^3 \frac{\partial}{\partial x_i} K_i \frac{\partial q}{\partial x_i} - \bar{\alpha} q, \quad (2)$$

where: q - calculated impurity; x_i - impurity coordinates, hereinafter denoted by x, y, z ; u_i ; K_i - components of the average velocity of impurity transfer and coefficient of exchange related to directions of axis x_i ($i = 1, 2, 3$); α - coefficient determining change of concentration due to atmospheric metabolism (impurity transformation).

The use of this fundamental approach to mathematical modeling of turbulent diffusion, which often called K-theory, together with justified simplifications and empirical refinements, has found expression in the mathematical model (3) for emissions. This expression calculates the values of largest total concentration of harmful impurity C_M (mg/m^3), which is set at certain distance (x_M) from the place of ejection from vessels as from sources close to each other in separate sections:

$$C_M = \frac{AMFm'_3}{H^{7/3}}. \quad (3)$$

where A - coefficient that depends on the temperature stratification of atmosphere; M - mass of suspended substances emitted into atmosphere per unit time (g/s); F - dimensionless coefficient, taking into account rate of gravitational settling of solid particles (dust) in atmospheric air on underlying surface, recommended to take the values of parameter $F = 1$ when calculating the scattering in the atmosphere of soot during the operation of ship engines; m'_3 - dimensionless coefficient equal to 0.9; η - dimensionless coefficient taking into account the influence of terrain, in case of flat or slightly intersected terrain with height difference not exceeding 50 m per 1 km, $\eta = 1$; H - height, determined by the terrain.

Vessels of arbitrary geometric configuration and distribution of traffic intensity of ships are represented as set of point, linear and area sources of harmful substances, by summation of which the total air pollution is determined.

The use of such design scheme possible to take into account number of factors important for assessing the impact of ships:

- degree of unfavorability of local climatic conditions for the stable dispersion of impurities in the air, in particular, the inversion (stagnant) states of the atmosphere;
- influence of the terrain, the quality of underlying surface;
- photochemical metabolism of substances;
- possibility of operating with the database MPC, that is, in fact, have an extreme situational picture of air pollution.

To obtain reliable results of computed monitoring of atmospheric air pollution, real, that is, very specific (in terms of vessel's application) and, at the same time, complete (on the structure of vessels) information on the emission capacity and its distribution across the terrain is required. Direct instrumental monitoring of traffic intensities and structural distribution of vessels by characteristic groups and ecological classes solve this task.

The use of numerical methods for calculating impact of vessels on the environment and public health using direct observations of intensity and structure of flows will allow more balanced decision - making and urgent measures to improve environmental situation [16-22].

Difficulties in reducing the toxicity of exhaust gases are due to the selectivity of effect on particular harmful component. Therefore, to solve this problem, important to establish targeted priorities. The choice of these priorities is limited to regulatory standards and regulatory documents, but ways to achieve them can be very diverse. These difficulties are connected with search for rational solution that allows to meet the requirements of the standard at minimum costs and without significantly degrading operating cycle parameters of internal combustion engine.

Measures to reduce the impact of air pollution on the environment and public health are regulatory and legislative regulation (stricter air quality standards, maximum permissible emissions from various sources); structural changes (for example, reduced energy consumption, especially energy produced by burning fuel, changing modes of movement, land-use planning); and also changes in behavior at the individual level, which are expressed, for example, in use of ecology clean ways of transportation or household energy sources.

Conclusions

Thus, the main feature of the use of dual-fuel internal combustion engines on ships is that it operates on poor gas mixtures in which air is approximately twice as large as required for complete combustion. Consequently, a large amount of heat is expended on heating the air, and this contributes to a significant reduction in high values of combustion temperatures and a sharp decrease in the formation of nitrogen oxides, sulfur, and solid particles.

The use of bi-fuel internal combustion engines on ships carrying liquefied natural gas (LNG), possible to reduce cost of operating vessel by approximately 50% in comparison with option of equipping vessel with steam turbine power plant, completely eliminate SO_x emissions, drastically reduce NO_x emissions by 90% and significantly reduce CO_x emissions by 30%.

The main advantage of dual-fuel internal combustion engines is that they operate on cheap gas fuel and are rationally used on gas-carrier ships and onshore power plants in gas fields. In case of power outage, the engine can continue to run on liquid fuel.

The main incentives for expanding scope of application of dual-fuel internal combustion engines will be further tightening of environmental standards and rising prices for traditional types of marine fuel, caused by gradual reduction of world oil reserves. As result, it will be economically more profitable for shipowners to invest in construction of more expensive vessels when they are built, but cheaper to operate.

REFERENCES

- [1] Rumb, V.K., Serazutdinov, O.V. (2015) Toxicity of marine internal combustion engines [Toksichnost sudovyh dvigateley vnutrennego sgoraniya]: textbook. SPb.: Publishing house SPbGMTU. 124 p. (In Russian).
- [2] Kiselev D.M. (2013) Vessels on Natural Gas: Experience of Exploitation and Development Prospects [Suda na prirodnom gaze: opyt ekspluatatsii i perspektivy razvitiya]. J. River transport (XXI Century) [Rechnoy transport]. No. 3 (62). P. 62-64. (In Russian).
- [3] Janssen NAH et al. The impact of black carbon on health. Copenhagen, who regional office for Europe, 2012 [Electronic resource]. URL: <http://www.euro.who.int/en/what-we-do/health-topics/environmentand-health/air-quality/publications/2012/health-effects-of-black-carbon> (circulation date: 28.10.2012).
- [4] Chekhonadskikh, E.A. (2018) Impact of black carbon emissions on the environment and ways of their reduction [Vozdeystvie vybrosov chernogo ugleroda na okrughayuschuyu sredu i puti ih sokrascheniya]. J. collected materials of the 7 all-Russian interbranch STC "Actual problems of marine energy" [Aktualnye problemy morskoy energetiki]. SPb.: Its Spbgmtu. P. 477 – 480. (In Russian).
- [5] International Convention MARPOL 73/78 (2000). Annex VI "Prevention of air pollution by ships" [Predotvraschenie zagryazneniya atmosfery sudami]. Book. 3. - St. Petersburg: ZAO TsNIIMF, 2000. - 281 p. (In Russian).
- [6] Baranov V.A. (2010) Analysis of the prospects of application of various types of alternative fuels on marine vessels [Analiz perspektivnosti primeneniya razlichnyh vidov alternativnogo topliva na morskikh sudah]. J. Scientific and technical collection of the Russian Maritime Register of Shipping [Nauchno-tehnichesky sbornik Rossiyskogo morskogo registra sudohodstva]. No. 33. P. 99-126. (In Russian).
- [7] Cherkaev, G.V. (2014) Consequences of the development of environmental regulation [Perspektivy razvitiya ekologicheskogo normirovaniya]. J. Collected materials of 3 All-Russia inter-branch STC «Actual problems of marine energy» [Aktualnye problemy morskoy energetiki]. SPb.: IC SPbGMTU. P. 138 – 139. (In Russian).
- [8] International Convention for the Prevention of Pollution from Ships (MARPOL 73/78) [Mezhdunarodnaya konventsiya po predotvrascheniyu zagryazneny s sudov]. (2000) - Book. 3, app. VI. Prevention of air pollution by ships [Predotvraschenie zagryazneniya atmosfery sudami]. - St. Petersburg: ZAO CNIIMF. P. 281. (In Russian).
- [9] Khachiyani A.S. Comparative estimation of carbon dioxide emissions by various engines (2006) [Srvnitelnaya otsenka vybrosov dvoukisi ugleroda razlichnymi dvigatelyami]. J. Prospects for the development of power plants for the motor transport complex: coll. sci. tr. MADI (TU) [Perspektivy razvitiya energeticheskikh ustanovok dlya avtotransportnogo kompleksa]. P. 4-9. (In Russian).

[10] Koishina A.I., Kirisenko O.G., Koilybayev B.N., Agayeva K.K. (2018) Decision-making for choosing of geological and engineering operations: current status and prospects. J. News of the National Academy of Sciences of the Republic of Kazakhstan. Series of geology and technical sciences. N4.P.6-18. <https://doi.org/10.32014/2018.2518-170X>.

[11] Dorokhov A.F. Features of the use of gaseous fuels in ship power plants [Osobennosti primeneniya gazoobraznykh topghhiv in sudovykh energeticheskikh ustanovkakh]. J. Vestnik of the Astrakhan State Technical University. Seria: Marine technology and technology [Vestnik ASTU. Seriya: Morskaya tehnika and tehnologiya]. - 2012. - № 2. - P. 70-75. (In Russian).

[12] Voznitsky, I.V. (2007). Ship internal combustion engines [Sudovye dvigateli vnutrennego sgoraniya]. Volume 1. Moscow: Morkniga. 282 p. (In Russian).

[13] Lozhkin, V.N., Medeyko, V.V. (2005) Models of evaluation of environmental damage used in the Russian Federation, USA and EU countries with state regulation of the impact of vehicles on the environment [Modeli otsenki ekologicheskogo uscherba, primenyaemye v Rossiyskoy Federatsii, SShA i stranah ES, pri gosudarstvennom regulirovanii vozdeystviya transportnykh sredstv na okruzhayushchuyu sredyu]. J. Information Bulletin. No. 2 (32). «Issues of protection of the atmosphere from pollution» [Voprosy ohrany atmosfery ot zagryazneniya]. – SPb.: NPK «Atmosphere» with GGO im. A.I. Voeikov. P. 103–116. (In Russian).

[14] Examining the Exploitation of Methanol as a Fuel Type // Diesel facts. 2015. № 2. Pp. 6–7.

[15] Dual-Fuel L35/44DF Engine Moves towards Market Entry // Diesel facts. 2015. № 2. P. 11.

[16] Model of the wind field [Electronic resource]. URL: <http://www.indic-airviro> (date accessed: 22.02.2012). (In Russian)

[17] MSC 83/INF.3 «FSA – Liquefied Natural Gas (LNG) Carriers Details of the Formal Safety Assessment», IMO, 2007.

[18] Zhukov V.A. (2010) Prospects of conversion of automobile engines into ships in the aspect of ecological standards [Perspektivy konvertatsii avtomobilnykh dvigateley v sudovye v aspekte ekologicheskikh normativov]. J. Proceedings of the 11th International Conference "Actual problems of modern science" [Aktualnye problemy sovremennoy nauki]. - Part 3. Mechanics and mechanical engineering. - Samara: SamSTU. - P. 41-45. (In Russian).

[19] Blinkov A.N. (2011). Analysis of the methods of using gas fuel in ship power plants [Analiz sposobov primeneniya gazovogo topliva v sudovykh enereticheskikh ustanovkakh]. J. Scientific and technical collection of the Russian Maritime Register of Shipping (Rossiyskiy morskoy registr sudohodstva). No. 34. P. 177-179. (In Russian).

[20] Sorokin, N.D. (2008). The system of atmospheric air monitoring in St. Petersburg [Sishtema monitringa atghmosfernogo vozghduha in Sanghkt-Peterghburge]. Report of the IV intern. science. – practice. Conf. «Transport: from environmental policy to everyday practice» [Transport ot ekologicheskoy politiki do povsednevnoy praktiki]: VIII Intern. ecological forum 20–21 March, St. Petersburg. (In Russian).

[21] Zhukov V.A. (2015). Prospects for improving cooling systems for marine diesel engines [Perspektivy sovershenstvovaniya sistem ohlazhdeniya sudovykh dizeley]. J. Bulletin of the Admiral S.O. Makarov State Naval and River Fleet University. [Vestnik Gosudarstvennogo universiteta morskogo i rechnogo flota imeni admirala S.O. Makarova]- 2015. - No. 4 (32). - P. 131-137. (In Russian).

[22] Romanova S.M., Kazangapova N.B. (2018) Theory and practice of selfpurification capacities of natural water in Kazakhstan. J. News of the National Academy of Sciences of the Republic of Kazakhstan. Series of geology and technical sciences. N 1. P.41-49. <https://doi.org/10.32014/2018.2518-170X>

**К.С. Надиров¹, Г.В. Черкаев², Е.А. Чихонадских³,
Н.А. Маккавеева⁴, А.С. Садырбаева⁵, Г.Э. Орымбетова⁶**

^{1,5,6}М. АӘуэзов атындағы Оңтүстік Қазақстан мемлекеттік университеті, 160012, Қазақстан Республикасы, Шымкент қ., Тәуке хан даңғ., 5

²⁻⁴Санкт-Петербург мемлекеттік теңіз техникалық университеті, Санкт-Петербург қ., Ресей

ЕКІ ОТЫНДЫ ПЖ КЕМЕЛЕРДІҢ ПАЙДАЛАНЫЛҒАН ГАЗДАРЫМЕН ЗИЯНДЫ ЗАТТАРДЫҢ ШЫҒАРЫЛУЫНЫҢ ҚОРШАҒАН ОРТАҒА ЖӘНЕ ТҮРҒЫНДАР ДЕНСАУЛЫҒЫНА ӘСЕРІН ТАЛДАУ

Аннотация. Газдың төмен құндылығы және әсіресе оны өндіру аймақтарында электр энергиясын өндіру үшін, сонымен қатар газ тасымалдаушы кемелерде қолданудың пайдалылығына байланысты бірқатар қозғалтқыш жасаушы фирмалар өздері шығаратын қозғалтқыштарды газ отынымен жұмыс жасауға бейімдеп жетілдіре бастады. Жетілдіру екі бағытта жүреді: карбюраторлық бензин қозғалтқыштарына ұқсас карбюраторларды және тұтандыру білтесін қолданумен Отто циклы бойынша дизельді жұмысқа көшіру және газ және отын қоспасын тұтандыру үшін дизельдік отынның аз мөлшерін шашыратумен дизельдік циклды сақтау. Бұл кезде қажеттігіне қарай қозғалтқыштың тек қана дизельдік отында – екі отынды қозғалтқышпен

жұмыс жасауы да мүмкін. Жұмыстың мақсаты іштен жанатын екі отынды қозғалтқыштардың кемеді қолданылуын және ол жанған кезде қалқымалы бөлшектердің түзілуін зерттеу. Тақырыптың өзектілігі көптеген кемелердің отын ретінде мазут, бензин және дизельдік отындарды қолдануымен байланысты, бұл тұрғындардың денсаулығына және қоршаған орта жағдайына, әсіресе теңізге кері әсер етеді. Сондықтан мұндай жағдайдан шығу үшін екі отынды қозғалтқыштарды ендіру қолданылған, бұл кемелерден теңіз және ауа ортасына лактыруларды бірнеше есеге дейін азайтады.

Түйін сөздер: зиянды заттар лактырындылары, кемелердің іштен жану қозғалтқыштарынан шыққан газдар, қоршаған орта, тұрғындар денсаулығы, сығылған табиғи газ, атмосфералық диффузияны есептеу үлгісі.

**К.С. Надиров¹, Г.В. Черкаев², Е.А. Чихонадских³,
Н.А. Маккавеева⁴, А.С. Садырбаева⁵, Г.Э. Орымбетова⁶**

^{1,5,6}Южно-Казахстанский государственный университет им. М. Ауэзова, 160012,

Республика Казахстан, г.Шымкент, проспект Тауке хана, 5;

²⁻⁴Санкт-Петербургский государственный морской технический университет, г.Санкт-Петербург, Россия

АНАЛИЗ ВЛИЯНИЯ ВЫБРОСОВ ВРЕДНЫХ ВЕЩЕСТВ С ОТРАБОТАВШИМИ ГАЗАМИ СУДОВЫХ ДВУХТОПЛИВНЫХ ДВС НА ОКРУЖАЮЩУЮ СРЕДУ И ЗДОРОВЬЕ НАСЕЛЕНИЯ

Аннотация. В связи с низкой стоимостью газа и целесообразностью его использования для выработки электроэнергии, особенно в зонах его добычи, а также на судах-газовозах, ряд двигателестроительных фирм стали модернизировать выпускаемые ими двигатели для приспособления их к работе на газовом топливе. Модернизация идет по двум направлениям: по переводу дизеля на работу по циклу Отто с использованием карбюраторов и свечей зажигания подобно карбюраторным бензиновым двигателем и сохранению дизельного цикла с впрыском небольшого количества дизельного топлива для воспламенения смеси газа и топлива. При этом в случае необходимости не исключается работа двигателя только на дизельном топливе – двухтопливные двигатели. Цель работы заключается в исследовании применения двухтопливных двигателей внутреннего сгорания на судах и образуемых взвешенных частицах при его сгорании. Актуальность темы заключается в том, что большинство судов используют в качестве топлива мазут, бензин и дизельное топливо, что негативно сказывается на здоровье населения и состоянии окружающей среды, особенно, морской. Поэтому выходом из такого положения послужило внедрение двухтопливных двигателей внутреннего сгорания, которые в разы уменьшают выбросы от судов в морскую и воздушную среду.

Ключевые слова: выбросы вредных веществ, отработавшие газы судовых двигателей внутреннего сгорания, окружающая среда, здоровье населения, сжиженный природный газ, модели расчета атмосферной диффузии.

NEWS

OF THE NATIONAL ACADEMY OF SCIENCES OF THE REPUBLIC OF KAZAKHSTAN

SERIES CHEMISTRY AND TECHNOLOGY

ISSN 2224-5286

<https://doi.org/10.32014/2018.2518-1491.37>

Volume 6, Number 432 (2018), 150 – 155

UDC 533.6:519.6

**B.Kh. Khusain, K.K. Vinnikova,
A.S. Sass, K.S. Rakhmetova, N.R. Kenzin**

¹D.V.Sokolskiy Institute of Fuel, Catalysis and Electrochemistry JSC, Almaty, Kazakhstan
E-mail: bolatbekh@mail.ru

AERODYNAMIC MODELING OF EMISSIONS PASSAGE IN THE NEUTRALIZATION PROCESS

Abstract. This paper discusses an approach to analyzing the aerodynamics of a catalytic converter body using the Boltzmann lattice method and cellular automata. The LBM (Lattice Boltzmann Method) method is based on discretization of the Boltzmann kinetic equation, which at the microscopic level corresponds to the diluted gas model (particle model), and at the macroscopic level asymptotically goes to the Navier-Stokes equation for liquids and gases. Numerical approximation is carried out on the basis of the standard Batnagar-Gross-Kruk model.

Key words: aerodynamics, lattice Boltzmann method, numerical simulation, neutralizer.

1. Introduction

Recently, the Boltzmann lattice method has begun to gain popularity among problems in the field of fluid dynamics [1-3], as well as special cases in modeling multiphase, multicomponent and porous media [4-6]. The main advantages of the method in comparison with standard algorithms for the numerical solution of CFD problems based on solving the Navier – Stokes equations by finite volume/element methods are the ease of implementation, good parallelization and high computation efficiency. Cellular automaton provides the ability to set simple rules for mixtures and phases, a small interdependence of calculations between the cells of the lattice, allowing unlimited scaling of the simulation area. The LBM (Lattice Boltzmann Method) method was developed in 1986 [7] as a result of attempts to optimize calculations for gas and liquids, it is relatively new. Modern models, able to operate stably at high speed can solve applied problems for aerodynamics, laws of quantum mechanical systems and shock waves.

2. Mathematical model

Numerical simulation of the gas transfer process is based on the Boltzmann kinetic equation. The main idea of Boltzmann is to represent the gas as interacting particles whose behavior can be described by the laws of classical mechanics. However, due very large number of particles, in practice, it is not possible. Boltzmann proposed a statistical formulation of the problem in which the state of the system under study can be described by some distribution function $f^{(N)}(\mathbf{x}_1, \mathbf{x}_2, \dots, \mathbf{x}_N, \mathbf{p}_1, \mathbf{p}_2, \dots, \mathbf{p}_N, t)$, where N is

a number of particles, \mathbf{x}_i and \mathbf{p}_i are coordinates and momentum of the i-th particle respectively. Consider the one-dimensional case. Let the probable number of molecules with coordinates in the interval $\mathbf{x} \pm d\mathbf{x}$ and momentum in the interval $\mathbf{p} \pm d\mathbf{p}$ be defined as $f^{(1)}(\mathbf{x}, \mathbf{p}, t) d\mathbf{x} d\mathbf{p}$. Suppose that we have added some external force \mathbf{F} , which has a small magnitude in comparison with intermolecular forces. In case of the absence of collisions between molecules, the new positions of the molecules traveling from \mathbf{x} at time $t + dt$ will be equal to $\mathbf{x} = \mathbf{x} + \mathbf{v}dt = \mathbf{x} + (\mathbf{p} / m)dt = \mathbf{x} + d\mathbf{x}$, and the new impulses will be $\mathbf{p} = \mathbf{p} + \mathbf{F}dt = \mathbf{p} + (d\mathbf{p}/dt)dt = \mathbf{p} + d\mathbf{p}$.

Therefore, if the positions and pulses at time t are known, their increments allow us to determine the value of $f^{(1)}$ at time $t + dt$:

$$f^{(1)}(\mathbf{x} + d\mathbf{x}, \mathbf{p} + d\mathbf{p}, t = dt)d\mathbf{x}d\mathbf{p} = f^{(1)}(\mathbf{x}, \mathbf{p}, t)d\mathbf{x}d\mathbf{p} \quad (1)$$

Relation (1) describes the motion of particles without collisions. Collisions are taken into account by using the BGK model (Bhatnagar – Gross – Krook) - a classic choice among problems of physics:

$$f^{(1)}(\mathbf{x} + d\mathbf{x}, \mathbf{p} + d\mathbf{p}, t = dt)d\mathbf{x}d\mathbf{p} = f^{(1)}(\mathbf{x}, \mathbf{p}, t)d\mathbf{x}d\mathbf{p} + [\Gamma^{(+)} - \Gamma^{(-)}]d\mathbf{x}d\mathbf{p}dt \quad (2)$$

Here, the value of $\Gamma^{(-)}d\mathbf{x}d\mathbf{p}dt$ is equal to the number of molecules that did not arrive at the expected point of space with the coordinates $\mathbf{x} + d\mathbf{x}$ and momentum $\mathbf{p} + d\mathbf{p}$ due to collisions that occurred during time dt . The value of $\Gamma^{(+)}d\mathbf{x}d\mathbf{p}dt$ is equal to the number of molecules that began to move from points other than $\mathbf{x} + d\mathbf{x}$, but turned out to be in the region of space we are interested in due to collisions that occurred during time dt .

3. Boundary conditions

Usually during modeling the flow in channels or pipes using the LBM method, the channel walls are treated as a rigid boundary, from which particles are reflected, while periodic boundary conditions are applied to open channel sections [8].

In this case, the problem also has both types of boundary conditions. The computational domain (Fig. 1) consists of three boundaries - input, output and the rigid walls of the neutralizer. Reflection of particles will occur in a collision with the walls of the housing and the honeycombs of catalyst.

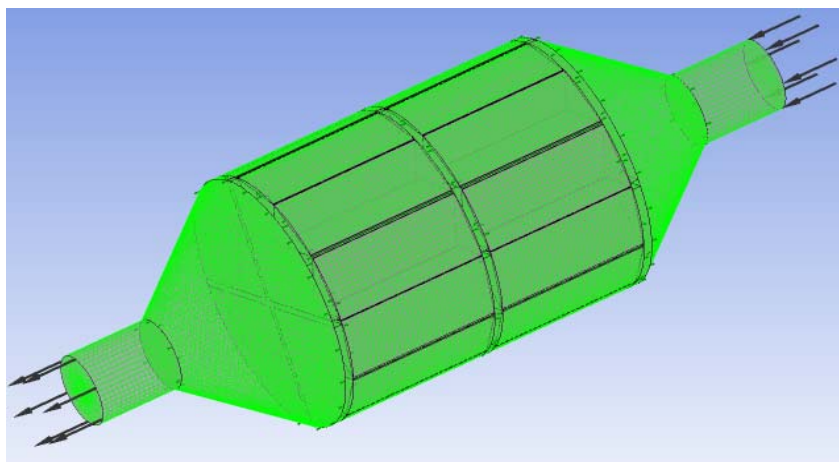


Figure 1 – Computational domain of the problem, catalytic converter housing

4. Numerical method

The method of lattice Boltzmann equations represents as a simplified implementation of the original Boltzmann idea through discretization of the equations. As a result, the number of particles, their possible velocities and positions in space is reduced. A uniform spatial grid called the Boltzmann lattice is built. Time is also discretized. Particles can be located only in the nodes of grid, the velocity of each particle can take a limited number of values, enough to reach the neighboring node during one time. Fig. 2 shows the lattice and directions of velocities \mathbf{e}_a , where $a = \overline{0,8}$ is an index of the direction (at $\mathbf{e}_0 = 0$ particles are at rest).

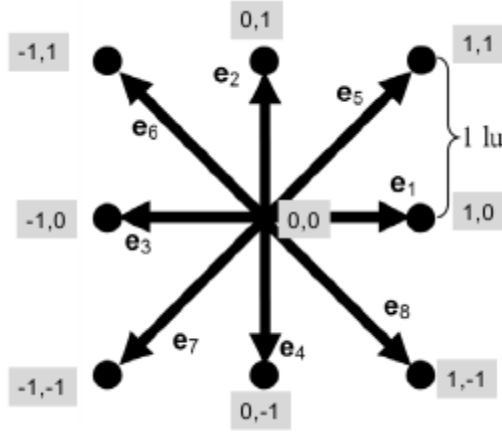


Figure 2 — Velocity components in D2Q9 model (2-dimensional with 9 velocity values)

The magnitude of the velocities $\mathbf{e}_1, \dots, \mathbf{e}_4$ is 1 lattice unit in 1 time step, i.e. $lu \cdot ts^{-1}$. The magnitude of the velocities $\mathbf{e}_5, \dots, \mathbf{e}_8$ is $\sqrt{2} lu \cdot ts^{-1}$. Such choice of velocities is very convenient, since all their x- and y-components have values 0, 1 or -1 (Fig. 2). The value of f_a determines the number of particles in a given node moving in the \mathbf{e}_a direction. The macroscopic density of gas in a given node is the sum of particles moving from a given node in all possible directions:

$$\rho = \sum_{a=0}^8 f_a$$

In the simplest case the mass of all particles is the same and equal to one. The macroscopic velocity \mathbf{u} is the average of the microscopic velocities \mathbf{e}_a multiplied by the number of particles moving in a certain direction f_a :

$$\mathbf{u} = \frac{1}{\rho} \sum_{a=0}^8 \mathbf{e}_a f_a$$

In the LBM representation, equation (2) will be:

$$f_a(\mathbf{x} + \mathbf{e}_a \Delta t, t + \Delta t) = f_a(\mathbf{x}, t) + \Omega_a(\mathbf{x}, t)$$

The term $\Omega_a(\mathbf{x}, t)$ describes the collision of particles. The authors of the model, Batnagar, Gross and Crook, suggested that if particles move without collisions, the system is in equilibrium. Any collision brings the system out of equilibrium. Then the iteration of the cellular automaton operating according to the LBM method will look as follows:

$$f_a(\mathbf{x} + \mathbf{e}_a \Delta t, t + \Delta t) = f_a(\mathbf{x}, t) - \frac{1}{\tau} [f_a(\mathbf{x}, t) - f_a^{eq}(\mathbf{x}, t)],$$

Where $f_a^{eq}(\mathbf{x}, t)$ is an equilibrium function given by the formula:

$$f_a^{eq}(\mathbf{x}, t) = w_a \rho(\mathbf{x}) \left[1 + 3 \frac{\mathbf{e}_a \cdot \mathbf{u}}{c^2} + \frac{9 (\mathbf{e}_a \cdot \mathbf{u})^2}{2 c^4} - \frac{3 \mathbf{u}^2}{2 c^2} \right],$$

Where weight w_a for particle at rest ($a = 0$) is equal to 4/9, for $a = 1, 2, 3, 4$ is 1/9 and for $a = 5, 6, 7, 8$ w_a is 1/36; c — the main velocity on lattice.

The model will qualitatively describe the flow at small values of the Mach number, and the kinematic viscosity depends on the relaxation time τ : $v = (\tau - 0.5)c^2 dt$.

5. Results

In order to calculate the numerical approximation, a software complex for the universal Windows platform was developed. The program calculates aerodynamics, regime and design parameters of the process of emissions passage through the catalytic converter. Basing on results, it builds the geometry of the converter housing. The realization is done in Python, C #, Java languages.

Figures 2 - 4 present the results of the calculation of the aerodynamic characteristics of a single-component single-phase flow in a neutralizer with an optimal configuration and composition [9] at different incoming gas velocities.

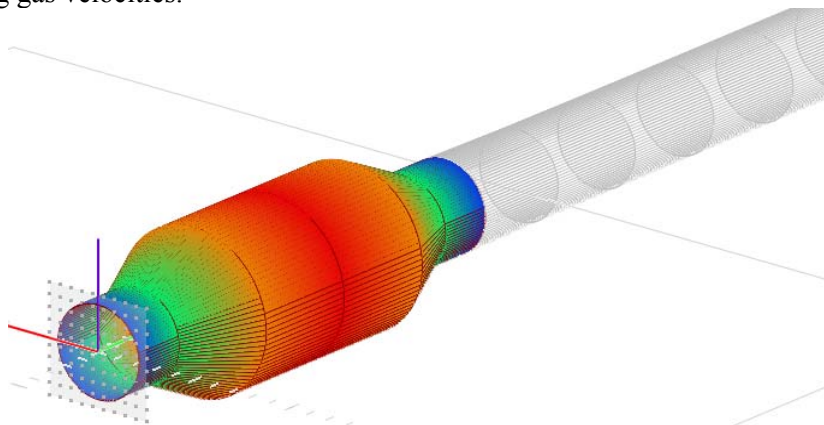


Figure 3 – Calculation at V=100 m/s

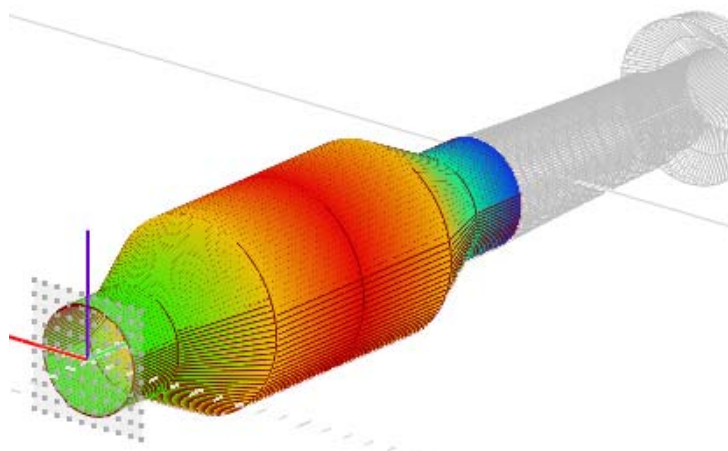


Figure 4 – Calculation at V=10 m/s

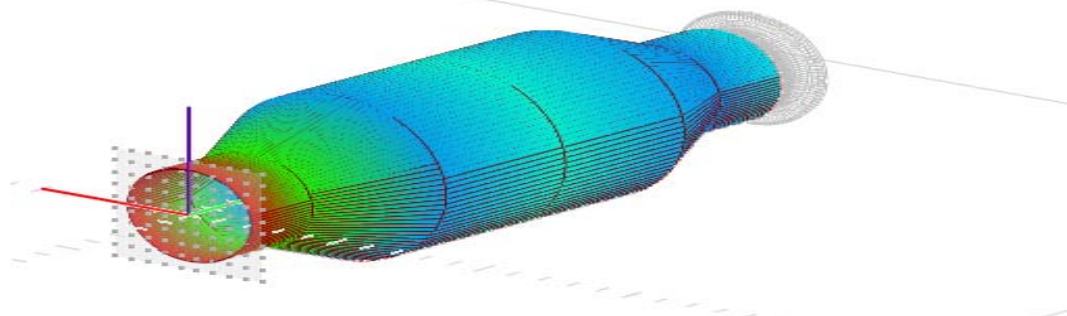


Figure 5 – Calculation at V=1 m/s

6. Conclusions

The developed software complex for modeling the passage of emissions in the neutralization process, based on LMB method, has two key qualities - high speed of calculations, and the ability to model problems with complex boundary conditions. In this case, the complexity of the geometry lies in the structure of honeycomb catalyst, the main element of the catalytic converter. The lattice Boltzmann method and cellular automata allow one to simulate the gas dynamics using simple arithmetic expressions. The statistical approach to the numerical analysis of gas motion simplifies mathematical apparatus, thereby reducing the amount of computational costs. This mathematical model allows making modifications and subsequent additions, which will take into account the chemical composition and temperature [10-11] of waste gases in neutralizer.

The work was carried out with the financial support of the State Institution "Committee of Science of the Ministry of Education and Science of the Republic of Kazakhstan" under project No. AR05131076 under agreement No. 173 of March 15, 2018

REFERENCES

- [1] Tyrinov A. I., Avramenko A.A., Basok B.I., Davydenko B.V. Modelirovanie mikrotechenij metodom reshetok Bol'cmana // NAN UKRAINY. Promyshlennaja teplotehnika, 2011, t.33, №2. – S. 11-19.
- [2] Ostapenko A.A. Modelirovanie techenij vjazkoj zhidkosti metodom reshetok Bol'cmana // Aktual'nye napravlenija nauchnyh issledovanij XXI veka: teoriya i praktika. T.2, № 5-1 (10-1). – Voronezh: 2014.– S.236-238. <https://doi.org/10.12737/6393>
- [3] Jeffrey D. Brewster (2007) Lattice-Boltzmann Simulations of Three-Dimensional Fluid Flow on a Desktop Computer. Analytical Chemistry 79 (7): 2965–2971. DOI: 10.1021/ac062178v
- [4] Kupershtoh A. L. Trehmernoe modelirovanie dvuhfaznyh sistem tipa zhidkost'-par metodom reshetochnyh uravnenij Bol'cmana na GPU // Vychislitel'nye metody i programmirovaniye: novye vychislitel'nye tehnologii. T.13 № 1. – M.:2012. – S.130-138. eISSN: 1726-3522
- [5] Xiaoyi He, Shiyi Chen, Raoyang Zhang, (1999) A Lattice Boltzmann Scheme for Incompressible Multiphase Flow and Its Application in Simulation of Rayleigh–Taylor Instability. Elsevier, Journal of Computational Physics Volume 152, Issue 2: 642-663. <https://doi.org/10.1006/jcph.1999.6257>
- [6] Xiaowen Shan, Hudong Chen, (1993) Lattice Boltzmann model for simulating flows with multiple phases and components. Physical Review E Vol. 47, Iss. 3. <https://doi.org/10.1103/PhysRevE.47.1815>
- [7] Kadanoff L. (1986) On two levels. Physics Today 39: 7-9. <https://doi.org/10.1063/1.2815134>
- [8] Jonas Latt, Bastien Chopard, Orestis Malaspinas, Michel Deville, Andreas Michler, (2008) Straight velocity boundaries in the lattice Boltzmann method. Phys. Rev. E (Vol. 77, Iss. 5). <https://doi.org/10.1103/PhysRevE.77.056703F>
- [9]
- [10][8] L.R. Sassykova, Sh.A. Gil'mundinov, A.T. Massenova, Zh.A. Akimbaeva, M.D. Gasparyan, M.K. Kalykhberiev, M.s. Nurakhmetova, V.N. Grunskii, N.R. Kenzin (2016) Catalysis on metal and ceramic carriers for neutralization of waste gases of industry and motor transport. News of the Academy of Sciences of the Republic of Kazakhstan. Series Chemistry and Technology 2, 416: 135-144. ISSN 2224-5286 <https://doi.org/10.32014/2018.2518-1491>
- [9] G. Barrios, R. Rechtman, J. Rojas, R. Tovar, (2005) The lattice Boltzmann equation for natural convection in a two-dimensional cavity with a partially heated wall. Journal of Fluid Mechanics, Volume 522: 91-100. <https://doi.org/10.1017/S0022112004001983>
- [10] Shiyi Chen, Gary D. Doolen, (1998) Lattice Boltzmann method for fluid flows. Annual Reviews. Fluid Mechanics. 1998: 329-364.

УДК 533.6:519.6

Б.Х. Хусаин¹, К.К. Винникова¹, А.С. Сасс¹, К.С. Рахметова¹, Н.Р. Кензин¹

¹Д.В. Сокольский атындағы жанармай, катализ және электрохимия институты, Алматы, Қазақстан

БЕЙТАРАПТАНДЫРУ ПРОЦЕСТЕГІ ПАЙДАЛАНЫЛҒАН ГАЗДАР ШЫҒУДЫҢ АЭРОДИНАМИКАЛЫҚ МОДЕЛЬДЕУ

Аннотация. Бұл мақалада каталитикалық түрлендіргіш корпусының аэродинамикасын Больцмандық торлы әдіспен және ұялы автомат арқылы талдау әдісі қарастырылады. LBM (Lattice Boltzmann Method) әдісі микроскопиялық деңгейде сұйылтылған газ үлгілеріне (бөлшектердің моделі) сәйкес келетін және сұйықтар мен газдарға арналған Навье-Стокс теңдеуіне бара-бар макрокопиялық деңгейде Больцмандық кинетикалық

теңдеуді дискретизациялауға негізделген. Сандық жақындау стандартты Батнагар-Гросс-Крук моделінің негізінде жүргізіледі.

Түйін сөздер: аэродинамика, Больцмандық торлы әдіс, сандық модельдеу, нейтрализатор.

УДК 533.6:519.6

Б.Х. Хусаин¹, К.К. Винникова¹, А.С. Сасс¹, К.С. Рахметова¹, Н.Р. Кензин¹

¹АО «Институт топлива, катализа и электрохимии им. Д.В.Сокольского», Алматы, Казахстан

АЭРОДИНАМИЧЕСКОЕ МОДЕЛИРОВАНИЕ ПРОХОЖДЕНИЯ ВЫБРОСОВ В ПРОЦЕССЕ НЕЙТРАЛИЗАЦИИ

Аннотация. В данной работе рассматривается подход к анализу аэродинамики корпуса каталитического нейтрализатора с применением решёточного метода Больцмана и клеточных автоматов. Метод LBM (Lattice Boltzmann Method) основан на дискретизации кинетического уравнения Больцмана, которое на микроскопическом уровне соответствует модели разреженных газов (модель частиц), а на макроскопическом уровне асимптотически переходит к уравнению Навье-Стокса для жидкостей и газов. Численное приближение осуществляется на основе стандартной модели [Батнагара-Гросса-Крука](#).

Ключевые слова: аэродинамика, решеточный метод Больцмана, численное моделирование, нейтрализатор.

Information about the authors:

B.Kh. Khusain - Candidate of Technical Sciences, researcher of “D.V.Sokolskiy Institute of Fuel, Catalysis and Electrochemistry” JSC, project supervisor, Almaty, Kazakhstan, e-mail: bolatbekh@mail.ru;

A.S. Sass - Candidate of Chemical Sciences, researcher of “D.V.Sokolskiy Institute of Fuel, Catalysis and Electrochemistry” JSC, Almaty, Kazakhstan, e-mail: aleksandr-sass@mail.ru;

N.R. Kenzin - Master Degree of Biotechnology, researcher of “D.V.Sokolskiy Institute of Fuel, Catalysis and Electrochemistry” JSC, Almaty, Kazakhstan, e-mail: nailkenz@gmail.com;

K.S. Rakhmetova - Master Degree of Technics and Technologies, researcher of “D.V.Sokolskiy Institute of Fuel, Catalysis and Electrochemistry” JSC, Almaty, Kazakhstan, e-mail: rahmetova_75@mail.ru;

K.K. Vinnikova – Master Degree Student of the 2nd academic year for the specialty of 6M070500 - "Mathematical and computer modeling", the Department of Mathematical and computer modeling, Al-Farabi Kazakh National University, junior researcher of “D.V.Sokolskiy Institute of Fuel, Catalysis and Electrochemistry” JSC, Almaty, Kazakhstan, e-mail: kseniayvinnikova@hotmail.com.

NEWS

OF THE NATIONAL ACADEMY OF SCIENCES OF THE REPUBLIC OF KAZAKHSTAN

SERIES CHEMISTRY AND TECHNOLOGY

ISSN 2224-5286

<https://doi.org/10.32014/2018.2518-1491.38>

Volume 6, Number 432 (2018), 156 – 162

L.A.Utegenova¹, A.K.Nurlybekova¹, Hajiakber Aisa^{2,3}, J. Jenis¹

¹Faculty of Chemistry and Chemical Technology, Al-Farabi Kazakh National University, Almaty, Kazakhstan;

²Xinjiang Technical Institutes of Physics and Chemistry, Central Asian of Drug Discovery and Development;

³Xinjiang Key Laboratory of Plant Resources and Natural Product Chemistry, XTIPC CAS, R. P. China

E-mail: lyazzat.utegenova@list.ru

LIPOSOLUBLE CONSTITUENTS OF *FRITILLARIA PALLIDIFLORA*

Abstract: Chemical constituents of the roots of *Fritillaria pallidiflora* collected in Kazakhstan were investigated for the first time. The quantitative and qualitative analysis of bioactive constituents of the medicinal plant have been made. The liposoluble constituents of hexane extract were obtained from the root parts of *F.pallidiflora* and analyzed by GC-MS method. More than thirty compounds were separated. Their relative contents were determined by area normalization in which 30 liposolubles were identified. The major liposoluble constituents of n-hexadecanoic acid (28.97%), linoelaidic acid (16.68%), oleic acid (11.30%), octadecanoic acid (6.95%), silanamine, n-phenyl- (4.41%), trans,trans-Dibenzylideneacetone(3.85%), gamma.-sitosterol (3.51%), ethyl 9.cis.,11.trans.-octadecadienoate (2.91%), hexadecanoic acid, ethyl ester (2.45%).

Key words: *Fritillaria pallidiflora*, GC-MS, liposoluble constituents.

Introduction

Fritillaria– is a genus of perennial herbaceous plants of the family Liliaceae, which in Latin translates into a glass for throwing out dice, in the shape of a corolla. One hundred and fifty species of hazel grouse, wildly growing in the temperate climate of the Northern Hemisphere, are known. Some species are found in the forests of East Asia, many in Western Asia. In the steppe zones, meadow places, on the slopes of the alpine and subalpine belt of Kazakhstan, there are 5 different species of *Fritillaria* growing[2]. Virtually all species of grouse contain alkaloids: peymin, verticin, peyminin, propymine, peymidine, peymifin, peymizin, peymithidin. They also include glycosides: peyminoside and zebaininoside. In addition, the bulbs contain organic acids, terpenoids, phytosterols and some vitamins. In small doses, the alkaloids contained in the bulbs have a therapeutic effect. Thus, in Chinese medicine, on the basis of the alkaloids contained in the bulbs, expectorants and soothing agents are made. In large doses of hazelnut bulbs are dangerous to health [4]. According to traditional descriptions, *Fritillaria* is slightly cold, and affects the lungs (to clear heat and moisten dryness, and used for hot-type bronchitis with dry cough) and the heart (to calm heart fire). *Fritillaria* is also used for treating lumps beneath the skin, such as scrofulous swellings and breast lumps. *F.pallidiflora* widely distributed in China and finds widespread applications as antitussive, antiasthmatic and expectorant medicine. Base on references, the main chemical constituents of *F. pallidiflora* be regarded as steroidal saponins and alkaloids [5].

In our continuously study of the plant, thirty liposoluble constituents in hexane part from medicinal plant, *F.pallidiflora* have been identified by GC-MS methods which grown in Almaty region of Kazakhstan for the first time.

Materials and Methods

Plant material. The root part of *F.pallidiflora* was collected in Almaty region of Kazakhstan, in May 2017 and identified by Dr. Alibek Ydyrys. Medicinal herbs were deposited in the Herbarium of Laboratory Plant Biomorphology, Faculty of Biology and Biotechnology, Al-Farabi Kazakh National

University, Almaty, Kazakhstan. The air dried roots of *F.pallidiflora* were cut into small pieces and stored at room temperature.

Extraction and isolation. The air-dried roots of *F. pallidiflora* (100 g) were pulverised then extracted with 70% ethyl alcohol (1:1) three times (seven days each time) at room temperature. After evaporation of the solvent under reduced pressure, the residues were mixed and suspended in water and then successively partitioned with hexane, EtOAc, and n- BuOH to afford the corresponding extracts. The obtained hexane extract was analyzed by GC-MS method.

Experimental part. The liposoluble constituents of from hexane extract of the medicinal plant were analyzed by using GC-MS method. GC-MS analysis: Electron Impact Ionization (EI) method on Agilent 7890A-5975C GC-MS (Gas Chromatograph coupled to Mass Spectrometer) fused silica capillary column (30m x 2.5mm; 0.25 μ m film thickness), coated with HP-5MS were utilized. The carrier gas was helium (99.999%). The column temperature was programmed from 50°C (held for 10min), at 10°C/min rate program to increase temperature to 300°C. The latter temperature maintained for 40min (Acquisition parameters full scan; scan range 30-1000 amu). The injector temperature was 310°C. Injection: with a 1 μ l: detector ion source (EI-70eV). Samples were injected by splitting with the split ratio 5:1.

Identification of the compounds: identification of compounds was done by comparing the NIST and Wiley library data of the peaks and mass spectra of the peaks with those reported in literature. Percentage composition was computed from GC peak areas on HP-5MS column without applying correction factors.

Results and discussion

The liposoluble constituents of hexane extract from the root parts of *F.pallidiflora* were analyzed by GC-MS. Thirty compounds were separated. Their relative contents were determined by area normalization. Table 1 showed the liposolubles contents of the root parts of *F.pallidiflora*. The liposoluble contents of *F.pallidiflora* have been identified in which the major constituents are n-hexadecanoic acid (28.97%), linoelaidic acid (16.68%), oleic Acid (11.30%), octadecanoic acid (6.95%), silanamine, n-phenyl- (4.41%), trans,trans-dibenzylideneacetone (3.85%), .gamma.-sitosterol (3.51%), ethyl 9.cis.,11.trans.-octadecadienoate (2.91%), hexadecanoic acid, ethyl ester (2.45%).

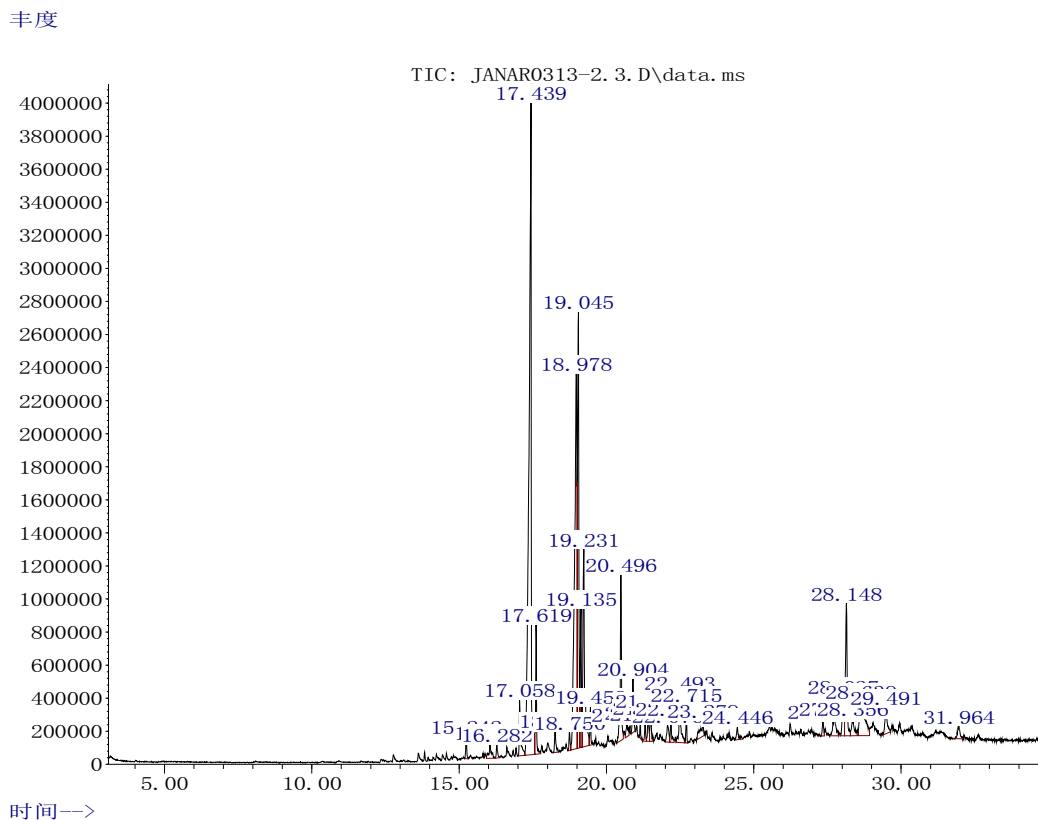
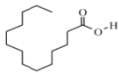
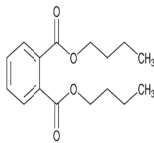
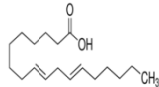


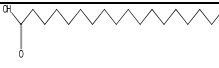

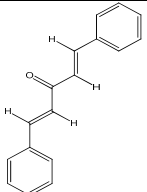
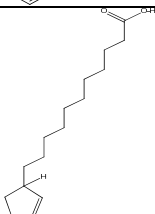
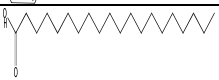
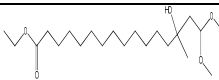
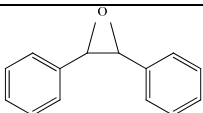
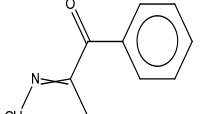
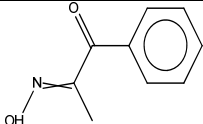

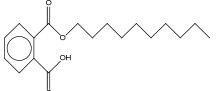
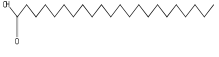
Fig. 1 Total ionization chromatogram of liposoluble contents hexane part from roots of *F.pallidiflora*


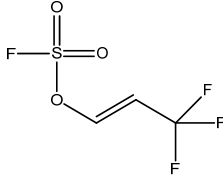
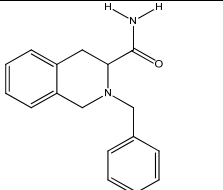
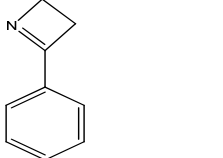
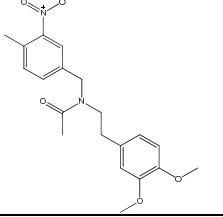
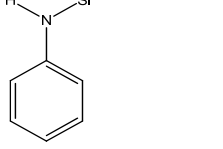
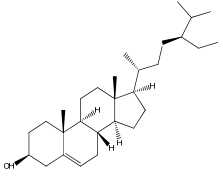
According to the report n-hexadecanoic acid (28.97%) is used in the production of stearin (a mixture with stearic acid), napalm, detergents and cosmetics, lubricating oils and plasticizers. And second major liposoluble constituents Linoelaidic acid (16.68%) showed rejuvenating and anti-inflammatory activities. Oleic Acid (11.30%) and its esters are used for the production of paint and varnish materials, as plasticizers. It is used in soap making, oleic acid and its salts are widely used as emulsifiers. It is part of cosmetic products [13].

Most of these constituents have been found to show interesting biological activity against certain illnesses and pathogens. For instance, the anti-inflammatory, antioxidant, hypocholesterolemic [14], antibacterial [15], activities reported for n-hexadecanoic acid (28.97%), may suggest the rationale for the traditional use of the species. Linoelaidic acid (16.68%) showed anti-inflammatory activity, oleic Acid (11.30%), and octadecanoic acid (6.95%) have antibacterial, antimicrobial activity [16], hexadecanoic acid, ethyl ester (2.45%) possess antioxidant, hypocholesterolemic, nematocide, pesticide, antiandrogenic flavor, and hemolytic activities [17].

Table 1 - The liposoluble constituents of root parts of *F.pallidiflora*

Peak No.	Constituents	t _R (min)	Molecular Formula	Structure	MW	Content (%)
1	Tetradecanoic acid	15,244	C ₁₄ H ₂₈ O ₂		228,209	0.43
2	9-Methyl-Z,Z-10,12-hexadecadien-1-ol acetate	16,051	C ₁₉ H ₃₄ O ₂		294,256	0.69
3	12-Bromododecanoic acid	16,28	C ₁₂ H ₂₃ BrO ₂		279,088	0.33
4	Dibutylphthalate	17,062	C ₁₆ H ₂₂ O ₄		278,152	1.44
5	n-Hexadecanoic acid	17,435	C ₁₆ H ₃₂ O ₂		256,24	28.97
6	Hexadecanoic acid, ethylester	17,622	C ₁₈ H ₃₆ O ₂		284,272	2.45
7	n-Decanoic acid	18,259	C ₁₀ H ₂₀ O ₂		172,146	0.62
8	Styrene	18,752	C ₈ H ₈		104,063	0.37
9	Linoelaidic acid	18,982	C ₁₈ H ₃₂ O ₂		280,24	16.68
10	Oleic Acid	19,05	C ₁₈ H ₃₄ O ₂		282,256	11.30
11	Ethyl 9.cis.,11.trans.-octadecadienoate	19,135	C ₂₀ H ₃₆ O ₂		308,272	2.91

Продолжение таблицы 1						
Peak No.	Constituents	t_R (min)	Molecular Formula	Structure	MW	Content (%)
12	Octadecanoicacid	19,228	$C_{18}H_{36}O_2$		284,272	6.95
13	Octadecanoicacid, ethylester	19,457	$C_{20}H_{40}O_2$		312,303	0.68
14	trans,trans-Dibenzylideneacetone	20,494	$C_{17}H_{14}O$		234,104	3.85
15	11-(2-Cyclopenten-1-yl)undecanoicacid, (+)-	20,698	$C_{16}H_{28}O_2$		252,209	0.47
16	Eicosanoicacid	20,902	$C_{20}H_{40}O_2$		312,303	1.26
17	Ethyl 14-methyl-hexadecanoate	21,148	$C_{21}H_{42}O_2$		298,287	0.25
18	Oxirane, 2,3-diphenyl-	21,318	$C_{14}H_{12}O$		196,089	0.35
19	1,2-Propanedione, 1-phenyl-, 2-oxime	21,42	$C_9H_9NO_2$		163,063	0.62
20	1,2-Propanedione, 1-phenyl-, 2-oxime	21,513	$C_9H_9NO_2$		163,063	0.76
21	Octadecylpropylether	22,074	$C_{21}H_{44}O$		312,339	0.67
22	Phthalicacid, monodecylester	22,193	$C_{18}H_{26}O_4$		306,183	0.61
23	Docosanoicacid	22,49	$C_{22}H_{44}O_2$		340,334	1.81

Peak No.	Constituents	t _R (min)	Molecular Formula	Structure	MW	Content (%)
24	Octadecanoic acid, 17-methyl-, methyl ester	22,711	C ₂₀ H ₄₀ O ₂		312,303	0.61
25	3,3,3-Trifluoroprop-1-en-1-yl fluorosulfate	23,28	C ₃ H ₂ F ₄ O ₃ S		193,966	0.89
26	2-Benzoyl-1,2,3,4-tetrahydro-isoquinoline-3-carboxylic acid	24,444	C ₁₇ H ₁₈ N ₂ O		281,105	0.47
27	Azete, 2,3-dihydro-4-phenyl-	27,349	C ₉ H ₉ N		131,073	0.38
28	Acetamide, N-[4-[[2-(6-chloro-3-cyano-4-methyl-2-pyridinyl)-2-ethylhydrazono]methyl]phenyl]-	28,038	C ₂₀ H ₂₄ N ₂ O ₅		355,12	1.32
29	Silanamine, N-phenyl-	28,148	C ₆ H ₆ NSi		123,05	4.41
30	Gamma.-Sitosterol	28,641	C ₂₉ H ₅₀ O		414,386	3.51

Conclusion

The liposoluble constituents were extracted by hexane from the root parts of *F.pallidiflora* which analyzed by GC-MS method. More than thirty compounds were separated. Their relative contents were determined by area normalization in which 30 liposolubles were identified. Active principles of hexane extract of the medicinal plant (*F.pallidiflora*) which collected from Almaty region of Kazakhstan were determined for the first time. While the major liposoluble constituents are n-hexadecanoic acid (28.97%), linoelaidic acid (16.68%), and oleic acid (11.30%) that possessing antifungal, insecticidal, larvicidalanti – inflammatory and analgesic activities separately.

Acknowledgement

The work was supported by grants from Ministry of Education and Science of Kazakhstan (0118PK00458).

REFERENCES

- [1] M.S. Baitenov Flora of Kazakhstan, Gylym, Almaty, 2001. - Vol. 2
- [2] *Brickell, Christopher, ed. (2016). RHS: A-Z Encyclopedia of garden plants (4th ed.). Dorling Kindersley. ISBN 978-0-241-23912-4.*
- [3] Nysanbaev A (1998) «Kazakhstan» National Encyclopedia, I: 328. Kazakh Encyclopediareduction, Almaty. [ISBN 5-89800-123-9](#)
- [4] Lozina-Lozinskaya A.S. Ryabchik - Fritillaria // Flora of the USSR / Botanical Institute of the USSR Academy of Sciences; Editor-in-chief and editor of the fourth volume of Acad. VL Komarov. - L.: Publishing House of the USSR Academy of Sciences, 1935. - T. IV. - P. 302-320.
- [5] Shuo Shen, Guoyu Li, Jian Huang, Chaojun Chen, Bu Ren, Ga Lu, Yong Tan, Jiaxu Zhang, Xian Li, Jinhui Wang. Steroidal saponins from *Fritillaria pallidiflora* Schrenk // *Fitoterapia* 83 (2012) 785–794
- [6] Dorni C, Sharma P, Saikia G, Longvah T. (2018) Fatty acid profile of edible oils and fats consumed in India, *Food Chemistry*, 238: 9-15. DOI: [10.1016/j.foodchem.2017.05.072](#)
- [7] Szymczycha-Madeja A, Welna M, Pohl P. (2012) Elemental analysis of teas and their infusions by spectrometric methods, *TrAC Trends in Analytical Chemistry*, 5: 165-181. DOI: 10.1016/j.trac.2011.12.005.
- [8] Yang B, Chen H, Stanton C, Ross RP, Zhang H, Chen YQ, Chen W. (2015) Review of the roles of conjugated linoleic acid in health and disease, *Journal of Functional Foods*, 15: 314-325. DOI: 10.1016/j.jff.2015.03.050
- [9] Bowen KJ, Kris-Etherton PM, Shearera GS, Westa ShG, Reddivaric L, Jones PJ. (2017) Oleic acid-derived oleoylethanolamide: A nutritional science perspective, *Progress in Lipid Research*, 67: 1-15. DOI: 10.1016/j.plipres.2017.04.001
- [10] Maechler P. (2017) Glutamate pathways of the beta-cell and the control of insulin secretion, *Diabetes Research and Clinical Practice*, 131:149-153. DOI: 10.1016/j.diabres.2017.07.009
- [11] Katane M, Kanazawa R, Kobayashi R, Oishi M, Nakayama K, Saitoh Y, Miyamoto T, Sekine M, Homma H. (2017) Structure–function relationships in human D-aspartate oxidase: characterisation of variants corresponding to known single nucleotide polymorphisms, *BBA - Proteins and Proteomics*, 1865: 1129-1140. DOI: [10.1016/j.bbapap.2017.06.010](#)
- [12] Liu L, Chen Y, Yang L. (2014) Inhibition study of alanine amino transferase enzyme using sequential online capillary electrophoresis analysis, *Analytical Biochemistry*, 467: 28-30. DOI: [10.1016/j.ab.2014.08.035](#)
- [13] <https://pubchem.ncbi.nlm.nih.gov/>
- [14] Kumar P.P., Kumaravel S., Lalitha C. Screening of antioxidant activity, total phenolics and GC-MS study of *Vitexnegundo*. *Afr. J. Biochem. Res.* 2010, 4, 191-195.
- [15] Rahuman A.A., Gopalakrishnan G., Ghose B.S., Arumugam S., Himalayan B. Effect of *Feronialimonia* on mosquito larvae. // *Fitoterapia* 2000, 71, 553-555.
- [16] Mustapha N. Abubakar, Runner R. T. Majinda. GC-MS Analysis and Preliminary Antimicrobial Activity of *Albizia adianthifolia* (Schumach) and *Pterocarpus angolensis* (DC) // *Medicines* 2016, 3, 3
- [17] Sudha T, Chidambarampillai S., Mohan V.R. GC-MS Analysis of Bioactive Components of Aerial parts of *Fluggealeucopyrus* Willd. (Euphorbiaceae) // *Journal of Applied Pharmaceutical Science* 3 (05); 2013: 126-130.
- [18] G.O. Kantureeva, E. Defrancesco, R.S. Alibekov, K.A. Urazbayeva, I.E. Efimova. New trends in the identification of the traditional food products of Kazakhstan. *News of NAS RK. Series of Chemistry and technology*. Volume 5, Number 431 (2018), 6 – 12. <https://doi.org/10.32014/2018.2518-1491.1> ISSN 2518-1491 (Online), ISSN 2224-5286 (Print)

¹Л.А. Утегенова, ¹А.К. Нурлыбекова, ^{2,3}Хажнякбер Анса, ¹Ж. Жәніс *

¹Әл-Фараби атындағы ҚазҰУ, Химия және Химиялық Технология Факультеті, Алматы, Қазақстан;

²Шыңжаң физика және химия техникалық институты, Қытайғылымдар академиясы;

³Шыңжаң табиғи ресурстар мен табиғи өнімдер химиясы зертханасы, Қытайғылымдар академиясы, Қытай

АҚШЫЛСЕПКІЛГҮЛӨСІМДІГІНЦМАЙДА ЕРИТІНҚҰРАМЫНЗЕРТТЕУ

Аннотация: Алматы өңірінен жиналған *Fritillaria pallidiflora* өсімдігі тамырының химиялық құрамы алғаш рет зерттелді. Дәрілік өсімдіктің биологиялық белсенді құрамының сандық және сапалық талдаулары

жасалды. *F.pallidiflora* өсімдігі тамырынан майда ергіш заттардан құрам тапқан гександі экстракті алынды және GC-MS әдісімен талданды. Сонымен гександы бөліктен отыз қосылыс сарапталды. Олардың салыстырмалы құрамы қалыпты аймақ көмегімен есептеліп, нәтижесінде гександы бөліктегі негізгі қосылыстар: п-гексадекан қышқылы (28,97%), линолейн қышқылы (16,68%), олеин қышқылы (11,30%), октадекан қышқылы (6,95%), силанамин, п-фенил- (4,41%), транс, транс-Дибензилиденацетон (3,85%), гамма-ситостерол (3,51%), этил-9-цис, 11-транс-октадекадиеноат (2,91%) және гексадекан қышқылдың этил эфирі (2,45%) болып табылды.

Түйін сөздер: *Fritillaria pallidiflora*, GC-MS, майда ергіш заттар

¹Л.А. Утегенова, ¹А.К. Нурлыбекова, ^{2,3}Хажиякбер Аиса, ¹Ж. Жәніс *

¹Факультет химии и химической технологии, Казахский национальный университет им. Аль-Фараби, Алматы, Казахстан

²Синьцзянский технический институт физики и химии, Китайская академия наук

³Лаборатория Синьцзянских растительных ресурсов химии природных соединений, Китайская академия наук, Китай

ИССЛЕДОВАНИЕ ЖИРОРАСТВОРИМОГО СОСТАВА РЯБЧИКА БЛЕДНОЦВЕТКОГО

Аннотация: Впервые был исследован химический состав корней *Fritillaria pallidiflora*, собранных в Алматинской области. Сделан количественный и качественный анализ биологически активных компонентов лекарственного растения. Жирорастворимые компоненты гексанового экстракта были получены из корневой части *F.pallidiflora* и проанализированы методом GC-MS. Было разделено тридцать соединений. Их относительное содержание было определено по нормализации площади, среди которых основными компонентами являются п-гексадекановая кислота (28,97%), линолеиновая кислота (16,68%), олеиновая кислота (11,30%), октадекановая кислота (6,95%), силанамин, п-фенил- (4,41%), транс, транс-Дибензилиденацетон (3,85%), гамма-ситостерол (3,51%), этил-9-цис., 11-транс-октадекадиеноат (2,91%), этиловый эфир гексадекановой кислоты (2,45%).

Ключевые слова: *Fritillaria pallidiflora*, GC-MS, жирорастворимые компоненты.

МАЗМҰНЫ

<i>Тунгатарова С.А., Ксандопуло Г., Кауменова Г.Н., Жумабек М., Байжуманова Т.С., Григорьева В.П., Комашко Л.В., Бегимова Г.У.</i> Метанды синтез газға каталитикалық риформингілеуде жану әдісімен композитті материалдарды жасау...6	
<i>Johann Dieck, Tатаева Р., Байманова А., Бакешова Ж., Капсалямов Б.</i> Ақаба суларды биологиялық өңдеу: теориялық негіздері және эксперименттік зерттеулер.....	16
<i>Орымбетова Г.Э., Conficoni D., Касымова М.К., Кобжасарова З.И., Орымбетов Э.М., Шамбулова Г.Д.</i> Сүт және сүт өнімдерінде қорғасын тәуекелін бағалау.....	23
<i>Талғатов Э.Т., Әуезханова А.С., Тумабаев Н.Ж., Ахметова С.Н., Сейтқалиева Қ.С., Бегмат Е.Ә., Жармагамбетова Ә.Қ.</i> Фенилацетиленді гидрлеуге арналған магнитті тасымалдағышқа отырғызылған полимер-палладий катализаторлары	29
<i>Ермагамбет Б.Т., Ремнев Г.Е., Мартемьянов С.М., Бухаркин А.А., Касенова Ж.М., Нурғалиев Н.У.</i> Майқұбы және Экібастұз көмір бассейндерінің диэлектрикалық қасиеттері.....	38
<i>Бейсенбаев А.Р., Жабаева А.Н., Сунцова Л.П., Душкин А.В., Адекенов С.М.</i> Оксима пиностробинның супрамолекулярлық кешенін синтездеу мен зерттеу.....	46
<i>Jadhav A. S., Mohanraj G. T., Mayadevi S., Gokarn A. N.</i> Йодты адсорбцияның саны бойынша катеху атты жаңғақтың қабығынан алынатын нано-беттік белсендірілген көмірдің көлемін анықтаудың жылдам әдісі.....	53
<i>Нүркенов О.А., Фазылов С.Д., Исаева А.Ж., Сейлханов Т.М., Животова Т.С., Шұлғау З.Т., Қожина Ж.М.</i> Функционалдық-орынбасылған изоникотин қышқылының гидразондары мен циклодекстриндердің комплекстік кешендері жән.....	57
<i>Ермагамбет Б.Т., Нурғалиев Н.У., Абылгазина Л.Д., Маслов Н.А., Касенова Ж.М., Касенов Б.К.</i> Көмір шлак қалдықтарының өнімдерінен бағалы компоненттер алудың әдістері.....	67
<i>Шоманова Ж.К., Сафаров Р.З., Жумаканова А.С., Носенко Ю.Г., Жанибекова А.Т., Шапекова Н.Л., Лорант Д.</i> Феррокорытпаны өңдеу қалдықтары негізінде алынған катализаторлар бетін электрондық микроскопия әдісімен зерттеу.....	79
<i>Баешов А., Гаишов Т.Э., Баешова А.К., Колесников А.В.</i> Мыс (II) иондарын үш валентті титан иондарымен цементациялау арқылы нано – және ультрадисперсті мыс ұнтақтарын алу.....	87
<i>Баешов А.Б., Мырзабеков Б.Э., Колесников А.В.</i> Құрамында титан (IV) иондары бар күкірт қышқылы ерітіндісінде мыс анодын қолдану кезінде электролит көлемінде дисперсті мыс ұнтақтарының түзілу заңдылықтары.....	96
<i>Чиркун Д. И., Левданский А.Э., Голубев В.Г., Сарсенбекулы Д., Кумисбеков С.А.</i> Өнеркәсіптік барабанды диірмендер жұмысын сарапталау және оларды жетілдіру жолдары.....	102
<i>Бродский А.Р., Григорьева В.П., Комашко Л.В., Нурмаканов Е.Е., Чанышева И.С., Шаповалов А.А., Шлыгина И.А., Яскевич В.И.</i> Молекула зонды бар Fe/γ-Al ₂ O ₃ катализдік жүйенің өзара әрекеттестігі I. γ-Al ₂ O ₃ және Fe/γ-Al ₂ O ₃ бастапқы жүйенің зерттелуі.....	109
<i>Бродский А.Р., Григорьева В.П., Комашко Л.В., Нурмаканов Е.Е., Чанышева И.С., Шаповалов А.А., Шлыгина И.А., Яскевич В.И.</i> Взаимодействие каталитической системы Fe/γ-Al ₂ O ₃ с молекулами-зондами II. Исследование носителя γ-Al ₂ O ₃ и системы Fe/γ-Al ₂ O ₃ после взаимодействия с водородом и аммиаком.....	120
<i>Доспаев М. М., Баешов А., Жумаканова А.С., Доспаев Д.М., Сыздықова Б.Б., Какенов К.С., Есенбаева Г.А.</i> Калий метасиликаты ертіндісінде мыс анодын поляризациялау кезіндегі нанодисперсті мыс силикаты ұнтағының түзілу механизм.....	130
<i>Надиоров К.С., Черкаев Г.В., Чихонадских Е.А., Маккаевева Н.А., Садырбаева А.С., Орымбетова Г.Э.</i> Екі отынды ііж кемелердің пайдаланылған газдарымен зиянды заттардың шығарылуының қоршаған ортаға және тұрғындар денсаулығына әсерін талдау	138
<i>Хусаин Б.Х., Винникова К.К., Сасс А.С., Рахметова К.С., Кензин Н.Р.</i> Бейтараптандыру процестегі пайдаланылған газдар шығудың аэродинамикалық модельдеу.....	150
<i>Утегенова Л.А., Нурлыбекова А.К., Хажиакбер Аиса, Жеңіс Ж.</i> Ақшыл сепкіл гүлөсімдігінің майда еритін құрамын зерттеу.....	156

СОДЕРЖАНИЕ

Тунгатарова С.А., Ксандопуло Г., Кауменова Г.Н., Жумабек М., Байжуманова Т.С., Григорьева В.П., Комашко Л.В., Бегимова Г.У. Разработка композитных материалов методом горения для каталитического риформинга метана в синтез-газ.....	6
Johann Duesck, Tатаева Р., Байманова А., Бакешова Ж., Капсалямов Б. Биологическая обработка сточных вод: теоретическая основа и экспериментальные исследования.....	16
Орымбетова Г.Э., Conficoni D., Касымова М.К., Кобжасарова З.И., Орымбетов Э.М., Шамбулова Г.Д. Оценка риска свинца в молоке и молочной продукции	23
Талгатов Э.Т., Ауезханова А.С., Тумабаев Н.Ж., Ахметова С.Н., Сейткалиева К.С., Бегмат Е.А., Жармагамбетова А.К. Полимер-палладиевые катализаторы на магнитном носителе для гидрирования фенилацетилена.....	29
Ермагамбет Б.Т., Ремнев Г.Е., Мартемьянов С.М., Бухаркин А.А., Касенова Ж.М., Нурғалиев Н.У. Диэлектрические свойства углей Майкубенского и Экибастузского бассейнов.....	38
Бейсенбаев А.Р., Жабаяева А.Н., Сунцова Л.П., Душкин А.В., Адекенов С.М. Синтез и изучение супрамолекулярного комплекса оксима пиностробина.....	46
Jadhav A. S., Mohanraj G. T., Mayadevi S., Gokarn A. N. Быстрый метод определения площади нано-поверхности активированного угля полученного из оболочки ореха катеху по числу адсорбции йода.....	53
Нуркенов О.А., Фазылов С.Д., Исаева А.Ж., Сейлханов Т.М., Животова Т.С., Шульгау З.Т., Кожина Ж.М. Комплексы включения функционально-замещенных гидразонов изоникотиновой кислоты с циклодекстринами и их антирадикальная активность.....	57
Ермагамбет Б.Т., Нурғалиев Н.У., Абылгазина Л.Д., Маслов Н.А., Касенова Ж.М., Касенов Б.К. Методы извлечения ценных компонентов из золошлаковых отходов углей.....	67
Шоманова Ж.К., Сафаров Р.З., Жумаканова А.С., Носенко Ю.Г., Жанибекова А.Т., Шапекова Н.Л., Лорант Д. Исследование методом электронной микроскопии поверхности катализаторов, полученных на основе отходов ферросплавного производства.....	79
Баешов А., Гаитов Т.Э., Баешова А.К., Колесников А.В. Получение нано- и ультрадисперсных порошков меди цементацией ионов меди (II) ионами трехвалентного титана	87
Баешов А.Б., Мырзабеков Б.Е., Колесников А.В. Закономерности образования дисперсных медных порошков в объеме электролита при использовании медного анода в растворе серной кислоты, содержащей ионы титана (IV)	96
Чиркун Д. И., Левданский А. Э., Голубев В.Г., Сарсенбекулы Д., Кумисбеков С.А. Анализ работы барабанных промышленных мельниц и пути их усовершенствования	102
Бродский А.Р., Григорьева В.П., Комашко Л.В., Нурмаканов Е.Е., Чанышева И.С., Шаповалов А.А., Шлыгина И.А., Яскевич В.И. Взаимодействие каталитической системы Fe/γ-Al ₂ O ₃ с молекулами-зондами I. Исследование γ-Al ₂ O ₃ и исходной системы Fe/γ-Al ₂ O ₃	109
Бродский А.Р., Григорьева В.П., Комашко Л.В., Нурмаканов Е.Е., Чанышева И.С., Шаповалов А.А., Шлыгина И.А., Яскевич В.И. Взаимодействие каталитической системы Fe/γ-Al ₂ O ₃ с молекулами-зондами II. Исследование носителя γ-Al ₂ O ₃ и системы Fe/γ-Al ₂ O ₃ после взаимодействия с водородом и аммиаком	120
Доспаев М. М., Баешов А., Жумаканова А.С., Доспаев Д.М., Сыздыкова Б.Б., Какенов К.С., Есенбаева Г.А. Механизм образования нанодисперсного порошка силиката меди в растворе метасиликата калия	130
Надилов К.С., Черкаев Г.В., Чихонадских Е.А., Маккаевеева Н.А., Садырбаева А.С., Орымбетова Г.Э. Анализ влияния выбросов вредных веществ с отработавшими газами судовых двухтопливных двс на окружающую среду и здоровье населения.....	138
Хусаин Б.Х., Винникова К.К., Сасс А.С., Рахметова К.С., Кензин Н.Р. Аэродинамическое моделирование прохождения выбросов в процессе нейтрализации.....	150
Утегенова Л.А., Нурлыбекова А.К., Хажиакбер Аиса, Жеңіс Ж. Исследование жирорастворимого состава рябчика Бледноцветного.....	156

CONTENTS

<i>Tungatarova S.A., Xanthopoulou G., Kaumenova G.N., Zhumabek M., Baizhumanova T.S., Grigorieva V.P., Komashko L.V., Begimova G.U.</i> Development of composite materials by combustion synthesis method for catalytic reforming of methane to synthesis gas.....	6
<i>Dueck Johann, Tatayeva R., Baymanova A., Bakeshova Zh., Kapsalyamov B.</i> Biological treatment of waste water: theoretical background and experimental research.....	16
<i>Orymbetova G.E., Conficoni D., Kassymova M.K., Kobzhasarova Z.I., Orymbetov E.M., Shambulova G.D.</i> Risk assessment of lead in milk and dairy products	23
<i>Talgatov. E.T., Auyezkhanova A.S., Tumabayev N.Z., Akhmetova S.N., Seitkaliyeva K.S., Begmat Y.A., Zharmagambetova A.K.</i> Polymer-palladium catalysts on magnetic support for hydrogenation of phenylacetylene.....	29
<i>Ermagambet B.T., Remnev G.E., Martemyanov S.M., Bukharkin A.A., Kasenova Zh.M., Nurgaliyev N.U.</i> Dielectric properties of the coals of Maykuben and Ekibastuz basins.....	38
<i>Beisenbayev A.R., Zhabayeva A.N., Suntsova L.P., Dushkin A.V., Adekenov S.M.</i> Synthesis and study of pinostrobin oxime supramolecular complexes.....	46
<i>Jadhav A. S., Mohanraj G. T., Mayadevi S., Gokarn A. N.</i> Rapid method for determination of nano surface area of arecanut shell derived activated carbon by iodine adsorption number.....	53
<i>Nurkenov O.A., Fazylov S.D., Issayeva A.Zh., Seilkhanov T.M., Zhivotova T.S., Shulgau Z.T., Kozhina Zh.M.</i> Complexes of inclusion of functionally-substituted hydrasons of isonicotic acid with cyclodextrines and their antiradical activity.....	57
<i>Yermagambet B.T., Nurgaliyev N.U., Abylgazina L.D., Maslov N.A., Kasenova Zh.M., Kasenov B.K.</i> Methods for extraction of valuable components from ash-and-slag coal wastes.....	67
<i>Shomanova Zh.K., Safarov R.Z., Zhumakanova A.S., Nosenko Yu.G., Zhanibekova A.T., Shapekova N.L., Lorant D.</i> Electron microscopy surface study of catalysts based on ferroalloy production waste.....	79
<i>Bayeshov A., Gaipov T.E., Bayeshova A.K., Kolesnikov A.V.</i> Synthesis of nano- and ultradisperse copper powders by cementation of copper (II) ions by three-valent titanium ions.....	87
<i>Bayeshov A.B., Myrzabekov B.E., Kolesnikov A.V.</i> Patterns of formation of dispersed copper powders in the body of electrolyte during the use of copper anode in sulfuric acid solution along with titanium (IV) ions.....	96
<i>Chyrkun D.I., Leudanski A.E., Golubev V.G., Sarsenbekuly D., Kumisbekov S.A.</i> Analysis of industrial drum mills' operation and ways of their improvement.....	102
<i>Brodskiy A.R., Grigor'eva V.P., Komashko L.V., Nurmakanov Y.Y., Chanysheva I.S., Shapovalov A.A., Shlygina I.A., Yaskevich V.I.</i> Interaction of the Fe/ γ -Al ₂ O ₃ catalytic system with probe molecules I. Research of the γ -Al ₂ O ₃ and the Fe/ γ -Al ₂ O ₃ initial system	109
<i>Brodskiy A.R., Grigor'eva V.P., Komashko L.V., Nurmakanov Y.Y., Chanysheva I.S., Shapovalov A.A., Shlygina I.A., Yaskevich V.I.</i> Interaction of the catalytic Fe/ γ -Al ₂ O ₃ system with probe molecules II. Study OF γ -Al ₂ O ₃ support and Fe/ γ -Al ₂ O ₃ system after interaction with hydrogen and ammonia.....	120
<i>Dospaev M.M., Bayeshov A., Zhumakanova A.S., Dospaev D.M., Syzdykova B.B., Kakenov K.S., Esenbaeva G.A.</i> Mechanism of forming nanodisperse copper silicate powder during anodic polzrization of copper electrode in potassium silicate solution.	130
<i>Nadirov K.S., Cherkaev G.V., Chikhonadskikh E.A., Makkaveeva N.A., Sadyrbaeva A.S., Orymbetova G.E.</i> Analysis of influence of emissions of harmful substances with exhaust gases of marine dual fuel internal combustion engine on the environment and human health.....	138
<i>Khusain B.Kh., Vinnikova K.K., Sass A.S., Rakhmetova K.S., Kenzin N.R.</i> Aerodynamic modeling of emissions passage in the neutralization process.....	150
<i>Utegenova L.A., Nurlybekova A.K., Hajiakber Aisa, Jenis J.</i> Liposoluble constituents of <i>Fritillaria pallidiflora</i>	156

Publication Ethics and Publication Malpractice in the journals of the National Academy of Sciences of the Republic of Kazakhstan

For information on Ethics in publishing and Ethical guidelines for journal publication see <http://www.elsevier.com/publishingethics> and <http://www.elsevier.com/journal-authors/ethics>.

Submission of an article to the National Academy of Sciences of the Republic of Kazakhstan implies that the described work has not been published previously (except in the form of an abstract or as part of a published lecture or academic thesis or as an electronic preprint, see <http://www.elsevier.com/postingpolicy>), that it is not under consideration for publication elsewhere, that its publication is approved by all authors and tacitly or explicitly by the responsible authorities where the work was carried out, and that, if accepted, it will not be published elsewhere in the same form, in English or in any other language, including electronically without the written consent of the copyright-holder. In particular, translations into English of papers already published in another language are not accepted.

No other forms of scientific misconduct are allowed, such as plagiarism, falsification, fraudulent data, incorrect interpretation of other works, incorrect citations, etc. The National Academy of Sciences of the Republic of Kazakhstan follows the Code of Conduct of the Committee on Publication Ethics (COPE), and follows the COPE Flowcharts for Resolving Cases of Suspected Misconduct (http://publicationethics.org/files/u2/New_Code.pdf). To verify originality, your article may be checked by the Cross Check originality detection service <http://www.elsevier.com/editors/plagdetect>.

The authors are obliged to participate in peer review process and be ready to provide corrections, clarifications, retractions and apologies when needed. All authors of a paper should have significantly contributed to the research.

The reviewers should provide objective judgments and should point out relevant published works which are not yet cited. Reviewed articles should be treated confidentially. The reviewers will be chosen in such a way that there is no conflict of interests with respect to the research, the authors and/or the research funders.

The editors have complete responsibility and authority to reject or accept a paper, and they will only accept a paper when reasonably certain. They will preserve anonymity of reviewers and promote publication of corrections, clarifications, retractions and apologies when needed. The acceptance of a paper automatically implies the copyright transfer to the National Academy of Sciences of the Republic of Kazakhstan.

The Editorial Board of the National Academy of Sciences of the Republic of Kazakhstan will monitor and safeguard publishing ethics.

Правила оформления статьи для публикации
в журнале смотреть на сайте:

www.nauka-nanrk.kz

<http://www.chemistry-technology.kz/index.php/ru/>

ISSN 2518-1491 (Online), ISSN 2224-5286 (Print)

Редакторы: *М. С. Ахметова, Т. А. Апендиев, Аленов Д.С.*
Верстка на компьютере *А.М. Кульгинбаевой*

Подписано в печать 05.12.2018.
Формат 60x881/8. Бумага офсетная. Печать – ризограф.
9,8 п.л. Тираж 300. Заказ 6.